NEW ZEALAND GEOTECHNICAL SOCIETY INC

AUSTRALIAN GEOMECHANICS SOCIETY

PROCEEDINGS OF THE 10TH YOUNG GEOTECHNICAL PROFESSIONALS CONFERENCE (10YGPC)

10 – 12 SEPTEMBER 2014

NOOSA, QUEENSLAND, AUSTRALIA

Major Sponsors:

IGS

Insitu Geotech Services Pty Ltd

CPTS

cone penetration testing services

ENGINEERS AUSTRALIA

HIRE

ATV

The experts in transporting personnel, machinery and sensitive equipment over difficult terrain under challenging conditions.

Used by engineers for:

- geotechnical investigations
- environment and resource management
- equipment transport
- forestry
- mine operations
- mineral exploration
- personnel transportation
- pipeline services
- power line maintenance
- reconnaissance
- seismic surveys
- surveying
- utility maintenance

We provide experienced operators and project-specific customised All Terrain Vehicles.

Making the inaccessible, accessible:

- marshlands
- mud flats
- flood plains
- low lying farmland
- bauxite, coal, gold and nickel tailings dams
- mountain tracks
- salt pans
- swamps
- tailings disposal areas
- reclamation works

We work with CPTS P/L to offer cone penetration testing in difficult to access sites.

CPTS

HIRE

ATV

YVO (EVO) KEULEMANS
M 0407 375 977

F (07) 3843 1386
E yvo@atvhire.com.au
W www.atvhire.com.au

CPTS
cone penetration testing services

Offering one level of service

....the best.

When projects need to be delivered on time and on budget, time is limited and reliable data is critical. CPTS is trusted by consulting engineers to provide faster high-quality, reliable CPT data every time.

For 13 years, CPTS has built a first-class reputation for expertise and experience in cone penetration testing services. Owner and exclusive site supervisor, Yvo Keulemans has more than 20 years hands-on CPT experience.

CPTS provides highly experienced CPT operators and a fleet of CPT testing vehicles. Our specialised insitu testing equipment includes:

- Standard cone (Qc & Fs) and Piezocone (Qc, Fs & Pore pressure)
- Vane shear testing with electronic inline torque sensor
- Dilatometer and Seismic dilatometer
- Electronic hand-held penetrometer
- Wireline soil samplers for sampling soft/loose strata
- Precision in-house systems to confirm highest accuracy calibration of CPT probes
- Vacuum chambers capable of completely saturating fully assembled piezocones prior to each test.

We often help clients solve unique soil testing and site access challenges, by developing job-specific solutions and working with ATV HIRE to transport personnel, sensitive equipment and machinery across difficult-to-access sites.

For site access without delay, data without query, and testing efficiency without rival; trust CPTS to deliver the best.

For your next project, contact:
Yvo (Evo) Keulemans • **M** 0407 375 977 • **E** yvo@cpts.com.au

we can access places you never thought possible

Australia, PNG and elsewhere

world class in situ testing, & sampling you always wanted

big rigs, little rig and rigs that float & fly

it's enjoyable working with IGS

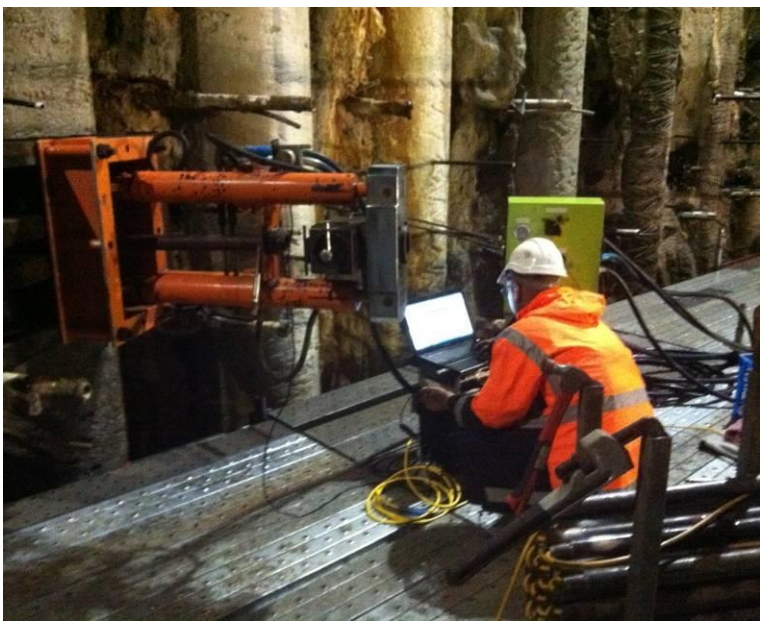

we can access sites you never thought possible

we can test ground you never thought possible

IGS

reducing geotechnical uncertainty

In Situ Testing

CPT & CPTu (piezo-cone)
DMT & Seismic DMT
Tee-Bar Testing
Push-in Vane Shear

Sampling

PPI Piston Sampler
Vertek Piston Sampler
Eziprobe Push-in Sampler
Gregg Sampler
Piston Flap (PF) Sampler
Bulk Sediment (BS) Sampler
Window Sampler

Other Things

Installation of piezometers
Installation of standpipes
In situ permeability testing

Innovation

We innovate to make things possible for our clients

0417-748-669
allan@insitu.com.au
www.insitu.com.au

Melbourne *Sydney* *Brisbane* *Townsville*

Additional Sponsorship provided by:

Additional Support provided by:

Preface

The YGP conference series aims at bringing together young people who may be studying for a Ph.D. or M.Sc. or at the early stage of their career in engineering or academia. The idea is to enable delegates to communicate with others who are doing research or starting out in the geotechnical profession and to share their experience. YGPC's provide the opportunity for all delegates to write and present a formal technical paper in a relaxed conference setting than the quadrennial ANZ Conference on Geomechanics.

The book presents the Proceedings of the 10th ANZ Young Geotechnical Professionals Conference (10YGPC) held at Noosa Heads, Queensland, Australia, on 10 – 12 September, 2014. This event was organised as an initiative of the Australian Geomechanics Society (AGS) and The New Zealand Geotechnical Society (NZGS).

The papers published in these proceedings were peer-reviewed by senior geotechnical personnel and experts in the field of geotechnical engineering. The topics covered are quite varied and include: laboratory testing; field testing; geology; groundwater; earthworks; soil behaviour; constitutive modelling; ground improvement; earthquake; retaining structures; foundations; slope stability; tunnels and observational methods.

I would like to acknowledge the work done by the reviewers, for their fundamental contribution in ensuring the quality of the published papers. We also gratefully acknowledge the financial supports from both the AGS and NZGS, along with the various sponsors (for both financial and in kind support). All contributing organisations were absolutely essential for the successful co-ordination of this conference.

David Lacey
10YGPC Organising Committee

Acknowledgement of Peer Reviewers

The papers published in these proceedings were peer-reviewed by senior geotechnical personnel and experts in the field of geotechnical engineering. The Australian Geomechanics Society (AGS) and The New Zealand Geotechnical Society (NZGS) were responsible for the peer review of the papers submitted by their own members.

The peer-review panel was comprised of the following personnel, each of whom are thanked for their donation of considerable time and effort to provide comprehensive paper reviews and comments to each submitting author:

Peer Reviewers provided by The New Zealand Geotechnical Society (NZGS):

Kevin Anderson
David Burns
Nick Harwood
Hamish Maclean
Mick Pender
Charlie Price
Ken Read
Ross Roberts
Laurence Wesley

Peer Reviewers provided by the Australian Geomechanics Society (AGS):

Bindumadhava Aery
Kam Chew
Chaminda Gallage
Adam Kemp
Patrick Kidd
David Lacey
Burt Look
Michelle Phillipson
Steven Rosin
Ian Shipway
Adrian Smith
Mogana Sundaram
Vipman Tandjiria
Ramtin Tejeddin
Bari Thomas
David Williams

Contents

This page intentionally left blank

Proceedings of the 10th ANZ Young Geotechnical Professional's Conference – 10YGPC
Noosa, Queensland, Australia
10 – 12 September 2014

CYCLIC SOFTENING CASE STUDY: WENDOVER RETIREMENT VILLAGE, CHRISTCHURCH

Richard HERITAGE
Aurecon, Wellington, New Zealand

ABSTRACT – Wendover Retirement Village is located in Papanui, Christchurch, New Zealand adjacent to a minor tributary of Dudley Creek on the edge of a drained peat swamp. The site suffered damage as a result of the recent major seismic activity in Canterbury, including ground settlement and lateral spreading.

The initial assumption was that liquefaction caused the ground damage on site. However, this was dismissed when investigations showed that the site is typically underlain by 5–6m of peat and organic clay with a high water table; which in turn overlies 1–2m of sand, then gravel. Analysis confirmed that liquefaction would be restricted to the sand that underlies the organic deposits.

To determine the cause of the ground damage, a cyclic softening assessment was undertaken based on the method of Idriss and Boulanger (Idriss & Boulanger, 2008). By comparing the results with the earthquake records from seismographs located nearby, it was demonstrated that cyclic softening was expected in the 22 February 2011 earthquake event and unlikely in the 4 September 2010 event. This correlated well with the observations of ground damage. In addition, by using probabilistic predictions of the magnitude of ground accelerations, the likelihood of cyclic-softening-induced ground damage reoccurring was able to be estimated.

1. Introduction

The Darfield Earthquake of 4 September 2010 caused significant damage to the land, infrastructure and buildings of Christchurch City and the wider Canterbury region. However, it was the subsequent Christchurch Earthquake of 22 February 2011 that caused the greatest damage to Christchurch City with liquefaction and associated lateral spreading causing severe ground damage on the flat land where the majority of Christchurch City is located. At Wendover Retirement Village, located in the suburb of Papanui on the flat land of Christchurch City, what appeared to be typical liquefaction induced lateral spreading had caused ground cracks and lateral movement towards the adjacent Dudley Creek. However, investigations into the nature of the soil below the site revealed that liquefaction was now the cause of the observed damage. This paper describes the assessment of the land at Wendover Retirement Village and presents the results of an analysis of what may have caused the observed land damage.

2. Background

Wendover Retirement Village is located on the floodplain of the Waimakariri River in the suburb of Papanui in Christchurch. The site is predominantly flat, surrounded by residential properties. The land to the northeast of the site is parkland that slopes gently down away from Wendover Retirement Village. Within 10–15m of the northeast boundary of the site is a small watercourse that is a tributary of Dudley Creek (see Figure 1).

The geological maps of Christchurch City (Brown & Weeber, 1992) describe the site as being on the edge of an area of "peat swamps, now drained" and historic maps of the area dating back to 1850 (Sibley, 1989) describe the land as "swamp, raupo and tussocks".

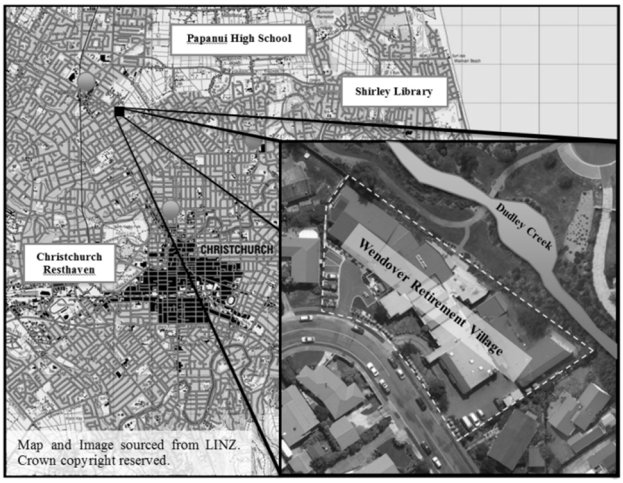

Figure 1. Site location plan

There is a seismograph in Papanui High School located approximately 1.0km northwest of Wendover Retirement Village which recorded the accelerations of all the recent earthquake events in the Canterbury Region. There are also seismographs located at Christchurch Resthaven (approximately 3km to the southeast) and Shirley Library (approximately 3.7km to the east). The assessed levels of shaking at Wendover Retirement Village during the most significant recent earthquakes are shown in Table 1.

3. Observed Land Damage

The Darfield Earthquake caused only minimal ground damage, whereas significant ground settlement and movement relative to the retirement village buildings was observed across the site following the 22 February 2011 Christchurch Earthquake. In places the ground settlement was upwards of 100mm, with the greatest relative settlement in the northern corner of the site along the grassed terrace area on the north-eastern boundary. What appeared to be lateral spreading was observed in the same grassed terrace area as well as in the banks adjacent the watercourse located within 10–15m of the buildings. In places lateral movements of up to 100mm were noted.

Some minor traces of liquefaction-induced surface expression (light grey fine silt sand material) were noted along the road frontage adjacent to Wendover Retirement Village. However, no notable damage to road pavements or other liquefaction-induced damage was observed

Table I. Levels of shaking on site

Name	Date	Moment Magnitude, Mw	Ave. PGA(1)
Darfield Earthquake	4 Sept 2010	7.1	0.26g
Christchurch Earthquake	22 Feb 2011	6.2	0.34g

(1) The peak ground accelerations (PGA) are based on averaging the values recorded at the nearby seismographs inversely proportional to the distance of the seismograph from site.

4. Soil Profile

To assess the local ground conditions, six Cone Penetration Tests (CPT) were undertaken, along with three hand-auger boreholes with Scala penetrometer testing in locations where the CPT rig access was not available. The tests were conducted between October and December 2011 because of access issues. The inferred ground conditions are shown in Table 2.

Table 2. Typical soil profile

Layer	Depth	Description	Consistency
1	0m	Peat and Organic Clay	Very Soft to Soft
2	5-6m	Sand and Gravelly Sand	Dense to Very Dense
3	6-8m	Sandy Gravel (inferred)	-

The water table was measured in the hand-auger boreholes at 0.2m to 0.7m below ground level, which corresponds to approximately the water level of the nearby watercourse. For the purposes of all analyses the groundwater level was assumed to be at the elevation of the average level of the nearby watercourse (typically 0.5m below ground level depending on the location measured).

5. Analysis

The ground damage on site appeared to be typical of liquefaction-induced lateral spreading. However, once ground investigations were undertaken, this became increasingly unlikely, as analysis predicted that the only soils susceptible to liquefaction were located below the organic deposits at 5–6m depth. The organic deposits of peat and organic clay were too cohesive to have undergone liquefaction. The failure mechanism being something other than liquefaction was further supported by the lack of liquefaction surface expression anywhere near the lateral spreading. It was postulated that the ground damage may have been caused by cyclic softening of the cohesive soils, and so an analysis of the investigation data was undertaken to verify this theory.

5.1. Cyclic softening methodology

In order to assess the soil's susceptibility to cyclic softening the method of Idriss and Boulanger (Idriss & Boulanger, 2008) was utilised. This method is based on the ratio of the cyclic stress ratio (CSR) to the cyclic resistance ratio in a similar approach to liquefaction susceptibility analysis of the NCEER method (Youd et. al., 2001). The main difference being that the CRR is calculated based on the undrained shear strength of the cohesive soil. The formulae that Idriss and Boulanger have recommended for calculating the CRR are:

$$CRR = 0.80\frac{S_u}{\sigma'_{vc}} MSF \cdot K_\alpha \quad (1)$$

$$MSF = 1.12 \cdot e^{\left(\frac{-M}{4}\right)} + 0.828 \quad (2)$$

$$K_\alpha = 1.344 - \frac{0.344}{(1 - \frac{\alpha}{0.22 \cdot OCR^{0.8}})^{0.688}} \quad (3)$$

$$\alpha = \frac{\tau_s}{\sigma'_{vc}} \quad (4)$$

Where: S_u = undrained shear strength of cohesive soil
σ'_{vc} = vertical effective stress at consolidation
MSF = magnitude scaling factor
M = earthquake magnitude
K_α = static shear stress correction factor
OCR = over consolidation ratio
τ_s = static shear stress

Note that the MSF formula is different from that used for a liquefaction analysis as clays are less susceptible to loss of strength and stiffness when subjected to cyclic loading.

The CSR is calculated in the same manner as used in a liquefaction method based on the method proposed by NCEER (Youd et. al., 2001):

$$CSR = 0.65 \frac{a_{max}}{g} \frac{\sigma_{vo}}{\sigma'_{vo}} r_d \quad (5)$$

Where: a_{max} = peak ground acceleration
g = acceleration due to gravity
σ_{vo} = in-situ vertical total stress
σ'_{vo} = in-situ vertical effective stress
r_d = stress reduction factor

As with the NCEER method, if CSR > CRR then cyclic softening will occur.

5.2. Assessment of parameters

The various parameters needed for these equations were assessed as follows:

- The undrained shear strength (S_u) was assessed based on an average value interpreted from the CPT logs.
- Using assumptions of typical soil densities for the soil types encountered and the depth of the water table as measured on site the vertical total and effective stresses were estimated (σ_{vo} and σ'_{vo}).
- The ground is essentially flat so it was assumed that the static shear stress (τ_s) is zero and hence the static shear stress correction factor (K_α) is also zero.
- The soil was assumed to be normally consolidated and so the overconsolidation ratio (OCR) is unity and hence $\sigma'_{vo} = \sigma'_{vc}$
- The stress reduction factor r_d was assessed based on the graph of r_d vs. depth produced by Seed and Idriss (Seed & Idriss, 1971)

5.3. Yield acceleration calculations

By substituting in the values assessed above the formula for the CRR can be simplified as follows:

$$CRR = 0.80 \frac{S_u}{\sigma'_{vo}} MSF \quad (6)$$

And hence for cyclic softening to occur:

$$0.65 \frac{a_{max}}{g} \frac{\sigma_{vo}}{\sigma'_{vo}} r_d > 0.80 \frac{S_u}{\sigma'_{vo}} MSF \quad (7)$$

The assessed calculations found that the yield accelerations for the Darfield and Christchurch earthquakes were as follows:

Table 3. Calculated yield accelerations

Name	Moment Magnitude, Mw	Ave. PGA	Calculated Yield Acceleration (ay)
Darfield Earthquake	7.1	0.26g	0.28g
Christchurch Earthquake	6.2	0.34g	0.29g

Note that the vertical stresses were calculated at the base of the layer of the peat and organic clay; and difference between the two yield accelerations is caused by the variation in the magnitude scaling factor. All other parameters are the same.

5.4. Time history comparison

The initial results suggest that the yield acceleration would have been reached during the Christchurch Earthquake but not during the Darfield Earthquake. This matches the observed ground behaviour as minimal ground damage occurred after the Darfield Earthquake whereas significant ground damage occurred following the Christchurch Earthquake. To have a closer look at what occurred during each earthquake, a time history analysis was undertaken based on the shaking records from three nearest seismographs. Illustrative results of this analysis are shown below in Figure 2 and the full results are tabulated in Table 4.

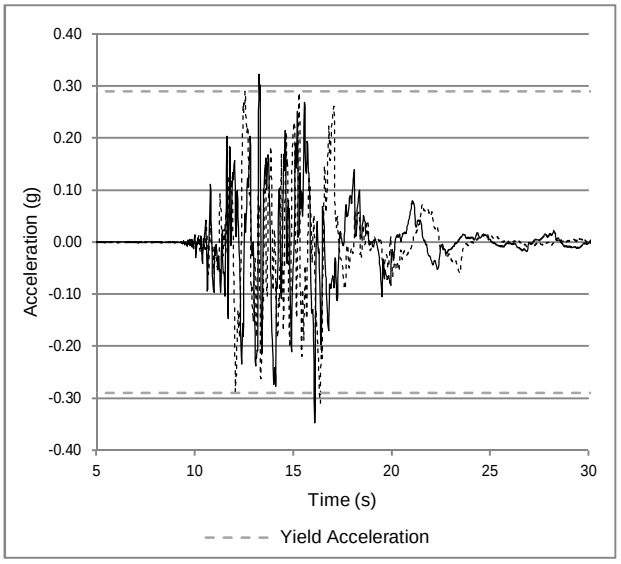

Figure 2. Christchurch Earthquake SHLC Accelerogram

The results show that the yield acceleration was never reached for the Darfield Earthquake and is likely to have been reached up to nine times during the Christchurch Earthquake. This indicates that the probability that cyclic softening occurred to a sufficient extent to cause ground damage is much more likely to have occurred following the Christchurch Earthquake. This matches the

observed ground damage and gives confidence as to the accuracy of the assessment.

Table 4. Frequency that yield acceleration is reached

Name	Location	Yield cycles in each direction(1)	
		X	Y
Darfield Earthquake	PPHS	0	0
	REHS	0	0
	SHLC	0	0
Christchurch Earthquake	PPHS	0	0
	REHS	4	5
	SHLC	1	2

(1) The number of times that a cycle of acceleration exceeded the yield acceleration for each earthquake.

5.5. Probability of reoccurrence

To predict the effect that future earthquake events would have on the Wendover Retirement Village land the analysis was re-run using predicted earthquake magnitudes and accelerations as recommended by the Ministry of Buisness, Innovation and Employment (MBIE, 2012, p. C2.2) for geotechnical design in Canterbury. The results are tabulated below:

Table 5. Design earthquake accelerations compared with yield accelerations

Design Earthquake Event	Magnitude	PGA	Calculated Yield Acceleration (ay)
Serviceability Limit State (SLS)	7.5	0.13g	0.27g
Ultimate Limit State (ULS)	7.5	0.35g	0.27g

The next step was to more accurately determine the probability that an earthquake would cause the levels of shaking that are predicted to trigger cyclic softening. To do this, the results of the GNS Science probabilistic assessment of liquefaction for Christchurch in the next 50 years (Gerstenberger et al., 2011) was referred to. This study gave estimates that various acceleration levels in Christchurch would be exceeded in seismic events in the next year, ten years and fifty years. By interpolating between the values given by GNS we were able to state that probabilities of cyclic softening reoccurring in the future. The GNS values along with the results that have been interpolated are shown in Table 6.

Note that these probabilities are based on magnitude weighted PGA and are based on earthquake likelihoods assessed in May 2011 and may need to be revised.

Table 6. Exceedance probabilities for liquefaction thresholds in Christchurch

Time-frame	GNS Results				ay
	>0.10g	>0.13g	>0.20g	>0.30g	>0.27g
0-1 years	46%	92%	60%	24%	34%
0-10 years	86%	70%	35%	12%	18%
0-50 years	98%	32%	14%	5%	7%

6. Discussion

This analysis was conducted in December 2011 and so some of the information used to assess the cyclic softening hazard at Wendover Retirement Village may be out of date. Notwithstanding this, the results of this analysis can be considered reasonably accurate – in a geotechnical sense – thanks to the density of seismographs in Christchurch City and the ongoing research being conducted in to the effects of the recent earthquake sequence.

The results predict whether or not cyclic softening will occur and lend support to the accuracy of the method of Idriss and Boulanger (Idriss & Boulanger, 2008). However, the analysis does not cover the magnitude of failure, which may be significantly more important when designing structures in soils where cyclic softening is considered a hazard.

7. Conclusion

The effects of the recent earthquake events on Christchurch have provided valuable insight into the behaviour of soils during earthquakes. The analysis of the cyclic softening that occurred at Wendover Retirement Village is an example of this. The high density of seismographs in Christchurch City, the huge amounts of data collected, and the ongoing research that is being conducted has allowed this analysis to be completed to a reasonably high degree of accuracy. The results lend support to the accuracy of the cyclic softening analysis methods proposed by Idriss and Boulanger (Idriss & Boulanger, 2008) and serve as a reminder to be aware of the potential for cyclic softening to cause ground damage in earthquake events.

8. Acknowledgements

I want to thank the following people for their help and assistance during this analysis and the publishing of this paper:

- Dominic Mahoney, Dr Jan Kupec, Ian McPherson and Alan Wightman – colleagues

whose advice greatly assisted me in conducting the analysis.
- Wendover Retirement Village – in particular Mr Charlie Hand – for permitting me to publish this paper.
- All the geotechnical engineers, geologists and support staff across New Zealand and overseas who have helped put together the huge amounts of research and information regarding the Canterbury Earthquakes.

9. References

Brown, L.J. & Weeber, J.H. (1992) *Geology of the Christchurch Urban Area*, Scale 1:25 000, Institute of Geological & Nuclear Sciences geological map 1.

Gerstenberger, M., Cubrinovski, M., McVerry, G., Stirling, M., Rhoades, D., Bradley, B., Brackley, H. (2011) *Probabilistic assessment of liquefaction potential for Christchurch in the next 50 years*, GNS Science Report 2011/15 30 p.

Idriss, I. M. & Boulanger, R. W. (2008) *Soil Liquefaction During Earthquakes.* Earthquake Engineering Research Institute Publication No. MNO-12

Kramer, S. L. (1996) *Geotechnical Earthquake Engineering*. Upper Saddle River, NJ: Prentice-Hall.

Ministry of Business Innovation and Employment (2012). *Repairing and rebuilding houses affected by the Canterbury earthquakes* Version 3, December 2012.

Seed, H. B. & Idriss, I. M. (1971) *Simplified procedure for evaluating soil liquefaction potential*, Journal of the Soil Mechanics and Foundations Division, ASCE, Vol. 107, No. SM9, pp. 1249-1274.

Sibley, K. (1989) *Waterways, Swamps and Vegetation Cover in 1856 Compiled from "Black Maps" approved by J Thomas and Thomas Cass, Chief Surveyors, (1856)*, Christchurch City Council Information Services, revised by Tibble, G. (1996)

Youd, T.L., Idriss, I. M., Andrus, R. D., Arango, I., Castro, G., Christian, J. T., Stokoe, K. H. II (2001) *Liquefaction resistance of soils: Summary report from the 1996 NCEER and 1998 NCEER/NSF workshop on evaluation of liquefaction resistance of soils*. Journal of geotechnical and geoenviromental engineering. Volume 127, Issue 10, pp. 817-833.

This page intentionally left blank

Proceedings of the 10th ANZ Young Geotechnical Professional's Conference – 10YGPC
Noosa, Queensland, Australia
10 – 12 September 2014

A CASE STUDY OF AN GROUND INVESTIGATION INTO A BUILDING COMPLEX DAMAGED DURING THE CANTERBURY EARTHQUAKE SEQUENCE, NZ

Frances NEESON
Opus International Consultants, Christchurch, New Zealand.

ABSTRACT – Following the Ms7.1 rupture of the Greendale Fault on 4th September 2010, the Christchurch area has experienced and continues to experience a sequence of aftershocks. The most destructive to date was Ms6.3 22nd February 2011 centred within 8km of Christchurch's CBD in which PGAs of up to 0.8g were experienced. This event caused structural damage and ground deformation of a building complex, located on the banks of the Avon River.

This paper describes the initial geotechnical inspection, investigations, resulting engineering geological model and the implementation of the model for remedial design and prevention of further lateral spreading induced structural damage at the building complex during subsequent seismic events.

A geotechnical assessment was undertaken to assess both general site stability and building stability issues. Ground deformation features that were observed included liquefaction, lateral spreading, tension cracking, voids and ground subsidence. Lateral spreading was most evident within the basement where the ramp structure showed 130mm of horizontal and 50mm of vertical displacement towards the river relative to the main basement structure. Up to 700mm of subsidence was visible between the building and the river, inducing tilting of the building. Liquefaction was most evident to the south and north of the complex, with up to 400mm thickness of ejected sand and silt observed. Site investigations included boreholes, piezometers, CPTs, ground penetrating radar and topographic survey.

1. Introduction

Christchurch is New Zealand's second largest city and is located on the east coast of New Zealand's South Island. The city is situated near the coast, on alluvial outwash plains and on the western flanks of the Lyttleton volcano of the Bank Peninsula volcanic complex. The South Island of New Zealand accommodates the Pacific and Australian tectonic plate boundary by a system of faults, most notably the Alpine Fault.

At 4:35am 4th September 2010 the Greendale Fault and at least two neighbouring blind faults ruptured inducing strong ground shaking felt across the South Island. This fault rupture has become known as the 'Darfield Earthquake' Ms7.1. The epicentre which was located 45km south of Christchurch's CBD; the earthquake had severe effects in Christchurch including widespread land damage such as liquefaction in addition to shaking induced damage and in some cases resulting in the collapse of unreinforced masonary buildings. Following this initial fault rupture there has been a well recorded aftershock sequence, an Ms6.3 aftershock of the Darfield Earthquake that occurred at 12:51pm 22nd February 2011 and located within 8km of the CBD has proved to be the most destructive event to date and has since become known as the 'Christchurch Earthquake'(Geonet, 2011).

The building complex is located within Christchurch's CBD and is bounded on one side by the Avon River. All buildings have shallow raft or basement foundations. During the February aftershock Peak Ground Accelerations (PGAs) of up to 0.8 g (vertical) and 0.7 g (horizontal) were recorded within the CBD (Geonet, 2011)

2. Initial Inspection Of The Building Complex

Opus was commissioned to conduct a rapid structural assessment of the building complex on the 24th February following the 22nd February aftershock. This structural assessment highlighted geotechnical issues which led to the initial geotechnical inspection of the 30th and 31st March 2011. The original structural assessment highlighted several areas where geotechnical inputs were required including the vehicle access ramp to the basement, separation of the annex link and general site instability.

2.1 Basement Ramp

Vehicle access to the complex basement is via a ramp which is orientated parallel to the Avon River and is offset by 20-30m. The western side wall of the ramp essentially acts as a retaining structure for another building within the complex and adjacent walkway and gradually increases in height from approximately 1m at the street frontage to 5m at the basement. Lateral spreading was most evident at the interface between the basement ramp structure and the basement which did not appear to have a structural connection.

Displacements of 150mm horizontal and 50mm vertical were evident where the two structures connect. Flooding of the basement occurred immediately following the February aftershock and this had been pumped dry during our initial inspection. The western wall of the ramp has an outer facing and concrete service box where the external wall has pulled away from the internal retaining wall and rotation was observed. This indicated 40mm of movement, which has accommodated some of the lateral movement expressed in the basement ramp below. No land damage distress at the adjacent building was observed during this initial inspection.

Lateral movement was also observed at ground level to the east of the ramp. Paving and steps to the basement level have moved laterally towards the Avon River, consistent with the ramp displacement. The river is approximately 25m east of the ramp wall and the basement floor level is approximately one metre above river bed level.

2.2 Annex

The Annex building structure links the ground floor of the Tower building to the second floor of the

building closest to the river all of which are underlain by the basement (refer to Figure 1). The Annex has paved areas to the north and south and the main entrance is to the south. Distress to the north eastern corner embayment was evident due to a column rotating slightly and leading to an approximately 20mm gap visible between structures. Cracks were noted in the basement beams and partition walls however, no structural connection between the ground floor/ second floor rotating column and the basement column was apparent. The external courtyard north of the Annex exhibited settlement of approximately 150mm and some surface expression of liquefaction was observed. During the inspection it was concluded that there does not appear to be an underlying geotechnical reason for the column rotation.

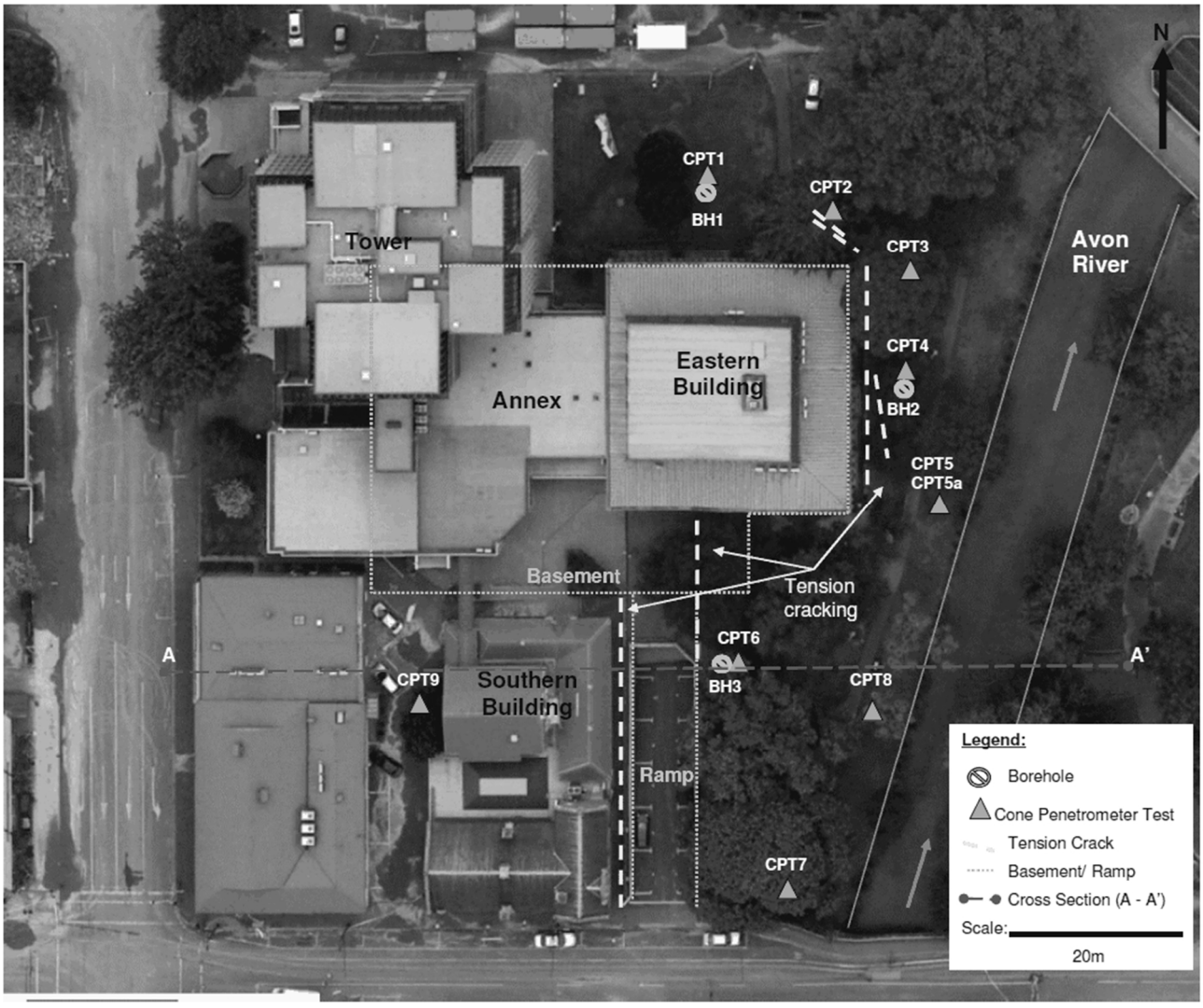

Figure 1. Site Location Plan

2.3 Observed Ground Damage and Geological Mapping

The initial geotechnical inspection included a general visual inspection of the complex; liquefaction and lateral spreading were observed in localised reas. Surface expression of liquefaction consisted of ejected sand and silt; liquefaction deposits were most prevalent in the north west corner of the site adjacent to the Tower. No obvious ground deformation induced distress appeared to affect the Tower building, however displacement and distortion of the steps and main access way indicates settlement or densification of soils or fill adjacent to the building.

Liquefaction was also evident between two of the stand-alone buildings in the southern extent of the complex, where ejected sand was being cleared away during the initial inspection. Paving stones showed visible distortion due to ejection of sand and silt. No distress to the foundations of these stand-alone buildings was observed during this initial inspection in March. However, a large void became obvious in October 2011 near the northern entrance of one building adjacent to the perimeter foundation which caused some concern. The void appeared to be a conduit or vent for ejected liquefaction deposits and is set back approximately 40m from the river. No evidence of liquefaction had been observed at this location during the initial inspection. However, it is located close to the external wall facing the basement retaining wall which exhibited signs of rotation and deformation consistent with the lateral spreading observed in the basement.

Lateral spreading and subsidence was also clearly evident adjacent to and east of the building nearest the river (eastern building). Tension cracking and slumping was exhibited in front of the retaining wall east of this building. Slumping of up to 0.7m was observed in front of the 1.2m high wall, but the slump toe was not evident. Tension cracking sub-parallel in front of the retaining wall persisted along the length of the wall. Hard landscaping features such as the retaining wall had pulled apart at the southern end and the footpath showed distortion. Lateral spreading was clearly evident east of the eastern building, as illustrated by the slumping, tension cracking and distortion to landscape structures, without surface expression of liquefaction.

2.4 Outcomes Of The Initial Inspection

Short-term remedial measures proposed included removal of liquefaction deposits and reinstatement of entrance steps. The complex was within the restricted CBD cordon therefore public access and immediate re-occupation of the complex was not possible.

3. Geological Setting and Site investigations

3.1 Geological Setting

Christchurch is situated on Holocene sedimentary deposits and on the slopes of Miocene aged volcanic rock (Brown & Weeber, 1992). The geological setting of Christchurch is comprised of swamp deposits behind beach dune sand; estuaries and lagoons; gravel, sand and silt derived from river channel and overbank flood deposits of the Waimakariri River floodplain.

The geology of the building complex site is mapped (Brown & Weeber, 1992) as Yaldhurst Member of the Springston Formation and is described as alluvial sand and silt overbank deposits. A river terrace is also identified by Brown & Weeber (1992) within the complex. In addition to the mapped Springston formation, localised fill was identified during the site investigation and Christchurch Formation was identified at depth across the site.

The Avon and Heathcote rivers originate from springs west of Christchurch and meander through the city to form the main drainage system. The Avon river meanders from west of Christchurch, through the CBD and eastern suburbs to the Avon Heathcote Estuary at the coast. The building complex is bounded to the east by the Avon River. Cubrinovski, and McCahon (2011) have produced a map overlaying river profiles from 1850 which shows a channel parallel to the main channel running through the site.

3.2 Site Investigations

Subsurface site investigations were undertaken to assess the ground conditions with particular emphasis on the building closest to the river and the wider stability of the complex site. Geophysical survey method Ground Penetrating Radar (GPR) was utilised near the southern building. A topographical survey was conducted to provide levels and displacements within the buildings and to provide a level survey across the site. Areas where slumping had been observed in March 2011 had been landscaped (filled) prior to the level survey and geotechnical site investigation.

3.2.1 Drilling Investigations

Three boreholes were conducted using Direct Push methods with standard penetration tests (SPTs) at 1.5m intervals to depths of 12-17m. Boreholes were intended to reach Riccarton Gravel formation, however this formation proved to be beyond the depth achievable using the Direct Push rig. Riccarton Gravel formation is inferred from boreholes at the neighbouring sites. Single standpipe piezometers were installed in all boreholes, upon completion of drilling and groundwater levels range from 2.2m to 4.6m below

ground level. Nine Cone Penetration Tests (CPTs) were conducted across the site to effective refusal.

Laboratory testing consisting of particle size distribution (PSD) analysis and plasticity indexes (PI) were conducted on eight samples recovered from the machine drilled boreholes.

3.2.2 Geophysical Survey – Ground Penetrating Radar (GPR)

A GPR survey was commissioned in October 2011 following the subsequent development of a void adjacent to the southern building. The survey was conducted in the area surrounding the southern building including the paved area between buildings and throughout the ground floor of the southern building. A total of 38 GPR survey lines were conducted to investigate the presence of voids. This survey picked up several anomalies across the area surveyed, some of which were suspected underground services, but also highlighted possible voids. A significant area beneath the paving between the buildings was identified as likely to contain sub-surface voids. This area was not deemed to adversely affect any of the neighbouring structures and therefore if these voids present a surface expression at a later date a backfill approach is likely to be employed to reinstate the ground.

3.2.3 Topographical Survey

A topographical survey was conducted across the site and level survey was conducted within the ground floor building level. This survey showed significant tilting towards the river of 100mm over 25m of the eastern building closest to the river. The survey also identified differential settlement of the basement floor slab with tilting of up to 6mm recorded towards the Avon River (east) and tilting of 118mm of the western section of the basement towards the west. The river terrace slope along the river varies from approximately 2m high east of the eastern building to 4m high north and south of the building with slopes typical of 1:7.

4. Developing the Geological Model

The geological model of the site was developed using the inspection observations, site investigation results and additional geotechnical information gained from a desktop review including published information from nearby sites. From this information the following geological formations and sub-units were identified to form the basis of the geological model presented in Table 1.

Piezometers installed in boreholes show an influence from the Avon River. The Basement level of the complex is approximately level with the Avon River. Groundwater incursion into the basement complex occurred on February 22nd and following snow melt in winter 2011.

Table 1. Geological Model

Geological Unit	Depth m	Sub-Unit (thickness m)	Description	N	N' corrected	Qc (MPa)	Liquefaction (settlement)	
							SLS	ULS
Fill	0.0 - 1.5	Silt and Gravel (0.0 – 1.5)	Soft to loose	0 - 2	0 - 3	-	-	-
Springston Formation	0.0 – 12.5	Silt (0.5 – 2.6)	Soft to firm	0 - 2	0 - 3	0 - 6	-	-
		Silty Sand and Sand (1.5 – 4.0)	Loose to medium dense	2 - 24	3 - 34	1 - 30	4.5 - 6m (2cm)	1.5-6.5m (8.5cm)
		Gravelly Sand and Sand (5.8 – 7.3)	Medium dense to dense	5 – 60+	7 - 85+	10 – 43	-	9 – 12.5m (5cm)
Christchurch Formation	12.5 - 21.0*	Sands and silty sands (2.5 - 4.5+)	Medium dense to very dense	48-60+	68 – 85+	2 - 32	-	-
		Silt and clay (0.0 – 0.5m)	Stiff	-	-	-	-	-
Riccarton Gravel	21.0+*	Sandy Gravel* (7.1m – 20+*)	Medium dense to very dense*	34 – 50+*	-	-	-	-

(* = inferred)

5. Geotechnical Assessment

Liquefaction modelling has been conducted to reflect Serviceability Limit State (SLS) M7.5 (0.13g) and ultimate limit (ULS) states using CPT results. It is likely that further liquefaction will occur in future seismic events. The main liquefiable layer has been identified as the upper 6m consisting of mainly fine sand with only the material below the groundwater table susceptible. Modelling showed additional liquefaction was possible between 9 to 14m depth under higher PGA. The contractor provided an energy calibration report for the Safety Auto SPT equipment. The SPT values were correlated for energy efficiency (N') and compared to raw SPT and CPT derived N60 values. A reasonable correlation is evident between CPT and SPT derived results at a shallow depth however, they are significantly different at greater depths. One of these comparisons are shown in Figure 3 below

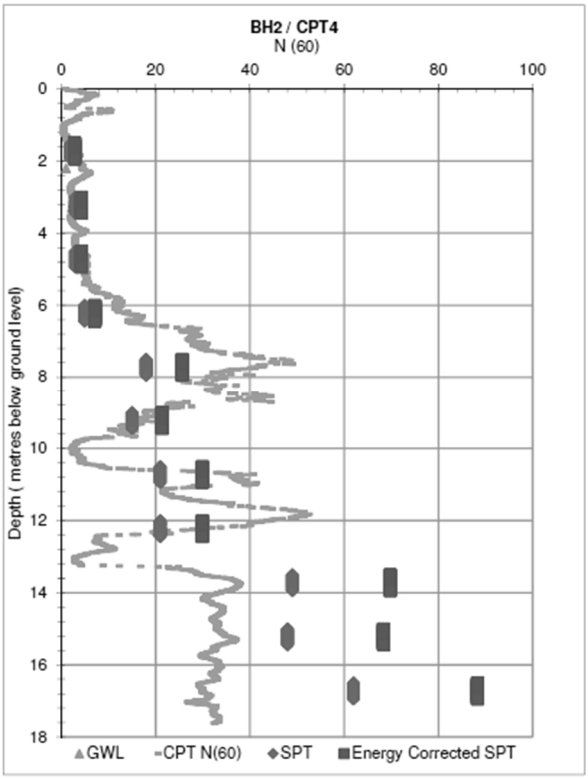

Figure 2. Comparison of CPT v SPT

The comparison of CPT and SPT data would suggest that neither CPT nor SPT data should be used in isolation when considering liquefaction potential at depth

Liquefaction induced settlements do not account for the observed slope induced movement towards the Avon on the east side of the complex where subsidence due to lateral spreading movement has occurred. Under ULS conditions lateral spreading has been calculated to be up to 0.2m in open ground and up to 0.005m for basement buildings. When back analysing the 22nd February event, two methods of lateral spreading analysis were employed; Youd et al (2002) and Zhang (2004). Predicted lateral movement from Youd et al was approximately 2 times higher than the observed movement in the February event, while Zang et al was even higher. No on-going ground deformation has been observed at the complex and damage due to the February seismic event has not appeared to worsen. Any movement towards the river appears to be seismically induced and progressive movement has not been observed. From these observations it also appears tilting of the building closest to the river is not ongoing. Analysis of future seismic events, such as an Alpine Fault event suggest liquefaction and lateral spreading will again occur at the site and tilting of the building is expected to continue towards the river. The Tower building is expected to have the least amount of settlement in future seismic events, due to its relatively deep foundations and set-back from the Avon River. The southern buildings are each separate structures with shallow foundations that appear to have performed well during the previous seismic events. The basement ramp however, acts as a retaining wall between the southern building and the Avon River and the ramp may have protected this building from some impacts of lateral spreading. Without remediation future earthquakes may result in increased lateral spreading effects on the ramp structure therefore, reducing its protection of the southern building and possibly having a detrimental effect on the foundations of this building.

6. Remedial Options

It is expected further tilting will occur during further seismic events of similar or greater magnitude. One proposed remedial solution is a piled retaining wall east of the eastern building and along the length of the river frontage to retain the slope during further seismic events. The design of this wall has been modelled by others in Plaxis. An alternative solution could consist of stone column ground densification/improvement however, due to site constraints this solution is currently not favoured. Current issues arising from the proposed remedial solution are interruption of the groundwater regime, protected trees and possible archaeological significance of the site.

7. Conclusions

PGAs of up to 0.8g were recorded within Christchurch's CBD during the Ms6.3 February 22nd 2011 aftershock. Evidence of liquefaction and lateral spreading was observed at the building complex site as tension cracking; voids; ejected sand and silt; and ground subsidence. Lateral spreading was clearly exhibited at the connection between basement and basement ramp and along the eastern river frontage. Sub-surface voids were

not observed until several months after the February event however, they are now known to be present within the complex. Voids have not undermined any foundations to date and while they currently appear to be concentrated near the southern building, further voids may become more evident in time and they are likely to be located where material was ejected as a result of liquefaction.

Liquefaction and lateral spreading has caused tilting of the eastern building and to a lesser extent the basement. The initial observations, geological mapping and development of the geological model aid in the best interpretation and computational analysis methods when conducting the geotechnical appraisal of the building complex site. Back analysis of the February event and comparison to on site observations allowed the 'best fit' analytical methods to be employed when assessing and designing remedial options for the building complex. Comparisons drawn between CPT and SPT data indicate that the liquefaction potential model requires further refinement at depth at this site.

8. Acknowledgements

I wish to acknowledge the support NZGS and EQC for the award to support my attendance to present this paper I also wish to thank Bing Ni, Glyn East, those people I worked with during the duration of the project and my colleagues especially Greg Saul, Glyn and Aaron George for their constructive reviews. In addition I would like to thank Opus for their support in the preparation of this paper and towards my attendance at this conference.

9. References

Brown, L & Weeber, J (1992) Geology of the Christchurch urban area. Scale 1:25,000. Institute of Geological & Nuclear Sciences geological map 1. 1 sheet + 104p Institute of Geological and Nuclear Sciences Limited, Lower Hutt, New Zealand.

Cubrinovski, M and McCahon, I (2011) Foundations on Deep Alluvial Soils. Technical Report Prepared for the Canterbury Earthquakes Royal Commission. University of Canterbury. 1-34

Geonet (accessed 2011, 2012, 2014) http://www.geonet.org.nz/ http://info.geonet.org.nz/display/home/Canterbury+Quakes

Youd, T.L, Hansen, C.M, and Barlett, S.F. (2002). Revised Multilinear Regression Equations for Prediction of Lateral Spread Displacement. J. Geotech. and Geoenvir. Engrg, Vol. 128, No. 12, 1007-1017.

Zhang, G, Robertson, P.K. and Bravhman, R.W.I. (2004). Estimating Liquefaction-Induced Lateral Displacements Using the Standard Penetration Test or Cone Penetration Test. J. Geotech. and Geoenvir. Engrg, Vol. 130, No. 8, 861-871.

A NEW METHOD OF PREDICTING INSTABILITY OF EMBANKMENTS ON SOFT GROUND FROM MONITORING DATA

Dominic TRANI[1] and Patrick WONG[2]
[1] *Senior Geotechnical Engineer, Coffey Geotechnics Pty Ltd, Wollongong, Australia*
[2] *Senior Consultant, Coffey Geotechnics Pty Ltd, Chatswood, Australia*

ABSTRACT – This paper tackles the challenge to predict impending failure of embankments on soft ground based on routine monitoring data as a way of controlling the rate of embankment construction to avoid failures. A literature study has been carried out on available methods of predicting embankment performance. The Authors then propose a method of plotting the inverse of incremental lateral displacement rate at the embankment toe against embankment height. Based on a case study, the Authors propose that an iterative prediction procedure be adopted as the embankment height increases and more data points become available. A projected limit of 0.05 days/mm or 50 days/metre (i.e. incremental lateral displacement rate of 20 mm/day following an embankment lift) be used as a guide to forecast the impending failure height, together with limiting the height of construction to between 80% to 90% of the predicted failure height at any time to control the rate of embankment construction to reduce the risk of embankment failure.

1. Introduction

Adequate instrumentation and monitoring of embankments constructed on soft ground are required for the purpose of validating predicted magnitude and rate of settlement when preloading is complete or when surcharge may be removed. It is also considered important that a good method of predicting embankment failure is available in order to either control construction or to impose appropriate immediate countermeasures to failure if necessary. When using monitoring data to assess embankment stability, there are many uncertainties and the ability to predict embankment performance (e.g., incremental excess pore pressure, lateral displacement) is not reliable. These quantities are in fact rarely predicted, and most engineers rely mainly on published literature for guidance on what the monitoring results indicate about embankment stability.

This paper provides an overview of existing methods of predicting embankment instability. A method is then proposed which will require additional testing of well instrumented and monitored case study, together with interim recommendations.

2. Review of Existing Methods

2.1. General

Embankments on soft ground are usually instrumented to provide data on pore pressures in the soft soil layer, vertical and lateral deformation. An idealised instrumentation for embankments constructed on soft ground is illustrated in Figure 1

Settlement plates, extensometers and piezometers beneath the centreline of the embankment and horizontal profile gauges installed across the width of the embankment are mainly used for monitoring the magnitude and rate of settlement beneath the embankment over time. However, these settlement plates and piezometers, together with survey monuments located at and beyond the toe of the embankment, piezometers and inclinometers located near the toe of the embankment, are also useful for the assessment of embankment stability.

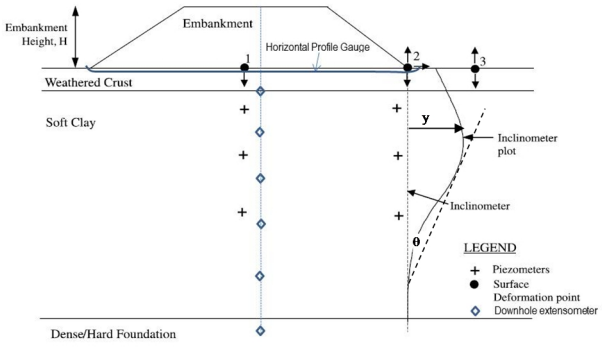

Figure 1. Idealised section of embankment indicating the types of monitored observations (modified from Hunter and Fell (2003)).

The following measured quantities have been reported to be useful in assessing the on-set of embankment failure:

- *Embankment height (H)* – it is typical to record embankment height every time survey readings are carried out.
- *Settlement at embankment centreline (s)* – settlement will occur due to consolidation of the soft soil. Linearly increasing or divergent rate of settlement is likely to be an indicator of impending failure. Based on the Authors' experience,

however, if this phenomenon is captured at all, it is often already too late.

- *Excess pore pressure* (Δu) – Tavenas & Leroueil (1980) proposed to use the excess pore pressure response of soft clays under applied undrained stress. When the soil is stressed less than its pre-consolidation pressure, the ratio $\Delta u/\Delta\sigma_v$ is less than 1. When the soil is stressed past its pre-consolidation pressure (i.e., OCR = 1), $\Delta u/\Delta\sigma_v$ should theoretically be equal to 1. Due to consolidation effects during actual construction, the incremental ratio $\Delta u/\Delta\sigma_v$ needs to be carefully measured at each increment of loading.
- *Lateral displacements at embankment toe (y)* – although the relationship between stability and lateral displacements at the embankment toe depends primarily on the soil condition, geometry of the embankment and construction sequence, an observed rate of lateral displacement is relevant to the occurrence of embankment failure.
- *Surface Cracking* – the development of longitudinal cracks at the embankment top that typically run parallel to the axis of the embankment are a common indication that embankment rupture is occurring. Embankment failure may be imminent depending on the width of the cracks and whether there are vertical displacements across the cracks.
- *Toe Heave* – toe heave is rarely obvious to the naked eyes until collapse of the embankment actually occurs. Hunter & Fell (2003) considered that monitoring of toe heave at an appropriate distance from the embankment toe may provide useful information on impending embankment instability.
- *Angular Distortion* (θ) – this measurement is inferred from measured lateral displacements from installed inclinometers at the embankment toe. The angular distortion is measured from a reference point which is likely to be the top of the dense or stiff material underlying the soft clay layer, or where the lateral displacement is zero.

2.2. An Overview of Existing Methods

The performance of embankment constructed on soft ground is not easy to predict from a single set of observed parameters, and is complicated by the nature of the soft soil, embankment geometry and rate of construction, process of consolidation and strength gain of the soft soil. The control of embankment construction to avoid failures had been attempted by various researchers and an overview is discussed below.

The use of soil deformation measurements to predict impending embankment failure had been identified by Johnston (1973) proposing a comparison between the displaced vertical volume (V_v) with the displaced horizontal volume (V_h).

To minimise the uncertainties stemming from estimating volumes of deformed soil, Tominaga & Hashimoto (1974) instead used the measured values of s and y. As presented by Todo et al (1996), Tominaga's method, which looks into the sudden change in the gradient of the s vs y plot, struggles to predict sudden embankment failures. This method had been refined by Tavenas & Lerouiel (1980) with a cautious approach of using the lower bound ratio of $\Delta y_{max}/\Delta s_{max}$ = 0.7 as a trigger level for review during loading above the pre-consolidation pressure in assessing embankment performance. The Authors have used this approach on a number of embankment projects with reasonably acceptable outcome. In the Gateway Upgrade Project (Brisbane, Queensland), a $\Delta y_{max}/\Delta s_{max}$ of 1.2 was reached for one particular section with no visually observed embankment distress.

A variation to the above method is to plot s_{max} vs $\Delta y_{max}/\Delta s_{max}$ against a set of failure criteria curves developed by Matsuo & Kawamura (1977). The Authors caution the use of this method as integrating factors of safety and settlement magnitudes may be unique only to the studied test sites and therefore not applicable to other sites.

Considering the element of time, Kurihara & Ichimoto (1977) suggested that rates of lateral displacement of 20 mm/day to 30 mm/day are relevant to the occurrence of minor cracks. Sudden changes, however, are difficult to capture and do occur without any warning of failure.

In 1979, researchers began to consider the applied load either in the form of embankment height or equivalent applied embankment stress. Sekiguchi & Shibata (1979) introduced the concept of load-deformation modulus ($\Delta\sigma_v/\Delta y$) and suggested to plot $\Delta\sigma_v/\Delta y$ vs $\Delta\sigma_v$ with embankment slope instability indicator proposed at $\Delta\sigma_v/\Delta y$ = 0. Todo et al (1996) showed this method to be difficult to implement and inconsistent on four different trial embankments.

In the event of embankment failure, Tavenas & Leroueil (1980) suggested the use of the excess pore pressure (Δu) increase developing at and near the slip plane. This is further refined by Leroueil & Rowe (2000) suggesting that localised failure is indicated when $\Delta u/\Delta\sigma_v$ exceeds 1 under the centre of the embankment. However, whether such increase would be captured would depend very much on the location of the installed piezometers relative to the potential slip plane which cannot be predicted with high accuracy. Wong & Petropulos (2013) showed a case study of an embankment failure where the ratio $\Delta u/\Delta\sigma_v$ exceeded 1 only at the time of, or shortly after failure.

The use of lateral deformation monitoring to predict impending embankment failure is relatively more commonly studied. Coutinho & Bello (2011) provided a summary of available methods for this purpose and illustrated the use of horizontal displacement methods via several case studies including the Juturnaiba trial embankment in Brazil reported by Cavalcante et al (2004). Coutinho & Bello (2011) presented different methods with the objective of evaluating the possibility of creep

rupture over time, where divergent behaviour in the evolution of displacements over time would indicate embankment instability, while a convergent behaviour would indicate consolidation and stabilisation. Due to the encountered limitations and many variables involved in the evaluation process, Coutinho & Bello (2011) recommended that more than one method should be used to obtain more confidence in decisions, and that all behaviour be analysed, not just the measured values.

2.3. Prediction of Time to Failure of Landslides

On Authors' experience, the observation of the rate of lateral displacement warrant further consideration. This is not to say that we should not continue to use other observed parameters such as increase in excess pore pressure, observation of surface cracking and toe heave to assess impending embankment failure.

Fukuzono (1985) presented a mathematical expression to estimate the time to collapse of a soil mass under laboratory controlled conditions simulating a rain fall. The empirical equation describes the relationship between inverse rate of slope creep movement under constant stress condition over time (t) and the eventual time to creep rupture (t_f).

When the inverse rate is plotted on the vertical axis against time on the horizontal axis as shown in Figure 2, it can be seen that collapse failure becomes imminent as the value of the inverse rate approaches the horizontal axis (i.e., infinite rate condition). As shown in the equation in Figure 2, different values of the equation constants define different shapes of the inverse rate versus time.

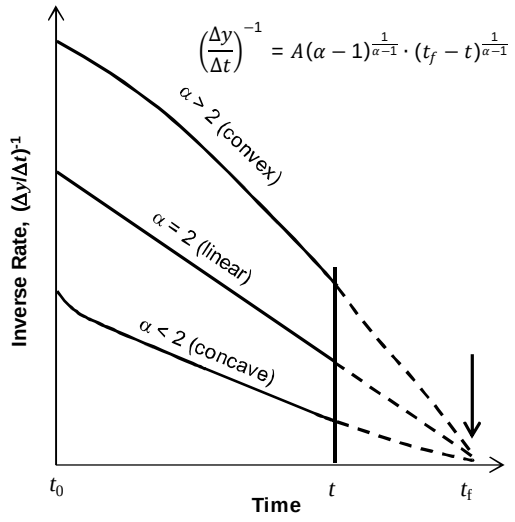

Figure 2. Relation of inverse rate and time to failure of slopes at constant stress (Fukuzono, 1985).

This method has been used extensively by mining engineers to monitor and manage the safety risk of open pit mines, using generally a linear line of best fit which is progressively updated with time records.

In road embankment construction, the total stress state increases at each increase in embankment height, and only reaches a constant state at the completion of construction. As excess pore pressures dissipate following embankment construction, the effective stress and shear strength of the soft foundation soil increases and the embankment becomes more stable. In rate sensitive soils, however, this may not be the case, and the above method may be useful in assessing the embankment stability following construction. The inverse rate concept may also be useful for assessing the embankment stability constructed on soft ground during construction, while taking into account the increase in applied stress.

3. Hypothesis and Proposed Method

3.1. General Hypothesis

For instrumented embankments constructed on soft ground, it is usual practice to plot embankment height and the maximum lateral displacement at the toe of the embankment (as measured by inclinometer) over time. An example of this from the Ballina Bypass Alliance Project, at the western approach to the bridge at Emigrant Creek South, is shown in Figure 3.

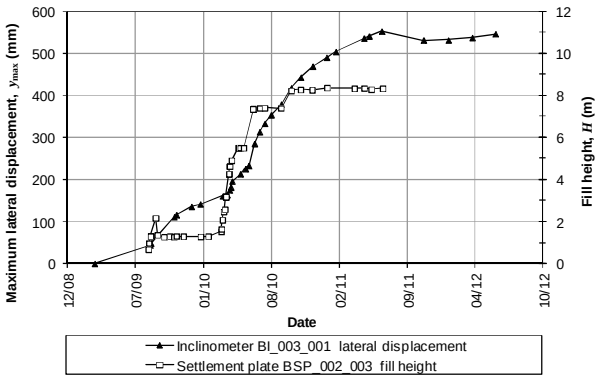

Figure 3. Example plot of embankment height and maximum horizontal displacement at the western approach to the bridge at Emigrant Creek South.

As indicated in Figure 3, the embankment is constructed in multiple stages until the final maximum height (H_{max}) is achieved. Both at intermediate stages and following completion of embankment construction for this example, the rate of increase in lateral displacement converges over time as the soft soil consolidates. It can also be seen that following each intermediate stage rest period, the lateral displacement rate increases again when the next lift is placed. The following observations, similar to those observed in Figure 3 have also been made by the Authors in many other instrumented embankments:

1. During staged embankment construction, the rate of lateral displacement increase immediately following each embankment lift is an important indicator of embankment stability.
2. Following embankment construction, the rate of lateral displacement should decrease over time. Rate sensitive rupture or creep rupture may occur with time if on-going linear increase or divergent behaviour is observed.

A hypothesis is therefore formed by the Authors that the "failure height" may be predicted from the instrumented data by plotting the inverse rate immediately after each embankment lift during construction using the principle described by Fukozono (1985). However, instead of plotting $(\Delta y/\Delta t)^{-1}$ against time, the embankment height (H) will be used in the horizontal axis, so that the vertical and horizontal axes are defined as follows:

- Vertical axis: $(\Delta y/\Delta t)^{-1}$ at $(H_i - H_{i-1})$
- Horizontal axis: embankment height at ith lift (H_i)

An iterative procedure will be required with the failure height updated as more data become available, and as the beneficial effect of any waiting time, consolidation and strength gain of the soft clay takes effect, giving rise to a potential increase in the failure height.

In order to test the above hypothesis, data from a case study have been utilised in this method as described below.

3.2. Case Study – Ballina Bypass Alliance – North Sandy Flat, Fill 5A Embankment

On the Ballina Bypass Alliance project, a stretch along the proposed road alignment located at North Sandy Flat was proposed to have an embankment of average design thickness of 4.6 m. At this particular stretch of the highway, the subsurface profile was assessed to comprise 1 m topsoil underlain by a very soft to soft alluvial clay layer which increases in thickness from zero at the base of hill, to up to approximately 10 m towards a swamp away from the toe of the side fill embankment.

Surcharging with wick drains was the nominated treatment method with a maximum surcharge thickness of up to 7.1 m was adopted to limit post construction settlement. Embankment construction started on the third week of November 2008 with wick drains installed a month earlier. On 20 April 2009, about 150 days since the start of construction, cracking of the embankment was observed the day after an embankment thickness of 5 m was achieved (Figure 4(a)).

As shown in Figure 4(a), limited data was available prior to H_i = 3 m. Also, since the interest of discussion is to verify the viability of the above hypothesis, data points post embankment cracking was also removed in Figure 4(b). Figure 4(b) demonstrates two possible trend lines wherein a lighter broken line represents a sign of imminent failure after reaching an embankment height of 4.4 m. At this embankment lift stage, the rate of lateral movement was just above 8 mm/day and no embankment cracking was observed. A second trend line represented by a darker broken line links the data points up to when embankment cracking was actually observed when the embankment height of 5 m was reached.

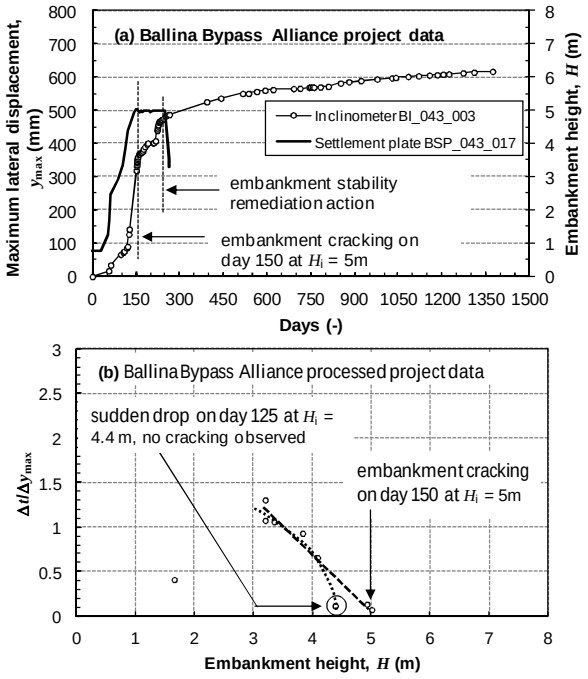

Figure 4. (a) Ballina Bypass Alliance project data at an embankment in North Sandy Flat, and (b) inverse rate approaching the horizontal axis at embankment imminent failure with embankment heights of 4.4 m (lighter broken line) and 5 m (darker broken line).

3.3 Discussion of Results and Proposed Method

In the case study presented, it would appear that plotting the inverse rate of lateral displacement against embankment height, and adopting a linear extrapolation technique could provide a conservative prediction of failure height at the early stages of construction. As the embankment height increases over time, consolidation and strength gain starts to take place. This causes an increase in the failure height and therefore a concave plot is expected as more data points become available. The case study, however, showed either a convex or linear fit without improvement. This is considered to be due to the geometry of the side fill with increasing soft clay thickness towards and away from the toe of the embankment. This case with accelerating lateral displacement resembles more like that of a natural landslide. Embankments constructed rapidly to failure without sufficient time for consolidation or strength gain may also exhibit concave or linear plots using this procedure. In any

case, it would appear that an iterative prediction procedure with the plots and prediction updated as more data are gathered with increasing embankment height could provide a reasonable control on embankment construction rate to avoid instability.

On the basis of the above case study proving the viability of the proposed hypothesis, the following method to predict the embankment height that would cause slope instability to embankments built on soft to very soft clay foundation is proposed.

1. To capture accurately and consistently the rate of lateral displacement with increasing embankment height, it is important that lateral displacement readings be taken as soon as practicable after each embankment lift, and at the same time lag each time.

2. Plot $(\Delta y/\Delta t)^{-1}$ at each lift against H_i and use a linear extrapolation technique to find H_f. It should be noted that when the embankment loading reaches beyond the pre-consolidation pressure of the foundation soil, a dive in the plot towards the horizontal axis of embankment height may result, and may lead to an under-estimate of the failure height. Care, however, should be exercised if flattening of the plot does not occur, which may signal other failure mechanisms such as brittle failure, rate sensitive soils, strain softening effects or non-uniform foundation failure conditions such as that observed for the case study above.

3. Continue construction if $H_i < 0.8H_f$. Hold and allow the foundation to consolidate if $(\Delta y/\Delta t)^{-1}$ is equal to or less than 0.05 day/mm until it reaches above 0.05 day/mm. The implied movement rate of ≥ 20 mm/day is consistent with the findings of Kurihara & Ichimoto (1977).

4. If attained lift $H_i \geq 0.9H_f$ and if $(\Delta y/\Delta t)^{-1}$ is ≤ 0.05 day/mm, hold construction and allow foundation to consolidate until $(\Delta y/\Delta t)^{-1}$ reaches above 0.05 day/mm.

5. If H_i is in between the limits stipulated in steps 3 and 4, review and allow construction if $(\Delta y/\Delta t)^{-1} > 0.05$ day/mm. If $(\Delta y/\Delta t)^{-1} < 0.05$ day/mm, hold construction and allow foundation to consolidate until $(\Delta y/\Delta t)^{-1}$ reaches above 0.05 day/mm.

6. In all steps above, review other tell-tales of possible embankment failure from other instrumentation and monitoring data, including daily visual observations.

Instrumentation data from a trial embankment TE2 (Magnani et al, 2009) is used to demonstrate the above procedure. As shown in Figure 5(a), a series of inclinometer readings taken after completing the 6th lift (H_i = 2.4m) indicate an increasing trend of $(\Delta y/\Delta t)^{-1}$. Based on the data, many possible extrapolation lines could be made and only two extrapolation lines are shown representing two possible estimates of H_f. At this stage where $(\Delta y/\Delta t)^{-1}$ is significantly above the proposed threshold of 0.05 day/mm, it is likely that extrapolation plots may under-estimate the predicted values of H_f.

Figure 5(b) represents the next iteration updating the previous iteration with the inclinometer reading taken 2 days after the lift was completed. This iteration shows a dramatic drop of $(\Delta y/\Delta t)^{-1}$ to 0.12 day/mm and the predicted H_f is estimated to be 2.8m implying that $H_i > 0.9\ H_f$. As such, Step 5 could be adhered and the ratio $(\Delta y/\Delta t)^{-1}$ should be kept above 0.05 day/mm.

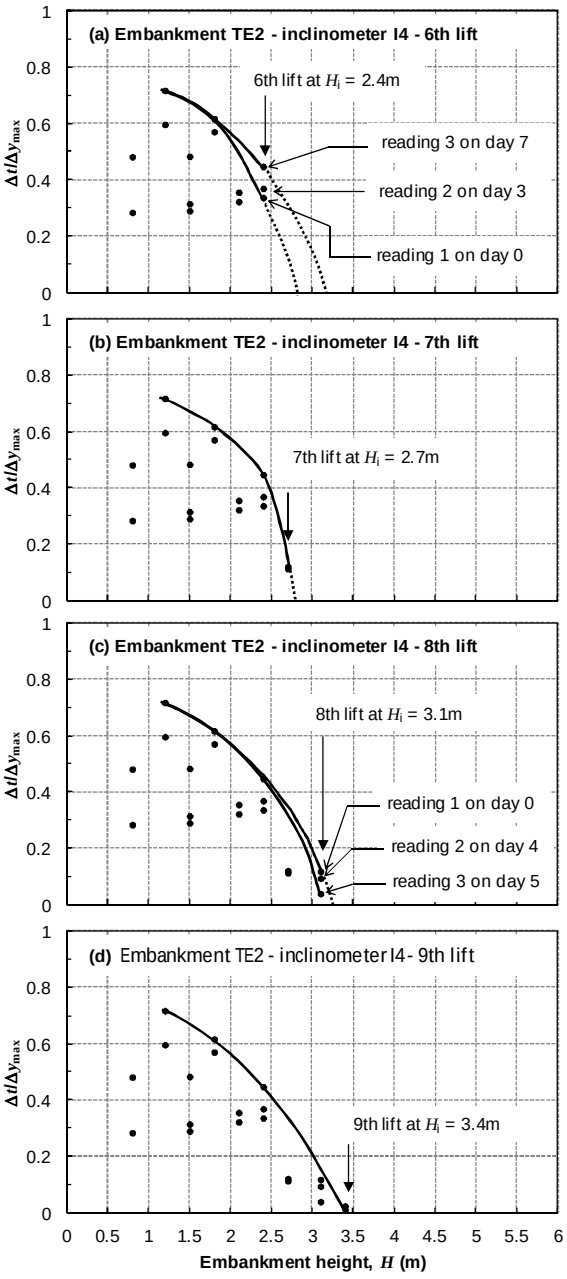

Figure 5. Iterations made to assess instability of the trial embankment TE2 (a) after completing lift 6, (b) after completing lift 7, (c) after completing lift 8, and (d) at failure after completing lift 9.

Figure 5(c) shows an updated data set with the series of inclinometer readings taken after the embankment was raised to H_i = 3.1m. The first

inclinometer reading taken right after fill placement is completed, which results in a $(\Delta y/\Delta t)^{-1}$ value close to 0.12 day/mm, is perhaps an indication of a delayed reaction in terms of lateral displacement of the underlying soft soil. The second inclinometer reading taken 4 days later shows a drop of $(\Delta y/\Delta t)^{-1}$ to 0.09 day/mm. The third inclinometer reading, which shows further drop of $(\Delta y/\Delta t)^{-1}$ to 0.04 day/mm, indicates that embankment instability may occur should raising the embankment be carried on. At this stage, Step 4 should be implemented in order to avoid embankment instability. Had the embankment construction been held and allowed the foundation to consolidate until $(\Delta y/\Delta t)^{-1}$ reaches above 0.05 day/mm, the resulting H_f could have been greater than the 3.2-3.3m estimated at the present stage.

The embankment was further raised to H_i = 3.4m and the subsequently inclinometer reading taken on the same day shows a calculated $(\Delta y/\Delta t)^{-1}$ dropping to 0.025 day/mm (Figure 5(d)). The next day when embankment cracking was already observed, a new inclinometer reading indicates a further drop of $(\Delta y/\Delta t)^{-1}$ to 0.01 day/mm.

4. Conclusion

Since 1970s, a number of methods of predicting impending failure of embankments on soft ground have been proposed and an overview is presented in this paper.

On the basis of a case study used to show the viability of presented hypothesis, a method to predict the embankment height that would cause slope instability to embankments built on soft to very soft clay foundation is presented. At each embankment construction lift, the proposed method requires plotting the inverse of incremental rate of lateral displacement measured at the embankment toe against embankment height. The plotted data points can then be linearly extrapolated until crossing the horizontal axis representing the possible maximum embankment height to cause failure. It is proposed that a projected limit of 0.05 day/mm or 50 days/metre (i.e., incremental lateral displacement rate of 20 mm/day following an embankment lift) be used as a guide to forecast the impending failure height and to hold construction and allow foundation to consolidate until the inverse rate significantly improved to 50 days/metre. An iterative procedure of prediction as the embankment height increases over time and more data points become available, with embankment construction hold points between 80% to 90% of the predicted failure height at any time, depending on the rate of movement and other observations.

This method has been tested only on limited examples, and needs to be further tested on more cases. This method should not be regarded as suitable in all circumstances. In rate sensitive soils for example, failure may occur sometime after embankment construction even though it may appear stable at its final lift. It is important that a number of different methods be used to assess the performance of embankments on soft ground.

5. References

Cavalcante, S.P., Coutinho, R.Q., & Gusmão, A.D. (2004). Analysis of behaviour of embankments on soft soils geotechnical investigationsand instrumental access embankments of the Jitituba River Bridge. *Proceedings, 15th ICCHGE, New York, pp1-9.*

Coutinho, R.Q. & Bello, M.I.M.C.V. (2011). Analysis and control of the stability of embankments on soft soils: Juturaiba and others experiences in Brazil. *Soils and Rocks, Special Issue: Construction on Soft Soils, Vol. 34, N.4, December 2011, pp331-351.*

Fukuzono, T. (1985). A new method for predicting the failure time of a slope. *Proceedings, 4th International Conference and Field Workshop on Landslides, 23-31 August 1985, Tokyo, Japan, pp145-150.*

Hunter, G. & Fell, R. (2003). Prediction of impending failure of embankments on soft ground. *Canadian Geotechnical Journal, Vol. 40, pp. 209-220.*

Johnston, I.W. (1973). Discussion – Session 4 in Field instrumentation in geotechnical engineering. *Halstead Press Book, John Wiley, New York, pp700-702.*

Kurihara, N. & Ichimoto, E. (1977). Case studies on construction of road embankments. *Application of Observational Method in Geotechnical Engineering, Kansai Chapter of Japan Society of Civil Engineers (in Japanese).*

Leroueil, S. & Rowe, R.K (2000). Embankments over soft soil and peat. *Geotechnical and geoenvironmental engineering handbook, Kluwer Academic Publishing, Norwell. USA, pp463-499.*

Magnani, H.O., Almeida, M.S.S., & Ehrlich, M. (2009). Behaviour of two reinforced test embankments on soft clay. *Geosynthetics International, 2009, 16, No. 3, pp127-138.*

Matsuo, M. & Kawamura, K. (1977). Diagram for construction of embankment on soft ground. *Soils and Foundations, 17 (3), pp37-52.*

Sekiguchi, H. & Shibata, T. (1979). Undrained behaviour of soft clay under embankment loading. *Proceedings, 3rd International Conference on Numerical Methods in Geomechanics*.

Tavenas, F. & Leroueil, S. (1980). The behavior of embankments on clay foundations. *Canadian Geotechnical Journal 17 (2), pp236-260.*

Todo, H., Sagae, T., Yamaguchi, M., & Chandra, Y.P. (1996). Comparison of stability control methods for embankments on soft ground in Southeast Asia. *Proceedings, 12th Southeast*

Asian Geotechnical Conference, 6-10 May 1996, Kuala Lumpur, Malaysia, pp297-302.

Tominaga, M. & Hashimoto, M. (1974). Embankment construction control by measurement of lateral displacement. *Tsuchi-to-Kiso Vol. 22, No. 11, Journal of Japanese Society of Soil Mechanics and Foundation Engineering (in Japanese).*

Wong, P.K. and Petropulos, P. (2013). Cockatoo Island Stage 3: seawall failure and remediation. *Proceedings, 2013 International Symposium on Slope Stability in Open Pit Mining and Civil Engineering, pp.393-407.*

This page intentionally left blank

Proceedings of the 10th ANZ Young Geotechnical Professional's Conference – 10YGPC
Noosa, Queensland, Australia
10 – 12 September 2014

APPLICATIONS OF INSITU TECHNIQUES IN RELATION TO CHARACTERISING SETTLEMENT POTENTIAL OF UNCONTROLLED FILL

Robert HARRINGTON
Geotechnical Engineer, Cardno, Brisbane, Australia

ABSTRACT – This paper presents a case study regarding the application of insitu testing techniques employed to characterise the settlement potential of uncontrolled fill. Uncontrolled and controlled filling had occurred over a 9 year period at the subject site, which had resulted in a typical profile of approximately 5m of controlled fill overlying up to 13m of uncontrolled fill. Traditional investigation methods including boreholes and SPT's were first utilised in order to characterise condition of this fill. However, settlements were not able to be accurately predicted using this methodology. It was subsequently proposed to implement insitu testing techniques to more accurately quantify the potential fill settlements. Investigations were carried out using CPT's, Flat Plate Dilatometers (DMT) and insitu dissipation tests, with the aim of characterising the vertical drained constrained modulus of the fill profile in order to calculate potential settlements due to building and infrastructure loads. Results of this analysis indicated that the site could be split into three separate zones. The fill was able to be classified into a number of different units. Based on the results of the work undertaken it was ascertained that creep settlement of the fill would be the governing component of the settlements which were likely to occur at the subject site. Several design alternatives were explored to either induce or control settlements based on anticipated loadings and options presented in order to design for expected settlements.

1. Introduction

The subject site was a backfilled quarry. The aim of the investigation was to characterise the settlement potential of the uncontrolled fill that had been placed during the backfilling as the owner's wish was to develop the lot into an industrial subdivision. The investigation was undertaken to assist in a development application for the site.

The subject site had been progressively quarried and backfilled between 2003 and 2012. Based on discussions with the client, the backfilling of the quarry was able to be broken down into three distinct phases.

Phase 1 had consisted of backfilling with clay overburden sourced from within the site. This material was placed in even lifts and heavily trafficked by plant at the time of backfilling. Phase 1 filling occurred predominantly across the southern portion of the site. Compaction control testing had been previously undertaken under 'Level 1' supervision over a small portion of the site between 2003 and 2005. Total fill height which could be considered "controlled fill" was approximately 3.6m of the full fill profile of up to 17m.

Phase 2 consisted of backfilling with offsite material. This backfill had been placed predominantly in the middle to the northeastern portion of the site, and was variable in nature. Phase 2 filling had occurred with minimal compaction and no moisture control.

Phase 3 consisted of controlled filling undertaken after 2011. Between 3m and 8m of controlled fill was placed to current finish level of the site. Prior to commencement of controlled filling the site was surveyed and contours of the vertical delineation between the controlled and uncontrolled fill were available.

The complete filling operations had resulted in a typical profile of 5m of controlled fill overlying up to 13m of uncontrolled fill.

The water table was measured at between 6.3m and 6.8m below surface level at the time of investigation indicating that the majority of the fill was saturated. This water level corresponded with the level of nearby river system.

An initial site investigation had been conducted (prior to the Author's involvement with the project) using boreholes and SPTs to try to ascertain the settlement potential of the fill. However, settlements had not been able to be accurately predicted using this methodology and dataset.

Following the initial investigation, a surcharge pad was constructed to attempt to assess likely settlements from subsequent loading. This surcharge pad assessment was not successful due to lack of proper monitoring.

Thus, it was proposed to use insitu testing techniques including Flat Plate Dilatometers (DMT), Cone Penetration Tests (CPTu) and dissipation tests to more accurately characterize expected settlements and the time rate of settlement of the previously placed fill.

1.1. Scope of Investigations

Between September 2013 and February 2014, two geotechnical investigations were carried out across the subject site. The first investigation was 'broadscale' and aimed to provide a more accurate estimation of settlements of the uncontrolled fill across the site. The second investigation was aimed at characterizing expected settlement due to construction of council infrastructure, including roadways and subsurface utilities.

The first investigation consisted of 7 CPTu's, 8 DMT's and 2 dissipation tests. The second investigation consisted of 8 further DMT's targeted in the proposed council infrastructure corridors.

2. Description of Tests

2.1. Flat Plate Dilatometer (DMT)

The dilatometer consists of a steel blade having a thin, expandable, circular steel membrane mounted on one face. When at rest, the membrane is flush with the surrounding flat surface of the blade. The blade is connected, by an electro-pneumatic tube running through the insertion rods to a control unit on the surface. The control unit is equipped with pressure gauges, an audio-visual signal, a valve for regulating gas flow (provided by a tank) and vent valves. The blade is advanced into the ground by using common field equipment, in this case, a CPT rig. Tests are generally performed in regular intervals of either 0.2m or 0.4m. At each testing depth, the membrane is inflated and takes two readings in about 1 minute: the A pressure, required to just begin to move the membrane ("lift-off"), and the B pressure, required to move the centre of the membrane 1.1mm against the soil. The pressures are then corrected to take into account the membrane stiffness. On the basis of the pressure readings, 4 parameters are provided to the user. These are as follows;

- I_D – Material Index – provides information on soil type (sand, silt, clay)
- M – Vertical Drained Constrained Modulus
- C_u – Undrained shear strength (clay soils only)
- K_D – Horizontal Stress Index – provides information of the stress history of the soil strata

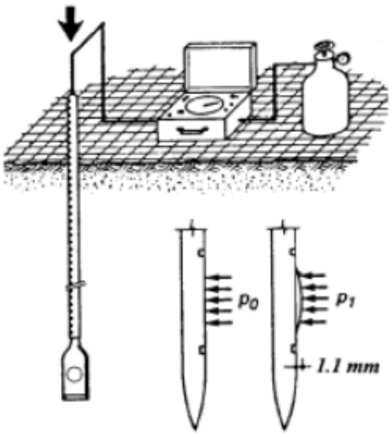

Figure 1. General layout of the flat plate dilatometer test (Totani et al, 2001)

2.2. Cone Penetration Test

The cone penetration test (CPT), consists of a cone at the end of a series of rods which is pushed into the ground at a constant rate with continuous or intermittent measurements taken of both cone resistance and the resistance along the surface, or friction sleeve. With the piezocone arrangement used in this investigation, the pore pressures are measured at the U1 and U2 positions. It was anticipated that an accurate measurement of pore water pressures would be difficult to obtain in the fill. Therefore the majority of the testing was undertaken with PWP being measured at the U1 position due to its greater sensitivity.

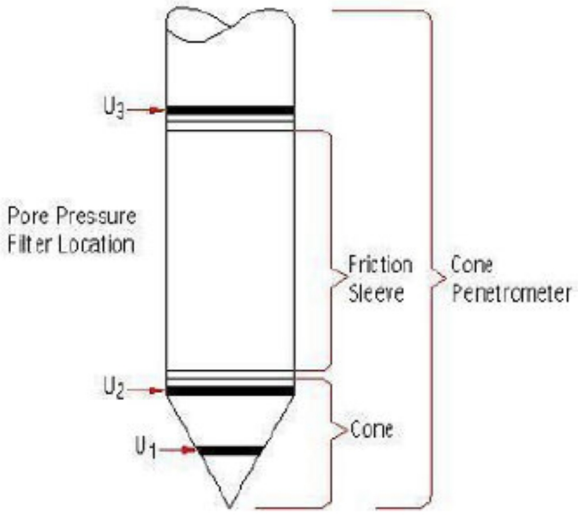

Figure 2. General layout of a CPTu cone

2.3. The Dissipation Test

During a pause in penetration, any excess pore pressures generated around the cone will start to dissipate once the cone is stopped. Dissipation tests are performed by stopping the piezocone and observing pore pressure with elapsed time (t). The pore pressures are plotted as a function of square

root of (t). The graphical technique suggested by Robertson and Campanella (1989), yields a value for t_{50}, which corresponds to the time for 50% consolidation. From the graphical data the horizontal coefficient of consolidation c_h can then be calculated using Houlsby and Teh's (1988) theory. (Lunne et al., 1997)

3. Use of test data in settlement analysis

3.1. Dilatometer Test Results

Analyses of settlement magnitudes were undertaken using Elastic Theory parameters derived from data obtained by pushing DMT's. Vertical drained constrained modulus (M) values were used either directly in one-dimensional settlement analysis or fed into the Finite Element Method (FEM) model for total stress linear-elastic settlement analysis. M values were converted to drained elastic Young's modulus, E, with the assumption of a Poisson's Ratio of 0.35.

The horizontal stress index, K_D, value was used to provide an indication of the initial level of compaction of the fill. The K_D is similar in shape to the profile of the overconsolidation ratio, OCR. $K_D \approx 2$ indicates in clays, which were the predominant fill material, an OCR = 1. $K_D > 2$ indicates over-consolidation. (Totani et al., 2001) This parameter was found to be very helpful for a quick initial assessment in order to ascertain the likely stress history of the deposit and the boundaries of the Phase 1 and 2 filling. No calculation was undertaken using this parameter.

3.2. CPTu data

CPTu data was used in order to classify the soil type of the fill which had been placed onsite. Soils were classified in accordance with Robertson et al, 1998. Shear strengths of clay fill and constrained modulus values were also calculated for the clay fill and were used to correlate with constrained modulus values and shear strengths calculated by the use of DMT's.

3.3. Dissipation Test Results

Dissipation tests were used in order to ascertain the expected time rate of settlements across the site. As the ratio of the horizontal coefficient of compression (c_h) and vertical coefficient of compression (c_v) is highly variable, and would be expected to vary across the site, only an order of magnitude estimate of how long consolidation settlements would take to occur was able to be provided. It was initially proposed to undertake 4 dissipation tests across the site. However, due to the pore pressure response of the cone during testing, time limitations resulted in only 2 tests were able to be completed.

The use of oedometer testing in order to ascertain c_v was not advocated as a part of this investigation. This was considered but not adopted as the site was filled and therefore, by definition, non-homogeneous; thus all samples collected would have to be non-representative or the results indicative of the full site. Instead, it was decided to attempt insitu data aquisition at multiple points by use of dissipation testing in lieu of laboratory oedometer testing.

4. Discussion of results

Based on the results of the DMT testing the fill was able to be split into a number of units, which directly correlated to the phases of filling (described previously).

The stress history of the well compacted and poorly compacted uncontrolled fill was very evident in the K_D and M values obtained from the dilatometer testing. The delineation of the controlled and uncontrolled fill was also able to the ascertained based on the data gathered.

5. Settlement Analysis

For the purpose of this assessment, the settlement of the controlled and uncontrolled fill was characterized as having four components which contributed to total settlement (from Waddell and Wong. 2005):

1. **Short-term settlement**, which occurs due to self-weight as the fill is placed and for a relatively short time after fill has reached full height.
2. **Elastic Settlement**, which occurs in the fill when subjected to loads from footings and floor slabs.
3. **Long-term or Creep Settlement**, which occurs over a period of years under effective stress conditions.
4. **Hydroconsolidation (Collapse) Settlement,** which can occur and is due to saturation of the fill.

5.1. Short-term settlement and Hydroconsolidation (Collapse) settlement

As the fill had been in place for a number of years prior to the investigation being undertaken short-term settlement due to self-weight was assessed to have little impact on the development of the site.

Most poorly compacted, partially saturated fills undergo a reduction in volume when inundated or submerged for the first time. Where clay has been poorly compacted and consists of lumps or clods of clay, these aggregrations may lose strength as he moisture content increases. Inundation may cause a collapse compression in stiff clay fill if it has not been properly compacted.

For this site, it was assessed that there may be a risk of collapse compression of the uncontrolled clay above the water table and below the layer of controlled fill caused by a rising of the water table, not a change in stress. Compression of 3% to 5% of the unsaturated, uncontrolled clay fill may occur due to saturation of this layer by either seepage from above or a rise in the water table level (Charles and Watts, 2001).

5.2. Methodology for Consolidation Settlement Analysis

For the subject site, consolidation settlement due to footing and earthworks loads were calculated based on both elastic theory parameters and via estimation of one-dimensional consolidation settlement magnitudes. One-dimensional settlement to analysis was undertaken using the following formula:

$$S = \sum \frac{\Delta \sigma_v}{M_{DMT}} \Delta z$$

Where:
S = settlement
$\Delta \sigma_v$ = change in vertical stress calculation in accordance with a Boussinesq stress distribution
M_{DMT}= Drained constrained modulus estimated from DMT
Δz = change in depth to the middle of the calculation layer (Totani et al., 2001)

One-dimensional analysis was undertaken for an assumed 40m x 40m area centered on each test location for various load conditions.

Finite Element Method (FEM) modelling was also completed in order to calculate expected settlement along council roadways. For the FEM modelling completed, the material parameters adopted for were linear-elastic total stress parameters derived from the results of the site investigation. A model of the anticipated subsurface conditions was developed for each of the three proposed roadways, based on the targeted testing completed. Figure 3 depicts the model developed for the longest road, Road 1.

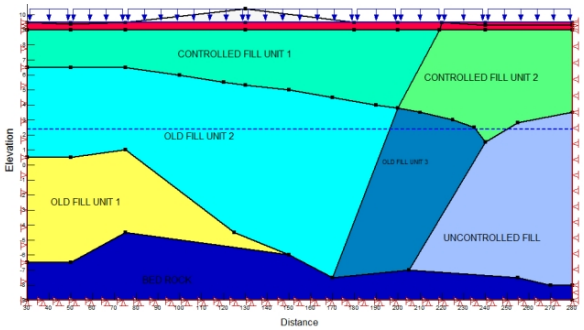

Figure 3. Model of soil units adopted for settlement analysis for Road 1

The complete soil profile model shown in Figure 3 was developed in six steps which broadly corresponded with the deposition of the fill.

5.3 Determination of the time rate of settlement from dissipation test results

Once c_h was determined (as per the methodology described in Section 2.3), c_v was calculated using the following formula:

$$c_v = c_h \frac{k_v}{k_h}$$

Where k_v/k_h is the ratio of horizontal and vertical permeability of the soil mass.

The k_v/k_h relationship is variable and would be expected to depend on the initial level of compaction of the clay strata and the presence, or otherwise, of permeable layers.

The range of k_v/k_h ratios adopted in the analysis was 3 to 15. Due to the uncertainties associated with interpretation, and difficulty in obtaining suitable dissipation test results at this site, an order of magnitude estimate was only able to be presented based on the data obtained (Lunne et al., 1997).

5.4 Creep Settlement

Long-term settlement (or creep settlement) continues to occur under conditions of constant effective stress after all excess pore-water pressures, which have occurred due to an induced change in stress (i.e. loading), have dissipated.

There is a linear relationship between settlement and the logarithm of the time that has elapsed since the load was applied (t_1). This continuing rate of compression of clay fills in one-dimensional compression can be described by the secondary compression or the creep strain rate (per log cycle of time), Cα.

Creep settlement per log cycle of time can be calculated in accordance with the following formula:

$$S_\alpha = C_\alpha \, x \, Fill \, Thickness \, (m) x \, log \frac{t_2}{t_1}$$

Where for the Log (t_2/t_1) term t_2 must be later than t_1.

For this analysis Log (t_2/t_1) was taken as a value of 2 for a 50 year design life. (Waddel and Wong, 2005), and Cα was estimated to fall within the range of 0.001 to 0.005 per log cycle of time (Charles and Watts, 2001).

Based on the adopted creep strain rates it was expected that secondary compression settlements in the order of 2mm to 10mm per metre of fill would occur, in addition to the expected elastic settlements. It was also considered reasonable to expect that creep strain rates would be dependent

on the initial level of compaction of the fill. Thus, the uncontrolled fill would be expected to settle more over the life cycle of the development than the controlled fill.

5.5. Results of settlement analysis

Based on the DMT test results, which correlated broadly with the history of fill deposition at the site, the site was split into three distinct zones, as shown in Figure 4.

Figure 4. Areas of expected settlements

Within Areas 1 and 3, total settlements over a 50 year design period were estimated to be in the order of 110 to 150mm, and consist of 30 to 40mm of consolidation settlements (due to estimated footing loads) and 70 to 110mm of creep (long-term) settlements.

Total estimated settlement for Area 2 was between 180 to 240mm, of which 80 to 100mm were expected to be consolidation settlement and 100 to 140mm attributed to creep settlement.

Based on the results of the dissipation test results it was estimated that consolidation settlements would take up to one year to occur, and from the completed modelling and analysis it was found that creep (long-term) settlements would likely be the governing (majority) component of the expected settlements.

6. Ground Improvement Options

Ground improvement options were presented as a part of the investigation report for the subject site for discussion purposes.

These alternatives were presented such that council had options to further investigate if they were not fully satisfied that other strategies presented would satisfactorily mitigate the risk of settlements to council infrastructure.

The following ground improvement options were explored to either induce (speed-up) or control settlement magnitudes based on anticipated loading conditions.

6.1 Preloading

Surcharging by construction of an embankment was considered in order to induce settlements prior to development and thus mitigate the risk of further creep settlement after development of the site had occurred.

The general strategy of preloading would have been to construct an embankment which would impart a stress of at least 1.5 times the working stress along the road alignments. Preloading was considered the most practicable and feasible option for this site because of the following reasons:

- The proposed embankment would have induced settlements in the uncontrolled fill
- Surcharge embankment may have been built sequentially reusing the same material
- Ease of construction and locally available material
- No requirement to engage specialist plant or contractors to undertake construction

Disadvantages identified to be associated with preloading included:

- Requires proper monitoring in order to evaluate the success of the surcharging
- Costs of construction
- Time required for settlements to occur (time can be shortened by using prefabricated vertical drains)

6.2 Heavy Dynamic Compaction (HDC)

Heavy Dynamic Compaction involves repeated dropping of a steel weight from a crawler crane. Tampers vary in weight and size but are generally between 5t and 25t. Drop heights are usually in the range of 10m to 25m. The combination of drop weight and height are a function of depth of strata required to be compacted.

HDC was not considered suitable for this site due to the relatively high water table and the nature of the fill at the subject site. This was because dynamic compaction will induce large pore pressures within the clay which may have resulted in failure.

6.3 Impact Rolling

Impact rolling involves a tractor towing a square or polygonal impact roller across the site. The depth of strata affected by the application of this energy is generally limited to approximately 2m. As the uncontrolled fill was at least 3m below surface level this technique was not considered viable.

6.4 Semi Rigid Inclusions

Options such as stone columns, controlled modulus columns or jet grouting could have been considered in principle. However, as they would have to be designed for specific structures they may not be cost effective for this site.

7. Options to mitigate the risk of damage to council infrastructure due to settlement

It was recommended that underground services to be installed during site development be designed to allow for the expected absolute and differential settlement.

Such design measures that were considered to be potentially suitable for implementation at this site included:

- Provision of additional fall in gravity sewers and drains so that flow is maintained under adverse differential settlement conditions
- Adoption of pipe and joint types tolerant of settlement
- Use of flexible couplings of service to buildings

For council roadways, similar techniques to those used for ground preparation and roadway construction upon reactive subgrades could also be appropriate for adoption for this project.

8. Conclusions

A site was investigated via employment of various insitu testing techniques. Additional data and insitu parameters were was thus gathered via use of these techniques, as opposed to the completion of boreholes and SPTs.

From the availability of the additional data obtained from non-traditional site investigation techniques, one was able to:

- Better understand the 'stress history' of the fill placed at the subject site
- Discretise the fill into units of different stiffness
- Estimate consolidation settlements of the profile due to the imposition of loads due to structures and roadways
- Provide an estimate of how long consolidation settlements would be expected to take
- Model the expected settlements across the site and along council roadways
- Separate estimated settlements in to consolidation and creep settlements

Having been able to complete such interpretation and analysis, geotechnical engineers were subsequently also able to provide further support to the Client and stakeholders. This included:

1. Provide options to mitigate the risk of settlement to structures and council assets and utilities.
2. Discuss strategies to either induce settlement prior to development or control settlements over the life of the development.

9. References

Charles JA., Watts KS. (2001) *Building on fill: geotechnical aspects*. 2nd ed. Building Research Establishment (BRE), Watford.

Lunne T., Powell Jm., Robertson P.K., (1997) *Cone Penetration Testing in Geotechnical Practice*. CRC Press, Florida, 352 pages.

Totani G., Marchetti S., Monaco P., Calabrese., M (2001) Use of the Flat Plate Dilatometer Test (DMT) in geotechnical design. *Proceedings IN SITU 2001, Intinl. Conf. On In situ Measurement of Soil Properties*, Bali, Indonesia, May 2001

Waddel PL., Wong PK., (2005) Settlement of Deep Engineered Fills *Australian Geomechanics Journal,* Vol. 40 No. 4, December 2005

ROCKHAMPTON WASTE TRANSFER STATION

Daniel McATEER
Design Engineer at Frankipile Australia, Brisbane, Australia

ABSTRACT – A recently delivered design and construct piling solution for the new waste transfer station located on a landfill site in east Rockhampton involved the construction of a multi-level industrial building, with surrounding access roads, on a geotechnically challenging site. The final building levels across the site varied in the order of 8-9m, necessitating a major earthworks operation before commencement of piling. The original scheme proposed by the client involved driving steel tubes, excavation of landfill material and driving octagonal prestressed piles with a bitumen coating. Original scheme was to be a two-pile and three-pile arrangement. The paper will aim to demonstrate the geotechnical and environmental challenges posed by the site as well as addressing the health, safety and construction implications of the original scheme. This paper explains the proposed piling solution, its advantages over the original scheme and the detailed geotechnical and structural design analysis involving lateral pile analysis, durability and pile settlement. Construction issues were overcome in relation to pile breakages and monitoring pile performance by the completion of dynamic pile testing.

1. Introduction

The proposed Waste Transfer Station is located on the Lakes Creek Road Landfill site in east Rockhampton.

The project involved the construction of a multi-level building with surrounding access roads.

The main building comprised three different building levels consisting of a tipping floor, surge pit and loading dock located above an existing ground level of 9.0m AHD. Waste enters the tipping floor, constructed at 16.6m AHD, prior to being pushed into a surge pit 3m below (13.6m AHD). Within the surge pit the waste is tipped and sorted, prior to being moved to the lower loading dock (at 9.0m AHD) is it is loaded into vehicles for distribution. A cross-section of the proposed building is outlined in Fig.1.

In order to complete this three (3) level arrangement, significant fill operations – in the order of 9m – was required before the commencement of piling operations.

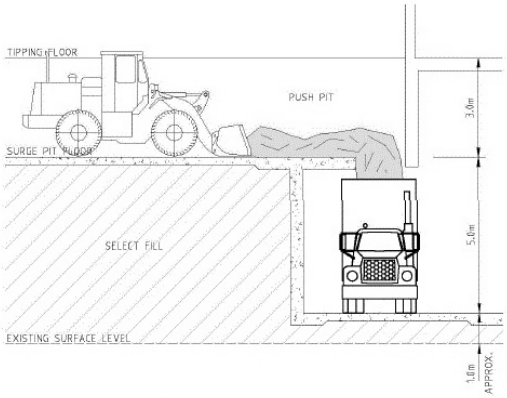

Figure 1. Building Cross-Section

1.1. Geotechnical Site Investigation

At the time of geotechnical investigation in 2010, the site was approximately level with the elevation of the existing ground surface varying slightly between 7.5m AHD and 8.9m AHD.

1.1.1. Extent of Site Investigation

The scope of the site investigation included four test pits excavated to depths of 6.5m below ground level of 9.0m AHD, seven boreholes in the vicinity of the building footprint, including three deep boreholes to depths of 34m and two shallow boreholes to depths of 4 to 8m.

Three cone penetration tests were conducted in three pre-formed boreholes, however, due to the difficult conditions obstructions encountered in the landfill material only shallow depths were achieved in two boreholes. A dummy probe was then used to push through the landfill material and the tests were continued.

This was an existing landfill site and contained material such as consisting of cardboard, glass, rubber, plastic, some kitchen waste, old tyres, mattresses, empty drums, timber fragments, concrete, builder's rubble, etc. The Landfill was considered to be well compacted

Finally standpipes were installed in two of the boreholes to facilitate groundwater monitoring.

1.1.2. Conditions Encountered

Original Fill was encountered in the first 3m which comprised of stiff silty clay and medium dense gravels.

The Fill material was overlying 6-8m of landfill. Underlying the landfill material was 12-16m of

estuarine deposits consisting of high plasticity soft to firm silty clay with standard penetration tests (SPT's) no greater than 11. In some instances values as low as 0 and 1 with notes on borelogs indicating hammer "fell under own self-weight". This material proceeded over 1-2m to stiff to very stiff silty clay with depth and CPT data indicating q_c values of 2-4MPa.

Below the estuarine deposits was 1-4m of alluvium consisting of very dense sands and gravels with SPT readings between 60 and 80.

Extremely weathered granite rock was encountered between RL-14.7m and RL-16.7m. Rock was considered to be extremely low strength and tender towards low strength with depth indicated by I_s50 values between 0.1 and 1.

Finally groundwater monitoring indicated that the groundwater was encountered at approximately RL5.0m.

A cross-section of the geotechnical profile is shown in Fig. 2.

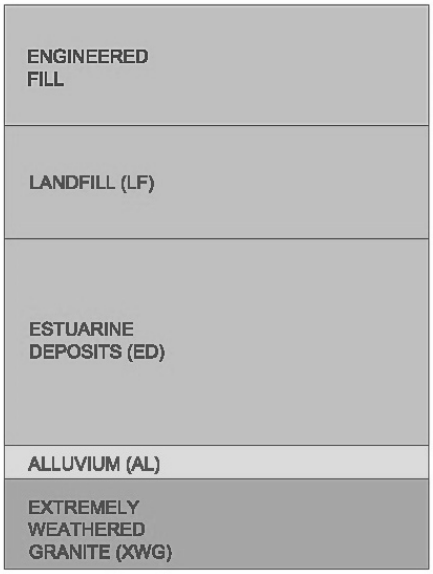

Figure 2. Geotechnical Cross-Section

1.1.3. Environmental Considerations

Medium to high inflows of leachate were also noticed at the base on the landfill material during test pit excavations and, in some instances, at higher perched levels in the landfill material. It was also noted that the problem of leachate inflow could become more pronounced with an excavate and replace foundation solution due to inflow from the surrounding embankments.

Furthermore, there were concerns that disturbance of the subsurface material from deep foundation construction (i.e. piling) could result in leachate transfer to the underground aquifer (i.e. the alluvium materials and permeable rock) located at depth.

1.2. Foundation System

1.2.1. Original Scheme

The use of octagonal pre-stressed concrete piles underneath a pilecap and tie-beam arrangement was originally proposed with pile groups between one and three under each pilecap. The design allowed for a total of 166 octagonal prestressed piles to carry the load of the building and a further 21 piles for the entry and exit bridges from the building.

The construction sequence involved driving a 1.0 metre diameter steel casing to the base of the landfill material, excavating inside the casing and driving an octagonal prestressed concrete pile with a bitumen coating to a suitable founding level. Then provide a sand infill to the surrounding pile in a PVC casing and finally fill the excavation with a cement bentonite grout before removing the steel casing.

1.2.2. Structural Considerations

Maximum ultimate column loads were in the order of 2200kN and ultimate lateral loads in the order of 135kN.

Six loading scenarios were considered, dealing with various arrangements of permanent, imposed, earthquake and wind actions. The structure required a design life of fifty years.

The structural specification outlined that all piled foundations required a settlement criteria of less than 10mm at safe working load and a positional tolerance of less than 75mm. This was considered consistent with *Australian Standard Piling – Design & Installation* (AS2159-2009).

1.2.3. Proposed Solution

Due to the low to moderate structural loads on each octagonal pre-stressed pile, an alternative precast concrete piled solution was adopted with piles driven to refusal and pile sizes of 300mm, 350mm and 400mm square. A maximum of a two pile group under each column location was also proposed.

This solution had various advantages over the original scheme most notably being a more efficient pile design by eliminating twenty piles (i.e. ten percent of project) based on the column loads provided.

Health & safety advantages included having less machinery and subsequent vehicle movement on site and no open excavations.

From a construction perspective it would also be very difficult to excavate landfill (highly variable) material to depths of 10m within the confines of a 1.0m steel casing.

The proposed solution would therefore reduce construction time due to fewer processes required to construct each pile.

An important environmental consideration with the original scheme was the treatment of the

excavated material. The proposed solution would not require any spoil removal.

Finally while prevention of leachate transfer to underground depths could not be guaranteed it was significantly diminished due to less disturbance of the waste layer.

1.3. Pile Design

1.3.1. Geotechnical Design

The structural specification called for a testing regime of ten percent dynamic testing of all piles. Based on this testing regime, experience in similar geotechnical conditions and the design method adopted, a geotechnical reduction factor, φ_g of 0.76 was adopted in accordance with Section 4 of AS2159- 2009.

As the piles would be driven to effective refusal their compression capacity would be governed by their structural capacity.

The effects of negative skin friction were also considered for material located above the soft estuarine deposits. Although the ultimate geotechnical strength in compression or uplift was not affected by negative friction, the serviceability design included the effects of such negative friction as outlined in *Australian Standard Piling – Design & Installation* (AS2159-2009). The ultimate geotechnical strength of the pile must be greater the combined effect of serviceability load and down drag associated with negative skin friction.

$$R_{d,ug} \geq E_{ds} + F_{nf} \qquad (1)$$

1.3.2. Durability

The structural specification outlined a design life of 50 years for the waste transfer station. Due to the geotechnical conditions encountered, particularly the material in the landfill zone, the exposure classification was assessed by the code and determined to be "very severe" and thus a minimum concrete strength of 50MPa and cover thickness of 40mm was required.

The durability and sustainability of these piles was also improved by the use of high strength concrete containing substantial quantities of supplementary cementitious material (i.e. fly ash greater than 20%) as noted under the durability requirements of the piling code. A higher performance and a lower water cement ratio results in a less permeable structure giving better resistance in the aggressive environment encountered.

1.3.3. Lateral Pile Analysis

Worst case failure for a laterally loaded pile will occur in a long pile with a fixed head as a plastic hinge will form in two places.

This idealization assumes that the moment-resistance at the pilecap is known (Poulos and Davis, 1980). As the moment-resistance at the pilecap was not known during design, a pinned connection to all piles was assumed. This was considered a conservative assumption, as maximum pile deflection magnitudes and soil deformations would be expected under this arrangement as shown in Fig. 3.

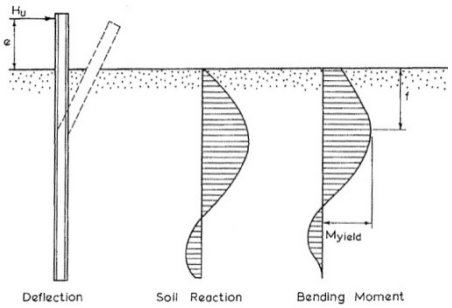

Figure 3. Lateral failure of Long Piles with free head (Poulos and Davis, 1980)

The behaviour of the piles under lateral loading was approximated using the commercial software package PIGLET (UWA, 2004). The initial lateral shear modulus and lateral shear modulus gradient parameters adopted are shown in Table 1.

Table 1. Pile Design Parameters

Parameter	Value
$G_{0.Lateral}$	4 MPa
dG/dz .Lateral	0.4 MPa/m

The parameters were based on a cohesionless engineered fill material with the shear modulus gradient reflecting the increase in effective pressure in the soil.

The completed lateral pile analysis indicated that piles subjected to lateral loading experienced a maximum moment at a consistent depth. Bending moments were observed to dissipate at a depth of approximately ten times the pile diameter.

Piles were also subject to an eccentric moment due to positional tolerance guidelines in the piling code. This resulted in the piles being assessed for the superimposed effect of the maximum moment due to lateral loading and the dissipation of the head eccentric moment at this depth as outlined in Fig. 4.

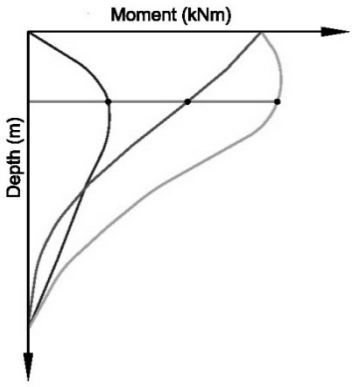

Figure 4. Bending Moment distributions

1.3.4. Lateral Restraint & Core Confinement

During the later stages of the design the findings of an instrumentation and monitoring report (AECOM, 2012) carried out on the site suggested that the site shall experience a settlement of 900mm over the life of the structure.

In accordance with Section 5.3.7 of AS2159-2009, a pile with a projection of more than two pile diameters above final ground formation level requires the tie or helix to have a minimum size. This requirement is defined by the *Australian Standard Concrete Structures* (AS3600-2009). The purpose of such a tie and helix arrangement was to provide confinement of concrete and lateral restraint of longitudinal bars against premature buckling.

Where the combined design action effects of combined axial force and bending moments on a pile fall within a region as detailed in Fig. 5, confinement of the core was required.

Core confinement checks were carried out in accordance with AS3600-2009. From this analysis, it was determined that a minimum spacing of 65mm for the helix was required for all precast piles to meet core confinement criteria. This potentially could have created pile constructability issues and undermined the pile's structural integrity, as getting vibration equipment between helix bars during pile casting would be difficult with this limited (small) helix spacing.

Furthermore increasing the helix spacing would result in a helix diameter greater than the standard 5-6mm bar providing difficulties during steel fabrication.

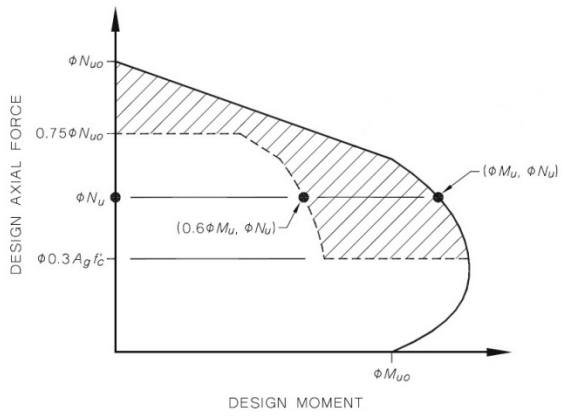

Figure 5. Confinement of the Core

To meet core confinement requirements all piles within the special confinement region were increased in size from a 350mm to a 400mm square pile to meet confinement requirements. This affected approximately twenty piles.

1.4. Evaluation

1.4.1. Pile Breakages

Based on previous experience driving precast piles in landfill sites, ten percent (i.e. sixteen in this instance) pile breakages could be expected. Overall there were six pile breakages observed during the construction phase of the project which was significantly less than our assessment during design.

Three of the breakages were during driving of the third section of pile. The increase in set recorded by our operators alluded to a structural breakage and the pile deviated off course.

One pile achieved anticipated founding depth but with a very high set of 26mm per blow.

Finally, the remaining two piles achieved set approximately 13m before piles in the immediate vicinity suggesting these piles may have hit an obstruction.

1.4.2. Pile Testing

As already mentioned, the testing criteria specified was ten percent pile dynamic testing including six CAPWAP® analysis.

The CAPWAP® analysis produces static-load versus deflection estimates using the best match soil profiles and pile model.

All piles were tested using a Junttan HHK7A piling rig operating a 7.0 tonne hydraulic drop hammer. A specified drop height based on the pile size being tested was proposed to ensure stresses in the head of the pile during driving did not undermine structural integrity. The maximum drop height for each pile size is outlined in Table 2.

Table 2. Testing Drop Heights adopted for CAPWAP testing

Pile Size (mm)	Drop height (mm)
300	500
350	700
400	800

As the ground will undergo settlement in the long-term, and as a result develop negative skin friction, the serviceability test load were determined in accordance with Table 8.3.3.3 of the AS2159-2009 and shown in Equation 2.

$$P_s \geq Eds + 2F_{nf} \qquad (2)$$

The pile tests results reported a maximum pile set of 5mm using pile dynamic testing and a maximum head deflection of 6.7mm using CAPWAP® analysis confirming compliance with the 10mm settlement criteria.

Furthermore the total pile resistance achieved through CAPWAP® was at least twenty percent more than the required load capacity.

2. Conclusions

This paper presented an alternative piled solution in difficult geotechnical conditions frequently encountered within landfill sites while complying with the structural design criteria specified by the client.

It demonstrated that a more sustainable piling solution can be achieved through a more efficient design, appropriate use of materials and resources and with greater appreciation for health, safety and environmental implications.

This project was a more "valued engineering" approach with the piling scope reduced by ten percent, significantly reducing construction time and at half of the cost comparable to the original scheme.

3. References

AECOM (2010). Factual geotechnical report - lakes creek road, waste transfer station, rockhampton.

AECOM (2012). Structural building specification - lakes creek road - waste transfer station.

AECOM (2012). Instrumentation & monitoring report – end of preloading.

Randolph M (2004), PIGLET Version 5.1

Australian Standard Piling – Design & Installation (AS2159-2009).

Australian Standard Concrete Structures (AS3600-2009).

Golder Associates (2009). Waste transfer station & sediment basin lakes creek road landfill, rockhampton.

Poulos H.G., Davis E.H. (1980). Pile fondation analysis and design. *Ch. 7, pp. 149-152.*

Ngamo Dynamics (2013). Precast concrete piles, waste transfer station, Rockhampton.

This page intentionally left blank

Proceedings of the 10th ANZ Young Geotechnical Professional's Conference – 10YGPC
Noosa, Queensland, Australia
10 – 12 September 2014

PROPOSED KOTUKU FLOOD DETENTION DAM – GEOLOGY AND GEOTECHNICAL DESIGN FEATURES

Daniel SCOTT
Riley Consultants Ltd, Auckland, New Zealand

ABSTRACT – In the North Island of New Zealand, volcanic soil and rock pose seepage issues for water retaining structures, and very careful investigation and design is necessary. The proposed Kotuku Flood Detention Dam has been designed to reduce flooding within Whangarei City, and is expected to commence construction in the 2014/2015 earthworks season. The proposed dam is classified a high potential impact classification (PIC) dam, and hence the geotechnical issues have been rigorously analysed. The proposed dam and catchment are located within a complex geological environment, where a basalt flow and flow margin, firm alluvial soils, and massive sandstone rock are present in the proposed dam foundation. This paper describes the geotechnical issues posed by site geology in preparing a detailed design of the 18m earth embankment dam. Investigation and testing has been undertaken to assess the site geology, including founding conditions, seepage potential and materials for dam construction. Permeability testing, including packer, falling and constant head tests, provided input to forming a geological model of the subsurface conditions. Transient groundwater analysis on the geological model was undertaken for a 36 hour, 1% annual exceedance probability (AEP) flood event. This analysis led to the development of a detailed design for the proposed dam, which comprises a clay liner, undercuts of alluvial and selected residual and flow margin materials, toe drains and internal drainage.

1. Introduction and Project Background

The Northland region of New Zealand, in which Whangarei is situated, has been subject to significant flood events over the past 10 years. In many cases, these events have highlighted the vulnerability of certain land areas to flooding and a requirement to improve/upgrade flood protection.

The proposed Kotuku flood detention dam is one such flood protection measure identified by Northland Regional Council (NRC). The concept for a dam at the proposed site, however, is not new, with studies dating as far back as 1966. Riley Consultants Ltd has been providing geotechnical and water resources engineering services for the proposed dam since undertaking feasibility studies in 2011.

The proposed embankment-type dam is located on the Nihotetea Stream to the south-west of the Whangarei Central Business District (CBD), as shown on Figure 1. The dam has a high potential impact classification (PIC) by NZSOLD Guidelines (2000).

The dam will be approximately 18m high and contain approximately 1.3 million m^3 of water during the design 1% Annual Exceedence Probability (AEP, which includes climate change) flood event. The 9.1km^2 catchment area shown in Figure 2 is predominantly covered in pasture, with some areas of scrub and bush. A predicted 1% AEP flood event currently results in a flood depth of 0.75m in the CBD, affecting approximately 620 buildings.

Three sites were initially considered, and the proposed dam site was selected after a feasibility study, cost comparison, and a reservoir stability investigation.

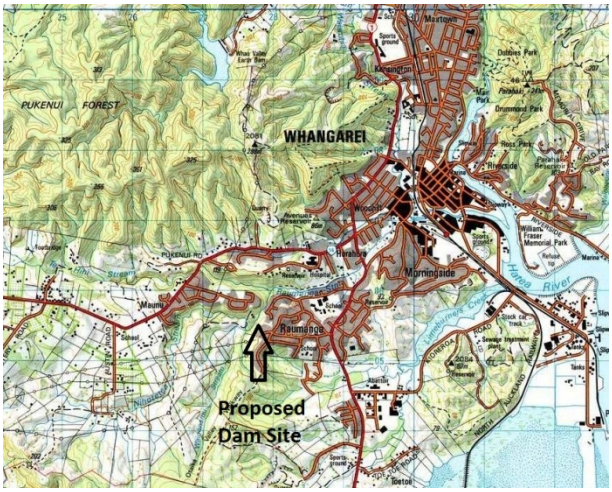

Figure 1. Map of proposed dam site

At the time of preparing this paper, August 2014, resource consent for construction of the dam has been obtained, and a contractor has been selected to undertake the construction works. Earthworks will be undertaken in the 2014/2015 earthworks season starting October 2014, and preliminary works to relocate services at the dam site were completed in July 2014.

2. Geology

The Institute of Geological Nuclear Sciences Ltd (GNS) 1:25,000 geological map of the Whangarei Urban Area (GNS geological map 26) indicates the site is underlain by several different geological units. The basement rock in the area is Waipapa

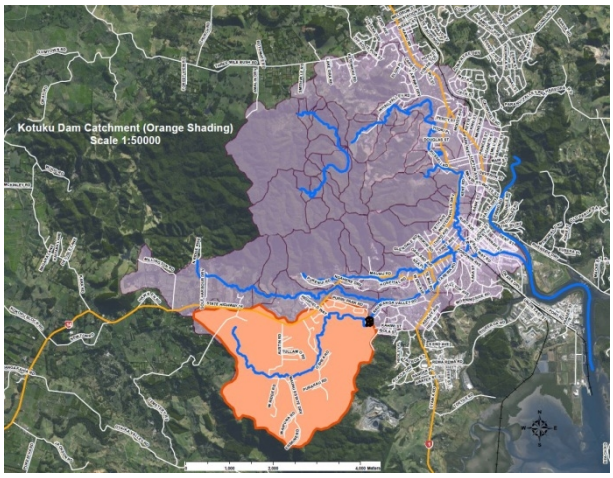

Figure 2. Kotuku Dam catchment

Terrane greywacke, which is overlain by Ruatangata sandstone, and is located near the ground surface on the southern and eastern slopes.

The northern and western slopes of the valley are underlain by basaltic lava of the Kerikeri Volcanic Group. The basaltic lava sourced from the Maunu Mountain volcano and associated scoria cone to the west of the site has flowed down and infilled a paleochannel of the Raumanga Stream and dammed associated tributaries. The basalt lava outcrops as cobbles and boulders at the ground surface and in the stream bed, and is exposed in a waterfall downstream of the dam site. The rocks are generally fine-grained and vesicular.

The lower-lying central portions near the watercourse are underlain by alluvium. The alluvium on the site is fluvial and lacustrine deposits consisting of clays, silts and gravels with generally minor organics. These are likely to have accumulated with the partial damming of streams by lava flows.

Site inspection, mapping, machine boreholes, test pits, and hand auger boreholes were undertaken at the dam site, in the borrow area, and reservoir to investigate the geology at the site. Three phases of investigation work were undertaken: feasibility study, preliminary design and detailed design.

2.1. Dam Site Geology

2.1.1. General

A plan layout of the dam site is shown in Figure 3. The proposed dam footprint extends over variable soil and rock types on both the left and right abutments and upstream to downstream. The right abutment is underlain by competent sandstone with a relatively shallow depth of overlying residual soil. The left abutment consists of a lava flow with mixed flow margin materials surrounding the basalt lava. The lava flow, which sits on the alluvium that overlies sandstone at depth, has filled a paleovalley. The firm alluvium varies in thickness from 2m to 5m in the valley floor at the dam centerline, increasing in thickness upstream into the old basin. Figure 4 presents a geological long section along the centre line of the embankment.

Investigations at the dam site were undertaken to develop and refine a geological model of the subsurface conditions. Testing was challenging due to access constraints from private properties, dense bush, steep slopes and large boulders at the ground surface. During drilling of the machine boreholes, falling head, constant head, and packer testing was undertaken in the Kerikeri Volcanic Group and Ruatangata Sandstone formation materials to assess soil and rock mass permeability. Angled machine boreholes were undertaken at the proposed dam abutments to maximise the likelihood of intercepting steeply dipping and vertical rock joints to provide a better understanding of defects and the rock mass permeability.

2.1.2. Subsurface Conditions

The central stream area has been infilled with alluvial material transported from the catchment upstream. The alluvial material is generally firm to stiff silty material with fractions of organics and a maximum thickness of 5m at the upstream end of the dam footprint.

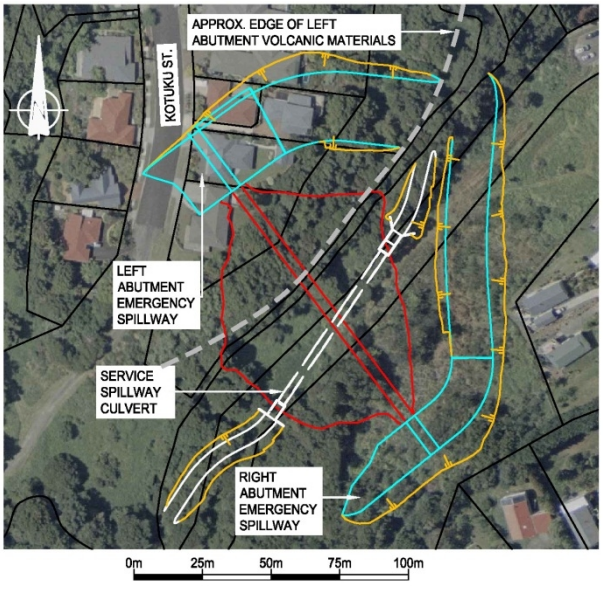

Figure 3. Plan layout of dam site

The right abutment comprises a steep slope of typically fine-grained and massive Ruatangata Sandstone of the Te Kuiti Group. The sandstone is generally completely weathered near the surface grading to unweathered at approximately 7.5m depth. Localised areas of colluvium and alluvium were encountered at the ground surface. Artesian pressures were encountered near the base of the slope, inferred to be from groundwater originating in the area upslope of the proposed dam site.

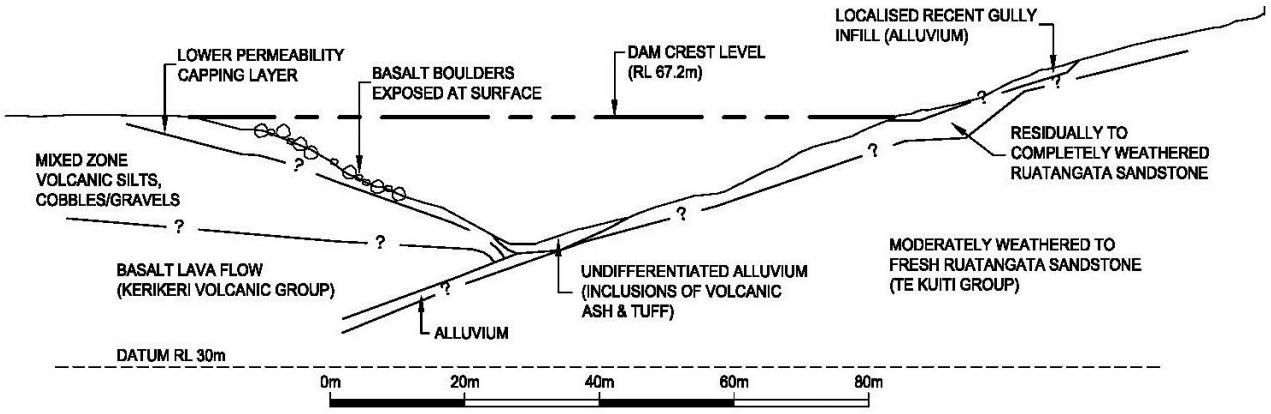

Figure 4. Geological cross section

The left abutment is located on the southern lateral margin of a large basalt lava flow of Kerikeri Volcanic Group material from the Maunu Mountain volcano and associated scoria cone to the west of the dam site. The lava flow margin generally comprises a mixed zone of materials including volcanic silts, gravels, and cobbles overlying the strong basalt lava flow at between 9m and 15m depth in the mid-slope to dam crest area. The basalt lava flow comprises strong fractured basalt rock. Defects in the basalt have a very narrow aperture with clay infill, and are vertical with moderately widely spaced sub-horizontal defects. A capping layer of lower permeability material overlies the mixed zone materials. The lava flow and flow margin are underlain by slightly weathered Ruatangata sandstone and, near the toe of the slope, with a firm to hard alluvial layer.

2.1.3. Permeability Testing

Packer testing was undertaken in the rock encountered at the dam site, with falling and constant head tests in the soils and weathered rock on the left abutment. In packer testing, pressurised water is pumped into an area of open machine borehole shut off by a packer, and the flow of water escaping through defects in the rock mass below the packer is recorded. The flow is recorded over five or more two minute intervals of water pressure being incrementally stepped-up and then down, and the pattern of the flowrate over the entire test is noted. Patterns can involve washing out of material (increasing flow during the test), filling of voids (decreasing flow during the test), higher flow when fractures are open at higher pressures (dilation), turbulent flow in fractures at higher pressures, and laminar flow where all the Lugeon values are the same for all pressures. One Lugeon unit corresponds to 1 litre/minute per metre length of test section at an effective pressure of 1 MPa. Following analysis, the most representative flowrate over the test is correlated to a Lugeon value for the rock mass.

Packer testing in the Ruatangata sandstone on the right abutment generally recorded Lugeon values of 0 to 6 (very low to moderate permeability) consistent with a massive rock with very tight to narrow defects. Packer testing in the basalt lava flow on the right abutment recorded Lugeon values of 2 to 100 (moderate to high permeability) indicating some variability between tight and many open joints.

Falling and constant head testing in the mixed zone of flow margin materials recorded permeability results of $8.3x10^{-5}$ m/s and $3.5x10^{-4}$ m/s, which are equivalent to the permeability of a silty sand to sand. A capping layer of lower permeability material was encountered between 3.7m and 6m at the left abutment, overlying the more permeable mixed zone materials.

2.2. Borrow Area Geology

The materials for constructing the dam are to be borrowed from the right abutment emergency spillway excavation and a borrow area located approximately 400m west of the dam site. The borrow area is a small hill underlain by residually weathered to unweathered weak sandstones and mudstones of Ruatangata Sandstone formation. Test pits were undertaken at the borrow area to determine the excavatability of the material and bulk samples were collected for laboratory testing.

2.3. Laboratory Testing

Laboratory testing was undertaken on samples from the left and right abutments and the borrow area. Key objectives of the laboratory testing were to assess the nature and strength of materials from the borrow area and right abutment spillway cut, and the grading of the flow margin soils on the left dam abutment to correlate to permeability and provide input for filter design. Compaction, grading and dispersivity tests were undertaken on the borrow materials to determine their suitability as dam construction materials, and strength tests were undertaken to assess the excavatability of the sandstone rock.

The borrow area and right abutment spillway materials are generally non-dispersive (ND1 and ND2), having over 65% fines (smaller than 0.063mm particle diameter, i.e. silt and clay sized particles), and achieving maximum dry density of around $1.35t/m^3$ (standard compaction) and over

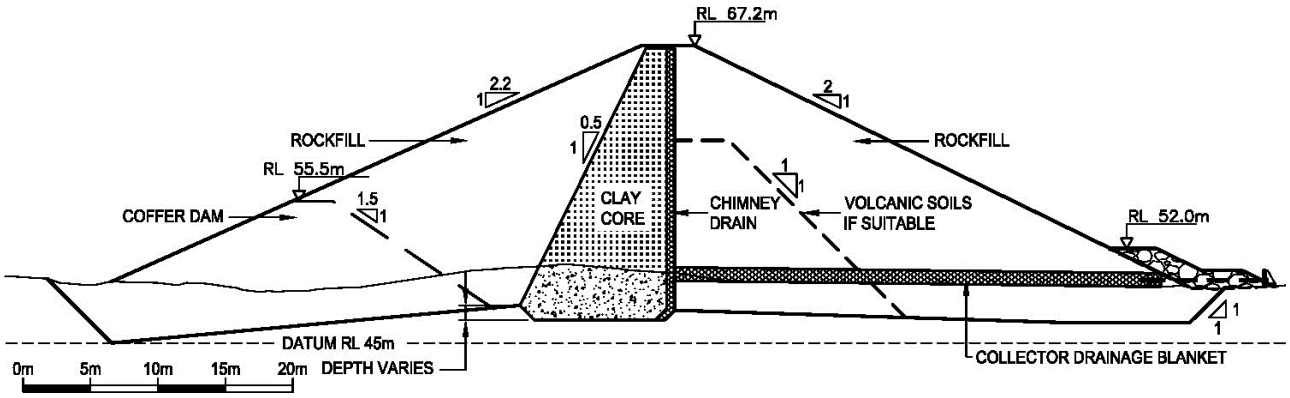

Figure 5. Typical embankment cross section

1.55t/m^3 (heavy compaction). The tests in sandstone material from the borrow area recorded uniaxial compressive strength in the range of 5 to 25MPa, and will likely require ripping to excavate. The flow margin material on the left abutment has gradings ranging from silty gravel to clayey silt.

2.4. Reservoir Stability

In the preliminary stages of investigation and design, when evaluating multiple dam sites, consideration was given to geological features that could lead to instability when the reservoir is temporarily at peak levels. This stage of assessment comprised a site walkover, field testing, and analysis of results from around the proposed reservoir.

The likelihood of large-scale instability within the basin slopes due to temporarily higher reservoir levels is considered low. In an extreme rainfall event, the slopes surrounding the reservoir will likely be saturated and localised surficial slumping may occur within the lower-lying areas of the basin, which is not considered to pose an unacceptable risk to the dam.

However, as part of prudent risk management, monitoring of reservoir stability will be incorporated into a long-term dam safety assurance programme.

3. Geotechnical Design Features

3.1. Foundation Treatment

As shown in Figure 4, the geological model for the dam foundation comprises volcanic materials on the left abutment, and weathered sandstone on the right abutment, with alluvium in the central valley. The volcanic materials are variable in composition, whereas sandstone on the right abutment is relatively uniform.

In the valley floor, the alluvium will be undercut to the stronger sandstone to minimise settlement and stability issues. At the upstream toe of the dam, the undercut may be 4m to 5m or greater, which is considered achievable. Such an earth embankment dam is typically expected to settle less than 0.7% of its height (i.e. less than 140mm), and undercutting the alluvial and completely weathered sandstone materials and compacting the dam construction materials well will ensure that the settlement is maintained in that range.

On the right abutment the moderately weathered sandstone is typically shallow (less than 2m) and is an acceptable founding material. Overlying soil, including completely weathered rock and any localised areas of alluvium and colluvium, will be stripped. There is no evidence of significant defects within the massive sandstone rock.

On the lower left abutment, where the dam height is greatest, any weaker near-surface materials and the mixed zone materials will be removed to sandstone or the basalt lava flow. Treatment of basalt defects will possibly be required when the lava is exposed in the dam foundation. As the dam section rises up the relatively steep abutment, the depth to the basalt rock increases significantly and it is not practical to sub-excavate to that depth. Consequently, rubbly flow margin materials comprising variable cohesive soils mixed with gravels and volcanic materials will be left in place in the foundation. There is no evidence of continuous highly permeable or erodible materials in the flow margin, but there are gap-graded materials that may be susceptible to piping if significant sustained seepage flow were to occur. Although peak reservoir levels are only sustained for a matter of hours, seepage control features are considered essential in the left abutment foundation, which are discuss in section 3.3 and include an upstream clay liner.

3.2. Embankment Design

The proposed dam zoning consists of a central clay core, a zone of volcanic soils immediately downstream of the core, and upstream and downstream rockfill shoulders. Figure 5 presents a typical cross section through the embankment.

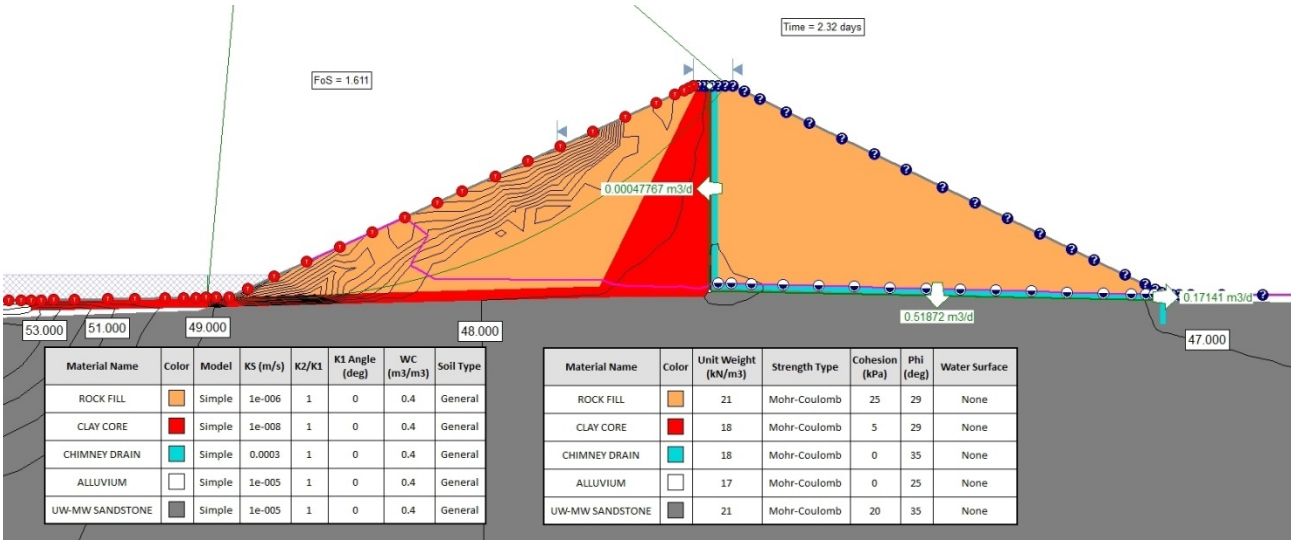

Material Name	Color	Model	KS (m/s)	K2/K1	K1 Angle (deg)	WC (m3/m3)	Soil Type
ROCK FILL		Simple	1e-006	1	0	0.4	General
CLAY CORE		Simple	1e-008	1	0	0.4	General
CHIMNEY DRAIN		Simple	0.0003	1	0	0.4	General
ALLUVIUM		Simple	1e-005	1	0	0.4	General
UW-MW SANDSTONE		Simple	1e-005	1	0	0.4	General

Material Name	Color	Unit Weight (kN/m3)	Strength Type	Cohesion (kPa)	Phi (deg)	Water Surface
ROCK FILL		21	Mohr-Coulomb	25	29	None
CLAY CORE		18	Mohr-Coulomb	5	29	None
CHIMNEY DRAIN		18	Mohr-Coulomb	0	35	None
ALLUVIUM		17	Mohr-Coulomb	0	25	None
UW-MW SANDSTONE		21	Mohr-Coulomb	20	35	None

Figure 6. Rapid drawdown slope stability analysis

The core materials will be obtained from the surficial soils or completely weathered rock. Completely weathered rock (especially siltstone) is likely to be an acceptable core material, as it breaks down/compacts to a fine-grained material. Sheepsfoot rollers are nominated in the construction specification so that gravel-sized particles are broken down by roller action.

The rockfill and clay materials will be obtained from the nominated borrow area and the right abutment emergency spillway excavation. As the rockfill is sourced from a weak rock, the compacted material will have a lower percentage of gravel-sized particles, and permeability is expected to be low. Selected soils from the left emergency spillway excavation are proposed to be used in the downstream shoulder. A high standard of compaction is necessary for the clay core and clay liner. It is recommended that 200mm loose layers of material with greater than 65% fines content are compacted to achieve a shear vane strength of greater than 120kPa and air voids of less than 8% (5% average). The rockfill on the upstream and downstream shoulders will be compacted to 95% of the dry density standard compaction with air voids less than 10% (8% average).

3.2.1. Slope Stability

Slope instability is most likely to occur during rapid drawdown conditions when the dam freeboard is much greater than at the peak flood level. The likelihood of a slope failure causing a large wave and potentially overtopping the dam is therefore much less with a detention dam compared with a permanent reservoir.

Slope stability analysis was undertaken using the Slide software package on three sections through the dam (two on the left abutment) for a variety of cases, including effective stress, total stress, seismic loading from an operating basis earthquake (OBE: 1:150 year event, 0.1g) and maximum design earthquake (MDE: 1:10,000 year event, 0.32g), and a rapid drawdown analysis on the upstream slope. Input for geotechnical material parameters came from triaxial testing on typical rockfill material from the borrow area (c' = 25kPa, φ' = 29°) and assumed parameters for other materials in the dam embankment and foundation based on in-situ strength testing. Sensitivity analyses were undertaken on all the geotechnical material parameters used. A typical Slide printout for the rapid drawdown analysis is shown in Figure 6. The required Factors of Safety (FoS) adopted from NZSOLD Guidelines (2000) are 1.5 under steady state seepage, 1.2 under OBE, a FoS of greater than 1 under MDE, and 1.2 to 1.3 during rapid drawdown conditions on the upstream slope.

A deformation analysis was also undertaken for the OBE and MDE events, which showed minor to moderate damage including 40mm crest settlement and 30mm crack width in an MDE event.

3.3. Seepage – Internal Drainage and Clay Liner

The internal drainage consists of a fully intercepting 600mm wide chimney drain that extends to peak maximum flood level and connects to a base horizontal drainage/filter blanket, as shown in Figure 5. The horizontal drain is locally thickened in the vicinity of the service spillway culvert (beneath the dam and in the current stream bed location), where there is a greater risk of cracking and concentrated leaks. A 250mm thick continuous filter layer is provided on the left abutment foundation surface with a series of 1m thick high capacity strip drains, consisting of a filter layer surrounding a coarser drainage material. A toe drain is provided on each abutment.

The filters have been designed to allow for compatibility with the embankment and foundation soils at site, with the critical surfaces being the clay core to vertical drain interface and the foundation to horizontal/toe drain interface. The filter design was undertaken according to guidelines set out in Fell et

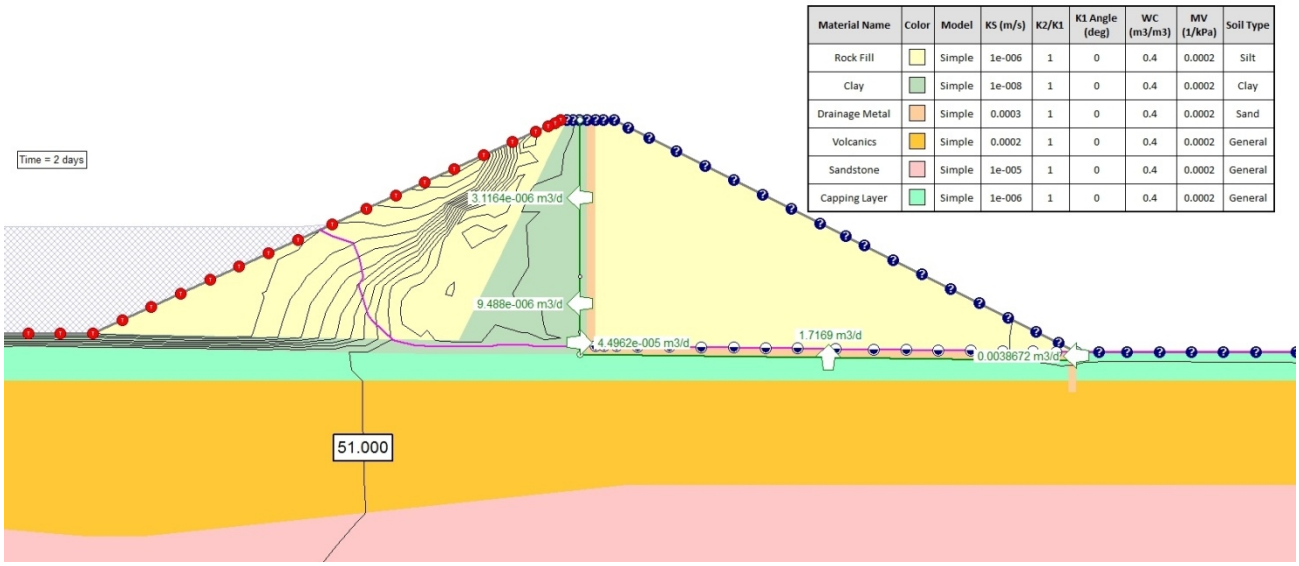

Figure 7. Transient groundwater analysis

al (2005), which has specific criteria for determining the filter design gradations for the critical filters. Two filter gradings are recommended, with the coarser (all gravel-sized, >2mm particle diameter) drainage material only to be used in the high capacity strip drains. The second filter material consists of well-graded sandy gravel with less than 2% fines. A horizontal drain thickness of 250mm, which is approximately 20 times the maximum particle diameter, has been adopted to prevent segregation of particles in the filter blanket.

An upstream clay liner on the left abutment is provided as a means to reduce seepage potential and pressures in the left abutment foundation. The clay liner is 1m thick and extends 20m from the upstream toe of the dam. This liner was modeled in the seepage analysis.

A transient groundwater analysis of flow through the dam embankment and foundation was prepared using the Slide software package groundwater function. An input hydrograph of the three day 1% AEP storm event on the upstream side of the dam was provided, which has a maximum water level after 1.32 days and no water in the basin after 2.32 days. The permeabilities for the embankment and foundation materials were inferred from the packer test and falling and constant head test results and from assumptions based on the geological model for the dam embankment and foundation materials. A key assumption in the Slide model is a pressure head of zero in the horizontal drain on the downstream shoulder, which assumes the drain is flowing in a large detention event. A printout from the Slide groundwater model is shown in Figure 7. The analysis is sensitive to input parameters and assumptions.

The highest flowrate into the horizontal drains was obtained on a mid-slope section on the left abutment, with the most likely flowrate into the drains ranging between 0.3 and 2 m^3/d/m. Assuming the most conservative parameters in the analysis, a value of 34 m^3/d/m is obtained. Lower flowrates were calculated for the lower left abutment and central dam sections. A design flowrate of 1 m^3/d/m has been used in design of the horizontal drains on the left abutment. The proposed strip drains on the left abutment achieved a FoS of 11 for this design flowrate, which is greater than a FoS of 10 that is considered acceptable for the drains.

4. Conclusions

The proposed 18m high Kotuku flood detention dam is a high PIC embankment dam to be constructed on the Nihotetea Stream to reduce flooding in Whangarei City. The dam is located within a complex geological environment with three different geological units including a moderately permeable basalt lava flow and flow margin within the dam foundation. Detailed site investigation has been undertaken to assess the subsurface conditions and prepare a geological model. Foundation treatment, embankment, seepage, and internal drainage designs have been prepared for the proposed dam, which include a clay liner, undercuts of alluvial and selected residual and flow margin materials, toe drains, and internal drainage. The dam is scheduled for construction in the 2014/2015 earthworks season.

5. References

Fell R., MacGregor P., Stapledon D., Bell G. (2005). *Geotechnical Engineering of Dams.*

Martin V., Tate D., Camuso J., Howse B. (2013). *Proposed Kotuku Flood Detention Dam.*

NZSOLD (2000). *New Zealand Dam Safety Guidelines.*

Proceedings of the 10th ANZ Young Geotechnical Professional's Conference – 10YGPC
Noosa, Queensland, Australia
10 – 12 September 2014

DESIGN CONFIGURATIONS OF STONE COLUMNS AS A MITIGATION MEASURE AGAINST LIQUEFACTION-INDUCED LATERAL SPREADING

Elby TANG
Tonkin & Taylor Ltd, Auckland, New Zealand

ABSTRACT - Liquefaction-induced lateral spreading is a common phenomenon after strong seismic events. Typically lateral spreading occurs in sloping ground close to waterways in regions with liquefiable underlying soils and may result in significant damage and lead to significant replacement expense of existing buildings and structures. The installation of stone columns may be used to reduce liquefaction potential for foundations in level ground but there is little literature on stone columns being used to mitigate liquefaction-induced lateral spreading. This paper presents findings of a study to evaluate the effectiveness of stone columns to mitigate liquefaction-induced lateral spreading. A case study from the recent 22 February 2011 Christchurch Earthquake was used as a basis of the study and the study was carried out using effective stress analysis with the finite element software package FLAC v7.0. Current state-of-the-art design procedures for stone columns to prevent liquefaction have been used to assess its applicability to mitigate lateral spreading. The effects of lateral extent of the improvement zone and the area replacement ratio of stone columns have been investigated. Generally, it was found that stone column remediation was found to be effective in reducing the lateral displacement that was caused by liquefaction due to the seismic event in the numerical analyses. However, complementary ground improvement measures may be required to eliminate lateral displacement adjacent to the waterway.

1. Introduction

Liquefaction has been responsible for many failures of man-made and natural structures. Liquefaction-induced lateral spreading has been commonly documented after strong seismic events such as the sequence of Christchurch earthquakes that began on 4 September 2010. In this paper, two dimensional numerical analyses were used to assess the effectiveness of stone columns in mitigating liquefaction-induced lateral spreading. The state-of-the-art design procedures for stone columns to prevent liquefaction were used in the numerical modelling as the basis of assessing their applicability to mitigate lateral spreading. A case study from the Christchurch 22 February 2011 Earthquake was used to calibrate the numerical model for the study. Focus is placed on the reduction in accumulated surface lateral deformation and excess pore water pressure within the improved ground. The effects of lateral extent of the improved zone and the area replacement ratio of stone columns have been investigated.

2. Stone Columns

The installation of stone columns mitigates the potential for liquefaction by increasing the density of surrounding soil and allowing drainage to control pore water pressure generated. The introduction of stiffer elements, which can potentially carry higher stress levels and reduce the stress levels in the surrounding soils (Priebe 1991), provides resistance to deformation. These effects may reduce the build-up of excess pore water pressure which in turn, reduces the liquefaction potential, and the associated ground deformations.

Recently, installation of stone columns to mitigate liquefaction-induced lateral spreading has been investigated (e.g. Elgamal et al 2009) and it was concluded that stone columns were effective in reducing lateral deformation in sandy stratum. However, the current stone column design methods for liquefaction mitigation available in literature (Priebe 1998; Baez and Martin 1995) are largely focused on its implementation on level ground and foundation design, and not for lateral spreading.

3. Methodology

3.1 Model Definition

3.1.1 Representative site location

The selected site for the analysis is adjacent to the Avon River in the suburb of Dallington. It is located near the artificially straightened reach of the Avon River known as Kerrs Reach, about 2km to the east of the Christchurch CBD. Figure 1 below shows the site location map of the representative section.

Following the 4 September 2010 and 22 February 2011 earthquakes, Robinson et al. (2011) took field measurements of lateral spreading at various sites in Christchurch. The results from the field measurements show that the cumulative displacement along the closest transect, which was approximately 200m to the south, was approximately 0.8m. The lateral displacement data from this study was used as the basis to calibrate the FLAC numerical model.

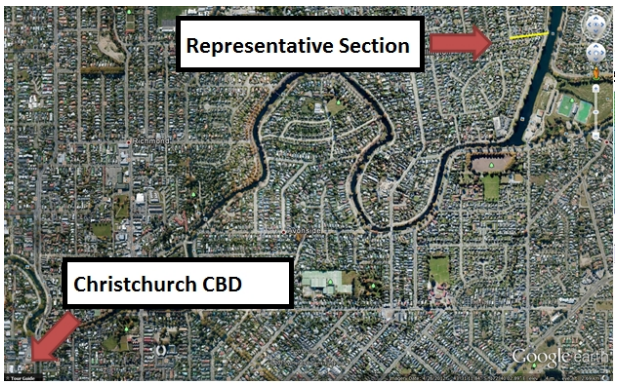

Figure 1. Site Location map of the representative section

3.1.2 Geological Section

To avoid complex geometries in the numerical modelling, the subsurface geological profile has been simplified to represent a generalised profile in the vicinity of the site and subsoil strata have been assumed to be horizontal. The slope geometry has been approximated from LiDar surveying results. Based on available CPT data (CGD 2012), the site is assumed to consist of three geological units: a sandy gravel crust 1.7m thick, overlying 8.2m of loose to medium dense sand which is underlain by dense sand with interbedded silt layers. Figure 2 shows a FLAC screenshot of the geological section used in numerical analyses. The groundwater levels which underlie the subject area are assumed to range from 0.9m to 3.2m below the existing ground surface. The model defines the centre of the river as x=0m, and the crest of the river is at approximately x=-31m.

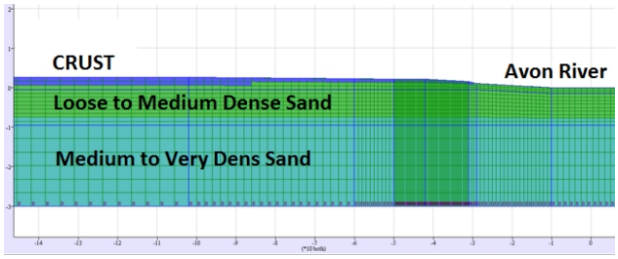

Figure 2. FLAC geological section for modelling

3.2 Static and dynamic material parameters

Subsoil material parameters have been interpreted from the borehole and CPT logs results. The materials subsurface shear wave velocities and dynamic characteristics were derived from the MASW geophysical testing results in the area. The dynamic characteristics of all soils in the model were assumed to be governed by the Seed and Idriss (1971) modulus reduction and damping ratio curves.

3.3 Strong motion record used for analyses

Seismic records from Riccarton High School (RHSC) station were considered to be suitable because no liquefaction was observed here. As the ground motion recorded at the RHSC station was recorded at the ground surface, where the input motion in the FLAC numerical model is at the base of the model, a Deconvolution analysis is required in order to model the representative motion at the base of the mode. The strong motion record was corrected into the direction perpendicular to the cross section and deconvoluted to the depth of engineering rock using a 1-D wave propagation programme Strata (University of Texas, 2009) prior to input to the numerical model. Figure 3 shows the input motion for the numerical analyses.

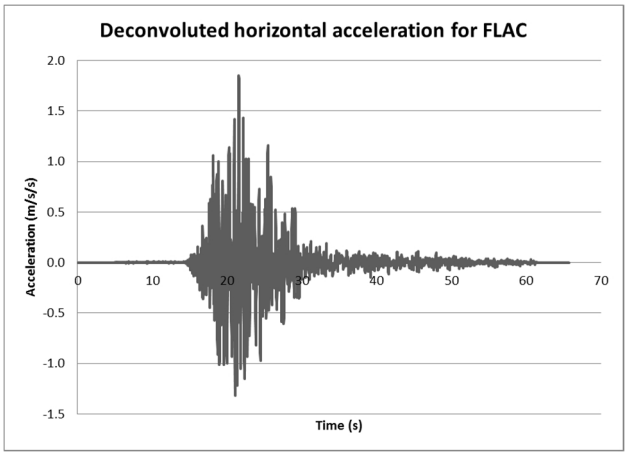

Figure 3. Deconvoluted horizontal acceleration for input into FLAC

3.4 FLAC numerical modelling

The finite difference numerical analysis program FLAC v. 7.0 (Fast Langrangian Analysis of Continua) in 2D was employed in this study. A coupled effective stress analysis was performed using a simple material model to simulate the behaviour of the soils, including liquefaction. The soil behaviour is based on the Mohr-Coulomb plasticity model with material damping added to account for cyclic dissipation during the elastic part of the response and during wave propagation through the site. Liquefaction was simulated using the Finn-Byrne model, which incorporates the Byrne (1991) relation between irrecoverable volume change and cyclic shear-strain amplitude into the Mohr-Coulomb model. Further details of the modelling are presented in Tang (2012).

3.5 Stone column modelling

3.5.1 Stone column parameters

The basic design parameters of stone columns include the stone column diameter, D, pattern, spacing and the backfill material to be used. The diameter of the stone columns in this study has

been chosen to be 750mm. For the purpose of this study, a square pattern has been modelled with an effective diameter (De) equal to 1.13S where S is the spacing of stone columns. The resulting equivalent cylinder of material having a diameter De enclosing the tributary area of soil and one stone column is known as the unit cell. For this site, the Area Replacement Ratio, ARR (ratio of area of the stone column after compaction (Ac) to the total area within the unit cell) was determined to be 15%. The stone columns were modelled to be installed immediately adjacent to the crest of the waterway.

3.5.2 Modelling a 3D problem in 2D

A series of parallel trenches was used to represent the 3D stone column grid in 2D. The stiffness as well as the permeability of both soft soil and coarse grained inclusion needs to be adapted in order to model the deformation behaviour and drainage conditions correctly. Hird et al. (1992) and Indraratna & Redana (2000) recommended methods to perform a conversion of permeability. These transformations are also applicable to model smear effects. The ideal drainage performance of stone columns can be reduced by a smear zone. During the installation of stone columns, the structure of the soil immediately adjacent to the stone column may be disturbed, leading to a reduction of horizontal permeability. This zone of disturbed soil is called the smear zone.

3.5.3 Stone column mechanisms

3.5.3.1 Densification effect

The effect of granular pile installation on the modifications induced in loose to medium dense granular deposits was studied by Murali Krishna and Madhav (2009). Their findings were presented in the form of design charts that can be used design the required degree of treatment for the expected improvement or to estimate the improved SPT N_1 values of treated ground for respective area replacement ratios and SPT N_1 values of insitu ground. The improved SPT N_1 value for the studied site has been determined to be 26 from these charts,. Moreover, studies have shown that densification of the in-situ soil surrounding the stone columns decreases with distance away from the stone column (Obhayashi et al. 1999 and Weber et al. 2010). They determined that the extent of the disturbed zone is approximately 2.5 times the radius of the stone column and this was adopted in this study.

3.5.3.2 Reinforcement effect

As the current study is a 3D problem being modelled in a 2D model, the stiffness of the stone columns needs to be modified in order to model the deformation behaviour correctly. In a 2D plane strain model, the stone columns will be represented as an infinite trench with a width equal to the diameter of the stone column rather than a single column. The vertical stiffness of the column material used in the 2D model was calculated as an equivalent stiffness of individual columns in a 3D space.

3.5.3.3 Drainage effect

The drainage condition needs to be revised from a 3D problem into a 2D simulation. The excess pore pressure dissipation should be similar in both systems – the radial drainage system must equal the plane drainage system. The Idraratna & Redana (2000) equations to estimate plane strain permeabilities were used in the study. Weber et al. (2010) studied the smear zone and densification zone around stone columns and the smear zone was described as a strongly sheared and remoulded zone, which leads to a reduction of horizontal permeability in this zone. In this study, the smear zone was assumed to be 1/3 of the column radius, i.e. 0.125m. The horizontal permeability of the smear zone was determined by formulae defined by Indraratna & Redana (2000).

4. Numerical Results

4.1 Control model – no stone columns

Figure 4 illustrates the calculated surface displacements by the FLAC numerical model and the measured cumulative lateral displacements at transect CH_DAL_15 by Robinson et al. (2011). The figure shows that there is a similar 'exponential decay' distribution where the lateral spreading displacements rapidly decrease with the distance from the waterway. This is consistent with the conventional liquefaction induced lateral spread mechanism where the lateral spreading displacements reduce exponentially away from the riverbank. The calculated surface lateral displacements by FLAC were compared to the field measurements by Robinson (2011). The magnitude of lateral spread between the field measurements and the FLAC calculations at the crest off the bank differed by about 20%. This could be due to the stream bank in FLAC being modelled on the loose silty GRAVEL, where in real life the bank may be supported by vegetation or small man-made structures. The difference in lateral displacements between the calculated and measured values reduces to zero at approximately 100m away from the centre line of the river. Such difference is considered acceptable and comparable considering the displacement trend is reasonably similar.

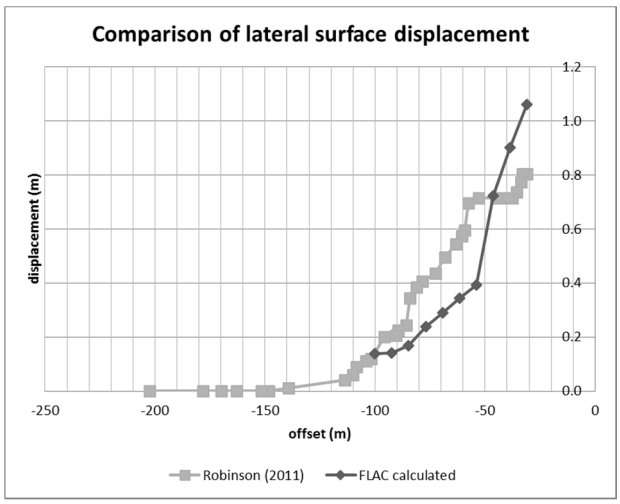

Figure 4. Comparison of lateral surface displacement between Robinson (2011) field measurements and FLAC calculated displacements with distance away from river centre line.

4.2 Stone column models

4.2.1 Varying lateral extent of improvement zone

Figure 5 illustrates the comparison of lateral surface displacements between the different numbers of stone columns modelled. There is an obvious trend that as the improvement zone is increased, the lateral displacement along the surface on the cross section is reduced. It can be seen that as the number of stone columns increases, the curvature of the lateral displacement distribution increases. The lateral surface displacement reduces more rapidly with respect to distance away from the crest of the waterway as more stone columns modelled. It should be noted that there is little difference in the lateral displacement at the crest of the riverbank for all cases, varying by approximately 0.1m. This could be explained that the sloping riverbank is still vulnerable to gravitational inertia forces close to the crest of the river driving the soil mass down the slope. Furthermore, the first stone column was modelled at 1.0m away from the crest of the slope, so the 1.0m column of soil directly adjacent to the crest of the riverbank may have benefit from the densification effect, but does not have an increased stiffness. The stone columns could be installed right on the edge of the riverbank for improved results.

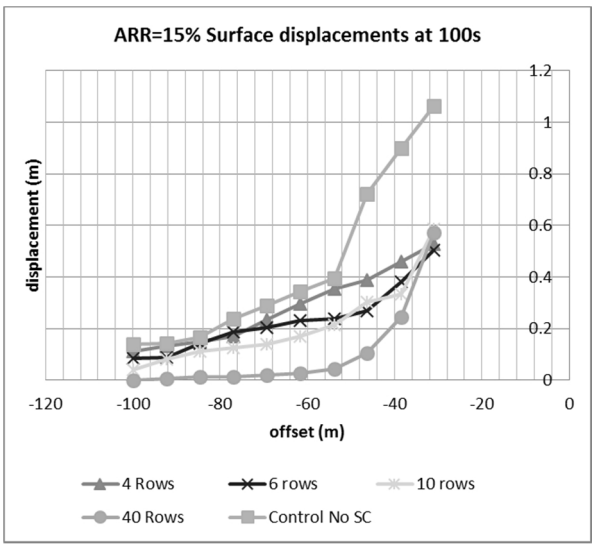

Figure 5. Comparison of lateral surface displacement for stone columns with ARR=15% with varying improvement zones with distance away from river centre line.

The figure shows that four rows of stone columns are not adequate to mitigate liquefaction and the associated lateral spreading towards the riverbank in this subject site. Even though structures may not be built directly adjacent to the Avon River, the displacements are still relatively high at distances further away from the crest. In contrast, in the model where 10 rows of stone columns were modelled, there is a steep gradient over the first 8m away from the crest of the riverbank, which reduces lateral displacement from 0.59m to 0.34m, reducing further to 0.2m to approximately 23m away from the crest of the riverbank. Typically, in the area of the subject site in the Dallington suburb, the closest structure adjacent to the Avon River is the road, which is at least 20m away from the crest of the riverbank, and the closest residential dwelling is approximately 40m away from the crest of the riverbank. At 20m away from the crest of the river (x=-51m), the models with 6 rows and 10 rows of stone columns recorded a lateral displacement of approximately 0.25m whereas the model with four columns recorded a lateral displacement of 0.38m. The model with 40 rows of stone columns recorded a lateral displacement of 0.06m, which may be within the tolerance of these man-made structures.

The lateral surface displacement close to the crest of the riverbank is between 0.5m to 0.6m where stone columns are modelled at ARR=15% even when the improvement zone is extended to 40 rows of stone columns. This implies that the ground improvement near the crest of the riverbank is not adequate to withstand the gravitational inertia forces caused by the sloping geometry of the cross section.

Another way to improve the system of stone columns is to increase the ARR, i.e., installing the stone columns at closer spacing to achieve a stiffer and more densified improvement zone with shorter

drainage paths. This should reduce liquefaction potential in the improved zone. Stone columns with an ARR of 20% were analysed.

4.2.2 Stone columns with ARR = 20%

Figure 6 illustrates the surface lateral displacements along the cross section plotted for the different stone column configurations. For four rows of stone columns with an ARR of 20%, the maximum lateral displacement at the crest of the riverbank is approximately 0.51m. The surface lateral displacements then drop rapidly to 0.36m at approximately 8m away from the crest, which is just outside the improvement zone. It should be noted that the closest man-made structure to the Avon River is the road along the Avon River which is approximately 20m away from the crest of the riverbank. At 20m away from the crest of the riverbank, the ARR=20% with four rows of stone columns recorded a lateral displacement of 0.3m, compared to the ARR=15% case which recorded a lateral displacement of 0.38m, which is a 21% improvement.

The distributions of lateral surface displacement along the cross section showed a similar trend to the ARR=15% case. An increase in the number of stone columns, results in a greater rate of decrease in lateral displacements with respect to distance away from the crest. At 20m from the crest, the model with 6 rows and 10 rows of columns showed lateral displacements of 0.26m and 0.20m respectively.

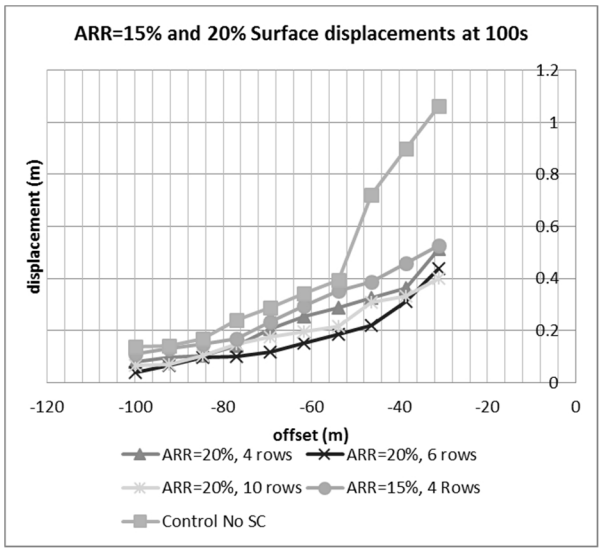

Figure 6. Comparison of lateral surface displacement along the cross section with an ARR=15 and 20% and varying the improvement zones with distance away from river centre line.

5. Discussion

It was found through the analyses that the recommended area replacement ratio estimated using the Priebe and Grundbau (1998) method did not totally eliminate lateral spreading towards the Avon River with a system of four rows of stone columns, resulting in lateral displacements in excess of 0.5m close to the crest of the riverbank. Even this 0.5m of lateral displacement could be very damaging to any underground pipelines, cables or structures that may be constructed close to river. However, it was noted that large displacements at the crest of a waterway may not be critical as the closest structures may be several metres away. The closest structure next to the river for the case study is the road that runs along the Avon River, which is approximately 20m away from the crest of the riverbank. A lateral displacement of 0.35m was calculated at a distance of 20m away from the crest of the riverbank. This magnitude of lateral displacement is considered to be detrimental for any underground services, which are commonly laid beneath roads.

More rows of stone columns were also modeled with the same ARR. It was found that as more rows of stone columns were added, lateral surface displacement decreases at a higher rate with distance from the crest of the riverbank. Where the ground improvement zone is extended to 40 rows behind the crest of the riverbank, the lateral surface displacement at the crest was still in excess of 0.5m, but at 20m away from the crest was approximately 0.1m, which could be acceptable.

6. Limitations and Recommendations

Many assumptions have been made in this study. These assumptions have largely been made on the basis of current literature, but it is understood that there are various limitations to the study. These have been summarised below.

- Only one input ground motion has been used
- Only one cross section has been analysed
- Results were compared to lateral displacement data that was recorded at a site 200m away
- Numerical model in 2D for a problem that is essentially 3D

Further studies would be recommended to produce design charts for stone columns used for mitigating liquefaction induced lateral spreading. A much more comprehensive parametric study analysing different slope geometries, subsoil parameters, groundwater levels and varying input motions would be required to create design charts that would determine the area replacement ratio and the extent of improvement zone required. It would be recommended that these studies be performed using three dimensional numerical modelling to mimic the physical problem as closely as possible. The current study could be further developed into a three dimensional analyses using FLAC 3D, and results from the 2D model and 3D model compared to investigate any differences and the validity of the current 2D model.

7. Conclusions

A study was carried out to assess the effectiveness of stone columns against liquefaction induced lateral spreading using the finite difference programme FLAC. A site in Christchurch which was affected by the February 2011 earthquake was used for this purpose.

Overall, the investigations have shown that the current design procedures are adequate for design of stone columns against earthquake induced liquefaction on a level site, but complementary improvement around the crest of the slope may be required to reduce lateral displacements to tolerable levels close to the crest of a slope or a waterway.

The installation of more rows of stone columns was shown to greatly decrease lateral displacement. However, the installation of some 40 rows of stone columns along a 500m stretch of the Avon River would not be feasible considering there are residential buildings 40m away from the river, and the economic costs of constructing this system of stone columns. It is therefore a problem of optimisation between displacement tolerance, available space and economic costs to decide the extent of the improvement zone width behind the river.

8. References

Baez, J. I., and Martin, G. R. (1995). Permeability and shear wave velocity of vibro-replacement stone columns. Geotech. Spec. Publ., 49, 66-81.

Byrne, P. M. (1991) A Cyclic Shear-Volume Coupling and Pore-Pressure Model for Sand. Proceedings: Second International Conference on Recent Advances in Geotechnical Earthquake Engineering and Soil Dynamics. 1.24, 47-55.

Canterbury Geotechnical Database (2012) "Liquefaction and Lateral Spreading Observations", Map Layer CGD0300 - 11 Feb 2013, retrieved April 2013 from) from https://canterburygeotechnicaldatabase.projectorbit.com/

Elgamal, A., Lu, J., and Forcellini, D. (2009). Mitigation of Liquefaction-Induced Lateral Deformation in a Sloping Stratum: Three-dimensional Numerical Simulation. J. Geotech. Geoenviron. Eng., 135(11), 1672–1682.

Hird, C. C., Pyrah, I. C., & Russel, D. (1992). Finite element modelling of vertical drains beneath embankments on soft ground. Geotechnique, 42(3), 499-511.

Indraratna, B., & Redana, I. W. (2000). Numerical modeling of vertical drains with smear and well resistance installed in soft clay. Canadian Geotechnical Journal, 37(1), 132-145.

Murali Krishna, A. and Madhav, M. R. (2009). Treatment of loose to medium dense sands by granular piles: Improved SPT 'N1' Values. Journal of Geotechnical and Geological Engineering, 27 (3): 455-459.

Obayashi, J., Harada, K. and Yamamoto, M. (1999). Resistance against liquefaction of ground improved by sand compaction pile method. Earthquake Geotechnical Engineering, Seco e Pinto (ed.), Balkama, Rotterdam, 549-554.

Priebe, H. J. (1991). The prevention of liquefaction by vibro replacement. Proc., 2nd Int. Conf. On Earthquake Resistant Construction and Designs, S. A. Savidis, Ed., A. A. Balkema, Rotterdam, 211-219.

Priebe, H. J. and Grundbau, K.(1998). Vibro Replacement to prevent earthquake induced liquefaction. Ground Engineering, 31(9), 30-33

Robinson, K., et al. (2011) Field measurements of lateral spreading following the 2010 Darfield earthquake. Proceedings of the Ninth Pacific Conference on Earthquake Engineering.

Seed, H. B. and Idriss, I. M. (1971). Simplified procedure for evaluating soil liquefaction potential. Journal of the Soil Mechanics and Foundations Division, 97(SM 9): 1249-1273.

Tang, E. (2012). Stone columns as a mitigation measure against liquefaction-induced lateral spreading. Master's Thesis, University of Auckland, Auckland, New Zealand.

Weber, T. M., Plötze, M., Laue, J., Peschke, G., & Springman, S. M. (2010). Smear zone identification and soil properties around stone columns constructed in-flight in centrifuge model tests. Geotechnique, 60(3), 197-206.

Proceedings of the 10th ANZ Young Geotechnical Professional's Conference – 10YGPC
Noosa, Queensland, Australia
10 – 12 September 2014

BIRDS HILL REMEDIATION FOLLOWING 2011 TASMAN FLOOD EVENTS – A CASE STUDY.

Rebecca RYDER
MWH New Zealand Ltd., Nelson, New Zealand

ABSTRACT – In 2011 674 mm of rain fell over a 48 hour period in Golden Bay, Tasman, triggering a devastating one in 500 year flood event. As a result several Golden Bay communities were isolated from the rest of the Tasman region and multiple lifeline networks were severed. Slope failure cut off crucial roading networks, flood waters caused extensive damage to waste water and water supply systems as well as communication and power line networks.

This case study focusses on the slope failure at Birds Hill on SH60 near Takaka, Golden Bay. Both lanes of the road were completely lost due to a slip below the carriageway. This failure required rapid reinstatement as SH60 provides the only road access to a number of towns north of Takaka. A temporary access road was cut into the hill-side, however a long term solution was needed.

A reinforced fill slope was selected as the preferred remedial solution. SlopeW modelling software was used to verify the design and assess the potential impact of geological and geometric variations to the design. The opportunity to realign was used to improve the safety of this section of road and provide additional space for cyclists. Remedial works were completed December 2013.

1. Introduction

Following persistent rainfall over 13-15 December 2011 in the Nelson and Tasman region (New Zealand) a number of landslides occurred along with widespread flooding damage.

The region was declared to be in a state of civil emergency on the 14th December (Wopereis, 2014). Teams of geotechnical specialists were deployed to inspect the affected properties and life-line structures around central and rural areas.

The heavy rainfall caused two ground failures on Birds Hill located along SH60 in Golden Bay, Takaka, New Zealand (Wopereis, 2014). One of these two noted failures was a smaller slumping failure and the other a more significant drop-out which removed the full road width, severing the only access route to the settlement of Collingwood, north of Takaka. This paper summarises the rainfall event before focusing on the large Birds Hill drop-out failure and subsequent design and remediation.

2. Rainfall Event 13-15 December 2011

The December 2011 rainfall caused a 1 in 500 year flood event in the Nelson and Tasman regions. Rainfall was not particularly heavy, but it was persistent over a 48 hour period. This weather system was caused by a trough stalled between a low in the Tasman Sea and a high to the east of New Zealand (Stephens, 2012). The recorded rainfall for various Tasman/Nelson regions is recorded in Table 1 below. The total rainfall for the event in Takaka was recorded as 674mm which is around a third of the regions normal total annual rainfall (Stephens, 2012). This excessive volume of rain fell within 48 hours which set a New Zealand record for coastal rainfall (Wopereis, 2014).

Table 1. Nelson/Tasman region rainfall recorded over 48 hour period, December 2011 (Tasman District Council, 2012).

Region/Zone	Rainfall Recorded over 48 hours
Takaka	674mm
Richmond	281mm
Nelson	300mm

3. Civil Defence Emergency Response

The heavy rainfall caused widespread flooding and landslips. Many residential homes were impacted and had to be evacuated. Some rural towns were temporarily cut off by surface flooding and land-slips. After the state of emergency was declared on the 14th December, the Nelson/Tasman Civil Defence response was initiated. As a significant part of this emergency response, geotechnical specialists, both from within the region and around New Zealand, were deployed to carry out inspections of properties impacted during the event.

Teams of geotechnical engineers and engineering geologists travelled from Nelson to the rural settlement of Takaka which had been badly affected with damage to many lifeline access roads. The Birds Hill Slip was quickly identified as a critical site which needed urgent attention.

As a result of the drop out on Birds Hill the only access route to Collingwood was lost (Stephens, 2012). This had economic implications as there are numerous dairy farms in the area requiring road access to export milk on a daily basis. Temporary single lane access was created by cutting into the hill side and side-casting fill material. The steep

terrain prevented further widening of the road, so it was not possible to provide more than one lane using this temporary solution (MWH, 2012).

4. Birds Hill Slip – Geotechnical Assessment

Birds Hill is located in Golden Bay approximately 3km north of Takaka on the Takaka-Collingwood Highway / SH60. The road carriage-way was constructed in the 1960's. It traverses the lower hills crossing a series of ridges and gullys. It is likely that the cut material produced from the road excavation through the rocky bluffs was then re-used as fill material in the gullys (Wopereis, 2014). The toe of the hill merges with the flood plain that extends to the sea. An abandoned historic highway reportedly built around the 1870's is still visible at the toe of the slope. The land above the site is covered with regenerating native forest. The floodplain downslope is generally covered in pasture (MWH, 2012).

The underlying geology of the site is mapped by GNS Sciences and illustrated in the published geological map of Nelson Area (Geology of the Nelson Area, Scale 1:250,000, GNS Map 9, 1998). The map indicates that the site is generally underlain by the Onekaka Schist that is locally covered by the Motupipi Coal Measures. The Onekaka Schist exposed in cut batters alongside the highway is moderately to highly weathered. Clayey soils mantle the slopes in the vicinity of the sites. The flood plain at the toe of the hill is comprised of recent fluvial deposits.

The large under-slip at Birds Hill SH60 affected the full road width but did not impact the slope above the road. It was identified that the area which failed was an old gully which had been filled to allow the road to pass between the rocky spurs on either side (Figure 2). The failure appeared to have originated in the fill material, likely to have been placed during the construction of the road. The failure extended vertically to expose the Onekaka schist bedrock at the steepest part of the headscarp. It was also noted during the initial inspections that a services duct which ran along the back of the slip could have contributed to the failure. The services duct was observed after the slip event to be conducting water from further up the road. The duct had ruptured and water was spilling out at the head-scarp of the Birds Hill slip. This theory was not conclusive however, as the pipe may have been ruptured during the slip movement rather than contributing to the failure.

5. Site Investigation / Reconnaissance Data

Investigations carried out at the location of the main slip comprised 12 Dynamic Cone Penetration Tests completed at the top of the slip with six Scala Penetrometer tests and test pits on the face and toe of the slip. This information was used to develop a geological model. A bedrock profile was inferred based on the outcropping rock spurs and mapped geology above the slip. The four main geological units encountered during the site investigation were: Onekaka Schist, Motupipi coal measures siltstone, sandstone and clayey colluvium fill comprised of clay/sandy silt (MWH, 2012).

Groundwater was reportedly located between 1.0m and 3.0m depth at various points down the slip face. It is likely that insufficient drainage was a significant contributing factor to the slope failure (MWH, 2012). This assessment is based on the lack of culverts through the natural low point of the gully as well as the possibility of the services duct leaking water directly into the gully at the head-scarp of the slip.

6. Birds Hill Remedial Solution Concept

As this section of road is a state highway (SH60), the basis of design was controlled by NZ Transport Agency (NZTA) requirements. NZTA framework dictated the design life, seismic loading and factors of safety that had to be met in the analysis.

No lab testing was carried out on any of the geological deposits. Geological design parameters were based on literature and engineering judgment. Due to the high uncertainty associated with the design input information, sensitivity analysis was carried out during the modelling phase. This ensured that there was sufficient robustness in the design and that the model was not disproportionately dependent on a particular input parameter. The analysis explored the sensitivity of the model to geological material parameters, the inferred depth to bedrock and the inferred ground water level down the slope. These parameters were varied within a range of approximately +/-15% and were analysed individually to ensure that results could be interpreted correctly. It was verified that the design was sufficiently robust and would still maintain acceptable stability if the conditions were not as exactly as assumed for modelled purposes. If further site investigations or lab testing of the site materials had been carried out, the design may have been further refined at this stage, possibly reducing the cost of materials and therefore construction. However, the client preferred that a more robust design was adopted to account for the unknown conditions.

The final conceptual design consisted of an engineered fill slope providing sufficient width to reinstate the double lane carriageway, as well as space for cyclists and a berm.

The fill used to construct the slope was to be taken from the rocky bluffs above the road. This method of cut-to-fill was efficient and simple to monitor. This was particularly beneficial for the Birds Hill site which had limited storage space for fill materials. By removing material from the inside

slope above the road it also allowed for improved traffic sight distance as the sharp corners were removed from the cut batters.

7. Model Development

The remedial design for Birds Hill was developed using the slope stability analysis software program SlopeW by Geo-Slope International Ltd. Physical geometry of the slope in cross-section was obtained from survey information captured immediately after the main slip occurred and again after single lane access had been reinstated. A simplified geological model was created based on the available site investigation data.

The gully where the slip failure occurred was assumed to be roughly v-shaped, with out-cropping bedrock mapped along two ridgelines. It was known that an engineered fill slope could be founded on bedrock at either edge of the gully. The worst case however was a section through the middle of the gully which had a thick layer of colluvium silt/clay overlying the bedrock. Bedrock was estimated to be much deeper in the middle of the gully as it was not encountered during site investigations. Using the mapped (visible) profile of the bedrock from above the road, along with the spurs of rock on either side of the gully below, the inferred bedrock profile indicated that through the middle of the gully bedrock was potentially up to 10m below the existing ground level. For this depth to bedrock, it was not financially viable to dig out and replace all the colluvium material. A fill slope design solution had to be found that would satisfy the design criteria without needing the slope to be excavated down to bedrock across the width of the slip.

Figure 1 is the design cross-section through the middle proposed fill slope footprint. This was identified as a 'worst case design scenario' through the deepest part of the gully as the colluvium is at an estimated maximum thickness of 10m over the bedrock. The design of the fill slope shown was verified to meet NZTA criteria based on this assumed 'worst case' where the slope toe is founded on colluvium. However the reality is that approximately one half of the engineered fill slope toe is founded on bedrock rather than on colluvium, at the edges of the gully. The sections of wall with a bedrock foundation were found to have a much higher FOS against significant failure than that of the design sections founded on colluvium (Figure 1). By limiting the width of the engineered fill slope which is founded on colluvium rather than bedrock, it is inferred that the stability of the slope has been maximized, while keeping within financial constraints of the project.

Using the SlopeW program, both circular and wedge failures were analysed. Circular failures gave the most critical slip planes, so these were used in the sensitivity analysis. The design process focused on the risk of failure to the road carriage-way. Some minor surficial failures below the road were identified as having a FOS lower than the design threshold of NZTA requirements; however these failures were very shallow, small in extent and did not impact the road carriageway or berm.

Subsoil drains were trenched in below the engineered fill slope face with cut-off drains running laterally across the width of the slip. Installation of this drainage network reduces the chances of future landslips as a result of high rainfall/flooding in the area.

In addition to the fill slope design, new drainage provisions and road layout design were implemented. Both provided improvement to the road, compared to its condition prior to the slip.

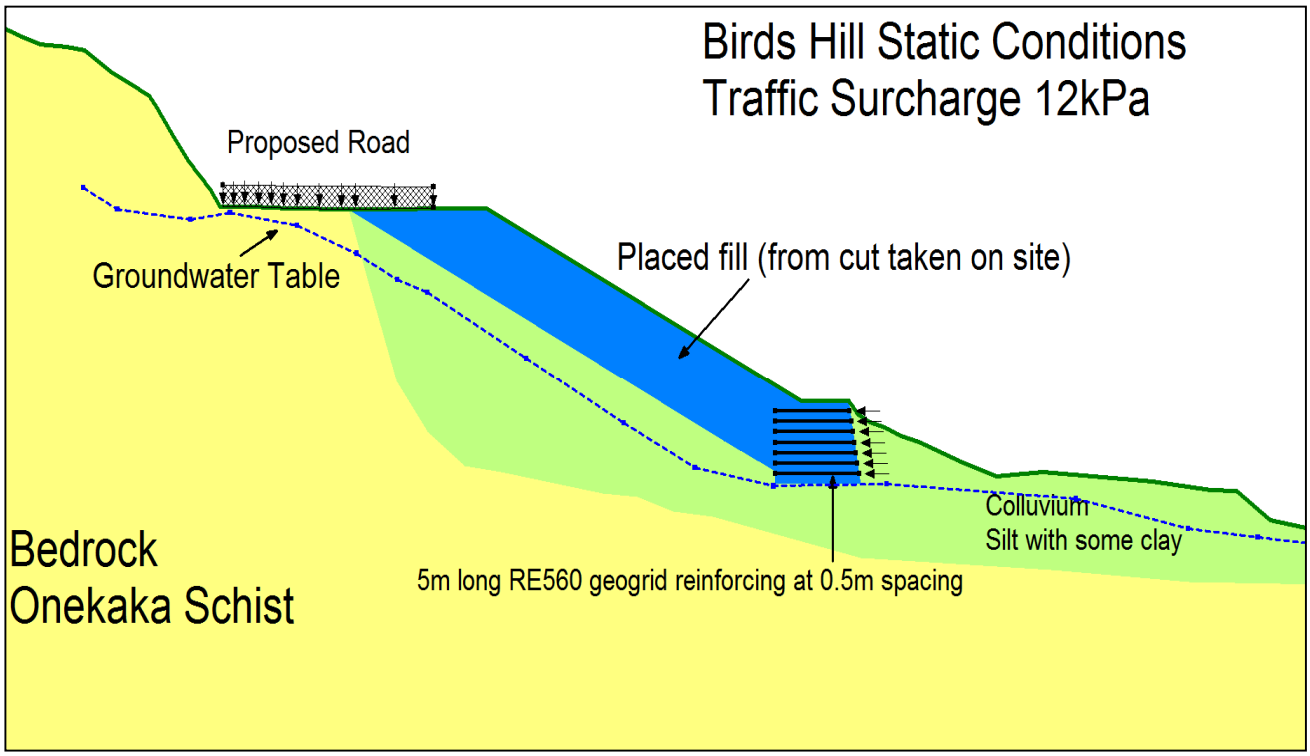

Figure 1. SlopeW model used for the analysis of remedial solutions at Birds Hill.

8. Fill-Slope Construction and On-going Works

Side-cast material had been cut and dumped downslope as part of the emergency works to provide the temporary single lane access through Birds Hill. To prepare the Birds Hill slip site for construction, excavation of the side-cast material was required to provide a stable foundation for the engineered fill slope. To reduce the likelihood of future instability or settlement all of the uncontrolled side-cast fill needed to be removed. The excavation proved to be difficult as it was not clear exactly where the boundary was between the *in-situ* colluvium and end-tipped fill material. Information gathered from survey data was used to verify that excavation was taken deep enough to remove all of the uncontrolled fill.

Originally, a long length of the road cut-batter through Birds Hill was to be trimmed during the construction phase of the engineered fill slope. This would have allowed good quality fill material to be selected from a large volume of cut. A change was made to the construction program that reduced the extent of the cut-batter excavation completed. This meant that fill material was suddenly limited in volume and the engineered slope had to be constructed out of whatever material was provided at that particular stage of the program. The cut material available was much more weathered, and therefore poorer quality, than assumed in the design model. This more weathered, weaker rock had to be used in the fill slope, or the project program would be jeopardized.

Sensitivity analysis provided valuable insight for assessing how a weaker fill source would impact the design. It was concluded that this change of fill strength posed a significant risk to the slope stability. It was agreed that this fill could be used at the toe of the slope, if sufficient reinforcement could be implemented to provide the additional strength required. The design was revised to include a reinforced soil block constructed with layers of geogrid at 0.6m center spacings, extending 5m horizontally at the toe of the slope (Figure 1). The reinforcement eliminated the critical circular failures which were predicted by the SlopeW model for the revised model with a weaker fill material.

To avoid having to include geogrid reinforcement up the full height of the fill slope, less weathered (stronger) material had to be sourced quickly without incurring a significant cost to the project. Alternative fill was located in nearby areas, however to allow the use of this new material additional compaction laboratory testing and plateau testing verification had to be carried out. Some storage and carting costs were also incurred by this change in fill source. The alternative fill sources had a distinctive weathering profile which ranged from highly weathered at the surface, though to moderately weathered deeper into the rock mass. The contractor then had to make an adjustment to the excavation methodology to account for this varying degree of weathering. The most weathered surficial rock was to be removed and dumped. Further cutting of the rock was then made in a way that mixed the highly weathered rock with less weathered rock before it was placed on the fill slope below the road. The SlopeW model was updated and re-analysed with revised fill parameters. By making these changes to the fill

source and excavation methodology it was confirmed geogrid reinforcement was only required at the toe of the slope. Fill was monitored closely to ensure that the material was of an acceptable standard throughout the construction of the engineered slope.

To verify the compaction of the placed fill, Nuclear Densometer (NDM) testing was carried out. Compaction curves were completed on the various fill sources and plateau tests were carried out on site using the rock fill. It was found to be difficult to achieve the required compaction on site, despite the use of heavy compaction plant and applying a methodology verified through plateau testing completed on site. The fill was highly variable having been sourced from multiple locations and appeared to be very sensitive to moisture. This was a particular problem as the main construction period ran through wet winter months of 2012. Moisture content of the fill material had to be preserved by covering stockpiles on site and allowing time for fill to dry after a rain event. A significant amount of time was spent on site attempting to adjust moisture contents and repeating NDM tests to ensure the required compaction was achieved.

The re-construction of the road had to be coordinated with service providers. The construction works provided an opportunity for buried services in the road carriageway to be accessed and improved. Timing of such additional works had to be carefully planned so that the road could be safely trafficked while work continued. Land ownership issues also slowed the progress of the construction. Disagreements between NZTA and local land owners meant that excavation of the various fill sources was delayed while land boundary lines were discussed and defined. It was very important that all of these issues were dealt with as quickly as possible especially as local media was following the project and residents were eager to see the two-lane road reinstated.

As part of the Bird's Hill remediation, trimming of the road cut-batters was undertaken on either side of the main slip zone. During this additional work, a historic landslide was uncovered in one of the new cut-batters above the road (Wopereis, 2014). Despite numerous attempts to trim back the batter in this area, continuing instability and failure of the batter occurred. Geotechnical specialist inspection and instruction along with significant earthworks were required to ensure the safety of this area. As a result the cut batter had to be laid back on a very low angle to prevent on-going instability.

9. Conclusions

The value of investing time and funding in site investigations and laboratory testing was strongly emphasized through this project. Many of the design assumptions and construction issues could have been avoided with a greater emphasis on site investigation and testing early in the project life.

Changes to the construction program meant that the fill material was limited in volume and therefore could not be preferentially selected based on quality. To account for the use of poor quality fill geogrid reinforcement was added to the toe of the slope. Additional fill was later sourced from other near-by areas to prevent the need for geogrid reinforcement up the whole height of the engineered slope.

The additional time and expense of finding additional fill sources, carrying out the required laboratory/site testing and completing further design verification as a result of this was a significant cost to the project. However it was a necessary step to ensure that the engineered fill slope was constructed correctly while keeping to the project program and meeting the expectations of the client and road users.

Today Birds Hill is a much improved section of road (Figure 3) with a wide carriage-way shoulder and improved site distance for motorists and cyclists (NZTA, 2013).

10. References

GNS Science. (1998). Geology of the Nelson Area Map 9, Scale 1:250,000.

MWH. (April 2012). *Geotechnical interpretative and concept options report, State Highway 60, Birds Hill reinstatement* RP89/7.57 and RP89/7.75, Prepared for NZTA.

NZTA. (2013) *State highway projects – SH60 at Birds Hill*:
http://www.nzta.govt.nz/network/projects/project.html?ID=234

Stephens, Joy. (2012). N*elson and Tasman floods* report:
http://www.theprow.org.nz/events/nelson-and-tasman-floods/#.U0-G41WSwso

Tasman District Council, (January 2012). *A storm like no other*. Newsline 237 – January 27 article:
http://www.tasman.govt.nz/tasman/newsline-online/2012/newsline-267-27-january-2012/#storm

Wopereis, Paul – Principal Engineering Geologist, MWH, pers. comm. (December 2011-April 2014)

Figure 2. Birds Hill SH60 Slip, December 2011.

Figure 3. Birds Hill SH60 post-remediation construction, December 2013.

Proceedings of the 10th ANZ Young Geotechnical Professional's Conference – 10YGPC
Noosa, Queensland, Australia
10 – 12 September 2014

A UNIQUE APPROACH TO ROCKFALL PROTECTION – USING A HIGH ENERGY ROCKFALL EMBANKMENT AT COALCLIFF RAILWAY LINE.

Laura STUBBS[1] and Gary MATTHEWS[2]
[1] *Maccaferri, Civil Engineer, Laura Stubbs, Sydney, Australia*
[2] *Maccaferri, National Technical Manager, Gary Matthews, Brisbane, Australia*

A new rockfall protection countermeasure; a reinforced soil embankment has recently been applied along the Coalcliff railway edge. The rockfall embankment is designed and constructed using a "green" reinforced soil technique to intercept and arrest falling rocks. It is called a "green" rock fall embankment or more commonly a Green Terramesh® embankment as the embankment can be completely covered with vegetation to become a living structure.

To develop the reinforced embankment system, rockfall simulation techniques developed by Maccaferri and Polytechnico Di Torino (Italy) were used to evaluate the geometry and size of the structure required to withstand various impact energies, and the interaction between the reinforcement and backfill was checked using Maccaferri's reinforced soil software program, MacStarsW.

This paper looks at solving a common rockfall problem by designing and implementing a highly efficient and environmentally friendly rockfall embankment for Sydney Trains.

1. Introduction

The Coalcliff train line is part of the Illawarra railway network that loops the scenic south coast of New South Wales. In this area, the railway runs along the lower escarpment which has a long history of rockfalls and slope instabilities on the upslope side.

The geology and geomorphology in this area along with intense rainfall events cause boulders and debris to break away from the upslope region. An effective countermeasure for protecting the public and railway infrastructure from the possibility of such rockfall events was therefore needed. The countermeasure would need to absorb the potentially high energy impacts with minimal (if any) maintenance to the structure, be cost effective, easy to construct, withstand a coastal environment and be visually appealing on this scenic part of Wollongong (the establishment of vegetation on the embankment was extremely important to reduce the visual impact and minimise the impact to public consciousness).

A review of possible solutions by the author and client showed rockfall embankments (Figures 1 and 2) optimal for the Coalcliff site. This review was based on previous performance of these structures in protecting communities in the mountainous regions of Italy that are prone to rockfalls and debris flows, and confidence in Maccaferri's design experience for the construction of reinforced soil embankments with heights up to 20 meters and energy capacities up to 20,000 kilojoules.

Figure 1. View of two grassed embankments in the surrounding environment, Cogne, Italy

Figure 2. Areial view of two embankments after the collapse of blocks (>10,000 kJ), Cogne, Italy

These rockfall barriers are typically trapezoidal-shaped soil embankments constructed using reinforced soil techniques that allow locally available materials to be used (Figure 3).

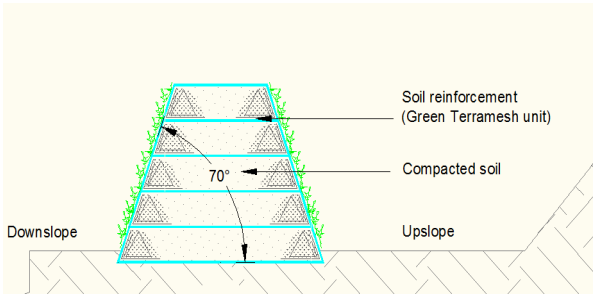

Figure 3. Components of a rockfall embankment

This paper details various phases in rock fall embankment design; kinematics of the block (rock), impact of the block on the embankment and the stability of the embankment itself. The last section of this paper will discuss the construction of the green embankment to guarantee a satisfactory outcome and service life of the structure.

2. Why use a reinforced soil embankment?

Engineers often choose cable mesh rockfall protection barriers to intercept individual falling blocks and falls composed of numerous smaller rocks. However, a disadvantage of a rockfall fence in certain applications is its deflection, limited energy capacity, and the fact that following successful rock impacts, maintenance of the system is often required to reset the barrier for subsequent impacts.

In contrast, rockfall embankments have been designed and constructed worldwide for rock fall protection and are proven to be an effective and reliable solution that can absorb very high energy impacts with little to no downslope deflection and without the requirement for extensive, complicated or expensive maintenance works. Also, the Green Terramesh facing can fulfill the environmental requirements of the client; in a matter of months vegetation can be established to blend in with the local landscape (Figure 4).

Figure 4. Close up of the block which struck the upstream embankment (7,500 kJ impact)

The principle differences between embankments and dynamic cable mesh rockfall fences are compared in Table 1:

Table 1. Feature comparisons between embankments and cable mesh rockfall protection

Feature	Rockfall embankment	Cable mesh rockfall fence
Energy absorption capacity	Tests to 5000 kJ Computational checks for higher capacity systems, greater than 20000 kJ	Tested up to 8500 kJ
Ability to intercept maximum velocity impacts	Very high (no theoretical limit)	Variable (approximately 35 m/s maximum)
Downslope deformation of structure from impact	Very low to none Falling blocks are retained behind, or embedded within the embankment	Yes (current fences are all "dynamic" or semi-dynamic systems)
Installation in immediate proximity to vulnerable structure	Yes (due to low/negligible deformation of structure)	No, minimum standoff distance due to required elongation of the fence (varies between fence types and manufacturer)
Maintenance requirement after low energy impact	None (under normal circumstances)	Variable (depending on fence type and set up)
Installation tolerances (geometric)	Few specific requirements	Small geometric installation tolerances (to ensure correct functioning)
Required slope topography for installation	Suitable only for medium to low gradient slopes/sites	Can be installed on any type of slope in any orientation

3. Design concept

The impact of rockfall is significant in the Wollongong area as most of the railway sites are found near steep rock slopes. To develop an effective rockfall protection system, it is necessary to first identify the design boulder size and then

the characteristics of the trajectory through a thorough site investigation in order to describe the geometric characteristics of the slope such as angle, launch points, ridges, and gullies that largely define the path and mode (rolling, bouncing etc.) of the rockfall. Once the rockfall area has been evaluated, it can be further analysed and quantified by both empirical and computer modeling to estimate the trajectory, bounce height and velocity for a given rock. This key information is then used to establish the overall dimensions of the rock fall embankment.

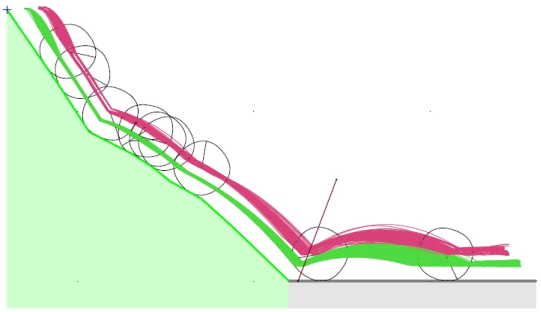

Figure 5. Example of rock fall trajectory analyis using Rocscience

The proposed embankment at Coalcliff had to withstand a design impact from rocks that would vary in size up to 3 m^3. Also, it was required to fit into the existing rail corridor respecting strict space constraints.

While the height of the embankment is based on the calculated impact trajectory height, the embankment depth is proportioned according to the energy (and therefore force) of the impacting rock. Figure 9 shows a simple procedure developed by Maccaferri in conjunction with the Polytechnico Di Torino (Italy). It presents a unique graphical approach which determines the greatest expected impact penetration depth into the embankment thereby enabling the dimensioning of the embankment; these graphs are based on evidence already reported in literature from full-scale tests and a systematic series of numerical models.

Given this information, the feasibility of the rock fall embankment was evaluated using the simplified design approach and approved by the client to be a robust solution for the site.

4. Detailed design of the reinforced soil embankment

The detailed design of the rockfall embankment began in August 2012 with a review of the site layout, environmental issues and budgetary constraints.

To mimimise cost and enhance the neighbouring green environment, it was decided to use a reinforced soil structure in lieu of a conventional rockfall barrier. Green Terramesh was chosen to strengthen and stabilise the soil embankment. The wall face is made of flexible mesh panels that can be faced with topsoil and planted with vegetation to create a "green" wall that can tolerate some differential movement. The body of the embankment is in filled with granular soil, compacted in layers with the Green Terrramesh reinforcement placed at intervals of 600 mm. It is the inclusion of the Terramesh reinforcement that allows a stable energy absorbing structure to be formed with sides as steep as 70^0.

The reinforced soil technique places tensile elements in the soil to improve stability and control deformation. To be effective, the reinforcements must intersect potential failure surfaces in the soil mass. Deformation in the soil mass generates strains in the reinforcements, which in turn, generate tensile loads in the Green Terramesh reinforcements. These tensile loads act to restrict soil movements and thus impart additional shear strength. This results in the composite soil/reinforcement system having significantly greater shear strength than the soil mass alone.

A significant advantage of a rockfall embankment when compared to more conventional systems is that they can be constructed easily and economically with site won soils; additional reinforcement, if required, can be provided with supplementary mesh or polymeric geogrids.

The Green Terramesh system was designed for the project as an efficient combination of flexible facing that retains vegetative soil and reinforced engineered backfill core.

4.1. Green Terramesh® system

Green Terramesh is an environmentally friendly modular system used for soil reinforced applications such as retaining walls and rock fall embankments.

The main unit is made of 8 x 10 double twisted steel woven wire mesh, as per EN10233-3 (Figures 6 and 7). The facing and the soil reinforcing tail elements are made from the same mesh panel. The use of a single integral facing and reinforcing unit substantially reduces the potential risks associated with a facing connection failure as the connection has been engineered into the system. Attached behind the woven wire mesh is a welded wire mesh panel. Two steel brackets (8 mm dia.) are used to form a fixed 70^o degree face angle.

The steel wire used in the manufacture of Green Terramesh is heavily Galmac (zinc/aluminum alloy) coated soft temper steel. A PVC coating of 0.5 mm nominal thickness is then applied to the steel to provide added protection for use in potentially aggressive environments, typically where they are buried in soil and where

water is prevalent: In salt or fresh water, or wherever the risk of corrosion is present.

Green Terramesh units are typically supplied as 2 m wide units with a single layer of woven wire mesh reinforcement having a tail length determined by the project's structural design. These units are commonly used in conventional reinforced soil applications.

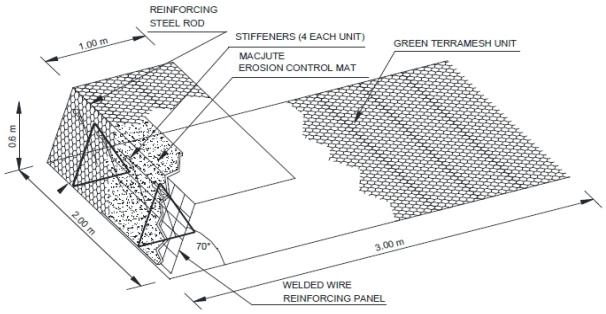

Figure 6. Green Terrmesh® unit

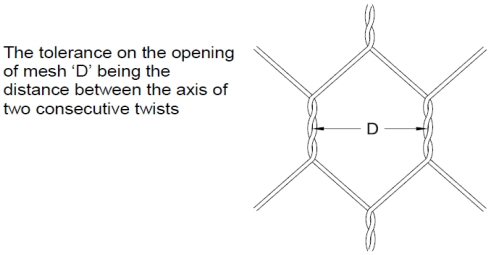

Figure 7. Green Terramesh mesh dimensions: 80 x 100 mm

4.2. Reinforced embankment design

The first step of the design process at the Coalcliff site was to check the footprint area of the embankment to make sure that it would effectively fit the site. A detailed design was then required to determine the structures:

1. Ability to control the block's trajectory and structural stability to withstand the impact and;
2. Constructability

4.3. Design process

4.3.1. Dimension of embankment versus impact response

To determine the structural dynamic response of the embankment during an impact, it was necessary to determine the penetration of the block into the embankment.

The results of extensive finite element (FE) simulations show deformation of the rockfall embankment induced by impact. The mechanisms presented in Figure 8 shows that mutual layers of reinforcement deform with the impact and plastic deformation developed in the soil related to the formation of the impact crater.

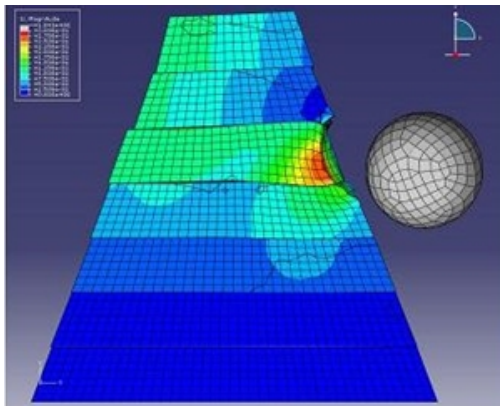

Figure 8. Example of FE modeling of the impact of a block on a Green Terramesh embankment

However, the relevancy of these analytical methods is limited due to the complex nature and usability of the process. As a result, a simplified method for approximating the maximum depth of penetration was introduced into calculations. Calvetti and Di Prisco (a design approach developed by Maccaferri in conjunction with the Polytechnico Di Torino, Italy, 2007) developed the correlation between impact energy and impact force for falling blocks with variable radius to estimate the maximum penetration depth (Figure 9). For example, a 3 m^3 block travelling at 25 m/s is calculated to have a maximum depth of penetration into the embankment of approximately 0.5 m.

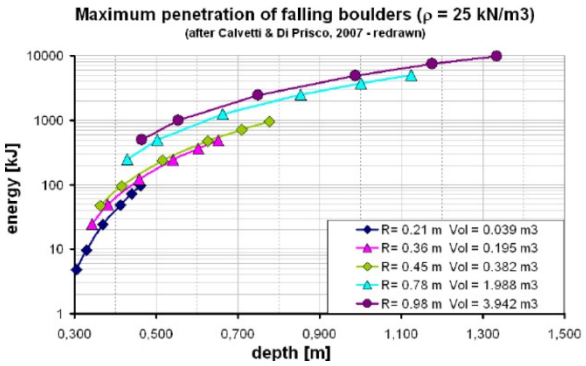

Figure 9. Derived maximum penetration of an impacting block in relation to impact energy

The penetration of the block on the facing portion of the embankment is used to determine the thickness of the embankment; at the point of its highest probable impact. The minimum thickness of the reinforced embankment is estimated to be twice the maximum penetration depth:

$$t_W \geq 2\ p_b \qquad (1)$$

Where:

t_W = minimum thickness of the embankment at the point of impact

p_b = penetration of the block into the embankment

In the case of a trapezoidal embankment, the top width of the embankment is obtained when:

$$t_E \geq t_W - 2\, u_f/\tan(\alpha) \qquad (2)$$

Where:

t_E = width of the top section

U_f = upper free section of embankment

Tan(α) = inclination of the uphill embankment

The upper section of the embankment, where impact should not occur (due to high potential deformation) should be at least equal to the diameter of the rock mass.

The minimum height of the embankment is determined as:

$$h_E \geq h_d + U_f = h_d + ((t_W - t_E)/2)\tan(\alpha) \qquad (3)$$

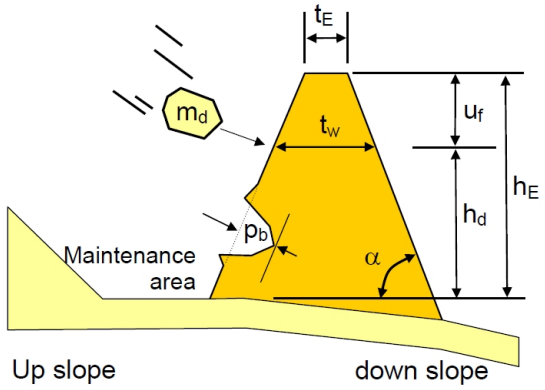

Figure 10. Indicative embankment layout and definition of the relevant embankment parameters

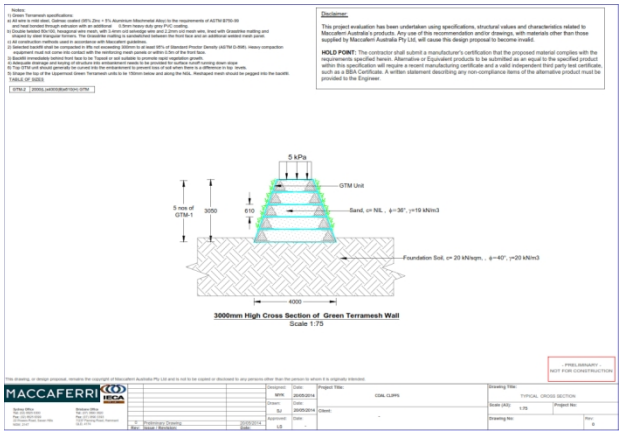

Figure 11. Embankment layout at Coalcliff

Figure 11 shows the overall configuration of the 3 m high embankment at Coalcliff. The reinforced soil core of the embankment is 4 meters wide at the base and forms a trapezoidal section using Green Terramesh units laid back-to-back at an inclination of 70^o degrees.

By adopting this pseudo approach in Figure 9 the structure is designed to absorb an impact of 650 kJ.

4.3.2. Stability of the rockfall embankment

After addressing the embankment's impact response, the stability of the rockfall embankment must be checked to ensure the embankment structure and its reinforcement have a safety factor satisfying the design criteria.

The static analysis of the embankment (bearing capacity of the foundation and sliding) and the internal stability of the embankment (tensile and pull-out strength of the reinforcement elements) were performed in MacStarsW (Figures 12 and 13).

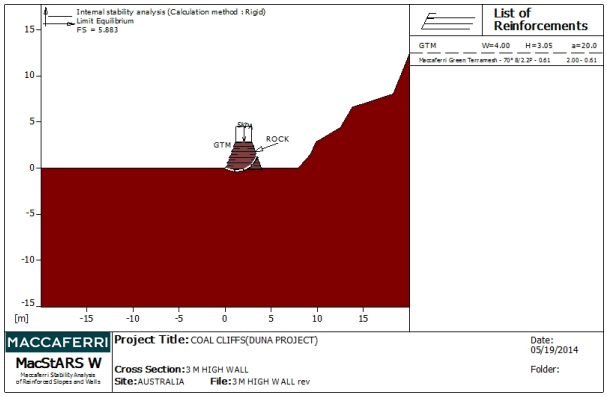

Figure 12. The interaction between the reinforcement and backfill soil at the Coacliff embankment is checked using MacStarsW

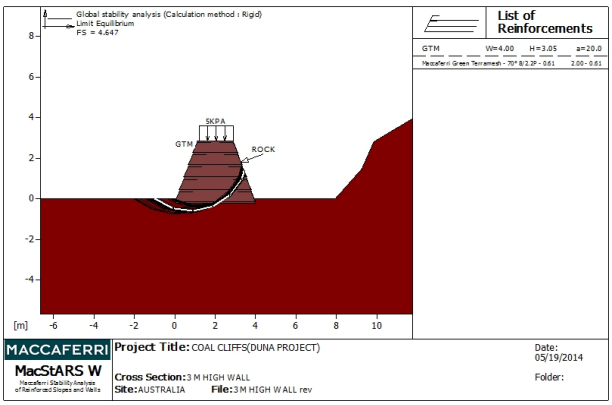

Figure 13. Global stability check of the embankment at the Coacliff is performed with limit state methods in MacStarsW

5. Construction

Construction of the 750 m^2 rockfall protection system started in February 2014, with two separate embankments, 65 m and 50 m long, built in phases by Sydney Trains at Coalcliff.

The construction began with the foundation layer which was prepared in order to ensure adequate load-bearing and vertical alignment of the embankment. The Green Terramesh reinforcing elements were installed, taking care to place 300 mm thick of seeded topsoil next to the facing lined with MacJute, a bio-degradable erosion blanket to promote plant growth. The embankment fill consisted of good quality, free draining, granular material (with a high internal angle of friction) compacted in layers to 95% Standard Proctor using conventional compaction equipment (rollers, vibrating plate etc.).

Figure 14. Assembly of Green Terramesh units

Figure 15. South access ramp to embankment

Figure 16. The mesh front face acts as framework during construction

Figure 17. Factory fitted biodegradable facing layer which retains good quality topsoil

Figure 18. Vegetation growth before hydroseeding

After the embankment is completed, the outer face will be hydroseeded and climbing plants natural to the area will be planted in order to "green" the facing.

The embankments were constructed rapidly, as the number of operations performed on site were reduced using the pre-assembled double-twist mesh fascia units and soil reinforced structural elements. Typically, the installation rate for Green Terramesh is 8 to 10 m^3 a day.

Figure 19. Embankment one: 65 meters long

Figure 20. Embankment two: 50 meters long

6. Conclusion

Embankments or back-to-back reinforced soil structures have been used successfully by Maccaferri throughout the world for rockfall protection. Internationally, the embankment barriers are the first choice rockfall protection systems in situations where the total kinetic (impact) energy is greater than 15,000 kilojoules and where space permits. This is the first use of a "green" embankment along the Illawarra railway line as a rockfall protection embankment.

Such a system is cost effective and robust for Sydney Trains as the rockfall embankments can intercept high impact energy levels without any appreciable deformation resulting in minimal maintenance requirements.

An unintended benefit of using a rockfall embankment with a layer of double twist mesh is that any rockfall impacting on the structure creates an impact record for Sydney Trains, thus providing an empirical method of tracking the actual number of rockfall events between inspection visits.

7. Acknowledgements

The authors would like to thank Sydney Trains for their contributions to this paper and the 10YGCP reviewers.

8. References

Gharpure A, Kumar S, Scotto M, 2012,
Composite soil reinforcement system for retention of very high steep fills – A case study, 5th European Geosynthetics Congress, Valencia

Flentje P, Chowdhury R, 2002,
Landsliding in an urban ara, The Geological Socity of London, England

Hendrix M, Wilson R.A, Moon A.T, Stewart I.E, Flentje, 2002,
Slope hazard assessment on a coast road in New South Wales, Australia

Leventhanl A, Flentje P, 2012,
Illustrative sections depicting landslide susceptibility of the Illawarra escarpment, Australian Geomechancis, Australia

Ronco C, Oggeri C, Pelia D, 2009,
Design of reinforced ground embankments used for rockfall protection, Politechnico di Torino, Italy

Simons M.J, Pollak S, Peirone B, BC Ministry of Transportation and Infrastructure, 2010,
Design and construction of a high energy embankment on the Trans-Canada highway, Maccaferri, 2011, Technical data sheet – Green Terramesh, Maccaferri, Australia

Maccaferri, 2011,
Technical note – Green Terramesh rockfall protection embankments, Maccaferri, New Zealand

Officine Maccaferri, 2009,
Case History, Rockfall embankment – in Cretaz (Cogne – AOSTA), Officine Maccaferri, Italy

Officine Maccaferri, 2010,
Numerical modeling of ground reinforced embankments used for rockfall protection, Officine Maccaferri, Italy

Officine Maccaferri, 2009,
Protection from high energy rockfall impacts using Terramesh, Embankments designs and experience, Officine Maccaferri, Italy

Officine Maccaferri, 2010,
Technical data sheet – MAC.RO. systems – rockfall protection embankments, Officine Maccaferri, Italy

This page intentionally left blank

Proceedings of the 10th ANZ Young Geotechnical Professional's Conference – 10YGPC
Noosa, Queensland, Australia
10 – 12 September 2014

MANAGING A SIGNIFICANT SLOPE MOVEMENT AT CLERMONT COAL MINE

Alison LANGSFORD
Rio Tinto Clermont Coal, Clermont, Australia

ABSTRACT – From July 2012 until January 2013 significant movement on the western wall of Clermont Coal Mine required geotechnical management to ensure coal could be extracted without exceeding an acceptable level of risk. A complicated structural package forms the western wall of the pit. This area includes a high angle fault zone at the slope toe and pitward dipping foliation from metamorphic phyllite. Movement was detected in the wall soon after exposure and, as mining progressed, the wall condition continued to degrade. Slope monitoring systems, including an IBIS radar, were used along with controlled mining practices and a Trigger Action Response Plan. The movement was successfully managed by identifying movement triggers and implementing controls to mitigate the risk. The coal at the toe of the wall was recovered to design without incident. A description of the geology, perceived mode of slope failure, monitoring practices, and detailed account of the slope management and practices used during coal mining will be discussed here.

1. Introduction

Clermont Coal mine is a truck and shovel operation producing high volatile export quality thermal coal. Overburden removal began in 2008, with the first coal produced in 2010.

The mine is located approximately 220 km southwest of Mackay and 10 km north of the township of Clermont in central Queensland, Australia (see Figure 1). The mine lies near the western edge of the Bowen Basin, a region well known for coal production.

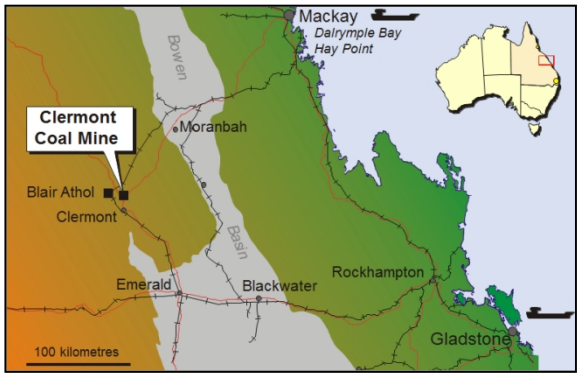

Figure 1. Location of Clermont mine

2. Regional geology and structure

Clermont mine extracts coal from the Wolfang Basin. The coal is thought to have been deposited during Early Permian northward extension of the Denison Trough structures in response to east-west crustal extension. Sedimentary units (including coal, conglomerate, sandstone, siltstone, shale and carbonaceous mudstone) were deposited unconformably on the Hurleys metamorphics unit of the Cambrian Anakie Group (Smith 2009).

During the Triassic Era, regional compression halted deposition and folded the sequences into north-westerly trending synclines. This folding lead to the Wolfang seam sometimes being sharply upturned, or thickened by thrusting. The present day structure at Clermont mine is an isolated half-graben with a defining fault on the western side.

A sequence of Tertiary sediments made up of gravel and claystone covers the Permian strata of the Wolfang Basin. Nearby volcanism produced basalt flows that covers almost the entire proposed mining area. Up to three Tertiary basalt flows have been identified. The basalt exhibits a large degree of variability, ranging from plastic clay to hard and durable, massive fresh rock.

3. Pre-Failure

3.1 Wall design

The sudden termination of coal measures to the west of the basin was recognized to be fault related very early in the exploration and pit design process. The foliation in the metamorphic units is quite variable so identifying the overall defect direction was a challenging task from drill hole samples.

Several options were considered, including more conservative and more aggressive designs for the western wall. With a final wall height of over 150 m, slight angle variations in slopes and changes to bench widths had a significant impact on cost Lowering the overall angle of the wall reduced risk and increased the strip ratio and therefore cost. The wall design needed to be economically viable while maintaining an acceptable level of risk to the mine workers.

Significant work and independent reviews were conducted prior to the final design selection.

Wall angles ranges between 80° and 40° (depending on the estimated stability of the different rock types) were assigned. The review work highlighted the importance of dewatering, monitoring piezometric pressure to ensure wall stability. The uncertainty around the design also ensured that slope movement monitoring, particularly within the metamorphic unit, was a requirement to maintain the acceptable level of risk.

3.2 Mine Progression

In the initial box cut tertiary sediments made up the exposed western wall. As the pit progressed south the metamorphics units were exposed by the advancing face.

When the metamorphic unit was exposed some small scale wall failures occurred. Small cracks were observed on some of the benches and some isolated rock falls were observed. These were managed as individual events and localized controls were successfully implemented to reduce risk and allowed work to continue.

An IBIS-M radar was acquired in June 2012. It was installed in a shipping container to protect it from the elements. The radar was placed on the eastern side of the pit ~1.2km from the area of interest. On installation of the radar small movements in the metamorphic unit were detected. This movement occurred across multiple benches and fine cracks, which had previously been identified in the area, were observed to have increased in length and separation distance.

At this time the pit was ~140 m deep and the top of coal had only recently been exposed in the western portion of the pit

4. Progression of the failure

From July 2012 until January 2013 significant movement was detected on the western wall. Movement began in a small section of exposed metamorphic unit on the southern end of the wall. This area increased both in size and velocity until ~0.5km^2 of wall was considered to be moving. The sedimentary material which had stood in front of the metamorphic unit was undermined by this movement and began to flake and fail, sliding along the scree slope.

Clermont Pit progresses in a southerly direction so the southern extent of movement was limited by the remaining overburden in the next pushback and to the north a large sub-vertical crack formed through the Tertiary sedimentary and volcanic units. Movement north of this crack was very minimal and it was considered likely that, beyond this point, the me tamorphic unit lay far enough behind the wall that it did not influence the wall stability.

As the movement progressed it became apparent that there were two main parts to the failure process. At the top of the wall material was failing along the foliation creating a scree slope. At the toe of the slope the coal and conglomerate units were bulging out and failing along defects created by the sheering movement of the fault.

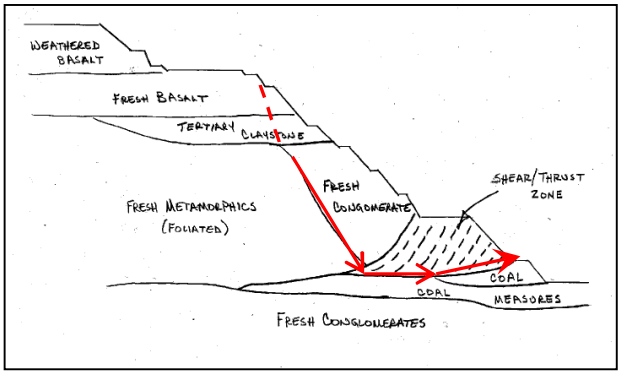

Figure 2. Section looking at the western wall showing the geology and interpreted direction of movement of material during failure (Mattern 2013).

There were three main triggers which increased movement; rain, excavating the coal at the toe of the wall and blasting. Blasting, particularly at the toe of the wall, generally only increased the rate of movement for the next 24-48 hours. Rain and excavating coal had a much bigger influence on triggering movement. Figure 3 shows a graph of the displacement observed during the wall movement by the IBIS-M radar it also highlights some of the key events which triggered an increase in the rate of displacement observed.

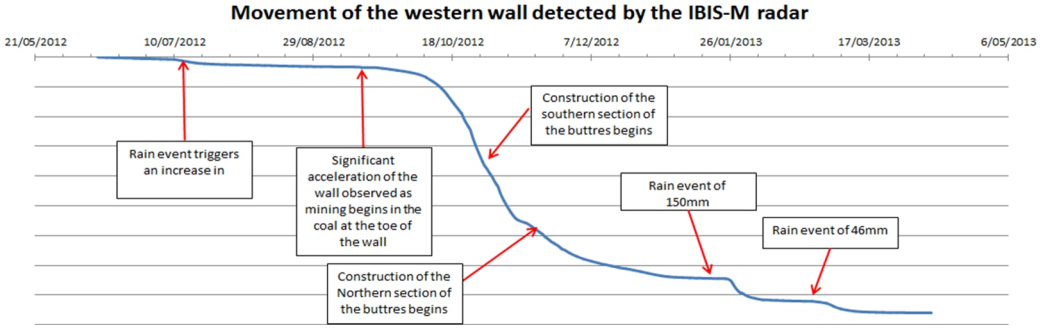

Figure 3. Graph of the average displacement (mm) observed on the western wall at Clermont Mine during the movement. Note the y scale has been deliberately removed for data privacy reasons.

4. Monitoring of wall movement

4.1 IBIS-M Radar

The IBIS-M radar was key in monitoring and managing this failure. It is an interferometric radar using Stepped-frequency Continuous Wave (SF-CW) coherent radar with SAR (synthetic aperture radar) technology. It has an accuracy of 1/10 mm (according to OEM specifications) and it's quick scan rate of ~6 minutes for an area ~0.5Km2 (Farina et al 2011) made it a good choice to monitor the fast displacement rates at the peak of the wall movement.

The radar data was initially monitored daily but this was re-assessed regularly and monitoring became much more frequent when the movement was greatest. The software also allowed for email alarms to be set based on movement of assigned areas. These alarms were customizable so, during the highest movement, email alarms were set to send to key personnel at 2 hourly intervals so that up to date information was always accessible.

Initial displacement rates indicated by the IBIS radar were questioned as visual observations estimated it to be significantly less than the data indicated. A Maptek I-Site laser scanner was used in the first few months to compare scans taken before and during movement. These scans indicated that that magnitude of movement recorded by the radar was plausible.

The use of inverse velocity graphs to predict the critical failure point was considered but it was found that this was not a useful tool in this context. As regular work was required at the toe of the wall to extract coal the movement was not following a natural failure path, as a result the predictions produced from inverse velocity graphs were inconsistent with observed wall behavior and displacement rates better predicted rock fall.

4.2 Crack Pegs

During the initial stages of wall movement crack peg monitoring was used to assess displacement rates. The original cracks were less than 100 mm wide. Monitored daily, the total displacement and the rate of displacement were considered in the Trigger Action Response Plan (TARP). Measurement of these cracks continued until October 2012 when it was deemed unsafe to enter the area. At this time some cracks were showing total displacement of over a metre and opening at a rate of up to 3 cm per day.

4.3 Ground Water monitoring

Vibrating wire piezometers had been installed behind the pit shell prior to the detection of movement. Data was collected monthly and monitored for sudden changes which could indicate imminent failure. The site model suggested the metamorphic unit would hold little water and this was supported by very little change observed in pressure prior to and during the movement.

Visual observations of water seeping from the wall proved to be a good indication of wall movement. Small seeps which had been present for months prior to the wall moving dried up or became significantly less evident. These seeps returned after movement had ceased.

5. Management of the risk to mine workers

Initially the area was managed by stopping work below the movement. As a larger section of the wall was exposed the movement became more frequent and over a larger area hampering coal mining progress. The quality and quantity of the coal directly beneath the movement was high so it was a priority to find a way to mine it. The coal was successfully recovered according to design and without a single incident.

5.1 Trigger Action Response Plan

The Trigger Action Response Plan (TARP) was developed to allow personnel to work at the toe of the wall in a safe manner by considering the triggers and ensuring that risk was minimized. It was used in conjunction with Job Hazard Analysis which were created by a cross section of the workforce and reviewed every 5 days.

The TARP was color coded with a traffic-light system for ease of understanding;

- Level 1 (green) permitted work in the area for vehicles with falling object protection (no access on foot or in light vehicles,
- Level 2 (yellow) allowed work in the area with a JHA, spotter, geotechnical advice and regular radar checks by a trained person
- Level 3 (red) no access was permitted within 50 m of the toe of the wall until geotechnical advice was received.

The 50 m exclusion zone was calculated from the potential slope run out distance that could occur if the whole wall was to fail instantaneously.

The IBIS-M Radar was key in assigning these trigger levels. Initially absolute values of displacement were used as the triggers between the different levels. It became clear however that the scree slope forming at the top of the slope was resulting in high displacement readings without endangering the personnel working at the toe. It was identified that changes in the rate of movement was more representative of risk than the absolute values which had previously been selected. Accordingly the TARP was updated.

When the wall was moving at a rate that put it in 'Level 2' conditions;

- The radar was monitored every 2 hours by a geotechnical engineer while personnel under the wall
- A spotter visually monitored the wall at all times while personnel were working under the wall
- Visibility of the wall was essential. No night shift work was permitted
- In the case of a rain event >10 mm work stopped for at least 12 hours, with re-entry allowed only after approval of the geotechnical engineer and Open Cut Examiner.
- After any in-pit production blast, work stopped until the radar data was reviewed by a geotechnical engineer. For blasts within 1,000 m, re-entry was delayed for 6 hours to allowed for more data to be used in the decision to re-enter the area
- Work was only permitted if the wall was showing an average acceleration of less than 10 mm per day

If any of the above conditions were breached Level 3 conditions were implemented with a 50 m stand off until a geotechnical engineer reviewed the data. The 50 m stand off was increased to a 100 m stand off if an average displacement rate faster than 400 mm per day was observed until rates slowed.

5.2 Selective mining

Removing coal at the toe of the wall was a key trigger that increased movement observed on the wall. With less support the lower section bulged significantly and cracks formed along the lower benches. This lower bench movement de-stabilized the upper slope and more material began to move down the screeslope.

A buttress of coal was left across the toe of the wall for as long as possible. The thickness of the buttress was determined by monitoring the wall, when an increase in the rate of movement was detected equipment walked away and began mining in a different area.

The wall was then attacked in 60 m wide sections and, as soon as all of the coal was removed, competent rock was dumped in as a replacement buttress. An in-pit dump had previously been planned against this wall and so this work was prioritized.

As soon as the work began on the buttress the rate of movement decreased significantly. Mining during buttress installation so this is difficult to see in the data shown in Figure 3. Though the wall continued to move the rate of displacement was less and the amount of time spent in Level 3 conditions was notably lower.

When the second section of buttress was completed in January 2013 wall displacement had dropped to movement rates which meant that, except for a couple of rain events, the wall stayed in Level 1 conditions (with the exception of two rain events which temporarily returned the wall to Level 2).

5.3 Involving the workforce

A key part in managing the wall movement was having a workforce that was willing to work beneath the wall. The cracks and wall movement was visually quite striking and so many of the operators were uncomfortable with working nearby.

The introduction of regular toolbox talks and daily communication on how the wall was progressing helped to demystify the mode of failure. The technology that was used could create clear visuals of what was occurring and when movement had been triggered, this created confidence in the geotechnical recommendations and effectiveness of controls.

Involving the workforce in the creation/review of Job Hazard Analysis every five days also allowed the operators to question the controls and provide feedback on how the TARPS were being used/ interpreted. Initial drafts of the TARP included some recommendations which were open to interpretation and this created confusion and made operators uncomfortable. A simple, easy to follow TARP was key in getting operators who were willing to work beneath the wall.

It is important to note that the clear visual displays produced by the radar and the regular updates lead to high confidence in the technology. It was important to ensure that the limitations were as clear as well as the benefits so that the workforce did not become overly reliant on the technology. Involving spotters in-pit to watch the wall for rock fall and other signs of movement helped to reinforce the limitations of the technology.

6. Conclusions

The hazards associated with the geology and structure of the western wall was a recognized risk prior to commencing mining. The metamorphic unit was identified as potentially unstable and the fault running through the area reduced the strength and created planes of weakness through the rock mass. The challenging nature of the wall required careful monitoring and Clermont Mine invested in multiple technologies to ensure the best understanding of what was going on.

This movement occurred as the metamorphic unit was exposed so there was limited previous data to compare it to. As the movement progressed the triggers between levels needed to

be re-assessed regularly to ensure that they appropriately represented the risk conditions being experienced in the pit.

As the mine progresses south it will continue to be affected by the metamorphic unit and fault. Future instability can be managed using the data that has been gathered during this process.

Moving forward, Clermont Mine will continue to implement this method of regularly re-assessing the appropriate trigger levels as movement is detected. Significantly more data has now been collected which provides information on the rates of movement that can be sustained without failure in the Clermont Mine rocks but the process of identifying and managing triggers will continue to be an important management technique. Re-assessing the data allowed flexibility in mining methods and minimized downtime.

7. Acknowledgement

The author would like to acknowledge the following people for their work in managing the wall movement and their help in explaining the mechanism and controls which were implemented; Jeff Mattern (RTCA Principal Geotechnical Engineer, Nathan Niaga (Clermont Mine Senior Geologist) and, Alex Hosssak (RTCA Senior Geotechnical Engineer) and the Clermont Mine Geology team

8. References

Farina, P., Leoni, L., Babboni, F., Coppi, F., Mayer, L. Ricci, P. (2011). IBIS-M, an Innovative Radar for Monitoring Slopes in Open-Pit Mines. *International Symposium on Rock Slope Stability in Open Pit Mining and Civil Engineering, Vancouver, Canada*

Gough, J. (various), reports to Rio Tinto Coal Australia

Hossak, A. (various), reports to Rio Tinto Coal Australia and personal correspondence

Mattern, J. (various), reports to Rio Tinto Coal Australia and personal correspondence

Smith, R. (2009) internal Rio Tinto Coal Australia reports

This page intentionally left blank

Proceedings of the 10th ANZ Young Geotechnical Professional's Conference – 10YGPC
Noosa, Queensland, Australia
10 – 12 September 2014

LANDSLIDE INVENTORY AND SUSCEPTIBILITY MODELLING OF THE SYDNEY BASIN

Darshika PALAMAKUMBURE[1], Phil FLENTJE[1] and David STIRLING[1]
[1] *University of Wollongong, Wollongong, Australia*

ABSTRACT – The authors have developed a series of large scale Landslide Inventory and Landslide Susceptibility zoning data sets for the wider Sydney Basin area, extending from Newcastle in the north to Batemans Bay and west to include the Blue Mountains, an area of 30,902 km^2 in NSW, Australia. The Australian Bureau of Statistics 2011 Census data show this area contains a population of 5.4 million people, approximately one quarter of the population of Australia. The team has been working on this project for a number of years following a successful 'proof of concept' trial. Over the last 3 years a PhD research program has been undertaken to refine the modelling processes and enhance the resolution of the input datasets. In particular, this work has involved the mapping of many landslides across the Sydney Basin region. In order to facilitate reliable modelling of landslide susceptibility, high resolution and large scale data sets, including the NSW Landslide Inventory, geology and Digital Elevation Models (DEM) have been compiled. With the data preparation now finalised, the research team has progressed onto the modelling phase of the project and we are currently post processing the Susceptibility grids. The regional, large scale GIS-based Susceptibility modelling outcomes are shown and discussed at the end of this paper. The Susceptibility modelling of Slide category landslides has classified 6% of the study area, approximately 1,996 km^2, as High Susceptibility. This High Susceptibility area contains 80% of the known landslides with a density of 1.3%. Almost 70% of the study area, approximately 21,509 km^2, has been classified as Very Low Susceptibility containing 0.4% of the landslide population with a density of 0.0006%.

1. Introduction

This paper discusses the current status, the successful development of the major datasets and the iteration of the new output Susceptibility models separately for both slide and flow category landslides. Updating and modelling of geology over the study area has been completed with the merging of the existing large scale geology datasets which cover some parts of the study area whilst the 1:250,000 NSW Geological Survey seamless state-wide geology covering the remaining area. The University of Wollongong GIS-based Landslide Inventory has been expanded from its Illawarra centric coverage to include landslides from across the Sydney Basin and some from further afield across New South Wales. A composite Digital Elevation Model comprising of high resolution Airborne Laser Scan datasets at 1m and CSIRO/Geoscience Australia/NASA Global DEM at 30m has been developed. This composite DEM has been resampled using the cubic convolution method to produce a DEM at 10m resolution. This DEM is over 980 million pixels and the DEM alone is a 3.65GByte ArcGIS GRID file. Furthermore, a new Toolbar embedded in ArcGIS v 10 has been developed (Palamakumbure et al., 2014) to complete the Data Mining knowledge based modelling, eliminating a previously used tedious and time consuming manual process.

With the data collection now finalised, (apart from the ongoing Landslide Inventory development) the research team has progressed onto the modelling phase of the project and we are currently post processing the Susceptibility grids. The regional, large scale GIS-based Susceptibility modelling outcomes are shown and discussed at the end of this paper. These datasets are still being post processed and validated. Whilst refinements and iterative development are likely, the authors can see that the susceptibility zoning outcomes are suitable for use as Preliminary and perhaps up to Intermediate level Susceptibility Zoning for Local Government Planning Development Control Plans where no other information exists.

All the data pertaining to this study including the landslide inventory, DEM and geology, are produced or obtained as GIS based digital data sets. The GIS work has been completed with the ESRI ArcGIS v10 environment.

The University of Wollongong Landslide Research Team have contacted numerous international organisations active in landslide risk management operations including the United States Geological Survey (USGS), Hong Kong Geotechnical Engineering Office (GEO), Italian National Institute for Environmental Protection and Research and British Geological Survey for information regarding the structure of their Landslide Inventories. The findings of this work have been incorporated in developing the structure of the new Landslide Inventory for the Sydney Basin (Flentje et al., 2012).

2. New South Wales wide Landslide Inventory

The Landslide Inventory has been the most vital component of the landslide susceptibility modelling work carried out by the landslide research team since 1990 and it has substantially grown in capacity every year since. Following a comprehensive literature review (Flentje et al., 2012), the structure of the landslide inventory has been updated to facilitate state of the art storage, querying, analysis and visualisation of landslide data. Information collected from numerous sources has been used in identifying and updating the landslide inventory, followed by field visits to verify the landslide boundaries in the field using a Trimble GeoExplorer 6000 XT GNSS device. With the cooperation of Transport for NSW Road and Maritime Services and Sydney Trains as well as numerous consulting firms, landslides across the Sydney Basin, including those in the Castle Hill and the Old Northern Road areas of the Hills Shire, have been mapped. Field mapping has also been undertaken in the Lake Macquarie and Newcastle areas. 'Unstable' areas in Soil Landscape maps and areas of landslide disturbance within vegetation mapping have also contributed to the growth of the inventory. Extensive mapping over the last several decades across the Illawarra, Southern Highlands and South Coast areas, with the support of the Wollongong City Council has resulted in a landslide inventory with 1522 landslide records across that area has now been expanded to include 1806 landslides across the Sydney Basin.

Whilst this inventory certainly does not contain all the recent landslides (those active during the last 100 years or so) within the Sydney Basin, (it may only contain perhaps 5 - 10% of them), the project time constraints were such that mapping and compilation work was finalised so we would proceed onto the modelling stage of the project. It is hoped that this work will continue into the future if financial support can be found. If it is assumed the inventory contains 5% of the total population of landslides, this suggests the Sydney Basin could contain perhaps 36,000 landslides.

3. Geology

One of the major challenges of this project was to obtain the most detailed GIS based seamless geology layer covering the entire study area (Figure 1). Even though detailed geology maps exist for some parts of the Sydney Basin, the disparities in defining and naming geological units limited the single step approach of merging the data sets. Therefore, several intermediate steps were involved in renaming some geology fields as appropriate and introducing a new field named Geo_num in each geology datasets to ensure the consistency in grouping the geological units across different map sheets. The detailed geology datasets at 1:4000, 1:50,000 and 1:100,000 covered approximately 75% of the study area and remainder was covered by the NSW state wide geology dataset at 1:250,000 (Minerals, 2003). The final merged geology integer grid

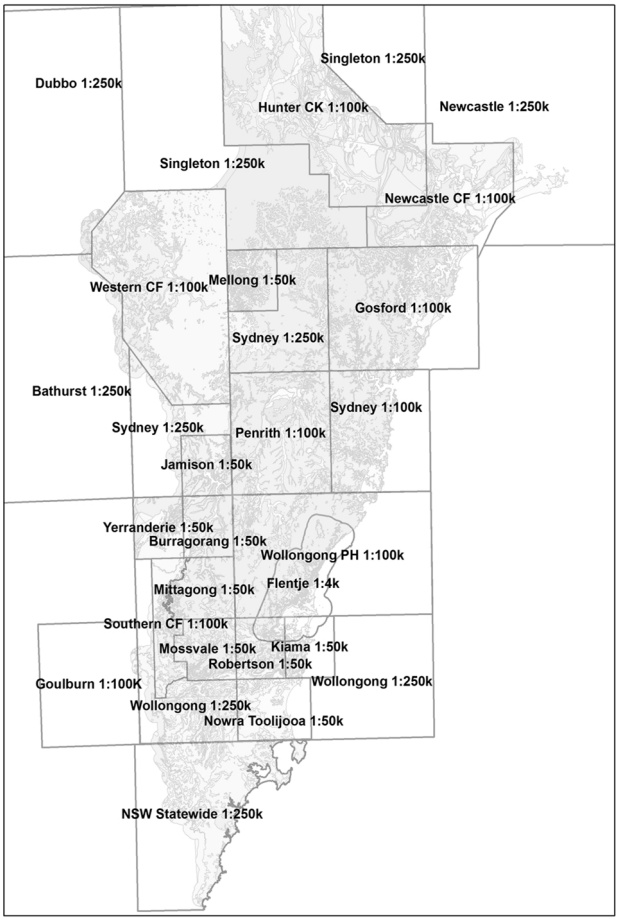

Figure 7. Merged source Geology datasets

includes a total number of 212 geology classes across the Sydney Basin study area. The extent of our Sydney Basin modelling was defined by the extent of the basal geology of the Sydney Basin sequence (generally the Shoalhaven Group) in this merged dataset and the 0m contour along the coastline of our merged DEM.

Authors are aware that the NSW Department of Trade is currently working on a seamless geology dataset for NSW. The Zone 56 area, coastal NSW, is scheduled for completion in 2015. When this data becomes available, our landslide model should be rerun.

4. Digital Elevation Model and its derivatives

CSIRO/Geoscience Australia/NASA Global DEM V2.0 (NASA, 2011) at 30m covers the entire Sydney basin but this resolution is not adequate to be applied in this detailed study of the landslide susceptibility. However, high resolution Airborne Laser Scan datasets are available for some parts of the study area. Therefore, a blend of low resolution and high quality DEMs was the best available option. The Airborne Laser Scan datasets at 10m and resampled Global DEM at 10m were combined to obtain the final DEM at 10m. In addition, eight other derivatives were developed from this DEM.

5. Knowledge based Data-Mining modelling of the slide category landslides

Among the three categories of landslides identified in the landslide inventory, namely slides, flows and falls, a total number of 1419 slides were used to build the knowledge based data-mining model. To train the model, build the See5 based decision tree (Quinlan, 1993) and derive rule sets, all the landslide pixels were used and an equal number of non-landslide pixels were selected randomly. Achieving an appropriate balance between the landslide and non-landslide training points is essential and an important aspect of our ongoing research (Palamakumbure, 2015). The Data mining process used in this project was proposed by the University of Wollongong, Landslide Research Team and described in detail by Flentje, et al. (2007)a and Flentje, et al. (2007)b.

6. Analysis of landslide susceptibility zones

To aid the visualisation of the data mining results, an ESRI GRID was developed based on the derived See5 rule sets (Figure 2). Using the Landslide Susceptibility Modelling Toolbar, the logic of the See5 rules was applied to the input grids and the final Landslide confidence was given as a decimal value for each pixel. This value is calculated by taking the cumulative sum of the confidence of the rules which contribute towards classifying a pixel as a landslide or a non-landslide, divided by the number of rules (in the winning class) that apply to each pixel.

If a pixel location satisfies the conditions of landslide and non-landslide rule/rules, the class which holds the highest confidence value is taken as the wining class. The pixels classified as landslides hold confidence values from 0 to 1 whereas the non-landslide pixels hold values from 0 to -1.

Table 1 summarises the contribution of landslide causative factors towards making predictions. *Geology* has contributed to the classification of the highest percentage of training cases followed by *Slope.*

The next step of this process is differentiating the classes of landslide susceptibility. The confidence distribution curves were plotted (Figure 3) and the threshold values for defining the Susceptibility classes were identified. It is essential that these distributions follow the objectives of Table 4(b) (AGS, 2007) included here as Table 2. Therefore, the maximum number landslides have been included in the highest susceptibility zones, while keeping their areas to a minimum. This was achieved by following the sudden increments or steps in the cumulative percentage of data (Figure 3). The study area was divided into four classes according to the landslide confidence values (Table 3). The highest susceptibility class includes 80% of the slide category landslides in the inventory, whereas the very low susceptibility class includes 0.4% of the slides.

The Susceptibility modelling of Slide category landslides has classified 6% of the study area (approximately 1,996 km^2), as High Susceptibility. This area contains 80% of the known landslides with a density of 1.3%. The moderate susceptibility class covers nearly 8% of the study area (2,607.92 km^2) and contains 15.6% of the slide population with a slide density of 0.19%.

Table 1. Training pixels % classified using the given attributes

Landslide causative factors	% data classified using the attribute
Geology	100%
Slope	38%
Aspect	11%
Curvature	9%
Profile Curvature	11%
Plan curvature	7%
Flow accumulation	0%
Wetness Index	12%
Terrain classification	4%

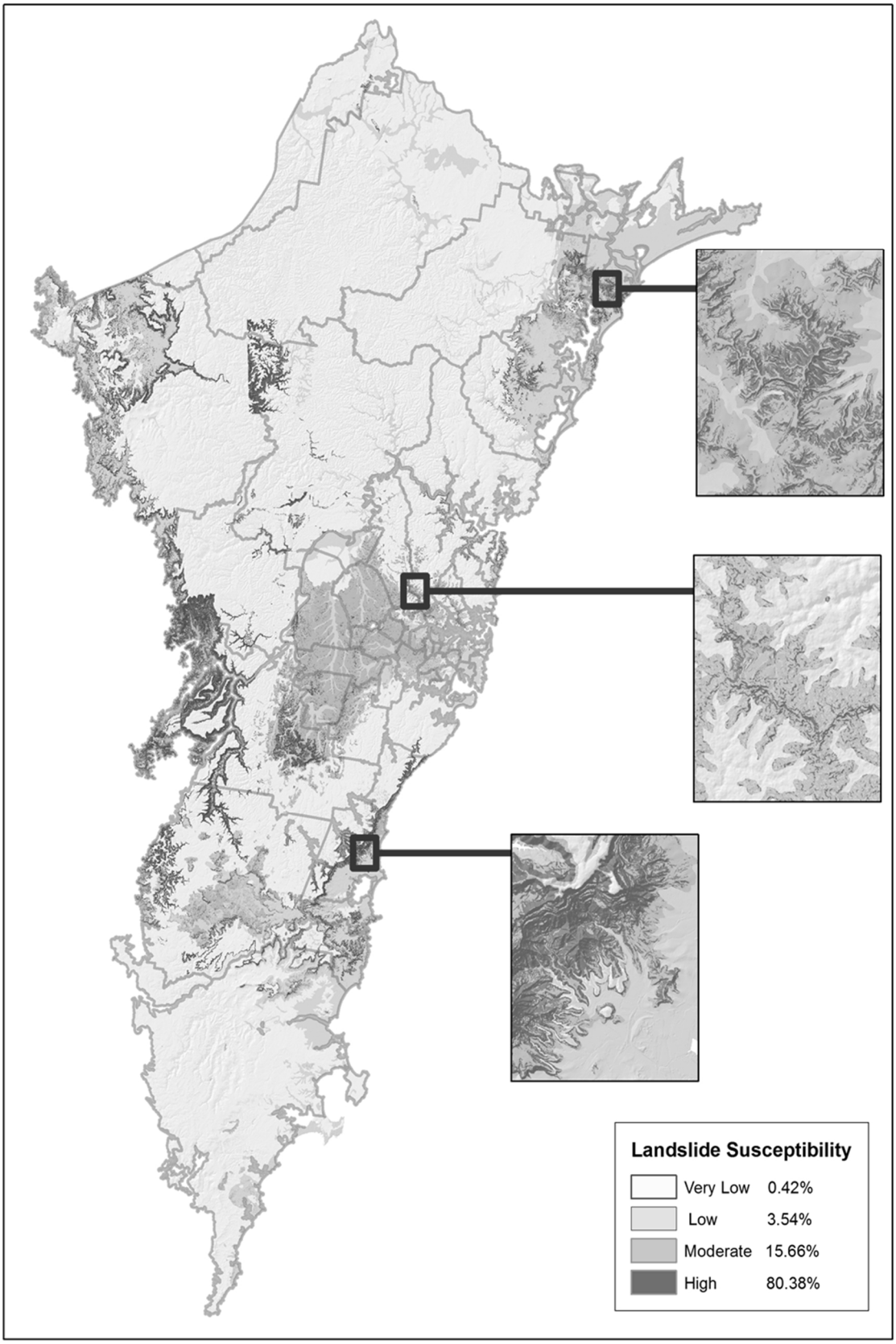

Figure 8. Study area and the Landslide Susceptibility map – attempt 1

Table 2. Relative susceptibility descriptors as in Table 4(b) of LRM Guidelines (AGS 2007)

Susceptibility Descriptors	Proportion of Large Landslides in inventory
Very Low	0 to 0.01
Low	>0.01 to 0.1
Moderate	>0.1 to 0.5
High	>0.5

Table 3. Distribution of slides in the landslide susceptibility classes

Susceptibility class	% of the Study Area	Area (km^2) of class	% slide population	Area of slides (km^2)	% of area effected by slides
High - 1	6.5	1,996	80.4	26.5	1.32
Moderate - 2	8.4	2,607	15.7	5.2	0.19
Low - 3	15.5	4,786	3.5	1.2	0.02
Very Low - 4	69.6	21,509	0.4	0.1	0.0006

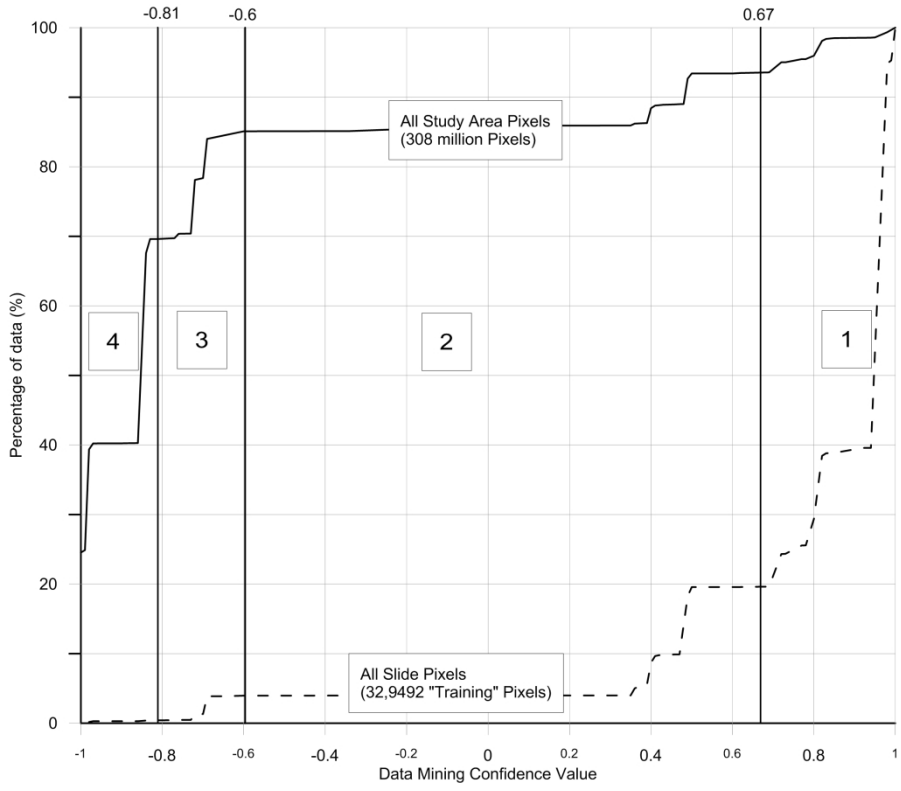

Figure 9. Classification of Susceptibility Zones using the distribution of the confidence values

The area of Low Susceptibility zone is 4,786.33 km^2 (15.5% of the study area) and contains 3.5% of the slide population with a landslide density of 0.02. Almost 70% of the study area, approximately 21,509 km^2, has been classified as Very Low Susceptibility containing 0.4% of the landslide population with a density of 0.0006%. Furthermore, considering the combined results of High and Moderate susceptibility classes, nearly 95% of the slides occur in 15% of the study area.

7. Conclusions

Large scale GIS based data layers and the NSW Landslide Inventory have been used in the modelling of the Landslide Susceptibility. The Landslide Susceptibility toolbar has demonstrated its suitability for application in modelling large scale high resolution datasets. The See5 based data mining approach was successful in meeting the AGS (2007) Table 4(b) objectives. Research is proceeding concerning the selection of the size of negative case training dataset and See5 modelling parameters suitable to conduct a large scale and high resolution modelling work. Assembling and preparation of data was one of the main challenges in this project and in particular the Landslide Inventory and geology datasets. As more than 100 geology classifications existed, the number of rules presented some challenges.

The authors note that the Slide Category Susceptibility Zoning outcomes are suitable for use as Preliminary and perhaps up to Intermediate level Susceptibility Zoning for Local Government Planning Development Control Plans where no other information exists. It is also of note that our Data Mining has also produced a Debris Flow Susceptibility Zoning as well and this will be discussed in a later paper.

The modelling will differentiate between man-made and natural failures but we have not progressed to that level of work thus far. The inventory does differentiate man-made failures although more data regarding these type of failures does need to be collected. It is an area for future development.

8. References

AGS (2007), "Guidelines for Landslide susceptibility, Hazard and Risk Zoning for Land Use Planning ", *Australian Geomechanics Journal,* vol. 42, issue (1), pp. 23.

Flentje P., Stirling D., Chowdhury R. (2007). Landslide susceptibility and Hazard derived from a landslide inventory using Data minig - an Australian case ctudy. *First North American Landslide Conference, Landslide and Society: Integrated Science, Engineering, Management and Mitigation*, Vail, Colarado.

Flentje P., Stirling D., Chowdhury R. (2007). Landslide Susceptibility and Hazard derived from a landslide inventory using data mining - An Australian case study. *10th Australia New Zealand Conference on Geomechanics*, Common Ground, Brisbane, Australian Geomechanics Society.

Flentje P., Stirling D., Palamakumbure D. (2012). An Inventory of Landslides within the Sydney Basin to aid the development of a refined Susceptibility Zoning. *11th Australia New Zealand Conference on Geomechanics (ANZ 2012), Ground Engineering in a Changing World*, Melbourne, Australia, Australian Geomechanics

Minerals (2003). NSW State Wide seamless Geology at 1:250,000 digital dataset. NSW Department of Minerals and Energy. sourced from NSW Geological Survey

NASA (2011). ASTER GDEM v10. T. The Advanced Spaceborne Thermal Emission and Reflection Radiometer (ASTER) Global Digital Elevation Model (GDEM) is concurrently distributed from the Ministry of Economy, and Industry (METI) Earth Remote Sensing Data Analysis Center (ERSDAC) in Japan and the National Aeronautics and Space Administration (NASA) Earth Observing System (EOS) Data Information System (EOSDIS) Land Processes (LP) Distributed Active Archive Center (DAAC) in the United States.

Palamakumbure D. (PhD thesis to be published). GIS based Landslide Inventory and Landslide Susceptibility Modelling across the Sydney Basin *University of Wollongong.*

Palamakumbure D., Stirling D., Flentje P., Chowdhury R. (2014). ArcGIS v.10 Landslide Susceptibility Data Mining add-in tool integrating data mining and GIS techniques to model landslide susceptibility. *IAEG XII CONGRESS*, Torino, Italy.

Quinlan J. R. (1993). C4.5: programs for machine learning, Morgan Kaufmann Publishers Inc.

Proceedings of the 10th ANZ Young Geotechnical Professional's Conference – 10YGPC
Noosa, Queensland, Australia
10 – 12 September 2014

QUANTITATIVE RISK ASSESSMENT FOR THE GREAT WESTERN HIGHWAY UPGRADE, MOUNT VICTORIA TO LITHGOW

David ANDREW[1], Steven ROSIN[2]
[1] *Geotechnical Engineer, Jacobs, Sydney, Australia*
[2] *Senior Principal Geotechnical Engineer, Jacobs, Sydney, Australia*

ABSTRACT – The Great Western Highway (GWH) from Mount Victoria to Lithgow (MV2L) comprises a road corridor that traverses through steep terrain and is bound by several high escarpment faces that generate risk to life for road users from a range of slope instability hazards. Where the risk to life is evaluated as unacceptable, it becomes necessary to implement risk reduction measures to ensure that an acceptable level of risk to road users is achieved. As part of the MV2L detail design stage, a Quantitative Risk Assessment (QRA) was undertaken for the reconstruction at Forty Bends. The conclusions and outcomes from the Forty Bends QRA presented in this paper demonstrate that quantitative risk assessment is a valuable technique that allows the assessment of multiple geotechnical hazards and the corresponding consequences. This framework facilitates sound decision making for geotechnical risk in projects that are located in complex geological risk environments.

1. Introduction

The GWH is a principal road transport link that connects the Central Tablelands of New South Wales (NSW), the Blue Mountains, and the Sydney Metropolitan Area. The highway is a significant freight corridor and conveys thousands of commuters per day between towns located along the route as well as Greater Sydney. In order to improve travel times and provide a safer environment for freight transport and commuters, a GWH upgrade program is progressively being undertaken. As part of this program, the GWH between MV2L has been proposed to be upgraded. The road corridor from MV2L comprises a route that traverses through steep terrain or is bounded by several high escarpment faces that generate risk to life for road users from a range of slope instability hazards. In accordance with Roads and Maritime Services (RMS) requirements, slopes within their road corridors require a slope risk assessment to evaluate the existing lives risk to road users. Where the risk to life is evaluated as unacceptable, it becomes necessary to implement risk reduction measures to ensure that an acceptable level of risk to road users is achieved.

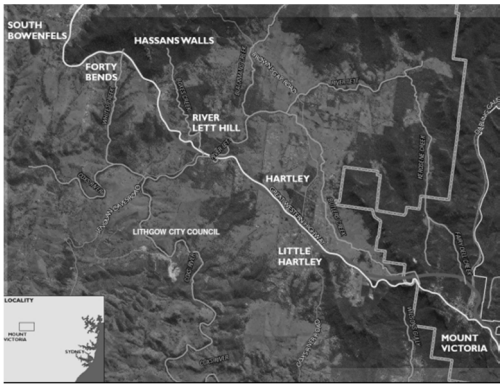

Figure 1. Location plan

As part of the GWH upgrade, the MV2L Alliance undertook detail design of the 4 kilometers Forty Bends section. The Forty Bends section upgrade includes realignment of the existing eastbound and westbound dual carriageway, reduced horizontal and vertical curves, improved line of sight for road users, and construction of several structures such as retaining walls, bridges, cuts, and fill embankments. A QRA was undertaken for the reconstruction at Forty Bends considering the complex nature of the slopes at this location and the range of potential instability hazards including post long wall mining of coal seams. An investigation of the landforms and geological formations for the Forty Bends section of the GWH allowed the formulation of the geotechnical domains and hazards for the QRA. These identified geotechnical domains were then used to develop the quantitative risk model and provide an assessment of the existing life risk for each geotechnical hazard based on acceptable societal risk. The comparison of the total life risk for each geotechnical domain with the As Low As Reasonably Practical (ALARP) principle provided an assessment for which the specification of risk reduction works for the Forty Bends slope would be developed.

2. Landforms and Site Geology

Forty Bends is located near the western boundary of the Sydney Sedimentary Basin (Bryan 1966), where Triassic age (230Ma) sediments of the Narrabeen Group overlie Permian age (270Ma) sedimentary rocks of the Illawarra Coal Measures and Shoalhaven Group. These strata dip approximately 1 to 2 degrees towards the east. The rocks unconformably overly basement granites of

Carboniferous age and steeply folded Devonian age meta-sedimentary rocks belonging to the Laclan Ford Belt. Younger Tertiary age (60Ma) mafic dykes have intruded within each of these regional geological formations.

The regional escarpment slopes in the Forty Bends area are located north of the existing and proposed upgrade alignment of the GWH. The elevation at the base of the escarpment along the existing alignment of the GWH is at approximately Reduced Level (RL) 890 metres Australian Height Datum (AHD) rising to RL 1130 metres AHD at the crest of the escarpment and therefore varying in elevation by approximately 240 metres.

The crests of the slope above the GWH are formed within the Burro-Moko Head Sandstone, which extends to approximately 40 metres thick and contains near vertical escarpment faces. The unit comprises medium to coarse grained, medium to high strength sandstone with thin shale interbeds in the upper half and occasional red brown claystone beds approximately two to five metres thick.

Directly below the escarpment, the natural slope is very steep (30 to 45 degrees) then reduces to more gentle slope (10 to 30 degrees) towards the road. The upper steep slopes directly below the Burro-Moko Head Sandstone is where the Caley Formation outcrops and this formation is approximately 30 metres thick. The Caley formation comprises medium to high strength, fine grained sandstone interbedded with shale, coarse lithic sandstone and claystone/siltstone seams up to 3 metres thick.

The Caley Formation is underlain by the Illawarra Coal Measures, which are approximately 100 metres thick in the Forty Bends area. The Illawarra Coal Measures are mostly buried below colluvium/talus which comprises a combination of transported soils and boulders fallen from the escarpments above. The formation includes interbedded claystone, siltstone, sandstone, and coal and has numerous, predominatly close to medium spaced rock defects.

The Shoalhaven Group underlies the Illawarra Coal Measures and is approximately 100 metres thick with the Berry Siltstone located at the top of the formation. The GWH is underlain by the Shoalhaven Group on the adjacent slopes above and below the road upgrade alignment.

The Berry Siltstone is predominately comprised of sandy grey micaceous siltstones, with thin sandy beds common in the upper section of the unit. Bioturbation is present throughout the unit, with bedding layers hard to distinguish. The lower section of the Berry Siltstone also contains large angular blocks and pebbles suggested to be of glacial (dropstones) origin.

Below the Shoalhaven Group, older basement rocks of Carboniferous age are located and are generally comprise granite (Kanimbla batholith). These basement rocks outcrop to the south of Forty Bends around Hartley and River Lett Hill.

Field mapping and site inspections (MV2L, 2013) were undertaken by MV2L alliance team members to define the geological formation boundaries in exposed cuttings and slopes, and confirm the site geological model that was prepared based on regional geological mapping. Figure 2 illustrates the geological formations on a typical cross section through the Forty Bends slope.

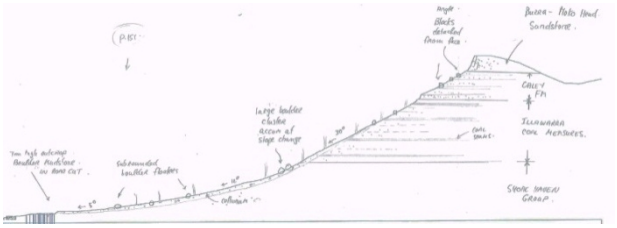

Figure 2. Typical cross section through slope

3. Geotechnical Hazards

3.1. Geotechnical Domains

The Forty Bends section was divided into seven geotechnical domains for the QRA based on areas of similar geology, slope profile, and type of slope instability hazards. The seven Geotechnical Domains (GD) included:

- Domain A – East End Spur (Stn 30.400 – 30.700).
- Domain B – Gabion Wall (Stn 30.700 – 31.050).
- Domain C – Hassan's Wall Escarpment (Stn 31.050 – 31.650).
- Domain D – Whites Creek Crossing (Stn 31.650 – 32.000).
- Domain E – West Ridge Spur of Whites Creek Gully (Stn 32.000 – 32.330).
- Domain F – East Side Embankment (Stn 32.330 – 33.000).
- Domain G – McKanes Falls Road Bend (Stn 33.000 – 33.600).

3.2. Hazards

A preliminary slope risk assessment (MV2L, 2011) was undertaken by the alliance to provide a systematic risk assessment for the entire upgrade alignment between MV2L. Six broad geotechnical hazards were identified during the preliminary slope risk assessment and were considered applicable to the QRA for the reconstruction at Forty Bends (MV2L, 2013). These geotechnical hazards were established because they were deemed to pose a risk to road users and applied to the geotechnical domains for Forty Bends. The six geotechnical hazards developed included:

- H1 - Small to medium rock block detachments from sandstone escarpment faces and ledges. Usually single blocks with size varying between 0.2 m to 1.0m in

diameter. The rate of movement is very rapid (5m/s).

- H2 – Medium to large rock block detachments from sandstone escarpment faces. Usually single or multiple blocks/sheets with size varying between 1.0 m to 4.0 m or greater in diameter. The rate of movement is very rapid (5m/s).
- H3 - Remobilisation of small boulders residing on steep slopes that have previously detached. Usually single boulders with size varying between 0.2 m to 1.0 m in diameter. The rate of movement is very rapid (5m/s).
- H4 - Remobilisation of large boulders residing on steep slopes that have previously detached. Usually single boulders with size varying between 1.0 m to 4.0 m or greater in diameter. The rate of movement is very rapid (5m/s).
- H5 - Debris flow of colluvium comprising a mixture of soil and boulder scree initiated on steep slopes. Usually triggered by concentrated rainfall run-off with volume varying between 500 m^3 to 1000 m^3. The rate of movement is moderate to rapid (1.8 to 180 m/hr).
- H6 - Slump or slide of deep colluvium and/or deeply weathered bedrock initiated on steep slopes. Usually triggered by prolonged rainfall periods with volume varying between 500 m^3 to 5000 m^3. The rate of movement is very slow to slow (1.6 to 5 m/yr).

The failure frequency of each hazard type was determined on the basis of past records, field assessment and engineering judgment of statistical information on trigger mechanisms such as rainfall intensity and earthquakes.

Hazard H1 and H2 are rock falls or topples triggered by a range of mechanisms and may be initiated by effects of weathering, wind, rain, root jacking, and earthquakes in combination with critical joint sets.

Hazard H3 and H4 involve the remobilization of large sub-rounded boulders that have previously detached from the Forty Bends escarpment and come to rest on steep slopes, generally poorly embedded and positioned in unstable orientations. These hazards may be triggered by erosion during periods of heavy rain, root growth or jacking, and bushfires. Boulders will typically remobilize on slopes steeper than 30 degrees however, remobilization and momentum over shorter distances may occur on reduced slopes of approximately 20 to 30 degrees under extreme rainfall events.

Hazard H5 is characterised by a flow occurring when a mass of cohesionless soil and rocks become saturated and flow rapidly down slope in a form that resembles viscous liquid. Hazard H5 is triggered by prolonged high intensity rainfall in combination with concentrated runoff discharging over the slope.

Hazard H6 is a deep seated mechanism and typically involves downslope movement of soil and weathered rock that initiate along surfaces of rupture or thin zones of intense shearing. Hazard H6 is activated by elevated pore pressures along failure planes as a result of prolonged high intensity rainfall. Geological mapping identified an active landslide that was repaired with top gabion wall in Domain B.

4. Development of QRA Model

4.1. QRA Model Inputs

4.1.1. Hazard likelihood reaching the road

Table 1 outlines the annualised hazard likelihood for reaching the GWH in each geotechnical domain that was adopted for the QRA. The likelihood is based on combined probability of detachment and run-out probability reaching the GWH while also a review of rainfall and earthquake data was also undertaken for guidance.

Table 1. Hazard likelihood for each domain

Domain	H1	H2	H3	H4	H5	H6
A	-	-	10^{-4}	10^{-4}	10^{-3}	10^{-5}
B	-	-	$5x10^{-4}$	10^{-3}	$2x10^{-3}$	10^{-2}
C	10^{-5}	10^{-5}	10^{-5}	10^{-5}	10^{-4}	10^{-5}
D	-	-	10^{-5}	10^{-5}	10^{-4}	10^{-5}
E	-	-	10^{-5}	10^{-5}	10^{-4}	10^{-5}
F	-	-	10^{-5}	10^{-5}	10^{-4}	10^{-5}
G	10^{-5}	10^{-5}	$2x10^{-4}$	$5x10^{-4}$	10^{-3}	10^{-4}

4.1.2. Traffic volume

The Annual Average Daily Traffic (AADT) for the GWH at Forty Bends was sourced from RMS and comprised 7900 vehicles per day for 2012 and was projected to 13000 vehicles per day for 2041. RMS supplied traffic movement counts as hourly distributions and therefore the day time distribution (6am to 6pm) was calculated as 79.7 percent and the night time distribution (6pm to 6am) as 20.3 percent. This day-night distribution split was incorporated into the QRA model.

4.1.3. Reaction time

The decision sight distance (L_{dsd}) was calculated (AASHTO, 1990) for the GWH at Forty Bends using an initial speed of 100 km/h. This speed resulted in a coefficient of longitudinal deceleration (d) equal to 0.39 and L_{dsd} equal to 170 metres. The value corresponds with the stopping distance outlined in RMS Guide to Slope Risk Analysis (2011), which is suggested between 150 to 170 metres.

The existing road alignment was assigned a line of sight factor (λ) equal to 0.75 for day traffic and 1.0 for night traffic representing 'good' and 'moderate' line of sight respectively. Therefore,

accounting for the line of sight factor, λL_{dsd} values were 127.5 metres and 170 metres respectively.

The adopted line of sight factor for the upgraded road alignment with improved line of sight was 0.5 for day traffic and 0.75 for night traffic. This corresponded to 'very good' and 'good' conditions with λL_{dsd} values that were 80 metres and 127.5 metres respectively. The upgraded road alignment for the GWH resulted in a 33 percent improvement in the stopping distance.

4.1.4. Vulnerability

The vulnerability values referring to probability of loss of life if impacted by hazards that were adopted for the QRA are presented in Table 2. These values were established in consultation with the RMS Guide to Slope Risk Analysis (2011) and considered the size of failure and speed.

Table 2. Hazard vulnerability ratings and values

Hazard	Annualised vulnerability probabilities
H1	0.055
H2	0.5
H3	0.055
H4	0.5
H5	0.055
H6	0.001

Hazard H6 has comparatively low vulnerability with the other hazards due to the mechanism and the slow nature of the hazard failure. This implies that there would be sufficient warning to respond to this hazard should a failure occur.

4.1.5. Element at risk

The element at risk for the QRA model was defined as vehicle occupancy and adopted as two people per vehicle for all traffic. Buses and trucks were not considered as part of the QRA model as the traffic volume did not delineate data for these vehicles types.

4.1.6. Road design structure factor

Design benefits from the upgraded road alignment are expected to reduce the likelihood of individual hazards reaching the road in a geotechnical domain. A review of the 20 percent detail design for Forty Bends identified the following benefits from the upgraded alignment regarding slope stability:

- Re-alignment of the road to the south away from the slope within Geotechnical Domain C and D.
- Elevated bridge structure within Geotechnical Domain D and free standing embankment in Domain E.
- Free standing embankment on the uphill side of the road for east bound carriageway that reduces hazards potentially reaching the carriageway.

Based on the considerations outlined, the following failure probability reduction factors for hazards reaching the road were implemented into the QRA:

- 50 percent reduction in the likelihood for all hazards reaching the road in Domain C.
- 80 percent reduction in the likelihood for all hazards reaching the road in Domain D.
- 40 percent reduction in the likelihood for all hazards reaching the road in Domain E.

4.2. ALR Calculation

The methodology and framework used to for the QRA included hazard assessment, consequence analysis, risk calculation, and risk assessment.

The annualised life risk calculation comprised the determination of the following:

- Probability of an event (hazard) occurring that may include release of a boulder or landslide that reaches the GWH.
- Probability that the element at risk is within the affected area (geotechnical domain) where the event occurs.
- Probability that the element at risk is within the failure zone at the time the event occurs (temporal probability).
- Vulnerability of the element at risk (probability of death if impacted by the event).
- The number of elements at risk.

The annualised life risk calculation implemented for the QRA was based on the equation presented in AGS (2007b) and augmented to include the number of elements at risk. The annualised life risk was calculated with Equation 1, as outlined below:

$$ALR = P_{(H)} \times P_{(S:H)} \times P_{(T:S)} \times V_n \times N \quad (1)$$

4.3 Bunce Equation

The annualized risk calculation for Forty Bends incorporated a method published by Bunce et. al. (1997) that evaluates the probability of an impact between a vehicle and rock using binomial theorem and inputs including traffic volume, number of failure events, vehicle speed, and an estimation of exposure to road users.

The Bunce equation considers the following hazard impact scenarios that when summed, equates the total risk to motorists:

- Impact of a falling rock on a stationary vehicle.
- Impact of a falling rock on a moving vehicle.
- Impact of a fallen rock on a moving vehicle.

The MV2L upgrade at Forty Bends does not include any intersections or road geometry features where stationary traffic would expect to be encountered; therefore the impact of a falling rock on stationary vehicle had been discounted for the QRA. The equations outlined by Bunce et. al.

(1997) for the two scenarios considered in the Forty Bends QRA are as follows:

- Impact of a falling rock on a moving vehicle.

$$P(S) = 1 - \left(1 - P\left(S:H\right)\right)^{Nr}$$

$$P(S:H) = \frac{\frac{N_V}{24}\frac{L_V}{1000}}{V_V} \quad (2)$$

- Impact of a moving vehicle on a fallen rock.

$$P(S) = 1 - \left(1 - P(S:H)\right)^{Nr} \quad (3)$$

$$P(S:H) = \frac{\frac{N_V}{24}\frac{L_{dsd}}{1000}}{V_V} \quad (4)$$

$$\lambda L_{dsd} = \lambda\left[\left(\frac{RT \times V}{3.6}\right) + \left(\frac{V^2}{254 \times d}\right)\right] \quad (5)$$

In principle the probability P(S:H) of vehicle impact given a rock fall is evaluated using the same equation for both scenarios. However, the impact of a falling rock on a moving vehicle involves a direct impact where the vehicle is occupying a small portion of the road within the geotechnical domain. Whereas, the impact of a moving vehicle on a fallen rock comprises a vehicle occupying a larger portion of the road within the geotechnical domain as a result of driver reaction time and stopping distance to avoid debris and thus is considered in the equation.

4.4 Societal Risk Criteria

Societal risk for the MV2L upgrade represents the annualized risk to which society is exposed by driving along the GWH at Forty Bends. The societal risk encompasses the total geotechnical risk from each hazard type in each geotechnical domain for which the traffic volume along the GWH at Forty Bends is exposed.

The Australian Geomechanics Society (AGS) has distinguished between Tolerable and Acceptable risks in the Landslide Risk Management Framework (AGS, 2007c), with tolerable risks being risks that society is prepared to live with to secure benefits and acceptable risks being risks that everybody in society affected is prepared to accept.

There are currently no widely agreed limits for an unacceptable level of ALR, however the ANCOLD Guidelines for Risk Assessment (2003) are widely referenced and denote that for existing structures, societal risk above 1 fatality in 1000 years (1 x 10^{-3}) is considered intolerable. A comparison of individual life loss risk criteria is presented in AGS (2007a).

Acceptable societal risk is typically considered to be less than one order of magnitude smaller (1 x 10^{-4}) than intolerable societal risks. Societal risk below an acceptable level (1 x 10^{-4}) are referred to as the target risk level and should be monitored and managed.

The 'As Low As Reasonably Practicable' (ALARP) principle should be applied to societal risks that fall between intolerable (1 x 10^{-3}) and acceptable (1 x 10^{-4}). Risk reduction measures should be implemented to societal risk that falls between these two thresholds until further risk reduction is unattainable without very significant capital investment or resource expenditure that would be deemed disproportionate to the level of risk reduction achieved.

Tolerable loss of life risk criteria for landslide risk has been developed by the AGS as part of the Landslide Risk Management guidelines. Table 3 outlines that the tolerable loss of life risk for 'new' slopes – defined by AGS (2007c) as any change to an existing slope through cut or fill, or new stabilization works – is 1 x 10^{-5}. However, this risk criteria is not directly applicable for roads.

Table 3. Tolerable risk criteria (AGS, 2007c).

Situation	**Suggested tolerable loss of life risk for the person most at risk**
Existing slope / Existing development	10^{-4} / annum
New constructed slope / new development / existing landslide	10^{-5} / annum

5. QRA Results and Discussion

The following cases were modelled for Forty Bends as part of the QRA:

- Case 1 – Existing Road 2012 traffic.
- Case 2 – Existing Road 2041 traffic.
- Case 3 – Road Upgrade 2012 traffic.
- Case 4 – Road Upgrade 2041 traffic.
- Case 5 – Road Upgrade 2012 traffic with risk reduction.
- Case 6 – Road Upgrade 2012 traffic with risk reduction.

The results of the QRA for the MV2L upgrade at Forty Bends were presented graphically using a series of plots of the annualized lives risk for each hazard type (H1 to H6) that applied within a specific geotechnical domain and road operating condition. The annualized lives risk for each hazard was then combined within the geotechnical domain and road operating condition.

Case 1 illustrated in Figure 3 shows that for the existing GWH alignment modelled with 2012 traffic volume, the ALR for Domain B and Domain G fell within the ALARP region. The total ALR combined for all geotechnical domains in Case 1 also fell within the ALARP region, with the predominant contributing risk from Hazard H4 reaching the road in Domain B. Case 2 is displayed in Figure 4 and illustrates that given the increased traffic volume for 2041, the ALR for each geotechnical domain increased and the combined risk for Domain B, Domain G, and Total Risk was close to the intolerable limit.

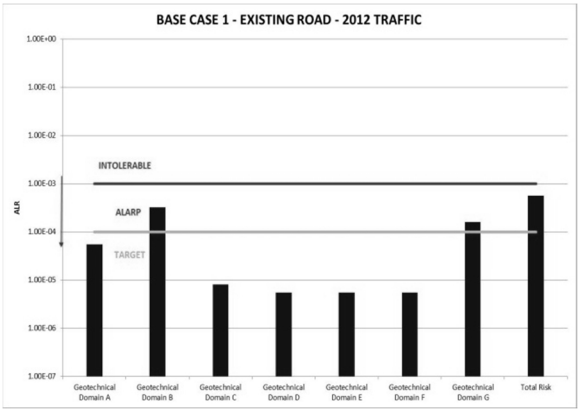

Figure 3. Case 1 existing road (2012)

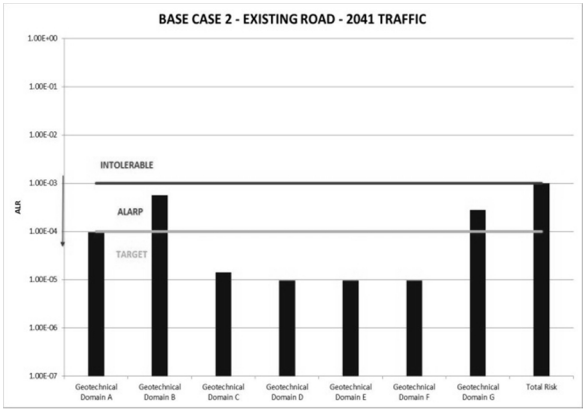

Figure 4. Case 2 existing road (2041)

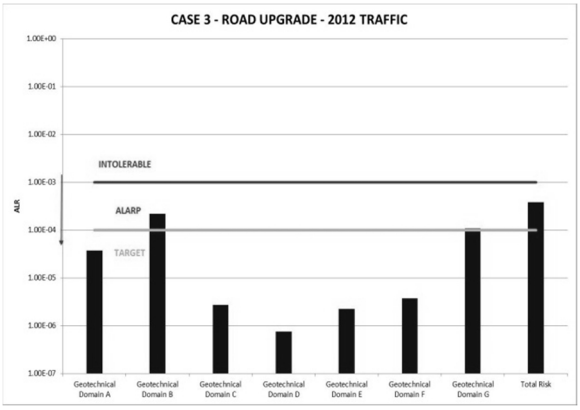

Figure 5. Case 3 road upgrade (2012)

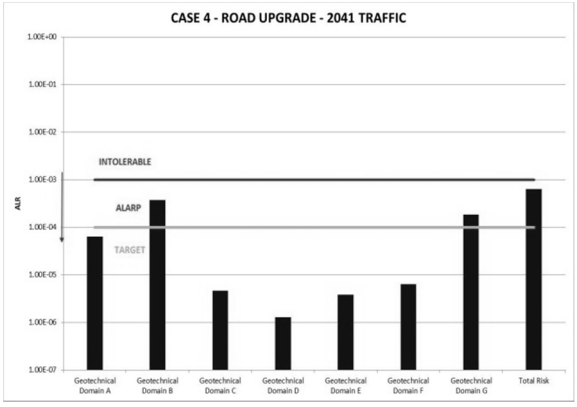

Figure 6. Case 4 road upgrade (2041)

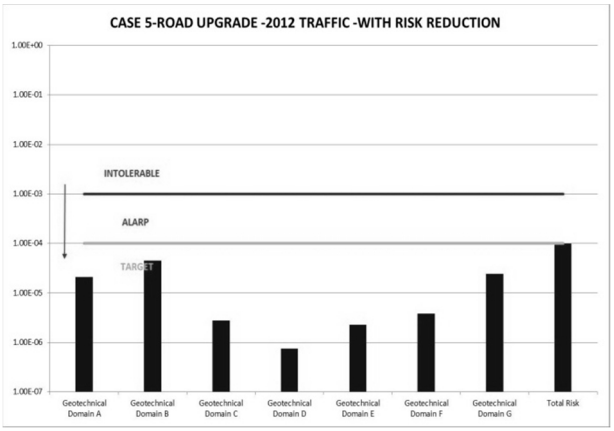

Figure 7. Case 5 road upgrade and risk reduction (2012)

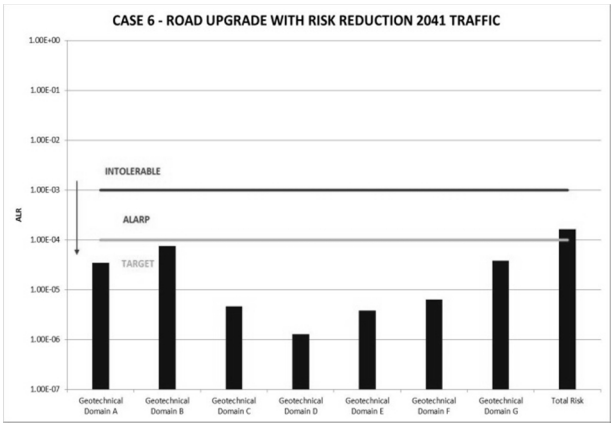

Figure 8. Case 6 road upgrade and risk reduction (2041)

Case 3 displayed in Figure 5 illustrates that for an upgraded GWH alignment modelled with 2012 traffic volume, the ALR for each geotechnical domain and the total risk has been reduced when compared with the results in Figure 3. However, ALR for Domain B and Domain G still falls in the ALARP category and therefore risk reduction works are considered justified for 2012 traffic volume. The results were replicated in Case 4 for 2041 traffic volume where the total ALR for Domain B, Domain G, and total risk fell within the ALARP region and risk reduction measures were considered. Case 3 and Case 4 have improved line of sight factors compared with Case 1 and Case 2 as a result of road alignment upgrades. Road design structure factors have also been incorporated into the QRA model.

Case 5 illustrated in Figure 7 shows that for an upgraded GWH alignment modelled with 2012 traffic volume and risk reduction measures for Domain B and Domain G, the total ALR for all geotechnical domains and total risk are below the target threshold. Figure 8 displays Case 6 QRA results with increased traffic volume for 2041 and

demonstrates that ALR for each geotechnical domain is below the target threshold however, the total risk for Case 6 marginally exceeds the target threshold. When considering the ALARP principle, risk reduction works for Case 5 and Case 6 were targeted to the highest ALR hazard types (H3 and H4). The risk reduction measures considered included breakup and removal of unstable boulders on slope, boulder anchoring directly upslope, or other appropriate measures. These risk reduction measures should be undertaken without disproportionate cost and excessive environmental impact for the project.

6. Conclusion

Quantitative risk assessment provides a framework for anticipating multiple hazard events, evaluating them, and making informed decisions about remedial solutions or the residual risk acceptance level for hazard events. It facilitates evaluation and comparison of geotechnical hazards across numerous geotechnical domains at a site and informs decision making for management of hazards and planning risk mitigation measures.

The application of QRA to Forty Bends for the GWH upgrade permitted the calculation of annualised risk to life for hazards before the road upgrade and after the implementation of mitigation measures or construction of protective structures as part of the upgrade. QRA is a tool that can be employed in conjunction with conventional deterministic methods of risk assessment such as slope stability modelling, rockfall simulation modelling, and RMS slope risk assessment approach that utilises a quantitative framework (Baynes et. al., 2002) with qualitative descriptions for hazards.

The Forty Bends QRA facilitated targeted geotechnical inspections within Geotechnical Domain A, B, and G that identified and flagged specific boulders that were deemed to have potential to re-mobilise and reach the road alignment. These boulders were targeted within a 50 to 100 metre zone upslope of the road alignment while boulders located further than 100 metres upslope were not targeted due to combination of cost, environmental impact of remedial works, and limited probability of reaching the road if remobilization occurred.

Remedial treatment measures targeting identified boulders within Geotechnical Domain A, B, and G were scoped based on the inspections. Treatment methods considered generally consisted of boulder break up, chain and anchor support, and structural toe support. It was also recommended that remedial treatments be undertaken for all boulders identified in Geotechnical Domain A to G within 5 to 10 metre zone upslope of the crest of a cutting on the road alignment due to the risk of remobilization and travel if crest slumping occurred.

7. Acknowledgments

The QRA for the MV2L upgrade described in this paper was the result of teamwork and would not have been possible without the input from the wider alliance project team. The authors would also like to acknowledge the MV2L alliance (Jacobs, PB, RMS) for permission to publish this paper.

8. References

AASHTO. (1990). *A policy on the geometric design of highways and streets*. American Society of Highway and Transportation Officials, Washington, D.C.

AGS. (2007a). Commentary on guideline for landslide susceptibility, hazard and risk zoning for land use planning, Australian Geomechanics Society, *Australian Geomechanics*, vol. 42, n°1, pp. 37 – 62.

AGS. (2007b). Practice note guidelines for landslide risk management, Australian Geomechanics Society, *Australian Geomechanics*, vol. 42, n°1, pp. 63 – 114.

AGS. (2007c). Commentary on practice note guidelines for landslide risk management, Australian Geomechanics Society, *Australian Geomechanics*, vol. 42, n°1, pp. 115 – 158.

ANCOLD. (2003). *Guidelines on risk assessment*, Australian National Committee on Large Dams, Sydney, New South Wales, Australia.

Baynes F. J., Lee I. K., and Stewart I. E. (2002). A study of the accuracy and precision of some landslide risk analyses, *Australian Geomechanics*, vol. 37, n°2, pp. 95 – 110.

Bryan J. H. (1966). Sydney 1:250 000 Geological Sheet SI/56-05, 3rd Edition, Geological Survey of New South Wales, Sydney.

Bunce C. M., Cruden D. M., and Morgenstern N. R. (1997). Assessment of the hazard from rock fall on a highway, *Canadian Geotechnical Journal*, vol. 34, n°3, pp. 344 – 356.

Mount Victoria to Lithgow Alliance (MV2L). (2011). *Preliminary slope risk assessment report*, Report No. GE-0086-D, Great Western Highway Upgrade, Mount Victoria to Lithgow Alliance, Sydney.

Mount Victoria to Lithgow Alliance (MV2L). (2013). *Reconstruction at Forty Bends slope risk assessment report*, Report No. GE-0828-D, Great Western Highway Upgrade, Mount Victoria to Lithgow Alliance, Sydney.

Roads and Maritime Services (RMS). (2011). *RMS Guide to slope risk analysis version 4*, Road Pavements and Geotechnical Engineering Section, Roads and Maritime Services, Parramatta.

9. Notation

ALR: Annualised Life Risk, defined as the annual probability of a fatality.
D: Coefficient of longitudinal deceleration.
L_{dsd}: Decision sight distance (AASHTO 1990).
L_V: Average length of vehicles.
N: The number of elements at risk exposed to the hazard.
N_r: Number of rocks.
N_V: The number of vehicles that pass through the domain per day.
P(H): Annual probability of hazard detaching and reaching the road. The probability of reaching the road is the probability of detachment p(d) multiplied by the probability of reaching the road p(t).
P(S): The probability that a rock hits a vehicle, the product of P(H) and P(S:H).
P(S:H): Probability of spatial impact given the hazard event reaching the road. It is a function of the spatial relationship between vehicles, geotechnical domain, length of vehicle, speed limit, traffic volume (ALR equation).
P(S:H): Probability of vehicle impact given a rock fall (Bunce equation).
P(T:S): Temporal spatial probability of the consequence occurring. It is the probability a vehicle is present within the impact zone for a portion of time throughout the year.
RT: Reaction time (seconds).
V: Initial speed (km/hr).
V_n: Vulnerability of the element at risk within the zone of impact due to the hazard event. The value varies between 1 (certain death) and 0 (no death).
V_V: Posted speed limit.
λ: Factor based on engineering judgment distinguishing good, moderate, and poor line of sight.

Proceedings of the 10th ANZ Young Geotechnical Professional's Conference – 10YGPC
Noosa, Queensland, Australia
10 – 12 September 2014

UNDERSTANDING RIVER BANK COLLAPSE HAZARDS: WHY PURSUING MANY SOURCES OF INFORMATION IS WORTH THE EFFORT

Matthew TERVET
Senior Engineering Geologist, Coffey, 33 Richmond Road, Keswick, SA 5000, Australia

ABSTRACT – Relatively large collapses of the banks of the River Murray in South Australia started in February 2008 as a result of very low river water levels in the lower reaches of the river. The location and timing of the collapses were difficult to predict and occurred quickly with little warning. In 2012 a review was undertaken of long term management options at four sites on the banks of the River Murray which had been judged to be at high risk because of the potential for river bank collapse.

This paper overviews the approach taken to develop an understanding of the river bank collapse hazards and demonstrates the benefit of assembling many sources of information (such as bathymetry, topography, observations from overview site visits). Selected examples from the project are presented which illustrate how a slope model was developed to understand the failure mechanisms. The use of back analysis to help understand the conditions leading to instability, how the slopes fail and why large river bank regressions can occur is also discussed.

The paper concludes by briefly discussing the range of potential management options for the four sites of interest.

1. Introduction

River bank collapses (landslides) were first recorded in 2008 in the lower reaches of the River Murray (below Lock 1) following a prolonged period of drought. River bank collapses and evidence of instability continued for a number of years whilst river levels remained low. Photograph 1 shows one of the most dramatic collapses that occurred in this period. Individual collapses up to at least 5,000 m^3 involving river bank retreats of 20 m occurred in places. From eye witness accounts it appeared failures occurred in tens of seconds to a few minutes.

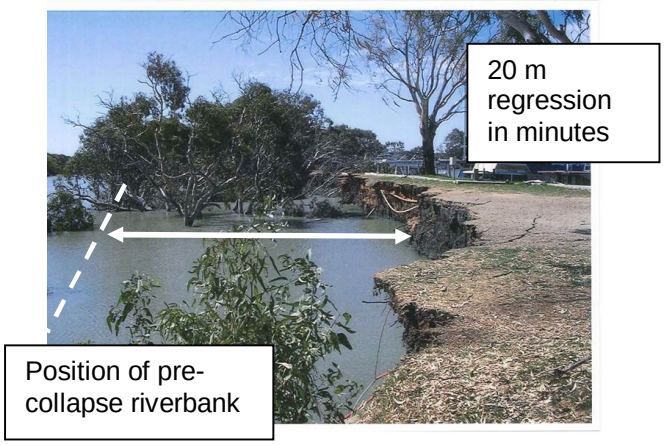

Photograph 1. Riverbank Collapse at Long Island Marina, Murray Bridge.

The pool levels at the time of the collapses were between RL -0.6 m and RL -0.9 m AHD, down from a normal operating range of approximately +0.75 m. In response to the collapses and the potential for further collapses public access was restricted at some sites as an interim measure.

In 2012 Coffey Geotechnics was engaged by the Department of Environment, Water and Natural Resources, South Australia (DEWNR) to carry out a review of long term management options for four sites on the banks of the River Murray which had been judged by DEWNR to be at high risk because of the potential for river bank collapse. Varying degrees of instability ranging from minor cracking to large river bank regressions had been previously documented at the four sites prior to the start of this project. Previous geotechnical investigations had also been conducted at the sites.

This paper describes the process of developing slope models for river bank collapse hazards as part of the review and highlights the value of incorporating many sources of information.

2. The importance of slope models

In landslide risk assessment understanding the hazards (what has happened, why it has happened and what else can happen) is probably the most time consuming and important task (Powell, 2002).

This process of understanding the hazards involves developing the most realistic slope model possible which incorporates and interprets the available information. In some cases, the information may be readily available (topographic maps) in other cases effort has to be put in to obtain the information (such as historical records, local knowledge or requesting more survey).

In some cases, failure to pursue and assemble key information can lead to unrealistic slope models and insufficient understanding of the

hazards and their consequences. Without this knowledge decisions about risk management or remediation may be ineffective or unnecessary or even counterproductive. Similarly, the value of stability analysis also depends on the degree to which the model is reflective of the actual conditions and failure mechanisms at a site. A factor of safety of 1.5 is irrelevant if the model is unrealistic or does not account for the actual conditions on site.

As described in Moon and Wilson (2004), assessments of landslide (e.g riverbank collapse) likelihood are evidence based judgments and the quality of these judgments improves when evidence is assembled and understood. It is therefore of great benefit to recognize the uncertainty in a slope model and make an effort to assemble a wide range of information sources to improve understanding of hazards. For most slope stability problems, this involves developing a slope model which considers how the slope formed, how it behaved in the past and how it might behave in the future (Moon and Wilson 2004).

3. Previous work and project approach

Previous work by others (mainly consultants working with DEWNR) had concluded that the principal failure mechanism causing river bank collapse was slope failures in soft Holocene aged clay due to the increased weight (effective stress) of the river bank resulting from lower pool levels in the River Murray.

Understandably, previous investigations had focused on particular sites where lives and infrastructure were judged to be at risk. The focus and approach taken as part of this review was to independently develop an understanding of the hazards in the wider region and the conditions which could lead to a large rapid failure. This involved overviewing existing primary information beyond the four sites of interest and pursuing other important information sources. No additional site investigations were undertaken. This approach is described in the following sections.

4. Pursuing, assembling and interpreting sources of information

Table 1 lists some of the information sources that were pursued and assembled for this project and outlines the benefit to the slope model. The information sources in Table 1 were pursued and assembled because it was realized they would improve the understanding of the hazards.

Table 3. Selected examples of information sources and benefits to slope model

Source of information	How it was used	Benefit to slope model
Geological history (maps, bulletins)	River channel evolution models (diagrammatic sketches) were prepared and presented in the report (Figure 1)	Helped understand the distribution, engineering properties and behaviour (including stability) of the materials in the ground, particularly the significance of soft Holocene aged clay.
Bathymetry	Slope profiles were prepared for comparison (Figure 2)	Demonstrated range of river bank slopes which had failed (ranging between 18º to 30º). Allowed comparison of pre and post failure slope geometries which were used in back analysis.
Field overview of 18 other river bank sites along more than 50 km of river.	Overview of other river bank failures used to improve overall knowledge of river bank collapses, their size, speed and occurrence.	Improved understanding of river bank collapse in the same geological environment elsewhere. Illustrated the range of sites where cracking or collapse had occurred. Helped understand the range in speed and magnitude of failure from very rapid and large to minor cracking.
Review of two well documented collapses	Back-analysis was undertaken	Improved understanding of hazards, magnitude and mechanism of failure, and possible future behavior.
NOTE: Other information sources not discussed above included; primary information from existing geotechnical reports (such as boreholes and CPTs), survey monitoring data at selected sites, site observations and review mapping (of topography, cracking, slope and river bank features) at the four sites needing review; topography from Digital Elevation Models (DEMs) and aerial photography.		

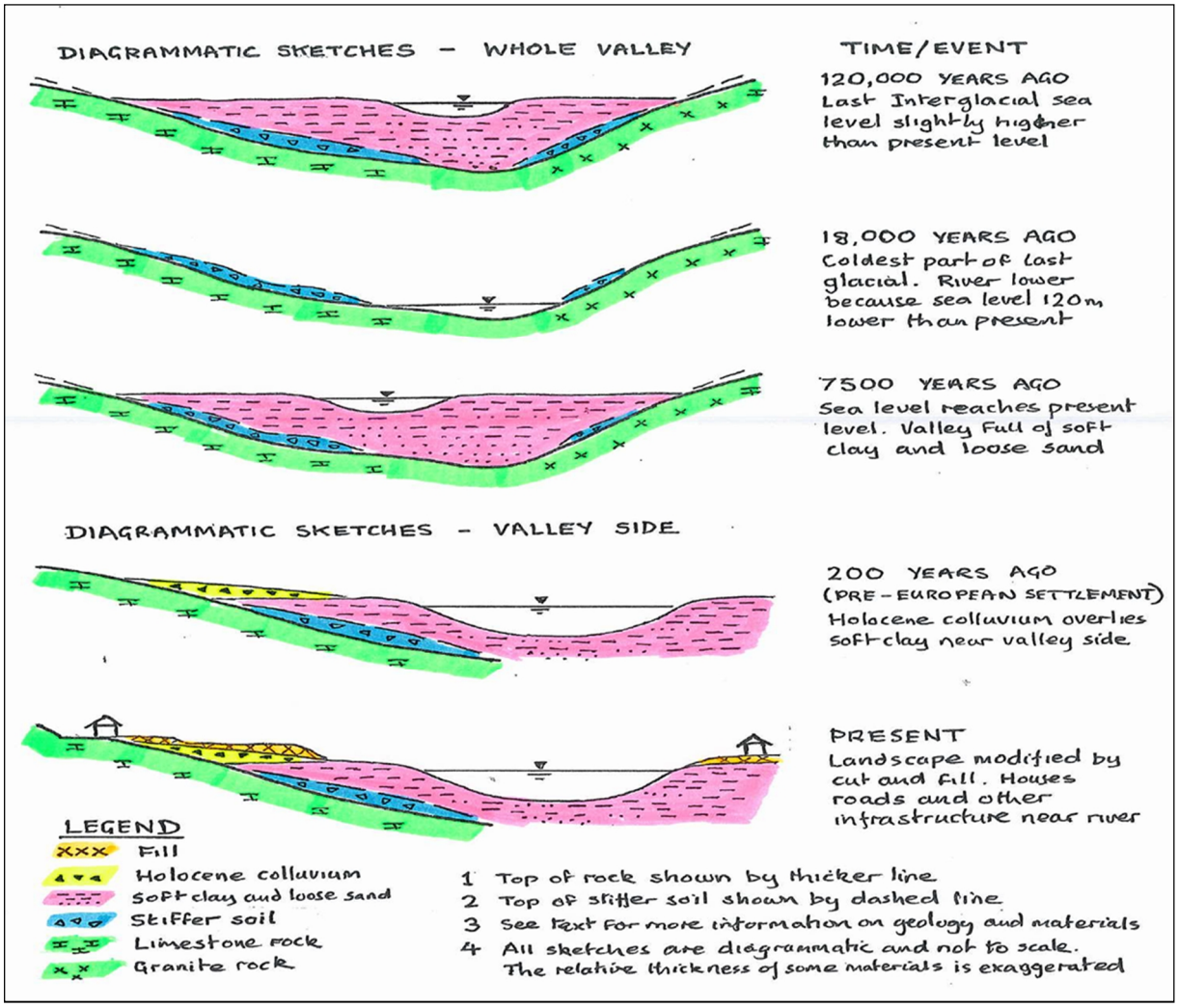

Figure 1. Diagrammatic sketches of geological history of the lower River Murray

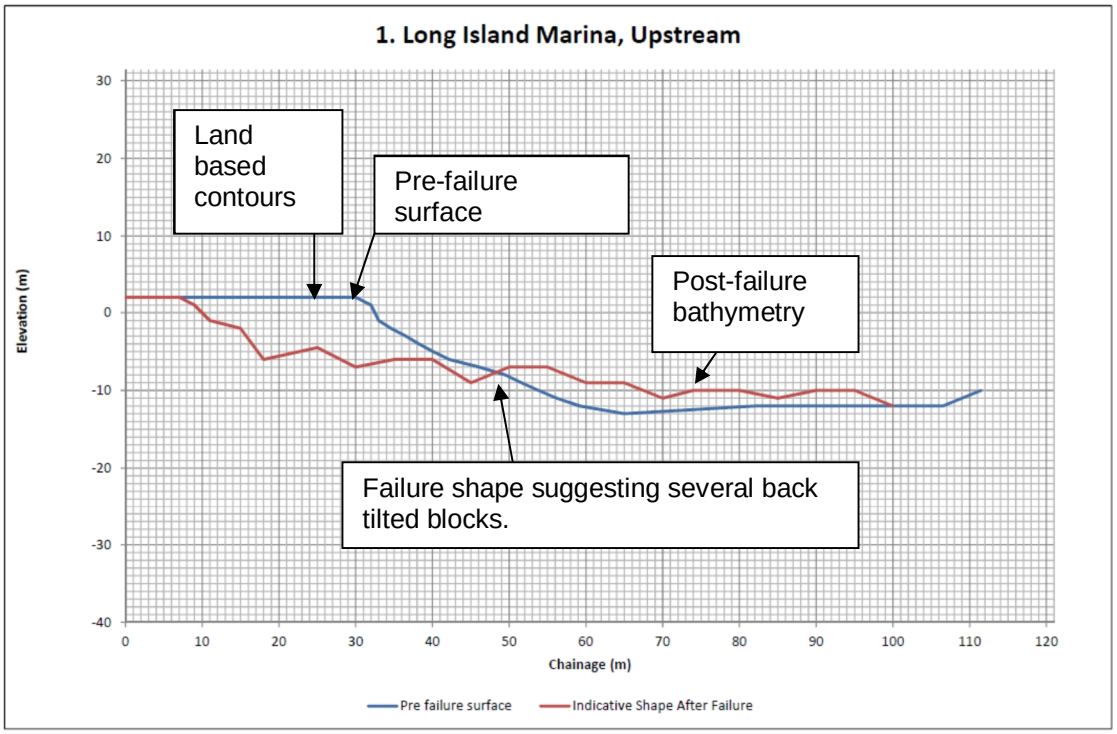

Figure 2. Example slope profile prepared from bathymetry showing pre and post failure surfaces.

For this project, the following activities were undertaken to interpret the information in Table 1 and better understand the hazards:

- Development of preliminary ground models, working maps and representative sections of the four sites.
- Preparation of simplified slope profiles using all available bathymetry and land based contours for eight sites in the region where failures had occurred (for example Figure 2). This involved graphical interpretation of the pre-failure profile based on the river bank contours upstream and downstream of the failure.
- Classification of the types of river bank failure into four categories (ranging from very rapid large collapses (failure within minutes) to relatively minor cracking) based on magnitude and speed of river bank collapse. A risk matrix was developed based on slope failure and land use categories (including infrastructure, public open space and restricted access) to enable a discussion of relative risk levels with respect to potential loss of life, injury or loss of assets.
- Back-analyses of two very rapid large collapses (this is described in more detail section 5) and stability analysis at the four sites of interest.

From the assembly and interpretation of the above information it was clear that a very rapid and large collapse (more than 15 m bank regression) had the greatest potential to cause loss of life or damage.

5. Back-analysis of larger failures

Back-analysis was undertaken of two of the most dramatic river bank collapses (Photograph 1) to better understand the conditions leading to a rapid failure and why large riverbank regression could occur.

Limit equilibrium stability analysis was undertaken using SLIDE software and the Morgenstern and Price method. The strength and density properties used in the back-analysis were selected based on existing geotechnical test results and experience. The material properties adopted in the base case model are summarised in Table 2. The back-analysis also required knowledge and judgements of the following:

- Pre- and post-failure geometries of the slope profiles assessed from bathymetry;
- The amount (distance) and speed of river bank regression, and local reports of further failures;
- The post-failure bathymetry of the slides which indicated a failure surface above the base of the river bed as opposed to a deep seated rotational failure.

The parameters were varied in a sensitivity analysis to assess the effects of water level changes, tension cracks, surcharge and changes in strength of the materials (particularly the soft clay). The results of some of the sensitivity analysis are summarised in Table 3. Calibration of the back-analysis with site observations was carried out. In particular it was found that the amount of head scarp regression (taken as the back of the slip circle) in the first stability run was much less than that observed. As a result, further analysis was undertaken of the initial and secondary failed slopes in selected models. The stability analysis of an initial failed slope is presented in Figure 3.

Table 3. Summary of some of the sensitivity analysis

Stability case	FOS	Head scarp regression
Base Case	0.88	11 m
Water level 1.4 m higher than base case	1.1	10.7 m
With 10 kPa surcharge	0.8	10.8 m
Initial failed slope	0.92	22 m
Secondary failed slope	0.61	28 m

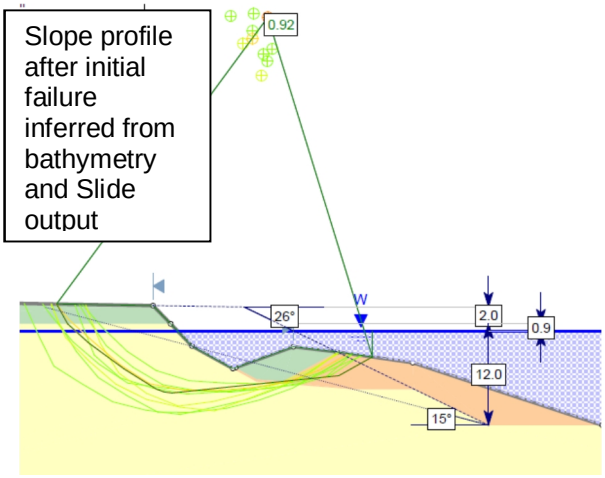

Figure 3. Stability analysis of initial failed slope to evaluate progressive failure mechanism

Table 2. Material properties used in back-analysis

Material Unit	Undrained C_u (kPa)	Drained		Unit Weight (kN/m^3)
		c' (kPa)	ϕ' (deg)	
Desiccated crust	50	2	28	18
Soft Holocene Clay	5.5 + 1.25 kPa per meter depth[1]	-	-	16
NOTE: [1]The undrained shear strength was a taken as function of reduced level with C_{u0} set at RL 0 m on the basis of the geological history and existing laboratory results.				

. The reassessment and back-analysis of the two large collapses lead to improved understanding of the hazards. From this work it was concluded:

- The drop in river level caused a large reduction in stability and appeared to be the major cause of river bank collapse.
- A fill surcharge on the bank also reduced the stability but field experience showed that riverbank collapse could occur where there is no fill.
- The collapses that cause large regressions (more than 15 m of bank) were probably the result of progressive failure (ie. a rapid succession of collapses)

6. Potential management options at four sites of interest

The information and evidence collected to understand the hazards for this review allowed discussion of a range of potential management options for the four subject sites which reflected the varying geological conditions and risks at each site. Such options ranged from; lowering road levels to enhance stability; pilling in front of properties underlain by a thin wedge of soft clay to recognition of the prohibitive costs of treatment in sites underlain by deep (> 20 m) soft clays.

7. Conclusions

This paper has overviewed the approach taken to develop an understanding of river bank collapse hazards for a project on the River Murray.

The focus on assembling many sources of information (such as bathymetry, topography and observations from overview site visits) beyond the four sites of primary interest and the back analysis of two larger failures lead to improved understanding of the conditions which lead to instability.

The following activities were of particular benefit in this project and could be considered when assessing similar landslide hazards:

- Reviewing and understanding relevant information of hazards in a wider area to better understand a site specific hazard (e.g how slopes are behaving in the region).
- Preparing working ground models, maps and sections which incorporate much information (ie. topography, bathymetry and observations). and the thinking time this provides to better understand the hazards and potential failure mechanisms.
- Undertaking back-analysis and reassessment of two larger failures which were not part of the project brief, but provided invaluable knowledge and helped understand the progressive failure mechanism.

8. Acknowledgement

The author thanks DEWNR for permission to publish this paper.

9. References

Powell G. (2002). Discussion "Landslide Risk Management Concepts and Guidelines". *Australian Geomechanics.*

Moon A.T., Wilson R.A (2004). Will it happen? – Quantitative judgements of landslide likelihood. *Proceedings of the Australia New Zealand Conference on Geomechanics, Centre of continuing education, University of Auckland,* pp 754-760.

This page intentionally left blank

Proceedings of the 10th ANZ Young Geotechnical Professional's Conference – 10YGPC
Noosa, Queensland, Australia
10 – 12 September 2014

RAIL EMBANKMENT FILL RETENTION WITH SOIL NAILS – CASE STUDIES

Louis KING
Golder Associates, Melbourne Australia

ABSTRACT – As part of the Regional Rail Link project in Melbourne's inner west, a number of near vertical slopes in variable fill materials were supported using soil nails. Pull-out testing of sacrificial nails indicated that significant variation in soil-grout adhesion could be expected, and in some instances the adhesions adopted in the original designs could not be achieved. The results of soil nail testing and observations made by engineers during site visits have been further investigated to understand the factors that influence the soil-grout adhesion, with results suggesting that the soil moisture content and hole stability greatly influence the load transfer between the nail and surrounding soil. This paper documents three soil nail wall case studies, including data obtained from soil nail testing in materials ranging from engineered fills to highly variable historic fills.

1. Introduction

In recent decades soil nails have increasingly been used to stabilise cut and existing slopes due to being an economic and efficient retention system. Soil nails typically comprise a 20 to 30 mm diameter steel bar that is inserted into a drilled hole at an angle that will generate tensile forces within the nail. Grout is then pumped into the hole, generally under gravity; however pressurised grouting can be used and has been found to achieve higher soil-grout adhesions (Sou et al., 2012).

Soil nails are not post tensioned like ground anchors; rather they act as passive elements that generate tensile forces through relative displacement between nail and surrounding soil. The load transfer between the nail and surrounding soil is influenced by soil properties, soil-nail interface roughness, soil moisture content, installation and grouting methods and applied vertical pressure (Chu and Yin, 2005; Su et al., 2007).

Typically when designing a soil nail retention system, the nail pull-out capacity or soil-grout adhesion is estimated based primarily on the shear strength of the soil, while taking into consideration other constraints that will impact the soil-grout adhesion. Design assumptions are then verified in the field through a series of pull-out tests, which are undertaken on sacrificial nails.

Favourable ground conditions for soil nails include firm to stiff low plasticity clays, fine to medium sands with some cohesion, engineered fills that have been placed and compacted in accordance with an earthworks specification and weak / extremely weathered rock (Phear et al., 2005). However, when constructing a number of soil nail walls as part of the recently completed Regional Rail Link – City to Maribyrnong River project, conditions such as variable and low strength fill materials, nails intercepting groundwater and unstable granular materials were encountered. Estimating appropriate pull-out resistances that take into consideration all of these factors proved challenging.

Field pull-out testing on these soil nails produced varying results, requiring in some instances changes to the nail configurations with reduced soil-grout adhesions. The observations from site and the results of pull-out testing have been investigated to better understand the influence these unfavourable conditions may have on the pull-out resistance of soil nails.

It is not the intent of this paper to discuss the soil nail design process in detail, rather to provide results of field verification testing and lessons learnt from the construction process. For further information on design processes the reader may refer to Australian Standards AS 4678-2002, CIRIA C6357 (2005) and FHWA SA-96-069R (1998).

2. Case studies

The Regional Rail Link project is a 47.5 km rail line running from West Werribee Junction to Melbourne CBD, creating dedicated tracks for regional trains to reduce bottlenecks in Melbourne's rail network. The most geotechnically complex section of the project is within the City to Maribyrnong River (RRL-CMR) package, which runs from Melbourne CBD to Hopkins Street, Footscray, and is typically constructed over Quaternary alluvium, known as Coode Island Silt (CIS).

As part of the project, a number of existing rail embankments required cutting and stabilising to allow the construction of new rail lines. Soil nails were generally adopted as the preferred retention option in these cases due to their construction and economic advantages over other design solutions, e.g. piled walls.

When designing the soil nail retention systems a two-stage design process was undertaken:

Stage 1: The first stage involved an assessment using the limit state equilibrium software SLOPEW.

This was used to confirm that the proposed design satisfied the design criteria; typically a minimum Factor of Safety (FOS) of 1.3 for short term and a minimum FOS of 1.5 for long term loading.

Stage 2: The second stage involved modelling the soil nail arrangement adopted in SLOPEW using the two-dimensional finite-element package PLAXIS (2D). Finite element modelling was used to assess the deformation of the soil nail wall, overall movement of the ground during excavation and confirm stability of the proposed design.

Top down construction was adopted for all the soil nail systems, typically comprising 1 m to 1.5 m bench heights. After each bench was nailed, steel-reinforcing mesh was placed against the cut face with a layer of shotcrete, approximately 150 mm thick, sprayed over the face. Once the shotcrete had cured, the next stage of excavations could progress, repeating this process until the final height of the wall was achieved.

Vertical strip drains were placed directly against the cut face to prevent the build-up of water behind shotcrete. Care was taken to keep these drains from becoming encapsulated in shotcrete, which would significantly reduce the effectiveness of the drains. Also, spoon drains were used at the top of the wall to collect and divert surface water.

2.1. Case study 1 – Maribyrnong viaduct

To construct the piers for a new viaduct structure next to an existing 8 m high railway embankment, soil nails were used over a length of approximately 160 m to steepen the batters from an existing 1.5H:1V slope to a near vertical (1H:6V) wall up to 4.6 m in height (refer to Figure 10). The soil nail wall was constructed with train lines remaining active on the adjacent embankment, meaning that movements resulting from the walls construction could not impact the safe operation of the train lines.

Figure 10. Maribyrnong viaduct soil nail wall

Due to limited access in the active rail corridor and construction sequencing, a geotechnical site investigation was not carried out within the footprint of the soil nail wall. Boreholes either side of the wall footprint indicated that beneath the existing embankment fill a 1.2 m thick layer of uncontrolled fill overlies soft silty clay (CIS).

One of the concerns raised at the design stage was uncertainty regarding the composition and consistency of the existing embankment fill and underlying uncontrolled fill. This caused difficulty in estimating soil properties. Based on the available information which included some slots excavated at the embankment toe, a preliminary ultimate soil-grout adhesion of 60 - 80 kPa was assumed prior to the testing stage of works.

In lieu of a site investigation a program of logging pull-out test holes, pull-out testing and rigorous construction monitoring and supervision was implemented to manage the additional risk. The construction supervision comprised a geotechnical engineer attending site during bench excavations and logging a nominated amount of soil nails to confirm fill materials were consistent and in accordance with design assumptions. Monitoring of the lateral and vertical movements of the rail track, gantries and soil nail wall was undertaken, with results forwarded to a geotechnical engineer and revised assessments made prior to proceeding with the next stage of excavations.

Six pull-out tests were undertaken at various levels along the length of the wall, with all nails comprising a 15 degree declination, 3 m bond length and 0.125 m hole diameter. Figure 11 presents the soil nail toe level plotted against the achieved soil-grout adhesion.

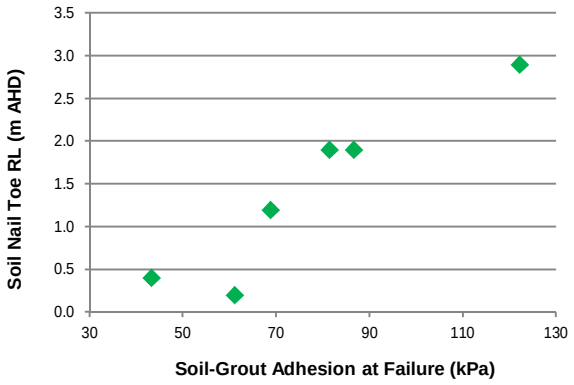

Figure 11. Nail toe RL v soil-grout adhesion – Maribyrnong viaduct

During the installation of the nails, fill material was observed to become moist below RL 0.5 m and deleterious material, such as brick and concrete rubble, was present in the drill cuttings of the tests which resulted in the three lowest soil-grout adhesions.

The results seen in Figure 11 and observations made during the installation of the sacrificial nails (i.e. the moisture content of drill cuttings increasing with depth) indicate that the moisture content of the surrounding soil influences the soil-grout adhesion. These observations are in line with the findings of Su et al. (2007) who performed pull-out testing on Completely Decomposed Granite (CDG) at four

different degrees of saturations. The study found that the peak pull-out resistance for CDG with a degree of saturation of 75% was about twice the resistance of the same material when fully saturated.

Based on the results of the pull-out tests, the soil nail wall design was modified to incorporate the lower soil-grout adhesions. The revised design comprised significantly lower soil-grout adhesions for nails in the lower benches, which encountered moist / saturated materials.

VicRoads Section 683 requires 5% of all production nails be proof tested to 150% of the allowable soil-grout adhesion. The results of these proof tests confirmed that the parameters adopted in the redesign were suitable. Construction of the wall with the revised nail configuration progressed quickly and the 160 m long wall was constructed without delay.

Post construction survey monitoring was undertaken along the wall and railway track, measuring both settlement and lateral movement. The results of this monitoring indicated that movements generally stabilised within two weeks after construction. Post construction settlements of the wall ranged between 22 mm and 36 mm and lateral movements between 3 mm and 6 mm.

2.2. Case study 2 – Arrivals yard

A dive structure to allow the passage of an access track beneath new rail lines was constructed using soil nails to support near vertical batters up to 4.6 m in height. The soil nails were installed beneath an adjacent track that remained active throughout construction, once again limiting the allowable movements of the soil nail wall.

Figure 12. Arrivals yard access dive structure

The site had limited space and was bound by busy roads and live rail. As a result, nails were moved and angles of nail declination varied as construction progressed in order to accommodate site constraints.

Site investigations within the vicinity of the dive structure indicated that the base of the excavation and the toes of the lower soil nails might encounter CIS and groundwater. These issues were identified at the design stage in addition to uncertainty regarding the composition of the fill materials.

Observations during the installation of sacrificial nails for pull-out testing suggested that the fill was variable in nature and consistency. The fill material was also more granular than expected, and some holes became unstable. Nails affected by instability required redrilling, more grout and resulted in lower soil-grout adhesions from pull-out testing.

Based on these observations and the site investigations, it is inferred that the fill materials are "historic" fills, which were not placed, compacted or selected to modern day standards. Phear et al. (2005) describes how in the past, railway embankments were "*constructed from end- or side-tipping of material and may contain loose or variably graded materials".*

To drill these variable materials in an efficient manner, the contractor experimented with using small amounts of water in some holes to assist in the removal of drill cuttings and hole stability. The water was sprayed into the drilled hole as a mist, with air pressure used to blow the wet material out of the hole. It was observed during site inspections that the drill cuttings were almost saturated upon removal. However, since these nails were within the upper bench it was considered unlikely that the saturated material was resultant of groundwater, and no evidence of perched water had been observed in nearby excavations or investigations.

Using this approach the results of the pull-out tests were extremely variable, as can be seen in Figure 13, with soil-grout adhesions ranging from 28 kPa to 81 kPa. Again the ultimate soil-grout adhesion assumed in the design could not be achieved with such low pull-out resistances. An option at this stage was to modify some of the drilling methods such as implementing casing to provide stability to the hole. However, to confirm that these methods could achieve the required soil-grout adhesions, further pull-out testing would have been required, which the project schedule did not allow. Modifications to the nail configuration were made, reducing the adopted soil-grout adhesion based on the results of testing. The revised nail configuration resulted in nails installed at closer intervals and under an increased level of geotechnical supervision. Production nails were installed without the water use, as this was considered to adversely impact soil-grout adhesion.

Production nail testing was again implemented, testing at least 5% of nails to 150% of the working load. Testing confirmed that the revised nail configuration and soil-grout adhesions could be achieved with the adopted drilling methodology.

With the tight construction program schedule there was no time to vary construction methodologies, i.e. using casing or auger drilling, which may have been able to achieve the soil-grout adhesions assumed in the preliminary design. Instead, the nail configuration was revised, which reduced project delays that would have likely resulted from further verification testing.

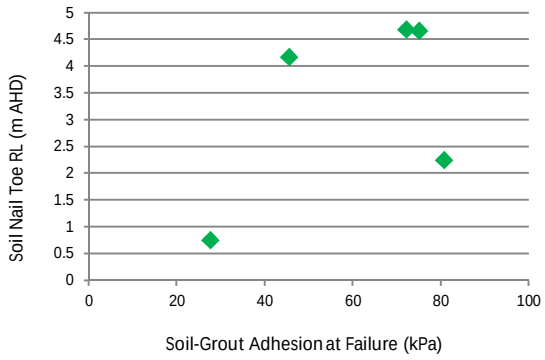

Figure 13. Nail toe RL v soil-grout adhesion – Arrivals yard

2.3. Case study 3 – North Dynon lead

As part of the RRL-CMR section of the project an existing rail embankment needed to be widened, which resulted in the temporary blocking of an adjacent access track. The widened embankment was constructed by keying into the existing batter and placing and compacting select fill (predominantly clayey material with varying amounts of gravel) at a 2H:1V batter, achieving a controlled engineered fill. This batter was left in place for over 6 months before commencing the construction of a soil nail wall, allowing the re-opening of the access track. The wall is up to 2.8 m high and extends for approximately 65 m as can be seen in Figure 14.

Figure 14. North Dynon lead soil nail wall

Site investigations within the vicinity of the wall indicated that the nails would not encounter groundwater and would be installed predominantly within the engineered fill. This provided the design engineers with greater confidence in the estimated soil-grout-adhesions.

During the installation of sacrificial nails, drill cuttings were easily removed from the drilled hole without the use of added water and appeared to remain relatively consistent in composition along the length of the wall. Some nail cuttings were observed to become more granular and variable in consistency as nails penetrated greater depths. The drilled holes remained stable without the use of any casing due to the high clay content in the engineered fill materials.

Pull-out testing on four sacrificial nails confirmed the design assumptions with ultimate soil-grout adhesions of between 70 kPa and 106 kPa achieved (refer to Figure 15). These results allowed construction of the wall to commence immediately and since the engineered fill was easily drilled, construction of the wall advanced quickly.

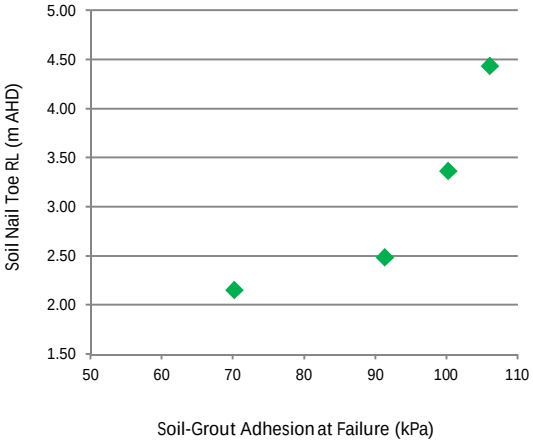

Figure 15. Nail toe RL v soil-grout adhesion – North Dynon lead

Based on observations from site, the relationship seen in Figure 15 is not considered to be due to moisture content of the surrounding soil, as seen in *case study 1*. Rather, sections of soil nails installed at lower levels have penetrated through the engineered fill, encountering more granular fill with lower shear strength, resulting in lower pull-out resistances with increasing depth.

As construction progressed, further production nail testing to confirm working loads was undertaken. The results of both pull-out and production nail testing as well as the rate of construction validated that engineered fill comprising stiff clays is an ideal ground condition for soil nails due to its uniformity and shear strength.

3. Conclusions

A number of soil nail walls have been constructed as part of the RRL-CMR section of the project to support near vertical slopes within various fill materials. The results of soil nail testing and observations made during site visits for three soil nail walls suggest that significant variability in soil-grout adhesion can be expected when nails are installed within such materials.

The influence of overburden pressure is argued by some to increase the shear resistance and therefore the soil-grout adhesion. However, due to shallow water tables and varying fill composition, this assumption could not be applied to the soil nail walls constructed as part of this project.

Pull-out testing typically indicated that nails installed at lower levels and encountered groundwater resulted in significantly lower soil-grout adhesions. Similar results were found for nails that encountered granular materials, where holes became unstable during drilling. Nails installed in these unstable materials resulted in lower pull-out resistances compared to nearby nails that remained stable during drilling.

Due to tight controls and site constraints, a high level of site supervision and survey monitoring was employed to confirm material consistency and ensure that the strict allowable movements were not exceeded. This approach has been found to be successful in reducing risk and satisfying stakeholders such as rail authorities and asset owners.

4. Acknowledgements

I would like to thank the Regional Rail Link City – Maribyrnong River Alliance for allowing the information presented within this paper to be published.

Thanks are also due to Dr Joel Gniel of Golder Associates, who has provided mentoring and leadership during the RRL-CMR section of the project as well as valuable feedback on this paper.

5. References

Chu L.M., and Yin J.H. (2005). Comparison of interface shear strength of soil nails measured by both direct shear box tests and pullout tests. *Journal of Geotechnical and Geoenvironmental Engineering*, Vol. 131 pp.1097-1107.

Hackney G. and Bridges C. (2014). Stabilisation of a fill embankment using soil nails. *Australian Geomechanics*, Vol. 49 (1), pp. 81-89.

Junaideen S.M., Tham T.G., Law K.T., Lee C.F., and Yue Z.Q. (2004). Laboratory study on soil-nail interaction in loose, completely decomposed granite. *Canadian Geotechnical Journal,* Vol. 41, pp. 274- 286.

Phear A., Dew C., Ozsoy B., Wharmby N.J., Judge J., and Barley A. D. (2005). *Soil nailing – best practice guidance*, C6357. CIRIA, London.

Seo H.J., Jeong K.H., Choi H., Lee I. M. (2012). Pullout resistance increase of soil nailing induced by pressurized grouting. *Journal of Geotechnical and Geoenvironmental Engineering*, Vol. 138 pp. 604-613.

Su L.J., Chan T.C.F., Shiu Y.K., Cheung T., and Yin J.H. (2007). Influence of degree of saturation on soil nail pull-out resistance in completely decomposed granite fill. *Canadian Geotechnical Journal,* Vol. 44, pp. 1314-1328.

Su L.J., Chan T.C.F., Yin J.H., Shiu Y.K., and Chiu S.L. (2008). Influence of overburden pressure on soil-nail pullout resistance in a compacted fill. *Journal of Geotechnical and Geoenvironmental Engineering*, Vol. 134 (9), pp. 1339-1347.

Zhang L.L., Zhang L.M., and Tang W.H. (2009). Uncertainties of field pullout resistance of soil nails. *Journal of Geotechnical and Geoenvironmental Engineering*, Vol. 135 (7), pp. 966-972.

This page intentionally left blank

Proceedings of the 10th ANZ Young Geotechnical Professional's Conference – 10YGPC
Noosa, Queensland, Australia
10 – 12 September 2014

THE IMPORTANCE OF CONSTRUCTION SUPERVISION IN GEOTECHNICAL ENGINEERING – A CASE STUDY

Edward HAIKAL
Golder Associates Pty Ltd, Melbourne Australia

ABSTRACT – This paper presents three case studies from the Regional Rail Link project to demonstrate the importance of construction supervision in geotechnical engineering. In geotechnical engineering, unlike other engineering disciplines, design conditions (particularly subsurface conditions) cannot easily be defined and in some instances can be altered as a result of construction activities or natural events. Allowing for construction supervision and monitoring provides opportunities to produce innovative designs during the design phase and optimize the design during the construction phase. The costs associated with construction supervision are nominal compared to these benefits.

1. The Regional Rail Link project

At the time of its construction, the Regional Rail Link (RRL) was Australia's largest public transport infrastructure project. Jointly funded by the Victorian and Commonwealth governments, the RRL is designed to separate metropolitan and regional trains travelling through Melbourne's west through the construction of dedicated regional tracks. The train link extends between Southern Cross Station and West Werribee Junction passing through suburbs including Sunshine and Footscray.

Due to the relatively long length of track (approximately 47.5 km), the project was divided into six work packages.

The case studies presented in this paper are from Work Package B which covered the length of track between Melbourne CBD and Hopkins Street, Footscray.

1.1. Site conditions

The RRL track is located adjacent to existing rail. To match existing rail levels, most of the RRL track was required to be constructed above ground level, in some places up to 6 m high. Partial excavation and trimming of the existing rail embankments was required, which in turn generated large quantities of excess fill.

Due to the cost of off-site disposal, the RRL City – Maribyrnong River Alliance (the project consortium) deemed it to be economically favourable to reuse the excess fill on-site. Their preference was to construct embankments reusing the excess fill rather than to support the track on a structure.

1.2. Subsurface conditions

Subsurface conditions in the Work Package B area varied considerably. Typically, a layer of uncontrolled fill between 1 m and 5 m thick was present at the surface. Below the uncontrolled fill, Coode Island Silt (CIS) comprising soft and compressible silt and clay was present and ranged from about 3 m to 20 m in thickness. The CIS was typically underlain by a stiffer unit (basalt, Fishermans Bend Silt or Werribee Formation).

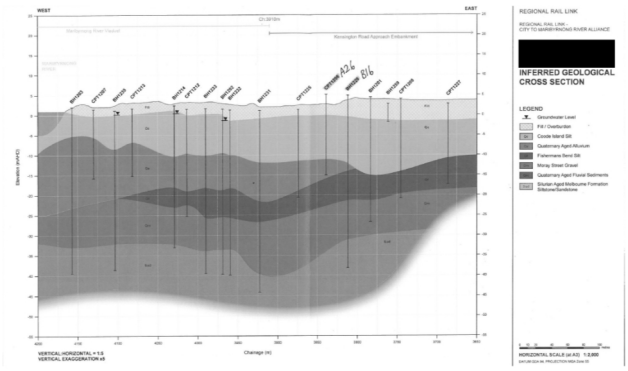

Figure 1. Geological section showing variable subsurface conditions

2. Case Study 1 – supporting innovation

Due to the relatively thick deposits of CIS, the embankment loads were required to be transferred to the stiffer underlying soils to prevent excessive settlements.

The design contemplated a less routine approach using controlled modulus columns (CMCs) to support the embankments rather than a more typical piled embankment solution.

Construction supervision provided the necessary assurance to the project proof engineers and rail authorities of the acceptability of the design.

2.1. CMC supported embankments

Some of the advantages of the CMC supported embankment solution include:

- higher production outputs than piles;
- cheaper material costs than piles due to the lesser amount of steel (CMC is not reinforced) and lower grade of concrete required;

- practically no spoil generated during installation, providing a cleaner project site, limiting the risk of surface contamination and minimising waste generated during drilling (CIS is expensive to dispose of off-site);
- minimal vibrations generated during installation enabling installation relatively close to sensitive structures; and
- reuse of potentially contaminated soil generated at various project locations.

These factors meant that the CMC supported embankment solution was significantly cheaper than other options available.

2.2. CMC design

A piled embankment supports its entire load on the piles. In contrast, a CMC embankment is supported by both the CMCs and the surrounding soil which is laterally compressed during installation. Therefore CMCs are considered a ground improvement option rather than a piled solution and are not required to satisfy pile design codes and standards.

The CMCs were designed to found at least 2 m into the stiff to very stiff layer below the CIS. Because of the variable subsurface conditions, each CMC was assigned a design installation depth based on expected subsurface conditions at the specific CMC location.

To limit differential settlement between adjacent CMCs, it was important that nearby CMCs found into similarly stiff materials.

Testing and construction verification were required to confirm that the CMCs were constructed to the required depths in accordance with the design intent and achieved the minimum 2 m penetration into stiff to very stiff material.

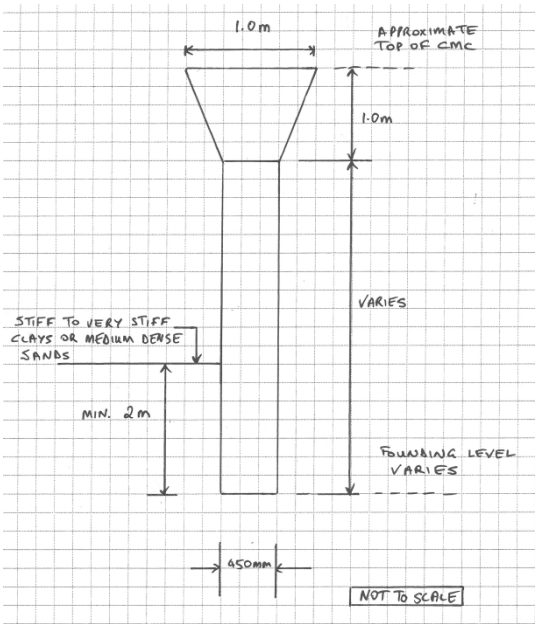

Figure 2. Typical CMC detail

2.3. Internal approval of CMC design

CMC supported embankments are becoming more popular in Australia due to their cost effectiveness but much research is still required regarding design and behaviour. There is no Australian Standard in relation to CMC design and installation. Given the risks of pursuing this relatively new solution, a comprehensive approach to CMC quality and assurance was required to both support adoption of the approach and its effective implementation.

The approach involved three integral elements:
1. Review of CMC installation rig data to confirm sufficient penetration into the underlying stiff layer and the required concrete shaft volume;
2. Limited and targeted testing to correlate rig installation data for quality assurance purposes and to assess the integrity of constructed shafts; and
3. Construction supervision to perform live assessments of conditions and respond to site and construction issues as they emerge.

Without such a rigorous approach, the project regulatory authorities would not have approved the CMC supported embankment design.

2.4. Design and testing savings

The Australian Standards for piling stipulate the frequency for testing and the appropriate factors for limit state design.

As CMCs are not required to comply with the pile design codes and standards and are not governed by any of the Australian standards, the quality control and targeted testing regime mentioned previously and a rigorous finite element based design approach were deemed required.

This resulted in significant cost and time savings for the project, for example, by removing the AS2159 – 2009 requirement that 5% of the over 1,000 CMCs be tested (assumed average risk rating of 4% to 4.9%).

The less stringent testing requirement of the CMC solution was compensated by a more rigorous site monitoring and review. Adoption of such ground improvement solution requires on-site presence of a geotechnical engineer.

3. Case Study 2 – responding to ad hoc issues

During the CMC installation works, unexpected construction problems were encountered. In many instances, the presence of a geotechnical engineer on-site allowed for an immediate assessment and judgment to be made, in turn reducing construction down-time associated with delays in resolving construction issues.

3.1. Construction supervision during initial stages

A geotechnical engineer was present on-site on a full-time basis to supervise the initial stages of

calibration, installation, testing and production. Based on site observations the geotechnical engineer was able to advise the RRL Alliance on appropriate revisions to construction practices and testing. This early identification and rectification of issues avoided the potential magnification of costs and delays to the project at a later date.

3.2. CMC production phase construction supervision

The on-site geotechnical engineer was able to observe live CMC rig data, installation and sequencing, enlarged head construction and hardstand conditions, and provide real-time confirmation or modifications to ensure the design intent was met.

3.3. Problems with CMC rig installation data

CMC installation rig data included the following:

- rig hydraulic pressure relating to drill torque;
- crown or down pressure;
- rate of penetration of the CMC drill head as each CMC was being installed; and
- concrete volume pumped versus depth used for the construction of each column.

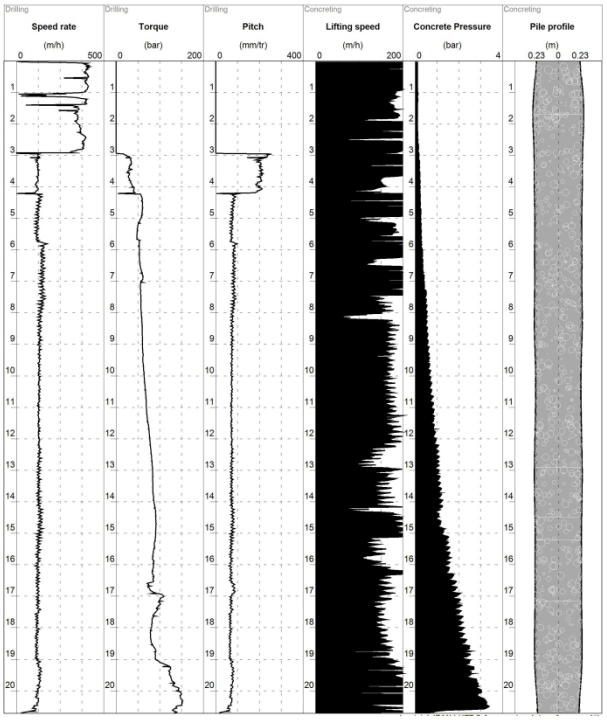

Figure 3. Example of CMC installation rig data

In one instance, the rig readout unit was malfunctioning and could not be relied upon. This would typically be a cause for the rig to shut-down and works to be delayed until the issue was resolved (possibly several days delay). In this case, the on-site geotechnical engineer was able to make an assessment of founding conditions based on live observations of the CMC rig response and a familiarity with the behaviour of a CMC rig during installation, based on observation of the installation of over 500 CMCs. For example when sufficiently stiff materials were encountered, the legs of the CMC rig would lift off the ground. This was supplemented by an increase in integrity testing.

If a geotechnical engineer was not present on site during initial stages of works and at the time problems with CMC rig installation outputs arose, construction works would have had to cease until the CMC rig instrumentation issues were resolved, resulting in significant time delays to the project and potential additional costs associated with installation of additional CMCs.

3.4. Consistency between different CMC contractors and crews

Three CMC contractors and several rigs and crews were involved in the CMC installation works for Work Package B. While CMC design information was provided to the contractors and crews, it was often difficult for the intent of the design (and lessons learnt) to be passed between contractors and from one section of the project to the next. This was facilitated by an on-site geotechnical engineer who was present throughout the production phase and resulted in process and operational improvements.

4. Case Study 3 – Customising design

Geotechnical design is typically based on the most unfavourable and conservative assumptions about geological conditions and soil engineering properties. Ralph Peck proposed an alternative approach to design (observational method) based on the most probable conditions with uncertainties accounted for by instrumentation measurements, geotechnical site investigation and construction supervision (Terzaghi and Peck, 1967).

This approach was successfully used on the design and construction of a soil nail wall built as part of Work Package B.

4.1. Design conditions

The soil profile at the soil nail wall comprised railway embankment fill underlain by an approximately 1 m thick layer of inferred uncontrolled fill underlain by CIS. The groundwater table was about 1 m to 2 m below the ground surface.

The soil nail wall consisted of three rows of soil nails installed sequentially to support three benches (upper, middle and lower).

Previous analysis indicated that the use of long-term (drained) parameters in conjunction with a 20 kPa live load surcharge applied across the width of the sleeper provided the most critical case with respect to stability. The project required a minimum

FOS against instability of 1.5 to be achieved using this approach.

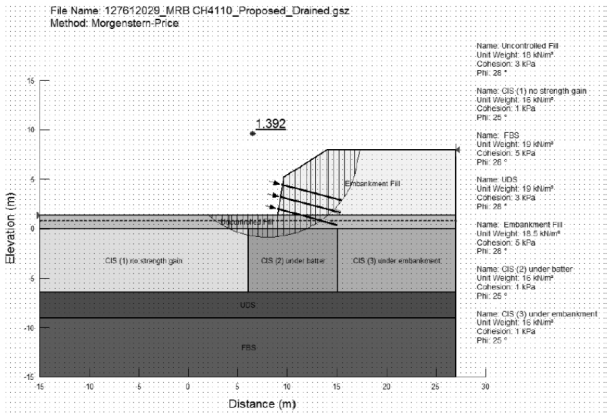

Figure 4. Slope/W output for soil nail wall

4.2. Adoption of more prudent soil engineering properties

Undrained and drained parameters adopted for the CIS were based on in situ and laboratory testing of samples of CIS obtained during the site investigation phase of the project.

The soil engineering parameters presented in Table 1 were adopted for modelling of CIS.

It was not possible to sample and test the embankment fill materials during the site investigation so the assessment of suitable parameters for design was made more difficult and had greater uncertainty.

Adopting overly conservative soil engineering properties consistent with limited investigation and extending the soil nail lengths was not practical due to the worsening soil strength and groundwater conditions with depth. Hence, it was important from a design perspective that the soil parameters adopted for the embankment fill were reasonable and prudent. A limited amount of sampling and shear box testing of samples taken from the embankment toe was therefore undertaken to provide greater confidence of soil parameters.

The soil engineering parameters presented in Table 2 were adopted for modelling of the embankment fill.

Although these soil parameters were still considered prudent, they were significantly less conservative than what had been adopted elsewhere on the project.

In view of the limited amount of testing, the geotechnical designer proposed that an observational method for design and construction be adopted to justify the use of the less conservative (but prudent) soil parameters used in design. The proof engineers and project regulatory authorities considered this approach to be acceptable.

The observational method adopted involved the review of design parameters and construction practices based on the results of:

- trial soil nail pull out tests;
- further laboratory shear box testing of soil samples recovered from the embankment fill;
- survey monitoring of the wall; and
- the full-time presence of a geotechnical engineer on site during construction to confirm that the materials encountered and the construction practices adopted were consistent with the design assumptions and intent.

Table 4 - soil parameters for CIS adopted in stability analyses (SlopeW)

Soil unit	Unit weight (kN/m^3)	Undrained shear strength (kPa)	Drained strength parameters	
			Friction angle (degrees)	Cohesion (kPa)
CIS (center of embankment)	16	32 + 1kPa/m	25	1
CIS (beneath batter)	16	22 + 1kPa/m	25	1
CIS (outside toe)	16	15 + 1kPa/m	25	1

Table 5 - soil parameters for fill adopted in stability analyses (SlopeW)

Soil unit	Unit weight (kN/m^3)	Undrained shear strength (kPa)	Drained strength parameters	
			Friction angle (degrees)	Cohesion (kPa)
Embankment fill	18.5	80	30	15
Uncontrolled fill (center)	18.5	50	30	10
Uncontrolled fill (beneath batters)	18.5	50	28	3

Photograph 1. Finished soil nail wall

4.3. Site observations during construction

During the construction of the soil nail wall, the site geotechnical engineer was able to confirm that the materials were consistent with the design assumptions.

The geotechnical engineer was also able to provide advice in regard to construction issues encountered on-site, such as collapsing holes (a result of occasional rabbit borrows in the embankment batter) and hole smearing.

In some instances elsewhere on the project where a geotechnical engineer was not present on-site during construction, there were issues and delays associated with confirming the design strengths.

5. Conclusion

It is evident from the case studies presented in this paper the important role that construction supervision by a geotechnical engineer played on the RRL project.

Firstly, in the case of the CMC supported embankment, this innovative and cost effective design solution would not have been approved by the proof engineers and project regulatory authorities without the support of a comprehensive approach to CMC quality and assurance.

Similarly, a numerical design approach was made possible by custom testing, more rigorous monitoring and review and site presence.

Secondly, construction supervision allowed issues encountered during construction to be promptly resolved on-site, reducing down-time associated with delays in resolving construction issues.

Finally, the adoption of less conservative soil parameters in design would not have been possible if it was not for the presence of a geotechnical engineer during construction works to confirm the materials encountered and construction practices were consistent with the design assumptions and intent.

The author considers the cost and time savings which were realised because of on-site presence of a geotechnical engineer outweigh the nominal costs of construction supervision.

The evidence suggests that further cost and time savings could have been achieved elsewhere on the project had there been a geotechnical engineer on-site during construction.

Although the examples provided in this paper are specific to the RRL project, the lessons learnt are applicable to other engineering projects, particularly larger scale projects where the savings in cost and time could be greater. Moreover the upfront cost of geotechnical supervision compared to overall project cost is relatively small.

6. Acknowledgements

Many thanks are due to the RRL City – Maribyrnong River Alliance for providing me with approval to share project information in this paper.

I would like to acknowledge the assistance of Dr Joel Gniel who provided valuable suggestions and feedback during the preparation of this paper.

Thanks are also due to Golder Associates Pty Ltd who have encouraged and supported me to prepare this paper.

7. References

AS2159 - 2009, *Piling – Design and Installation*, pp.60-69.

Terzaghi K., Peck R.B. (1967). *Soil mechanics in engineering practice*. J. Wiley, New York, pp.34.

This page intentionally left blank

Proceedings of the 10th ANZ Young Geotechnical Professional's Conference – 10YGPC
Noosa, Queensland, Australia
10 – 12 September 2014

DISPLACEMENT BASED BACK ANALYSIS OF BERM SUPPORTED RETAINING WALLS

Adrian KHO[1] and Michael MCAULEY[2]
[1] *Cardno, Brisbane, Australia*
[2] *GHD, Brisbane, Australia*

ABSTRACT - The use of earth berms left in place during bulk excavation is a cost effective method of enhancing the stability and reducing the size of a retaining wall. However, design guidance for berms is limited, especially in practice where a basic soil-structure interaction approach is more common. Several empirical methods of representing a berm have been previously published, including the equivalent surcharge method and the raised effective formation level method which are generally considered conservative and at times inaccurate. This paper presents a case study consisting three separate berm-supported retaining walls constructed as part of the Legacy Way tunnel in Brisbane. Monitoring data, collected following construction of the walls, was back analysed and used to compare against published empirical methods. The outcome of the study is a better understanding of the effect of berms on retaining walls as well as recommendations on a reasonable procedure for representing berms in design.

1. Berm supported retaining walls

The use of earth berms left in place during bulk excavation is a cost effective method of enhancing the stability and reducing the size of a retaining wall. Studies have shown that berms are more effective in reducing soil and wall movements than an increase in wall embedment (Powrie and Daly, 2002). Despite its known use for decades in underground excavation, design guidance for berms is fairly limited. This led Daly and Powrie (2001) to suggest that there is "generally no accepted procedure for determining their effectiveness".

Plane strain centrifuge model tests and finite element studies have been undertaken in the past. However, these may not be appropriate for routine use in design, where simpler methods of analysis are generally preferred (Daly and Powrie, 2001). The two most common of these methods, as described by Smethurst and Powrie (2008), are:

- *Equivalent surcharge method*

This method models the berm as an equivalent uniform surcharge, S*, added to the excavated soil surface and calculated from the weight of the berm. The surcharge is applied from the wall to the edge of the critical failure surface emanating from the toe of the wall. The lateral pressure exerted by the berm is neglected.

- *Raised effective formation level method*

This approach defines a design berm geometry that has the same based width, b, as the actual berm but has a slope of 1V:3H. The maximum height of the design berm is thus b/3. The design berm is modelled in the analysis by raising the formation level by half the design berm height (b/6). The portion of actual berm that extends above the design berm is then applied as surcharge to the new formation level using the equivalent surcharge method. The lateral pressure exerted by the berm is partly modelled in this method.

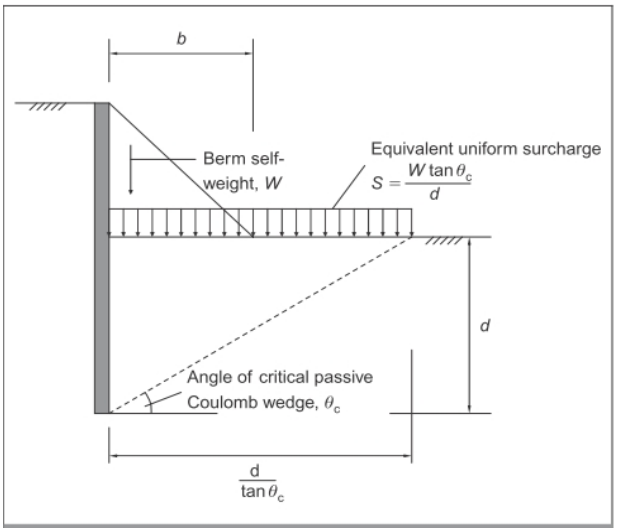

Figure 1. The equivalent surcharge method (after Smethurst and Powrie, 2008)

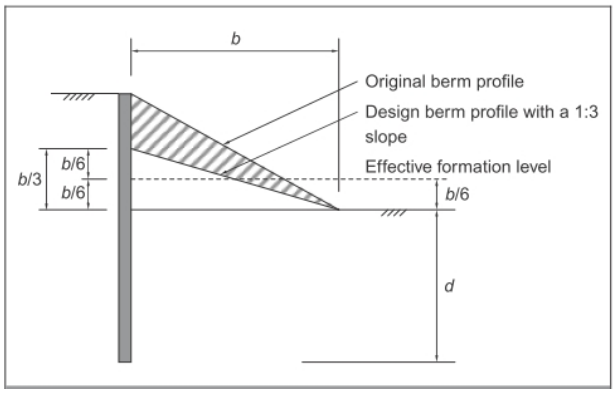

Figure 2. The raised effective formation level method (after Smethurst and Powrie, 2008)

A third method that has been frequently adopted by geotechnical designers is the minimum offset method which was introduced by the Geotechnical Engineering Office of Hong Kong through Geo Publication No.1 (Geotechnical Engineering Office, 2006). The publication suggests that lateral resistance of a pile is significantly reduced if the piles are positioned less than a distance of five to seven pile diameters from the slope crest.

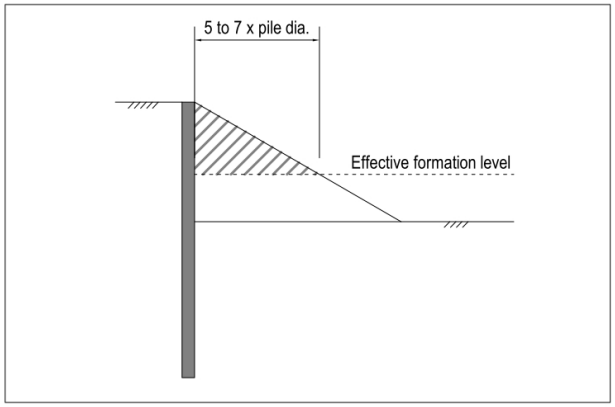

Figure 3. The minimum offset method (after Geotechnical Engineering Office, 2006)

Assessment of the first two methods by Smethurst and Powrie (2008) found that they are generally conservative while the minimum offset method can totally ignore the effects of the berm for large diameter piles. As such, an additional analysis method is proposed whereby the formation level in front of the wall is taken as the top of the berm level but with a reduction in its coefficient of passive resistance (K_p).

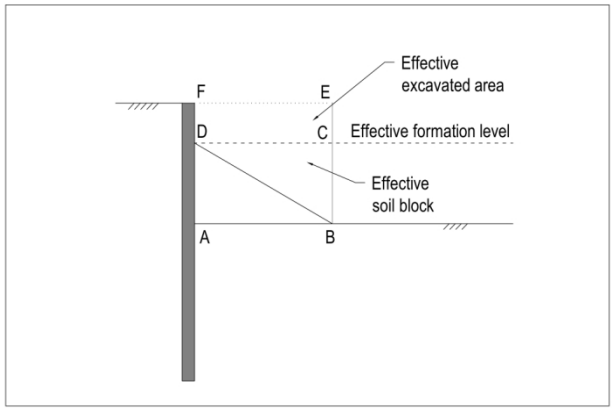

Figure 4. The reduced K_p method

The reduction in K_p is equivalent to the percentage area of the berm as compared with the entire block of soil if it were flat ground. Referring to Figure 4, the K_p value for the berm is taken to be:

$$\frac{Area\ ABD}{Area\ ABCD} \times K_p$$

where K_p is the coefficient of passive resistance of flat ground.

Compared to the other methods, this method is relatively quick and simple to model, yet still accounts for passive resistance of the berm.

2. The Legacy Way Tunnel Project

Legacy Way is a 4.6 km, twin 12.4m diameter road tunnel in Brisbane, Australia with approximately 3 km of surface connections to facilitate access to the tunnels. The new road bypasses Brisbane's Central Business District (CBD) to the west, and will connect the Western Freeway at Toowong with the Inner City Bypass (ICB) at Kelvin Grove.

The Western Connection comprises some 2 km of new roadway formed in trough and deep cut and cover structures and connects the Western Freeway to the western tunnel portal. The 12.4 m diameter parallel twin tunnels commence at the Toowong roundabout. The tunnels pass underneath sections of Auchenflower, Milton, Paddington and Red Hill before surfacing at Kelvin Grove, where the Eastern Connection (again trough and deep cut and cover structures) connect to the existing ICB.

Transcity, a joint venture between BMD Constructions, Ghella and Acciona Infrastructures, is responsible for the design, construction and initial operation of Legacy Way.

Design of Legacy Way has been carried out by Transcity Design Alliance, an Alliance between Cardno, GHD and URS.

2.1. Western Trough Structure

The Western Trough Structure provides a dual two-lane decline roadway connecting the existing Western Freeway to the Legacy Way tunnel and comprises approximately 485m of soldier pile retaining walls. The north wall supports the new realigned eastbound Western Freeway, whilst the south wall supports the existing Western Freeway. The soldier piles that were installed varied in diameter between 900 mm and 1500 mm, and were spaced at 2.4 m to 3.0 m center to center.

Figure 4. The Western Trough Structure with berm

Due to the curve of the realigned eastbound Western Freeway, an opportunity arose to leave a berm in place in front of the wall for a section approximately 160 m. The berm meant that retained heights were effectively reduced, thus also reducing wall support requirements.

Construction of the Western Trough Structure commenced late 2012 and was completed approximately a year later.

2.2. Eastern Soldier Pile Wall

In order to allow installation of secant piles as part of the Eastern Portal Structure, a temporary retaining wall was required. The wall was located directly in front of a private property and supports a temporary noise wall to attenuate construction noise.

The soldier pile wall comprised of 1200 mm diameter piles at 1.8 m to 2.4 m centre to centre. Sufficient space was available in front of part of the wall to leave a medium sized berm. This wall was constructed in early 2012 and was subsequently incorporated into the permanent works due to the ongoing need to attenuate noise from the roadway.

Figure 5. The Eastern Soldier Pile Wall with berm

2.3 Temporary Conveyor Tunnel Portal

In addition to the two mainline tunnels, a smaller, temporary tunnel was constructed (by drill and blast) to transport spoil from the Western worksite to the Mt Coot-tha Quarry via conveyor. This horseshoe shaped tunnel, called the Conveyor Tunnel, was 3.9 m wide and 4.7 m high and was some 550 m long.

The Western Worksite Conveyor Tunnel Portal comprised of 1200 mm diameter soldier piles spaced typically at 2.4 m centre to centre. Anchors were required locally above the tunnel. The tunnel entrance was some 3 m below the Finished Surface Level (FSL) of the surrounding area which meant that the excavation in front of the wall was in a somewhat "V" shape. This allowed a berm to be formed in front of much of the retaining wall.

Construction of the wall was completed in January 2012 while the conveyor tunnel broke through in March 2012. With completion of boring for the two mainline tunnels in June 2013, the conveyor tunnel was backfilled in late 2013. A section of the conveyor portal retaining wall has been incorporated into the buried Western Vent Station Building.

Figure 6. The temporary Conveyor Tunnel Portal with berm

2.4. Geology

The Western Connection, including the conveyor tunnel is located within the Bunya Phyllite beds which comprises mainly phyllite and quartzite. The Eastern Connection is located within the Neranleigh Fernvale beds comprising phyllite, metagreywacke, arenite, quartz arenite, quartzite and spilite. Both the Bunya Phyllite and Neranleigh Fernvale beds are considered meta-sedimentary rocks and are known collectively as the "Brisbane Metamorphics" (Transcity, 2011a and 2011b).

2.5 Original Design Method

The performance deed dictated that the wall design was undertaken in accordance with AS5100:3 using unfactored loads and a reduction factor on pile capacity. As per the deed and design standard, allowance was made for over-excavation, peak flood levels and surcharge loadings for future developments. Analysis of the retaining walls was undertaken using WALLAP (pseudo finite element method) and Phase^2 (by Rocscience) programmes.

3. Back Analysis

3.1. Critical Cross Sections

For the purpose of back analysis, critical sections at each berm supported retaining wall were selected based on berm size. These are summarized in Table 1. For the purpose of this assessment, berm sizes were defined as:

- Small – berm height is up to one third of the retained height of the wall;
- Medium – berm height is greater than a third, but less than two thirds, of the retained height of the wall;
- Large – berm height is within the upper third of the retained height of the wall.

Table 1. Details of critical cross sections

Location	Section Chainage	Retained Height (m)[1]	Berm Height (m)	Berm Size[2]	Soldier Pile Wall Arrangement	Retained Material and Layer Thickness[3]
Western Trough	Ch21640	8.4	2.3	Small	1.5m dia. at 3.0m c/c	a) Fill – 2.0m; b) Residual soil – 2.9m; c) Weathered phyllite (BP)
Western Trough	Ch21660	9.1	4.4	Medium	1.5m dia. at 3.0m c/c	a) Fill – 0.5m; b) Residual soil – 6.7m; c) Weathered phyllite (BP)
Western Trough	CH21700	8.6	6.5	Large	1.5m dia. at 3.0m c/c	a) Fill – 1.6m; b) Residual soil – 6.0m; c) Weathered phyllite (BP)
Eastern Soldier Pile Wall	CH15	7.0	2.5	Medium	1.2m dia. at 1.8m c/c	a) Residual soil – 3.7m; b) Weathered phyllite (NF)
Conveyor Portal	CH120	9.5	2.3	Small	1.2m dia. at 2.4m c/c	a) Residual soil - 5.4m; b) Weathered phyllite (BP)

1. Top of wall to excavation level (base of berm)
2. All berms 1(V):2(H)
3. BP = Bunya Phyllite beds; NF = Neranleigh Fernvale beds

3.2. Construction Records

The majority of piles installed on the Legacy Way project were logged by a geotechnical engineer/ engineering geologist as part of the construction oversight process. As-built geological data was available for the critical sections listed in Table 1.

In addition, monitoring prisms were installed and readings taken regularly as part of the monitoring program during and after construction. The monitoring trigger levels, for each of the critical cross sections, are summarized in Table 2.

Table 2. Monitoring trigger levels (mm)

Section	Alarm	Yellow	Red
	Plan contingency / remedial measures	Increase monitoring frequency, need for remedial action to be judged on trend of monitoring	Cease works, implement remedial measures
Western Trough			
Ch21640	11	15	20
Ch21660	12	17	22
CH21700	12	17	22
Eastern Soldier Pile Wall			
CH15	15	21	27
Conveyor Portal			
CH120	15	20	25

3.3. Back Analysis Methodology

The methodology for the back analysis was to use different analysis methods in WALLAP to model the retaining walls and berms with exact site conditions (i.e. geology, geometry and loadings) and compare the calculated displacements with actual results obtained from the monitoring program. The analysis methods that were considered in the assessment were:

- Phase^2 – using Phase^2 to model exact site conditions;
- WALLAP – using WALLAP to model exact site conditions;
- Equivalent surcharge method (ES);
- Raised effective formation level method (REFL);
- Minimum offset method (MO);
- Reduced Kp method (RKp)
- No berm – using WALLAP to model the wall without the berm.

3.4. Geotechnical Design Parameters

The adopted geotechnical design parameters are shown in Table 3.

Table 3. Adopted geotechnical design parameters

Unit	Unit Weight (kN/m^3)	φ (°)	c' (kPa)
Fill	21	30	5
Residual soil (BP)	22	30	5
Residual soil (NF)	22	28	2
Weathered Phyllite (BP)	25	43	34
Weathered Phyllite (NF)	25	40	32

4. Results

Results of the back analysis are shown in Table 4 and compared against actual monitoring data.

Table 4. Summary of results

Section	Description	Actual	Phase^2	WALLAP	ES	REFL	MO	RK_p	No berm
Western Trough CH21640	Deflection (mm)	6	10	10	13	12	13	10	13
	Bending moment (kNm/m)		430	451	659	544	658	424	658
	Shear force (kN/m)		144	142	242	196	241	118	241
	Required pile length (m)		8.9	9.1	10.1	9.3	10.1	8.3	10.1
Western Trough CH21660	Deflection (mm)	5	15	15	27	19	27	16	27
	Bending moment (kNm/m)		600	582	886	726	883	497	883
	Shear force (kN/m)		233	225	244	272	243	172	243
	Required pile length (m)		9.2	9.1	11.7	9.9	11.7	8.6	11.7
Western Trough CH21700	Deflection (mm)	4	9	6	25	18	18	8	25
	Bending Moment (kNm/m)		300	231	885	691	702	282	876
	Shear Force (kN/m)		120	64	277	246	261	117	274
	Required pile length (m)		6.6	3.0	11.2	9.3	9.4	4.1	11.2
Eastern Soldier Pile Wall CH15	Deflection (mm)	6	6	6	8	7	8	6	8
	Bending moment (kNm/m)		270	381	554	470	554	358	554
	Shear force (kN/m)		151	188	262	210	262	183	262
	Required pile length (m)		7.4	7.9	9.0	8.1	9.0	7.2	9.0
Conveyor Portal CH120	Deflection (mm)	7	8	17	28	19	18	18	28
	Bending moment (kNm/m)		340	441	690	509	474	451	691
	Shear force (kN/m)		160	190	370	226	207	197	380
	Required pile length (m)		10.5	9.2	11.0	9.5	9.4	9.5	11.0

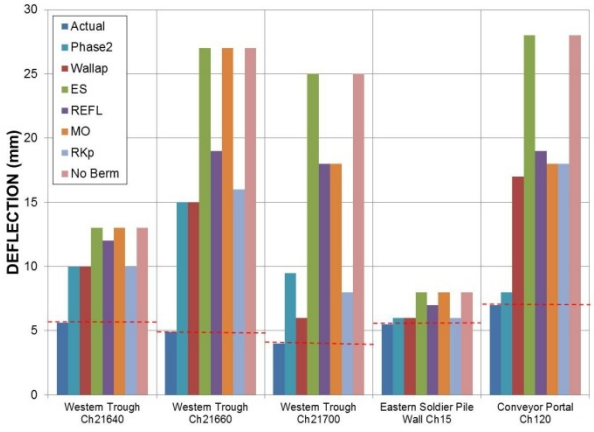

Figure 6. Comparison of back analysed deflections

5. Discussion

Back analysed deflections, as reported in Table 4, are compared with actual deflections in Figure 6. The modeled deflections compare reasonably well but are generally higher. This is not surprising as the design parameters are considered conservative.

The difference between modeled and actual deflections is slightly higher at Western Trough Ch21660 possibly due to the analysis methods not being able to account for the three dimensional effects of the concave wall. In addition, the difference between the modelled deflections in Phase^2 and in WALLAP at Conveyor Portal Ch120 is attributed to the sloping nature of the geology at this location. Phase^2 was able to model the entire cross section where the rock line was dipping towards the retaining wall while WALLAP assumed that it was flat.

The equivalent surcharge method, raised effective formation level method and minimum offset method were very conservative with respect to measured deflections, with the equivalent surcharge method the most conservative. In fact, the results from the equivalent surcharge method are very similar to the results if the berm were ignored altogether. As such, the equivalent surcharge method is considered too conservative.

Furthermore, it is argued that the REFL method can be simplified as to not include the equivalent surcharge component as that component of the calculation is expected to have negligible effect on the results.

The minimum offset method showed close matching for large berms, however, it allows little or no lateral contribution for small berms. It is argued that the underlying theory of this method, which assumes the top portion of the berm to contribute negligible passive resistance, is fairly sound. However, based on the analysis results, this may be too conservative, especially for large diameter

piles (>900 mm). In situations where ground conditions are fairly well understood, an offset distance of 3 to 5 times the pile diameter may be more appropriate.

Of the methods compared, it is clear that the reduced K_p method is the least conservative. The average difference in displacement calculated is 6.2 mm, which is reasonable considering typical survey tolerance for the project is ± 2 mm. Additionally, the reduced K_p method is expected to cause the least distortion of bending moment and shear force diagrams of the walls as no portion of the berm is ignored.

The bending moments and shear forces shown in Table 4 further highlight the effectiveness of a berm. By leaving a berm in place during excavation, the bending moments and shear forces in the wall can be reduced by up to 40% for small berms and 70% for large berms.

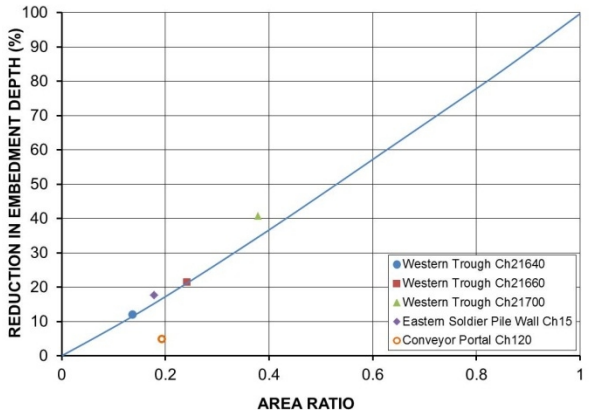

Figure 7. Comparison of back analysed deflections

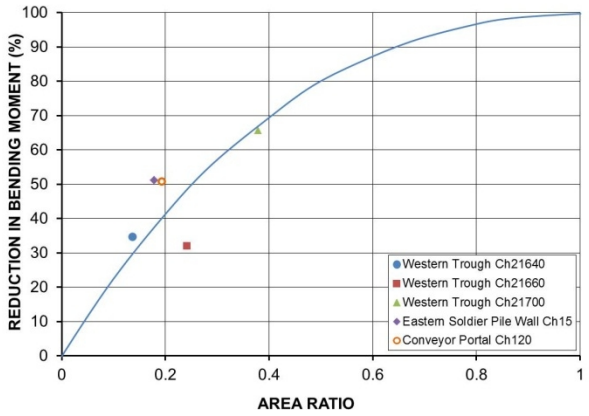

Figure 8. Comparison of back analysed deflections

Figures 7 and 8 show the reduction in required embedment depth and bending moment, as calculated using Phase^2, with increasing berm size. The size of berm is expressed as the ratio between the area of the berm, ABD, to the area of the effective excavated area, ABEF (refer Figure 4). As shown in Figures 7 and 8, leaving a berm in place can have significant advantages in terms of pile length and pile capacity.

6. Design and Construction Considerations

Some lessons were learnt as part of the design and construction of the permanent berm supported walls:

- Care should be taken where services are proposed at the top of the berm as this is a compression zone and is expected to experience the most lateral movement within the berm. This may cause higher levels of strains in the services.
- Over excavation in front of the berm should be allowed for. The temporary stability of the berm for over excavation works (e.g. installation of services) should be assessed.
- Incorporating berms in retaining wall designs have the potential of reducing embedment depths of the piles. Slope stability checks should be undertaken to ensure global stability of the wall and the berm. In most cases, it is recommended that the embedment depth of the piled wall is deeper than the base of the berm.
- The berm should be designed at as flat a batter as practical but no steeper than necessary to satisfy the relevant minimum factors of safety.
- Assessments undertaken as part of the Western Trough Structure design found that having a passive berm (Figure 9a) resulted in lower loads within the wall but positioning the wall at the bottom of the slope (Figure 9b) required shorter embedment depths. This was because the depth to rock was reduced. Under normal circumstances, it is expected that the passive berm arrangement would be the less efficient option but for the Western Trough Structure, over-excavation allowance of 2 m was required for the installation of the pavement and various services. The temporary excavation had less of an effect on the passive berm arrangement thus making it more attractive. This, along with other project constraints, meant that the passive berm arrangement was the preferred option for the Western Trough Structure.

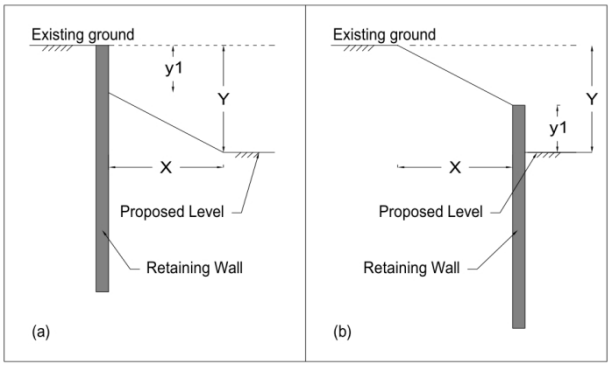

Figure 9. Different configurations for retaining wall on a slope. (a) passive berm and (b) wall at the bottom of the slope with backslope

7. Conclusions

Actual loads and pressures acting on retaining walls are difficult and expensive to monitor. In the absence of load monitoring data, it is difficult to fully understand the true effectiveness of berms. Nonetheless, this paper provides an indication of the lateral resistance provided by a berm.

The design and construction of berms to enhance the stability of permanent, large diameter soldier pile retaining walls at a major project in Brisbane was documented. In addition, four different methods of empirically representing berms in design have been compared to investigate their relative accuracy. The analysis results have shown that the equivalent surcharge method is conservative and provides little more lateral resistance compared to a case where the berm is ignored altogether. Of the analysis methods tested, the reduced K_p method is recommended as it was the least conservative and also best matched measured movements of the wall.

The study has shown that even small berms have the potential to substantially reduce loads on the wall thereby offering significant cost savings. The benefit of large berms is expected to be even greater, with reductions in bending moments and required embedment depths of up to 75% and 40% respectively.

8. Acknowledgements

The authors would like to acknowledge Transcity JV and Brisbane City Council for the procurement and construction of the Legacy Way Project. Transcity JV staff provided access to the Western and Eastern worksites during construction and photographs of the site as well as monitoring data. Michael McAuley was the Design Geotechnical Lead and Adrian Kho was the Design Geotechnical Engineer for the project.

9. References

AS 5100.3 (2004), Bridge Design – Foundation and soil supporting structures, Australian Standards

Daly M. P., Powrie W. (2001). Undrained analysis of earth berms as temporary supports for embedded retaining walls, *Proceedings of the Institution of Civil Engineers, Geotechnical Engineering, vol.* ***149****, no. 4, pp. 237-248.*

Geotechnical Engineering Office of Hong Kong (2006), *Foundation Design and Construction*, Geo Publication No. 1, The Government of Hong Kong Special Administrative Region.

Powrie W., Daly M.P. (2002), Centrifuge model tests on embedded retaining walls supported by earth berms, *Géotechnique, vol.* ***52****, no. 2, pp. 89-106.*

Smethurst J.A., Powrie W. (2008), Effective-stress analysis of berm-supported retaining walls, *Proceedings of the Institution of Civil Engineers, Geotechnical Engineering, vol.* ***161****, no. GE1, pp. 39-48.*

Transcity (2011a), *Geotechnical assessment report – Eastern* Connection, EC-0407-SR-02-0001, 219 p.

Transcity (2011b), *Geotechnical assessment report – Buried structures (Section 2) and Western Connection Trough*, WC-0403-SR-02-0001, 252p.

This page intentionally left blank

Proceedings of the 10th ANZ Young Geotechnical Professional's Conference – 10YGPC
Noosa, Queensland, Australia
10 – 12 September 2014

DESIGN AND CONSTRUCTION OF FOUNDATIONS FOR THE AUCKLAND RAIL ELECTRIFICATION PROJECT

Joshua TEAL
AECOM, Auckland, New Zealand

ABSTRACT – The Auckland urban rail network is being electrified with a 25kV AC overhead line traction system as part of a NZ$500M upgrade project. This involves wiring 80km of rail track that traverses a region of complex and widely varying geology from soft peaty alluvium to basalt rubble. Geotechnical input into the project included the foundation design for approximately 3,350 traction mast footings and various other support structures, retaining walls and electrical feeder stations. The traction masts were required to hold the electrified contact wire within certain deflection limits under various loading conditions. The design challenge was to produce a range of mast foundations able to cater for the varying ground conditions across Auckland within the narrow built-up rail corridor and be cost-effective to build. The track formation and state of the old embankments also impacted on the foundation design and construction. Embankments too steep for shallow spread footings, but with fractured basalt rock shallow enough to impede piling, was a common theme during construction.

1. Introduction

Auckland's public transport infrastructure suffered from serious under investment and general neglect over many decades, prompting local and central government to embark on a program of upgrades, most notably to Auckland's commuter rail network. Since 2006 this investment in rail has grown to more than NZ$1.6B, including double tracking and station upgrades. The New Zealand government announced in mid-2007 that as part of the upgrade the network would be electrified. Electrification includes construction of masts to support traction wires and associated infrastructure for 175 km of track. A significant portion of the civil engineering work required input by geotechnical specialists. This paper concentrates on the design and construction of foundations for the project.

Design of the overhead electric traction system necessitated design of mast foundations, footings for various minor ancillary and electrical buildings and retaining walls. Due to various designs aspects having to be resolved during construction, many tasks including minor mast foundation alterations had to be carried out by an onsite design team during the construction phase. Additionally, some unforeseen issues requiring geotechnical investigation and analysis arose during construction.

Major civil work construction and quality assurance checking for the traction system was completed by mid-2013 and the first electrified services began operating in late April 2014.

2. Project setting and geology

2.1. Project overview

The design contract for the electric traction system was awarded to AECOM in May 2008, with a view to operating electric train services by the end of 2013. The construction contract was awarded to a Hawkins Infrastructure and Laing O'Rourke joint venture ("HILOR") in mid-2010. The track system to be electrified included lines from the central city to western suburbs, eastern suburbs, and suburbs to the south. This represented about 80 km of double tracked line and included 2 major tunnels and an underground terminus station at Britomart.

2.2. Regional geology

The Auckland region is geologically complex with a number of significant geological units lying beneath the passenger rail network.

2.2.1. Waitemata Group

The basement rock of the Auckland region is a typically very weak to weak sandstone/siltstone of the Waitemata Group. Units relevant to this project included the East Coast Bays Formation and Kaawa Formation. This rock has a highly variable weathering sequence at its upper surface and typically varies from 0 – 50 meters depth below ground level. The rail network interfaces mostly with East Coast Bays Formation in the central Auckland isthmus area.

2.2.2. Tauranga Group

Overlying Waitemata Group rock across the Auckland region, and especially in the west and south of Auckland, are alluvial deposits of the Puketoka Formation, which is part of the Tauranga Group. This alluvium consists of soft to stiff, silty clays, clayey stilts, sands and soft peat. Puketoka Formation is dominated by pumiceous material in some areas.

2.2.3. Auckland Volcanic Field (basalt lava flows, scoria rubble, ash and tuff)

The Auckland region sits upon a volcanic field of some 50 vents. As such, volcanic rock and soil sit beneath, interlayered and on top of Waitemata and Tauranga Group units. Of significance to the rail network are the solid basalt flows, layers of scoria rubble, and weathered ash dominated sandy clayey silty tuff at near surface depth (0-5m), which is located particularly on the central isthmus area, but also in specific areas across south Auckland. All lines on the Auckland passenger rail network interface with materials of the Auckland Volcanic Field.

2.2.4. Rail embankments (age, construction, slopes)

Historic embankment fill constitutes a major geotechnical unit for the rail network. Most of the rail network alignment across Auckland was constructed from the 1880s to the 1920s. The fill embankment materials typically consist of stiff silty clay, however, certain sections of line are constructed with basalt gravel and boulders, particularly where the line passes through a narrow area where embankment slopes are steep (>>30deg).

3. Design of foundations

The design process commenced in mid-2008 by a multidisciplinary team from AECOM, assisted by experienced overhead lines design engineers from Balfour Beatty Rail. The electric traction system selected by the client to be designed and constructed was a 25kV AC overhead line system based on the Balfour Beatty Mark 3b system.

The overhead traction system utilised a standard range of ten different mast types that included portals, single and two-track cantilever mast and anchor masts. The masts were required to hold catenary and contact wire at precise positions over the track in varying wire configurations such as straight track, cross-overs and turn-outs, as well as supporting assemblies for tensioning and anchoring the wires. Aside from dead load cases, the key design cases were for wind loading on the mast and wires under serviceability, and ultimate limit state conditions. Foundation design included calculating contact wire-height deflections based on foundation rotation. Foundations were designed to ensure less than 35mm deflection under the principle serviceability case, and no collapse under the principle ultimate case.

Assisted by Balfour Beatty's experience from other similar electrified rail environments internationally, the geotechnical design team worked to develop a set of generic mast foundation designs that could be used in most geotechnical conditions expected to be encountered across Auckland. The client expected a set of robust designs that minimised the need for excessive customisation across the region and different geology. In keeping with overseas methods, a set of bored, cast-in-place concrete piles, shallow concrete pad footings, and grouted-bar rock anchor foundations were developed. These foundations could be selected and allocated to each mast location by way of a selection chart. This was a fine balancing act due to the need to minimise project cost and therefore over-design but also produce a design suitable for most cases.

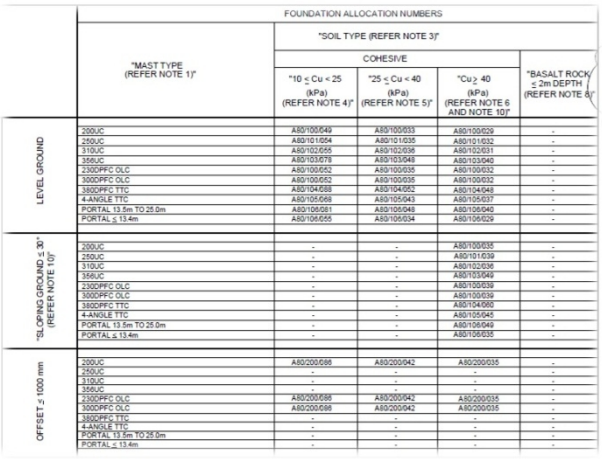

	"MAST TYPE (REFER NOTE 1)"	FOUNDATION ALLOCATION NUMBERS "SOIL TYPE (REFER NOTE 3)" COHESIVE "10 ≤ Cu < 25 (kPa) (REFER NOTE 4)"	"25 ≤ Cu < 40 (kPa) (REFER NOTE 5)"	"Cu ≥ 40 (kPa) (REFER NOTE 6 AND NOTE 10)"	"BASALT ROCK ≤ 2m DEPTH (REFER NOTE 8)"
LEVEL GROUND	200UC	A80/100/049	A80/100/033	A80/100/029	-
	250UC	A80/101/054	A80/101/035	A80/101/032	-
	310UC	A80/102/055	A80/102/036	A80/102/031	-
	356UC	A80/103/079	A80/103/048	A80/103/040	-
	2300PFC OLC	A80/100/052	A80/100/035	A80/100/032	-
	3000PFC OLC	A80/100/052	A80/100/035	A80/100/032	-
	3600PFC TTC	A80/104/088	A80/104/052	A80/104/048	-
	4-ANGLE TTC	A80/105/069	A80/105/043	A80/105/037	-
	PORTAL 13.5m TO 25.0m	A80/106/081	A80/106/048	A80/106/040	-
	PORTAL ≤ 13.4m	A80/106/055	A80/106/034	A80/106/029	-
"SLOPING GROUND ≤ 30° (REFER NOTE 10)"	200UC	-	-	A80/100/035	-
	250UC	-	-	A80/101/039	-
	310UC	-	-	A80/102/036	-
	356UC	-	-	A80/103/049	-
	2300PFC OLC	-	-	A80/100/039	-
	3000PFC OLC	-	-	A80/100/039	-
	3600PFC TTC	-	-	A80/104/060	-
	4-ANGLE TTC	-	-	A80/105/045	-
	PORTAL 13.5m TO 25.0m	-	-	A80/106/049	-
	PORTAL ≤ 13.4m	-	-	A80/106/035	-
OFFSET ≥ 1000 mm	200UC	A80/200/086	A80/200/042	A80/200/035	-
	250UC	-	-	-	-
	310UC	-	-	-	-
	356UC	-	-	-	-
	2300PFC OLC	A80/200/086	A80/200/042	A80/200/035	-
	3000PFC OLC	A80/200/086	A80/200/042	A80/200/035	-
	3600PFC TTC	-	-	-	-
	4-ANGLE TTC	-	-	-	-
	PORTAL 13.5m TO 25.0m	-	-	-	-
	PORTAL ≤ 13.4m	-	-	-	-

Figure 1. A part of the foundation allocation design chart, showing piled foundations.

Several design iterations led to a simplified foundation allocation chart with essentially five ground types matched to the ten mast types. The chart allocation method approved by the client required the contractor to complete a ground investigation at each mast location and determine the foundation type allocation. Any case outside the stated limits of the allocation chart, such as steep slopes greater than 30deg or very soft ground less than 10kPa undrained shear strength was to be referred back to the project Geotechnical Engineer for design resolution.

A key limitation for the foundation design was the information used as the basis of the design. Due to the client's need to produce a design based on a lidar topographical survey and without geotechnical investigations before the construction phase, the initial allocation of foundation types was only essentially a best estimate. The lidar survey did not provide a high degree of certainty with regard to embankment slopes and ground types were assumed based on published geological maps and some limited geotechnical investigation data previously collected by the designer. For example, track locations in central Auckland where solid basalt flows were expected to provide good conditions for grouted anchor foundations were eventually found to be rubbly basalt boulders overlain by a thin layer of alluvium.

4. Construction phase

From late 2010 construction work proceeded on day and night shifts, mostly between scheduled rail services and without full line closures. A number of issues arose during construction (see section 5.0), and the co-located multidisciplinary team structure made communication and resolution of issues and queries easier and more expeditious.

The vast bulk of contractor construction queries for geotechnical engineers related to clashes between buried services and the planned locations of electrification masts. The location of many underground services had been able to be determined during the design phase and de-conflicted with mast locations. However, de-confliction of along-track services including several fibre optical and signalling cables was deliberately left to the construction phase due to the uncertainty of their location.

When excavations for mast foundations began, it was found that the location of some of the services differed from the official CAD location by up to several meters. The basic design had been produced with a general plan location tolerance of +/- 1m, however, buried service conflicts often resulted in foundations moving more than 1m. This triggered redesign of certain wiring sections and often moved foundations into more geotechnically challenging positions, such as down steep slopes, into coastal revetments, retaining walls, and close to other existing building foundations. Most of these clashes with services, walls, and slopes were resolved by an alternative overhead wiring arrangement, a relocation of services, or a site-specific foundation design solution.

Figure 2. A pad foundation being constructed in a basalt gravel embankment near Morningside.

5. Geotechnical challenges during construction

A number of geotechnical challenges arose during construction particularly regarding difficult ground conditions and a heavily built up, space-constrained rail corridor.

5.1. South Auckland peat

During mid-late 2011, the contractor commenced foundation construction on a section of NIMT line in the Takanini area of south Auckland. It quickly became apparent that piling production rates were being affected by the presence of deep deposits of soft peat. The client tasked the onsite design team with investigating the implications for the current set of generic foundation designs. Shallow CPT investigations at each mast location in the affected construction area revealed a thin, stiff 'crust' clayey silt layer approximately 2m thick overlying the soft peat.

The resulting design solution involved changing all foundation types in the affected area to gravity pad type foundations. Because the section of line was relatively straight, structural design loads were lower than the generic design case, and thus the gravity pad foundations were able to be sized and installed at a depth that remained within the stiff surface crust, avoiding excavation or piling in peat.

5.2. Hobson Bay causeway

As the project progressed, the client became concerned about founding conditions for electrification masts across the Hobson Bay causeway portion of the NIMT line. This was due to the steep sides of the embankment, and age and unknown quality of the embankment fill construction. In addition, by early 2011 the client made a decision to change most mast types on the causeway from pin-based portals to single-track cantilever masts in response to public concern regarding perceived adverse visual effects of the planned large number of portal masts.

Due to the client's increased perception of design risk on a number of fronts, the onsite design team was tasked to undertake geotechnical investigations and allocate site specific foundation designs. This work replaced the contractor's relatively simple auger type investigation with higher quality cored machine boreholes and set aside the use of the foundation allocation chart. Project geotechnical engineers completed the works during scheduled periods of full track closure. However, the reporting timeframes became quite tight because the inconsistent location of along-track buried services resulted in a slower drilling work rate than expected. Designs were duly produced that mitigated project risk to the client's satisfaction and within the required timeframe (prior to the Rugby World Cup 2011).

5.3. The space constrained rail corridor

During the foundation construction phase of the project the design and construction teams were continually confronted with the real difficulty of installing significant new infrastructure into a well-established rail corridor that passes through a built-up urban environment. Two cases that highlighted this most clearly were, firstly, a section of rail line through Mt Eden with retaining walls close to the track on both sides, and secondly, a tight curve approaching the entrance to the Britomart Station tunnel.

The first case in Mt Eden involved a section of double track approximately 100m long bounded by retaining walls on both sides and at the minimum offset distance from the track. This left little or no room to install foundations for the new electric traction masts. The basic foundation design required in this area consisted of 1050mm diameter bored concrete piles supporting portals and twin-track cantilever masts (up to 9m long boom). The eventual solution involved piling in the line of, and behind existing retaining walls. However, this took months to achieve due to difficult negotiations for access for geotechnical investigations and ultimately some land acquisitions.

Figure 3. A twin-track cantilever mast foundation at Mt Eden.

The second case at the Britomart approach curve similarly involved a retaining wall very close to the inside of a tight curve. Added to this difficultly was the presence of development rights boundaries, owned by a third party, at certain heights and depths above and below track level. Development of the solution involved highly accurate re-surveying of the tracks, property boundaries, and retaining walls. Eventually it was determined that, when combined with a slightly altered overhead wiring configuration, specially modified, smaller gravity pad foundations could be fitted into the limited spaces available. This was achieved only after extensive consultation with key project stakeholders and numerous, time consuming site visits to measure and consider design options.

5.3. Construction difficulties in basalt

A typical problem encountered by construction crews through the duration of foundation construction was excavating and piling into basalt lava flows of the Auckland Volcanic Field. The difficulty manifested itself slightly differently depending on whether the contractor had initially selected a bored pile, or shallow gravity pad.

With the pile option, crews often had to attempt to hammer out basalt boulders encountered at the base of the pile hole. Sometimes large boulders were removed, which resulted in a significant increase in concrete volume to fill the hole.

When attempting to excavate for a shallow gravity pad, the rock encountered was frequently found to be a strong interlocked rock mass, despite the presence of voids, which ruled out the use of a grouted-bar anchor foundation. This required time consuming rock-breaking, and also resulted in larger than desired excavations, and increased concrete volumes due to the removal of large boulders.

Because much of the foundation work was carried out during night shifts, the contractor was also faced with the difficulty of having to minimise excessive noise from the rock hammering.

6. Quality Assurance

During the foundation construction the project experienced a number of quality related issues. These included basic issues such as structural detailing tolerances not being achieved and some foundations constructed at the incorrect level. These issues were generally confined to the early part of the project, and essentially because work crews did not yet fully understand the requirements of the design.

There were also difficulties related to the maintenance program of the rail corridor. In several instances third-party contractors were found to be digging up shallow pad footings while constructing new track-side swale drains. Issues of this type were resolved through ongoing consultation with all rail associated stakeholders and operators.

As part of the construction quality assurance program, the onsite design team carried out an inspection and audit program for all 3300 foundations constructed for the electrification project. This involved review of the construction quality documents and an onsite visual inspection of every foundation. A screening process was then used to check certain foundations to ensure asbuilt performance was likely to be in accordance with the design (i.e. serviceability deflection of the mast at wire height < 35mm).

7. Conclusions

The multidisciplinary onsite design team provided essentially a 'one stop shop' for design queries and most re-design work when it was required. This was a good arrangement for the project, in terms of ability to provide a timely and responsive service for the client and contractor.

Difficulties with the amount of geotechnical design work around steep embankment slopes and the huge number of buried services clashes highlight the need for accurate topographical surveys and maintenance of accurate buried services plans. When installing significant new infrastructure into a space constrained rail corridor, this information is invaluable. To that end, dedicated service trenches and standard offsets for buried services would also prove very useful.

The Auckland electrification project showed how difficult and complex the urban rail environment can be. There are many stakeholders and teams operating within client, contractor and design organisations as well as across the community. Good management of these interfaces is crucial to the success of such a construction project and operation of the new engineering infrastructure.

This page intentionally left blank

Proceedings of the 10th ANZ Young Geotechnical Professional's Conference – 10YGPC
Noosa, Queensland, Australia
10 – 12 September 2014

PILE LOAD TESTING AND VALIDATION OF FOUNDATION DESIGN ON THE MACKAYS TO PEKA PEKA EXPRESSWAY PROJECT

Martin BARRIENTOS
Geotechnical Engineer, Beca Ltd, Wellington, New Zealand

ABSTRACT – A regime of bored pile load tests was developed for validation of design assumptions around the capacity and behaviour of large diameter (2.1 – 3.0 m) bridge piles on the MacKays to Peka Peka (M2PP) Expressway project. Delivered by the M2PP Expressway Alliance, whose main partners are the NZ Transport Agency, Beca, Fletcher Construction and Higgins, the project is one of eight sections of highway improvements that form the Wellington Northern Corridor road of national significance, in the lower North Island of New Zealand. The expressway comprises 18 km of new four lane highway, crossing peat swamps and sand dunes. Given the high seismicity of the region, some of the ten expressway bridges are designated lifeline structures: designed to provide resilient emergency access into Wellington in the event of a natural disaster. This paper discusses the pile load test (Osterberg method) at the Waikanae River Bridge: measured vs. predicted performance, validation of design approach and considerations for later load tests.

1. Introduction

Large diameter (2.1 – 3.0 m) reinforced concrete bored pile foundations are being used to support the piers of the multi-span bridges on the MacKays to Peka Peka (M2PP) Expressway project. Four of these bridges have a mono-pile pier arrangement as shown in Figure 1 and, as per AS2159 (2009), are classed as a low redundancy system with little ability to redistribute loads. As such, the need to confirm design assumptions around the *axial capacity* of these pier piles was identified early on in the design.

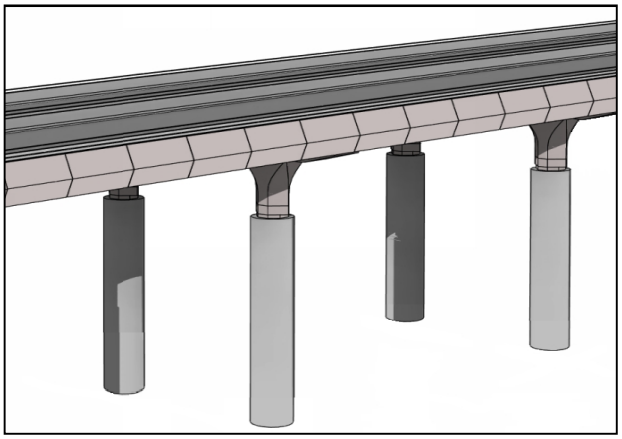

Figure 1. Simply supported, mono-pile bridge structural arrangement (decks not connected).

Three bi-directional load tests, undertaken using the Osterberg method, on sacrificial reinforced concrete bored piles have been proposed and located to reflect three different site soil conditions:

i) Waikanae River Bridge – founding strata comprises mostly gravels interbedded with silt,

ii) Te Moana Road Overpass – founding strata comprises partly sand and partly gravels interbedded with silt, and

iii) Wharemauku Stream Bridge – founding strata comprised entirely of sand.

The first of the load tests was undertaken on a 2.1 m diameter pile at the site of the Waikanae River Bridge on 11 and 12 March 2014. The results of this pile load test have been used to validate design assumptions and have provided valuable considerations for the two subsequent tests.

2. Project Description

The 18 km long, four lane M2PP Expressway is a realignment of State Highway 1 through the townships of Paraparaumu and Waikanae, located in the lower North Island of Zealand (Figures 2 and 3). The project is one of eight sections of highway improvements that form the Wellington Northern Corridor road of national significance; a strategic route key to the economic growth of the Wellington region and providing resilient emergency access to the capital in the event of a natural disaster. The NZ Transport Agency, Beca, Fletcher Construction and Higgins are the main partners of the M2PP Expressway Alliance, the consortium currently designing and constructing the route.

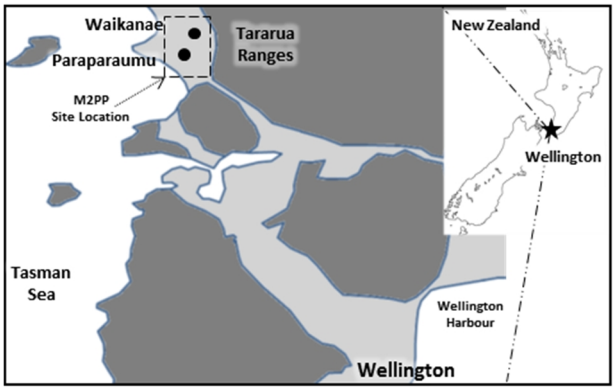

Figure 2. Site location.

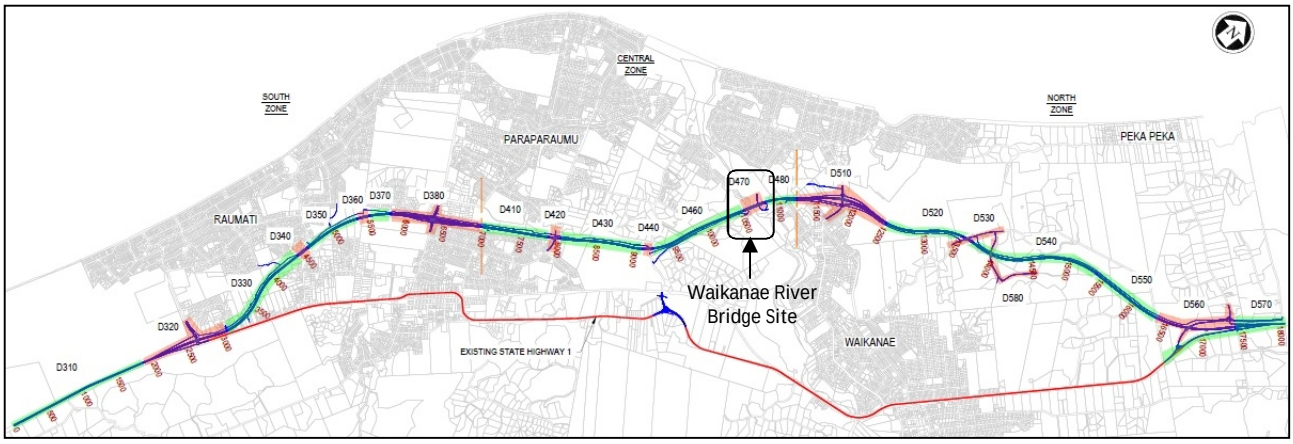

Figure 3. Expressway alignment and location of the Waikanae River Bridge.

3. Site Conditions

3.1. Geological Setting

The expressway route crosses the coastal plain to the west of the Tararua Ranges (Figure 3), in an area that has been shaped by repeated cycles of glaciation that have occurred in the past two million years. The Tararua Ranges, being steep greywacke (metamorphosed sandstone) hills formed through uplift and tilt of basement rock along northeast-southwest oriented faults, held valley glaciers during the glacial periods which resulted in severe erosion and generation of alluvial fans and floodplains. Eroded material deposited during glacial and interglacial periods along the coastal plain up until the last glaciation (some 10,000 – 15,000 years ago) form a thick wedge above the greywacke basement rock, known as the Pleistocene wedge. Deposited estuarine sands and gravels, dune sands, peat and river gravels above the Pleistocene wedge are Holocene-age materials.

The stratigraphic relationship between the materials encountered at this site is best illustrated in Figure 4.

3.2. Seismicity

The lower North Island of New Zealand is a seismically active region, producing large magnitude earthquake events. Although no major active faults are mapped passing directly through the expressway site, splinters of these faults are present. The design seismic event for bridge design has a 2500 year reoccurrence interval with a moment magnitude of 6.9, producing a peak ground acceleration of 0.68 g. All saturated granular Holocene deposits and medium dense to dense Pleistocene sands on the site are expected to liquefy under this high level of seismic shaking.

3.3. Ground Conditions at the Waikanae River

The site of the Waikanae River Bridge is underlain mostly by dense to very dense Pleistocene gravels interbedded with Pleistocene silt. The soil units present at the test pile location are summarised in Table 1 below, in the form of a general soil profile.

Table 1. Waikanae River Bridge soil sequence.

Layer	Depth (m bgl) [1]	Soil Unit	Deposition Type
1	0 – 4.7	Holocene sand / gravel	Interglacial (<10000 yrs)
2	4.7 – 12.8	Pleistocene sand	Interglacial
3	12.8 – 21.9	Pleistocene gravel	Glacial
4	21.9 – 22.6	Pleistocene silt	Interglacial (marine)
5	22.6 – 29.3	Pleistocene gravel	Glacial
6	29.3 – 31.0	Pleistocene silt	Interglacial (marine)
7	31.0 – 32.9	Pleistocene gravel	Glacial
8	32.9 – 34.7	Pleistocene sand	Interglacial
9	34.7 – 39.9	Pleistocene gravel	Glacial

[1] m bgl = meters below ground level.

Project-wide geotechnical parameters for the materials encountered beneath the expressway have been derived from correlations to numerous *in situ* tests, laboratory testing and, where appropriate, data from published sources. The interpretation of the pile load test is based on these established strength parameters and has not refined them specifically for the Waikanae River Bridge site.

4. Axial Pile Capacity – Design Philosophy

For the four bridges that have a mono-pile pier arrangement, the reinforced concrete bored piles are large in diameter (2.1 – 3.0 m) to accommodate the large horizontal seismic actions on the structure.

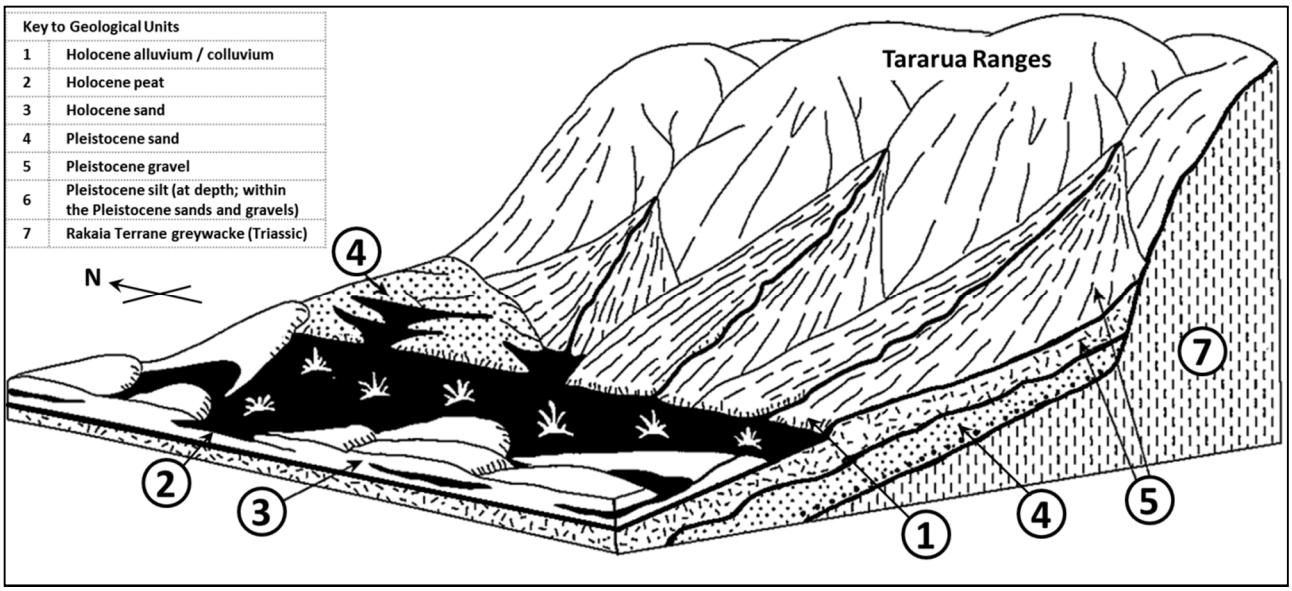

Figure 4. Isometric cross section of encountered materials at the M2PP Expressway and their relationship (modified from Maclean & Maclean, 2010).

The form of these multi-span bridges (separate decks for each carriageway, single pier per pile and simply supported deck; Figure 1) means that there is effectively no frame action. Critical axial load combinations are dead load in combination with live load and liquefaction induced negative skin friction.

Based on the scheme assessment for structures on the expressway, a five diameter clearance between the pile toe and any silt layers within the founding strata was to be provided (M2PP Alliance, 2011) for piles designed to derive their axial capacity in end bearing. This was to provide adequate stress reduction through the competent material before bearing onto silt layers.

From geotechnical investigations undertaken for the detailed design phase of the project, extending to greater depths than previous investigations, a greater prevalence of silt layers in the founding strata was identified at multiple locations along the alignment. The irregular distribution of the silt and hence difficulty in predicting their occurrence makes end bearing design difficult. Both avoiding silt layers within the stress bulb around the pile toe and providing certainty around pile founding levels made shaft resistance-only (skin friction) design an attractive option. Consequently, a skin friction axial capacity design has been adopted for determining the ultimate geotechnical capacity of bored pile foundations on the project.

The ultimate capacity, provided by skin friction alone, is computed using the following relationship:

$$V_u = V_{su} = \int_0^L C(\sigma_v' K_s \tan\delta' + \alpha s_u).dz \qquad (1)$$

The $\sigma'_v K_s \tan\delta'$ term is the adhesion against the pile surface from frictional soils and αs_u is adhesion from cohesive soils.

The self-weight of the pile is ignored in the calculation of capacity because it is assumed that this is satisfactorily carried in end bearing.

The way material properties are used in the design is affected by assumptions around:

i) The coefficient representing the horizontal effective stress in terms of vertical effective stress (K_s); taken as $K_s = 2.0$,

ii) The interface angle of shearing resistance (δ'); taken as 0.67φ' based on published correlations, and

iii) The adhesion factor (α); taken as α = 0.4, based on published correlations, for all cohesive deposits whether Holocene or Pleistocene.

The design $K_s = 2.0$ is optimistic compared to the conventional $K_s = K_0$ (at rest earth pressure coefficient) relationship (Figure 5). The formation history of the materials that underlie the expressway is the basis for selection of this value: repeated cycles of glaciation, faulting, aging and cementation, resulting in overconsolidation of these materials.

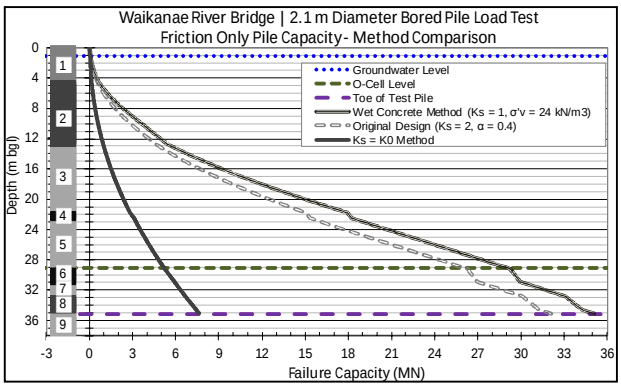

Figure 5. Estimation of skin friction capacity – method comparison (layering as per Table 1).

In terms of the load test, it is the product of K_s and δ' that is measured, though the relative proportions of K_s and δ' remain unknown. In the interests of consistency, only the K_s value has been selected for modification where a change in the product of K_s and δ' is warranted.

For reference, Figure 5 also includes the design capacity computed using the weight of wet concrete method (K_s = 1.0 and σ'_v = 24kN/m^3 inputs to Equation 1).

5. Test Pile Details and Loading Sequence

An sacrificial reinforced concrete bored pile – approximately 35.2 m long and 2.1 m diameter – was installed at the site of the Waikanae River Bridge by the M2PP Expressway Alliance and instrumented / tested by Fugro Singapore Pte. Ltd.

5.1. Instrumentation

An assembly consisting of two 510 mm Osterberg cells (O-cells) was provided at a single location near the toe of the pile (base of assembly at approximately 29 m bgl; three diameters above the pile toe). With reference to Figure 6, the following instrumentation was provided:

i) A pair of automated digital survey levels for measuring top of pile displacement;

ii) Seven levels of four vibrating wire strain gauges above the O-cell assembly, attached at 90° spacing within the reinforcing cage;

iii) Four telltale rods at 90° spacing monitored by displacement transducers (attached to the top of the pile) for measuring shaft compression above the O-cell assembly;

iv) Four displacement transducers for measuring expansion of the O-cell assembly;

v) Three levels of four vibrating wire strain gauges below the O-cell assembly, attached at 90° spacing; and

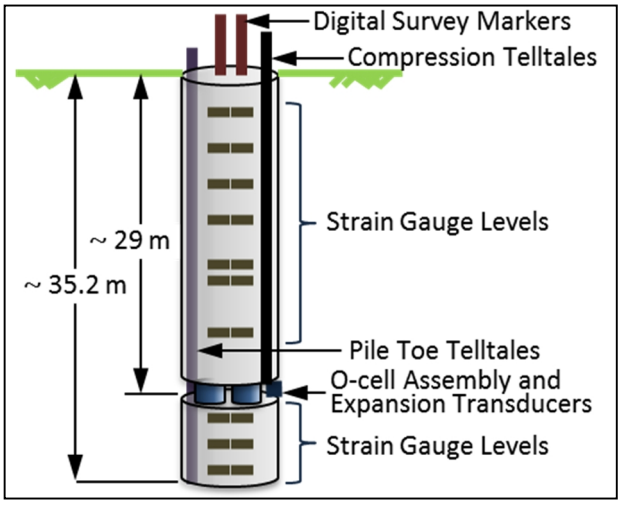

Figure 6. Indicative instrumentation arrangement (not to scale).

vi) Four telltale rods at 90° spacing monitored by displacement transducers (attached to the top of the pile) for measuring pile toe displacements.

5.2. Loading Sequence

A loading sequence was developed in general accordance with AS2159 (2009), adapted for use with an O-cell load test. Each successive load increment was held constant for either 20 minutes or until the creep criteria was met (0.5 mm per 15 minutes), whichever was longer. The load increment assessing pile serviceability (~10 MN) was held for four hours and the increment assessing the design ultimate capacity (~17.9 MN) for one hour.

Load increments were applied past the design ultimate capacity level with a view to assessing the failure capacity of the pile. For this load test, the limits of the equipment were reached at a maximum load of 28.73 MN. The ultimate load capacity of the pile was not reached.

6. Test Results

6.1. Above the O-cell Assembly

It is assumed that the O-cell does not impose an additional upward load until the expansion force exceeds the buoyant unit weight of the pile section above the O-cell assembly; calculated at 1.43 MN (based on an assumed 24 kN/m^3 unit weight for reinforced concrete).

At the maximum applied upward net load of 27.3 MN, the pile head moved 14.55 mm upward with an average shaft compression of 4.02 mm. Therefore, total displacement immediately above the O-cell assembly was 18.57 mm.

6.2. Below the O-cell Assembly

The O-cell applied a maximum downward load of 28.73 MN and at this loading, the displacement immediately below O-cell assembly was 49.78 mm. The pile toe was displaced downward by 48.05 mm and hence compression of the pile shaft in the lower portion was 1.73 mm.

7. Analysis of Results and Discussion

The results of the load test above the O-cell assembly have been interpreted and discussed in this paper; being relevant to skin friction axial capacity design.

It is worth noting that although this load test was undertaken to prove skin friction pile capacity, the results provide useful information for end bearing design considerations and also assessment of axial stiffness. These however, are beyond the scope of this paper.

7.1. Determination of Pile Modulus

The conversion of strain to load within the pile, between each strain gauge level, requires a pile modulus (AE; cross sectional area of pile multiplied by concrete stiffness).

Derivation of pile modulus was a two-step process:

i) Using the laboratory concrete stiffness (reported to be 30.35 GPa on the day of the pile load test; AE = 105 GN) to determine the theoretical load at the O-cell level (46.6 MN), and

ii) *Pro rata* the laboratory-based pile modulus by the amount required to reduce the theoretical load in step i. above to the actual applied test load (28.73 MN) (an approximately 40 % reduction).

The reduced pile modulus derived in this manner for strain gauge interpretation was approximately 64.8 GN and agrees well with Fugro's interpretation which used a back-analysis taking into account O-cell loads and compression telltale measurements (Fugro, 2014).

Thus, in the load test, the observed stiffness of the concrete (on which the observed pile modulus relies) is less than the value determined from laboratory testing. The elastic modulus of concrete is a function of the strains imposed in the pile as a result of loading and the load applied to the pile reduces as a result of load shedding into the soil surrounding the pile shaft (Fellenius, 2001).

7.2. Comparison of Design and Measured Values

Three approaches had been taken in comparing design values with load test results:

i) Overlaying theoretical versus interpreted capacities,

ii) Overlaying theoretical versus interpreted rolling average cumulative skin friction capacities, and

iii) Overlaying individual theoretical and interpreted unit skin frictional capacities.

Analysis of unit skin friction values (approach iii. above) was selected as the most appropriate method of assessing if changes to design assumptions were necessary. The distributions of measured unit skin friction and calculated values are shown in Figure 7.

7.2.1 Interpretation for Frictional Soils

The key input to skin friction capacity derivation for granular soils is the combination of K_s and δ' (as defined and described in section 4).

In the current design philosophy, the unit skin friction values in the upper layer of Pleistocene sand (layer 2 in Figure 7, between 4.7 and 12.75 m bgl) are overestimated. A decreased K_s = 0.7 has been determined for this material to bring theoretical unit skin friction in general agreement with measured values.

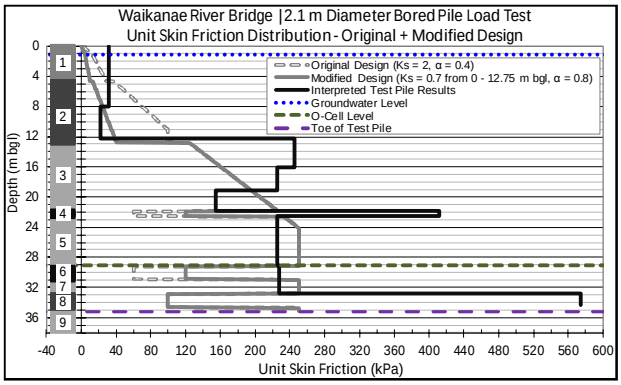

Figure 7. Measured, original design and modified design unit skin friction (layering as per Table 1).

It is likely that this upper layer of Pleistocene sand is not as heavily overconsolidated as the older, deeper Pleistocene deposits below 12.75 m bgl. In addition, the design K_s for Holocene materials have also been revised down to K_s = 0.7.

It is worth noting that the strain gauge level from which deductions around K_s have been made (Figure 7, ~12.3 m bgl) has been identified as potentially unreliable. It is located in the same material as the strain gauge at ~8.1 m bgl (Figure 7), in a zone with greater confining pressures, and yet indicates lower unit skin friction values. Considerations around strain gauge reliability and further investigation around the upper Pleistocene sands will be undertaken in the design of the next load test.

No change to K_s values for deep Pleistocene sands deposits are proposed based on the higher unit skin friction values calculated for this material between 32.9 and 34.7 m bgl (layer 8 in Figure 7).

In the Pleistocene gravels below 22.6 m bgl (layers 5 and 7 in Figure 7), measured unit skin friction is less than design estimates. Analysis of load steps preceding the ultimate indicated that unit skin friction was continuing to increase and therefore these soils do not appear to have reached failure.

7.2.2 Interpretation for Cohesive Soils

The unit pile skin friction for cohesive soils corresponds to the product of α (defined and described in section 4) and the undrained shear strength (s_u).

The results of the load test indicates an underestimation of either s_u or α, given that the product of these terms underestimates adhesion of the Pleistocene silt by a factor of at least two.

As per section 3.3, geotechnical parameters are not refined as part of this interpretation and hence the assumed α factor for Pleistocene silt has been increased to α = 0.8.

7.2.3 Interpretation of Capacity

An update of Figure 5, showing the theoretical capacity using the modified design parameters and

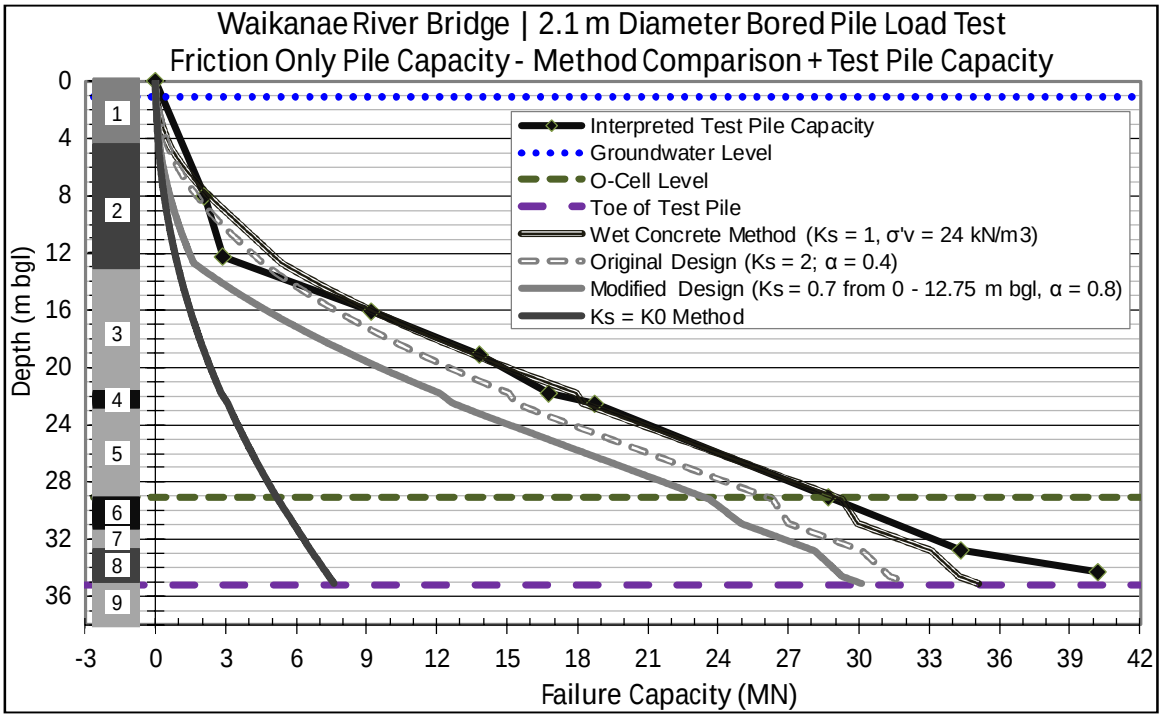

Figure 8. Estimated, modified estimated and measured skin friction capacity (layering as per Table 1).

results of the load test, is presented in Figure 8. The modified design provides a good curve fit with the measured capacity, compared to the original design or wet concrete method, and is more conservative.

It is worth noting that the increased rate of development of skin friction capacity between the lowest strain gauges is due to end effects and the influence of some mobilized end bearing.

8. Conclusions

8.1. Considerations for Design

Overall, the measured capacity of the test pile was greater than that predicted using the selected design approach for the project. Design assumptions are validated, with two modifications identified as part of the load test interpretation:

i) Adoption of a K_s = 0.7 for upper layers of Pleistocene sand and Holocene deposits at Waikanae River Bridge. The Pleistocene sand deposits at depth may continue to use a K_s = 2, and

ii) Use of a higher α = 0.8 value for the Pleistocene silt.

8.2. Considerations for Subsequent Load Tests

The next bored pile load test to be undertaken will be at the site of Te Moana Road Overpass. Greater thicknesses of Pleistocene sand are present at this location compared to at the Waikanae River Bridge site.

In order to better capture the capacity of the Pleistocene sand, a greater number of strain gauges is recommended within this unit and at the Pleistocene sand / gravel interface. Supplementary telltale compression rods with displacement transducers are also proposed. A two-level (push / pull) O-cell load test could also be considered.

Strain gauge reliability requires further consideration in the design of the pile load test at Te Moana Road Overpass.

9. Acknowledgements

The author would like to acknowledge the NZ Transport Agency and M2PP Expressway Alliance for permission to showcase this project and present the findings included in this paper.

The support of my colleagues, in particular Phil Clayton (Associate – Geotechnical Engineering, Beca), has been much appreciated and key in the composition of this conference paper.

10. References

AS2159:2009. *Piling – Design and Installation*. Standards Australia.

Fellenius, B. H. (2001). From strain measurements to load in an instrumented pile. Geotechnical News Magazine, vol. **19**, *n°1, pp. 35-38*.

Fugro Singapore Pte. Ltd. (2014). Report on Bored Pile Load Testing (Osterberg Method) (13830I-PD01-00).

M2PP Alliance (2011). MacKays to Peka Peka Expressway – Geotechnical Design Report (M2PP-SAR-RPT-GT-GE-279).

Maclean, C. & Maclean, J. (2010). *Waikanae*. Whitcombe Press, Waikanae.

Proceedings of the 10th ANZ Young Geotechnical Professional's Conference – 10YGPC
Noosa, Queensland, Australia
10 – 12 September 2014

FERRYMEAD BRIDGE REPLACEMENT – DESIGN AND CONSTRUCTION CHALLENGES

Gemma HAYES
Opus International Consultants Ltd, Wellington, New Zealand

ABSTRACT – The Ferrymead Bridge, which is a key lifeline to the Sumner and Redcliffs area in Christchurch, was identified as being vulnerable to damage in a major earthquake event. Seismic strengthening and widening of the bridge was started prior to the 2010 Darfield earthquake. The February 2011 earthquake caused extensive damage to the superstructure and partially constructed widening works. As a result it was decided to demolish the existing bridge and replace it.

This paper outlines the damage at the bridge site due to the 2010-2011 Christchurch earthquake sequence, and the extent of the site investigations. The resulting ground model used in the design of the replacement bridge structure is described. Key geotechnical issues associated with design, including the liquefiable nature of the soil, large lateral spread loads, the influence of the existing piles and implications of the highly variable nature of the founding volcanic layers on the bridge are discussed. The new bridge is supported by piles socketed into bedrock, and designed to resist the lateral spread loads on the bridge. The permanent pile casing was grouted into bedrock. Challenges and key findings from the piling operations for the replacement bridge are also presented.

1. Introduction

Ferrymead Bridge is located in Ferrymead, Christchurch. It crosses the mouth of the Heathcote River where the river opens into the Avon-Heathcote River Estuary, providing a link between the city and the south eastern suburbs including Sumner and Redcliffs (refer Figure 1). The bridge is a key lifeline to these areas as it carries all major services and, with the alternative road route expected to be closed due to rockfall following a major earthquake event, provides the only connection to the rest of Christchurch City. The liquefaction potential of the soils contributed to the vulnerability of the bridge in a seismic event. Construction works to widen and seismically strengthen the bridge began one week prior to the September 2010 Darfield earthquake. No damage occurred due to this earthquake event and construction works continued. The epicenter of the February 2011 Christchurch earthquake was within 5 km of the site. This earthquake caused liquefaction resulting in lateral spreading at both abutments and extensive damage to the superstructure and the partially constructed widening works. Due to the extent of the damage and health and safety risks associated with continuing the strengthening and widening works with continuing aftershocks it was decided to demolish the existing bridge and replace it.

2. Christchurch Earthquake Sequence 2010-2011

On the 4th September 2010 a M_W 7.1 predominantly strike-slip earthquake occurred. The epicenter was some 43 km west of the Ferrymead Bridge site and despite predictions, no significant damage occurred at the site as a result of this earthquake. The

Figure 1. Site location plan

subsequent aftershock sequence also resulted in no significant damage at the site until the 22 February 2011 earthquake (the Christchurch Earthquake) occurred. The epicenter of this M_W 6.2 earthquake was to the southwest of the site and within 5 km, associated peak ground accelerations at the bridge were estimated to be 0.68 g (Canterbury Geotechnical Database, 2013).

At the time of the Christchurch Earthquake all four of the 1.1 m diameter reinforced concrete seismic strengthening and widening abutment piles had been constructed, three with surveyed as-built locations. One of the abutment beams had also been constructed. Construction of the raked pier piles was well under way at one pier.

The Christchurch Earthquake caused extensive liquefaction at the bridge site resulting in lateral spreading of the approach embankments. Loads imposed on the seismic strengthening and widening abutment piles resulted in the piles rotating towards the river with measurements indicating movement at the top of the pile of 0.65 m to 0.74 m. In addition, rotation occurred at both abutments and displacements were obvious at the piers.

The bridge was able to be opened, with speed restrictions, to light vehicles just two days after the damaging earthquake. However, it took more than a year for the bridge to be opened to heavy vehicles such as buses and trucks. Temporary strengthening was carried out to allow this to happen.

3. Site Information

3.1. Geological Setting

Christchurch City is built on low-lying land that was previously swamp, sand dunes, estuaries and lagoons. Banks Peninsula borders the city to the south and is located on the eastern side of Ferrymead Bridge, towards Mount Pleasant. The bridge crosses the river mouth of the Heathcote River near the Heathcote-Avon Estuary on the margin between the low lying land and hilly Mount Pleasant area (Christchurch City Council, 2011).

Geological mapping of the bridge area shows the site is underlain by Holocene aged estuarine sand and silt, which makes up part of the Christchurch Formation. This is underlain by Late Miocene aged Mt Pleasant Formation comprising of basalt interbedded with breccia and tuff. The Mt Pleasant Formation forms part of the Lyttelton Volcanic Group.

3.2. Site Investigations

Due to the difference in design between the seismic strengthening and widening works and the replacement bridge, additional site investigations were required to provide information for design. With the form of the replacement bridge known, site investigations were able to target the proposed pile footprints. As the piles were to be fixed into the rock, the criteria for the termination of the boreholes was based not only on the requirement of finding an appropriate founding layer, but also a minimum depth into rock to provide lateral restraint.

There was to be at least one borehole at each of the 10 pile locations, however due to the large diameter, three boreholes were initially proposed at the pier piles. Restrictions associated with the existing bridge beams resulted in some of the boreholes being shifted so they were no longer within the proposed pile footprint. As a result all of the 10 proposed piles had at least one borehole in close proximity to the proposed pile location. In addition to the boreholes, seven cone penetration tests (CPTs) were carried out, two at each abutment and three at pier pile locations.

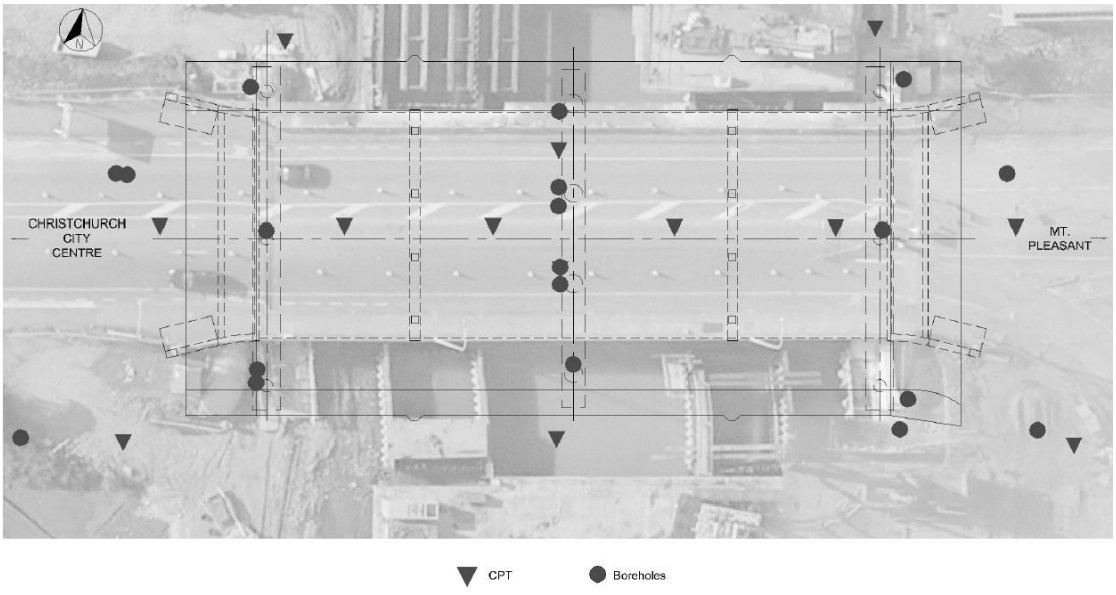

Figure 2. Site investigation location plan

By the time the investigations had been completed, a total of 12 boreholes had been drilled near proposed pile locations, a further five boreholes had been drilled in the approach embankments, and seven CPTs had been undertaken across the site (Figure 2). The additional site investigations were undertaken while the damaged bridge remained open to traffic.

Laboratory testing of the samples recovered was also undertaken, and included particle size distribution tests and unconfined compressive strength testing of the rock with stress stain measurements.

3.3. Ground Model

Development of the ground model relied heavily on the boreholes drilled specifically for the replacement bridge but also used information obtained during piling operations of the seismic strengthening and widening works.

Globally at the site, the ground model consisted of 2 m to 3 m of fill at the abutments overlying estuarine sediments varying in thickness from 6.8 m at the eastern abutment to 20.6 m at the western abutment. Underlying these sediments were the interbedded basalt, breccia and tuff (Figure 3). The breccia was further classified as Agglomerate or Volcanic Breccia based on the composition of the samples recovered and the expected in-situ behavior.

From the borehole results it became apparent there was significant variability within the rock and as such ground models were developed at each specific pile location.

4. Proposed Replacement Bridge Form

For various reasons including the thickness of liquefiable deposits, at the western abutment in particular, the presence of a large number of services and the large costs associated with ground improvement, the solution for the replacement bridge did not incorporate ground improvement. The decision to not improve the ground at the abutments resulted in a need to carefully consider the effects of liquefaction and resulting lateral spread loads and design the foundation system accordingly. In doing so fewer abutment piles and of a smaller diameter were utilised to minimise lateral spreading loads being imposed on the piles and bridge. The bridge has been designed such that lateral loads on the abutment piles are to be resisted by the larger diameter pier piles and the opposite abutment.

The final bridge form is a two span bridge with four large diameter (2.4 m) pier piles and three smaller diameter (1.1 m) piles at each abutment (Figure 4). A landspan at each abutment, which bridges a void behind the abutment piles, has been used to further reduce the lateral spread loads on the abutment piles. Piles have been socketed into the rock to prevent displacement should liquefaction occur.

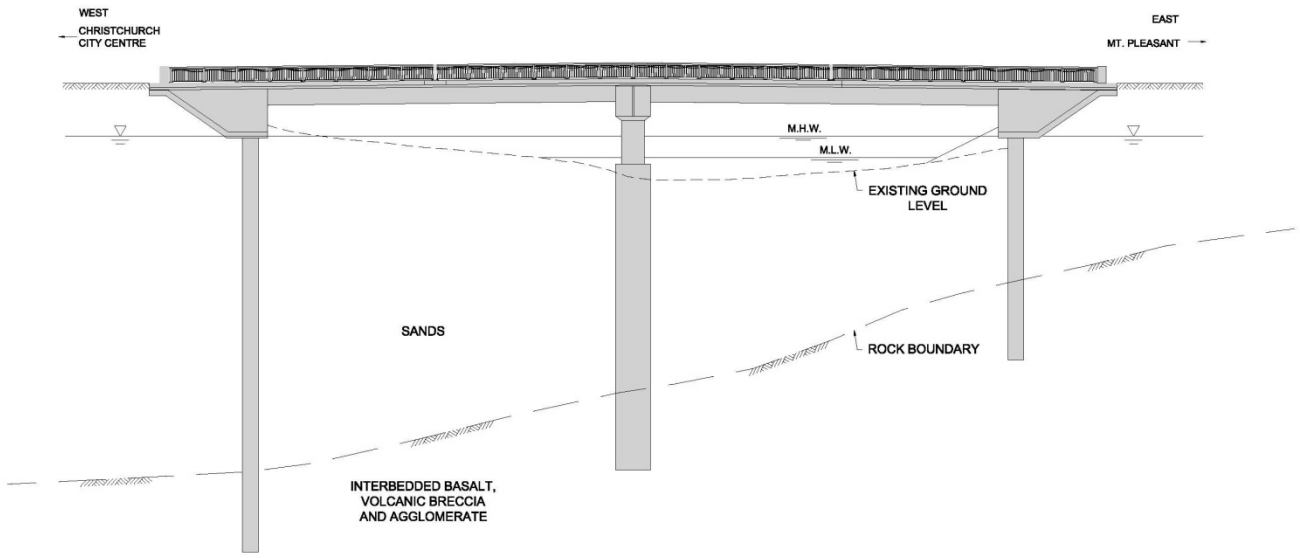

Figure 3. Simplified ground model

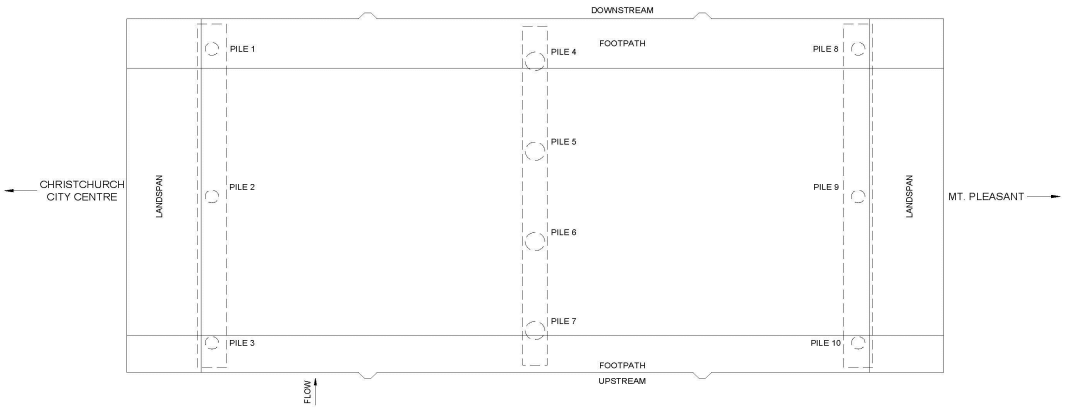

Figure 4. Proposed replacement bridge

5. Geotechnical Issues

As identified in early assessments pertaining to the seismic strengthening and widening of the existing bridge the soils at the site are susceptible to liquefaction. In addition the non-liquefiable crust at the abutments will impose large lateral spread loads at the abutments. The effects of lateral spread loads have been minimised through the use of a landspan in addition to specific construction detailing of the approach embankments (Figure 5). The approach embankments are to be constructed such that they are susceptible to liquefaction below a certain depth, this will reduce the thickness of the non-liquefiable crust therefore reducing the lateral spread loads. As the approaches can easily be reinstated following liquefaction in an earthquake event, the thickness of material susceptible to liquefaction at the approach embankments is unlikely to have long term detrimental effects on the post-disaster functionality of the bridge.

With the replacement bridge philosophy resulting in fewer abutment piles of a smaller diameter, soil is assumed to flow between the piles under cyclic loading. However, the foundations of the previous bridge, which consisted of two rows of closely spaced 0.4 m rectangular raked piles at each abutment, are likely to cause soil to arch between the piles. Arching of the soil will essentially cause the piles to act as a wall and ultimately result in the new abutment piles for the replacement bridge being subjected to much larger loads. In order to reduce the impact of soil arching a number of existing piles were removed from each abutment during demolition of the existing bridge.

As previously alluded to, ground conditions at the site are highly variable. Of particular importance is the variability in the layering and quality of the rock encountered. Strength testing of the rock material indicated a range from 2 MPa to over 100 MPa for the varying rock types encountered. The large variability in rock quality and uncertainty regarding the in-situ behaviour of the volcanic breccia and agglomerate required the piles to be founded in basalt layers of sufficient thickness. In addition to this, it was difficult to distinguish between boulders within the agglomerate material and thin basalt layers. This uncertainty made identifying founding layers, particularly at the abutments, difficult. The risk associated with this uncertainty and the

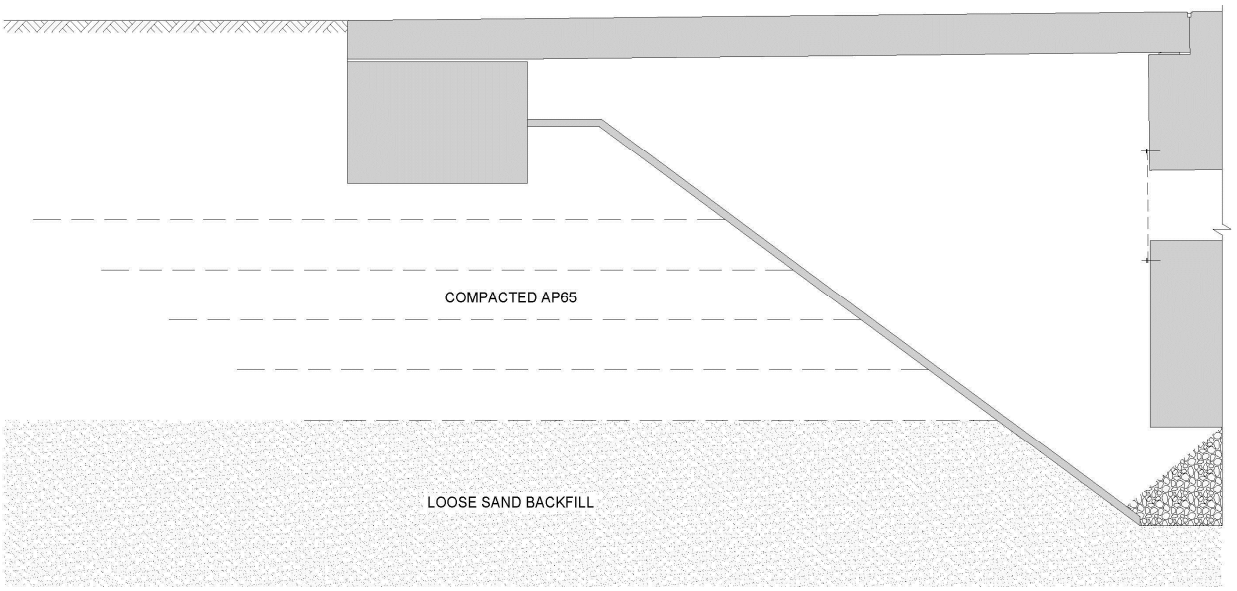

Figure 5. Approach embankment detailing

variable nature of the rock was considered during construction and as such a 1 m contingency of casing was ordered for every pile. The ongoing seismic activity posed a considerable risk to the construction of the replacement bridge. Geological and Nuclear Sciences (GNS) estimated a 9% probability of a magnitude 6.0 to 6.4 occurring in the Canterbury region in the following year (Opus, 2012). During construction, the bridge is more vulnerable to seismic activity, particularly prior to installation of the bridge deck, as loads cannot be transferred to the pier piles as per the design philosophy. The construction sequence was initially programmed to reduce the exposure time and hence the risk to the piles. This was achieved through constructing the pier piles first, as they are further from the river banks and less exposed to lateral spread loads, followed by the eastern abutment piles, which encountered rock at a significantly shallower level and as such were shorter piles, then construction of the western abutment piles. In addition to this sequencing a frame system was designed to prop the abutment piles off the pier piles (Sadashiva et al., 2014). These props were designed to minimise movement of the piles during construction and needed to be installed prior to driving the casing into rock.

6. Piling Operations

Piling for the replacement bridge began in June 2013 at the upstream pier pile, Pile 7 and concluded with the final pour of the upstream eastern abutment pile, Pile 10, at the end of April 2014. While piling was completed two months sooner than initially programmed it wasn't without its challenges.

The variation in ground conditions encountered during investigations was validated during piling operations with information obtained on site indicating some basalt layers dipping up to approximately 45°. Variations in the rock layering encountered, compared to that expected based on the site investigations, resulted in four of the 10 piles having an additional borehole drilled through the base of the pile excavation to prove the founding layer. At one pile in particular the top of the rock level, a critical aspect to the behavior of the bridge under seismic loading, was so much lower than that modelled during design that a revised model had to be analysed to assess the effect on the bridge behaviour.

The large diameter of the pier pile casings made driving a challenge. Piling through the basalt layer allowed excavation of the basalt up to 1 m in advance of the casing. However, due to the uncertainty of the stability of the agglomerate, excavation was only permitted 0.3 m in advance of the casing through these materials. Pile driving through the strong basalt layers required large driving forces which caused damage to the pile driving equipment, as a result the contractor mobilised larger plant. Pile driving through the agglomerate material was less of an issue as the casings were able to be vibrated into the ground relatively easily with minimal vibrations in the surrounding land.

A structural requirement of the design was for good contact between the pile casing and the ground, particularly for the length of pile embedded in rock. To achieve this, grouting of the pile casings was attempted using internal grout tubes and an external method using Tube-A-Manchette (TAM). The purpose of the grouting was to fill the void between the pile casing and the rock formed during excavation of the pile. While there was a significant focus on developing an appropriate method for TAM grouting with the contractor during the design and planning stages it was identified this method would need to evolve as grouting proceeded and more information and experience was gained. A specialist sub-contractor was engaged to undertake the grouting operations. Grouting initially involved internal grouting through tubes installed with the pile reinforcing cage prior to multiple stages of TAM grouting (Figure 6).

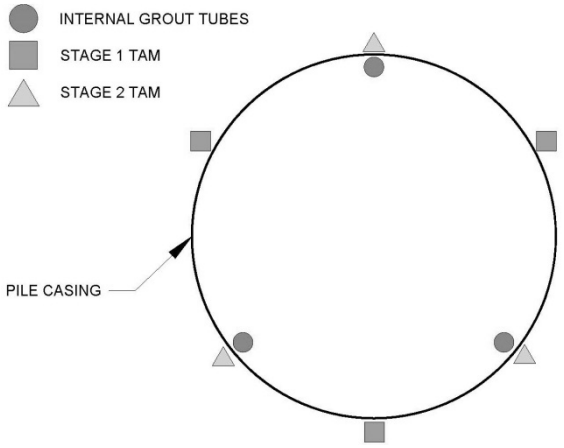

Figure 6. Internal grouting and TAM locations

As internal grouting appeared ineffective during grouting of the first two piles it was stopped and all grouting for the remaining eight piles was undertaken using TAM grouting. TAM grouting was conducted externally with the TAMs installed in boreholes drilled down the outside of the casing once the pile had been poured. Typically six TAMs were installed per pier pile and four TAMs were installed per abutment pile. TAM grouting was undertaken in two stages with half of the TAMs installed per stage and grouted over two to three days on average to ensure refusal was reached. Refusal was based on the pumping pressure reaching a maximum limit set prior to grouting commencing and was taken to indicate the void between the casing and the surrounding rock was full of grout. The volume of grout pumped through each node per day was limited to minimise the risk of losing excessive volumes of grout into the surrounding ground. Maximum grout volumes per node and maximum grouting pressures were

selected based on contractor experience and experience gained through the Ferrymead Bridge TAM grouting. These maximum volumes and pressures were the key adjustments made during the grouting operations.

7. Conclusions

Seismic strengthening and widening of the Ferrymead Bridge began one week prior to the September 2010 earthquake, with minimal resulting damage, and works continued. Extensive damage to the bridge and the seismic strengthening and widening works occurred as a result of liquefaction and lateral spreading caused by the Christchurch earthquake. Due to the damage and ongoing seismicity it was decided to demolish and replace the existing bridge.

A proposed replacement bridge form was developed and additional site investigations undertaken to assist with design. Significant geotechnical issues considered during design of the replacement bridge include the soils susceptible to liquefaction and lateral spreading, variable ground conditions particularly the volcanic rock, the influence of the existing bridge abutment piles and the ongoing seismic activity in the area. Solutions to reduce the risk from these issues involved careful consideration of the form of the replacement bridge, with smaller diameter and fewer piles at the abutments, incorporating a landspan to reduce lateral spread loads, removal of a select number of existing abutment piles and careful sequencing and propping of the piles during construction to minimise the risk posed by ongoing seismicity.

Construction challenges encountered during piling operations include the variable ground conditions, which required close monitoring and communication with the contractors, difficulties associated with driving the large diameter pier piles and undertaking pressure grouting to fill the void between the pile casing and the excavation.

Piling works were completed in April 2014, with bridge construction and associated approach works due to be completed in July 2015.

Given the knowledge gained from this project, if another structure, with similar risks and constraints, arose I would employ a similar strategy for the site investigations. This would include boreholes at each of the proposed pile locations, a further borehole at each of the approach embankments, minimal CPTs in the overlying sand and laboratory testing of the rock, with stress and strain measurements.

The only other change worthy of note would be to the grouting methodology. TAM grouting of the piles into the surrounding ground appeared to be effective. However, in the future I would adjust the methodology in the following ways:

- only attempt to grout using external TAMs;
- consider the overburden pressure at the depth being grouted when deciding on a limiting grouting pressure;
- consider the piling contractors methodology when deciding on limiting grout volumes and the likely void space required to be filled with grout; and
- in areas where grout take is high, use more attempts with smaller grout volumes with the aim of sealing the surrounding fractured ground, rather than larger volumes.

The extent of these site investigations and modified approach to grouting should allow adequate design and construction outcomes whilst contributing to an appropriate spread of risk across the entire project team.

8. Acknowledgements

The author gratefully acknowledges the permission of the Christchurch City Council, the client for this project, to publish this paper.

9. References

Canterbury Geotechnical Database. (2013). *Ground motion, map layer CGD5170 – 28 May 2013.* Retrieved April 2014, from http://canterburygeotechnicaldatabase.projectorbit.com/

Christchurch City Council. (2011, August 24). *Waterways, wetlands and drainage guide: Christchurch City Council.* Retrieved 2012 June, from Christchurch City Council: http://www.ccc.govt.nz/cityleisure/parkswalkways/evironmentecology/waterwayswetlandsdrainageguide/index.aspx

Kirkcaldie D., Brabhaharan P., Cowan M., Wang C., Hayes G., Greenfield L. (2013). Ferrymead Bridge – from widening and seismic upgrading to replacement, a casualty of the Christchurch earthquake. *New Zealand Society for Earthquake Engineering Annual Conference*. 26-28 April 2013. Wellington.

Opus International Consultants Ltd. (2012). *Ferrymead Bridge replacement – geotechnical interpretive report.*

Sadashiva V.K., Brabhaharan P., Novakov D., Cowan M., Krotofil M. (2014). Ferrymead Bridge – temporary seismic restrain system. *New Zealand Society for Earthquake Engineering Annual Conference*. 21-23 March 2014. Auckland.

Proceedings of the 10th ANZ Young Geotechnical Professional's Conference – 10YGPC
Noosa, Queensland, Australia
10 – 12 September 2014

PRACTICAL CONSIDERATIONS FOR DIRECT SHEAR TESTING OF COAL MINE SPOILS

Leonie BRADFIELD[1], Kai KOOSMEN[2], John SIMMONS[3], Stephen FITYUS[2].
[1] *Thiess Pty Ltd and University of Newcastle, Australia*
[2] *University of Newcastle, Australia*
[3] *Sherwood Geotechnical and Research Services, Peregian Beach, Australia*

ABSTRACT – Civil engineering laboratories use the direct shear test to provide shear strength parameters for soils under drained or undrained conditions. Standard shear boxes are of suitable capacity in terms of dimensions and load to provide reliable data for the testing of the majority of soils for civil engineering applications. However, the reliability of the data becomes questionable when extended to the field of mining engineering in which materials differ from traditional soils, and stresses may be much greater than those commonly encountered in general earthworks. When performing direct shear tests on coal mine spoil, geotechnical practitioners and laboratory technicians may be uninformed of the limitations of standard equipment and/or the consequences of applying unrepresentative data to geotechnical models. The purpose of this paper is to outline considerations for using standard laboratory equipment to derive shear strength parameters for coal measures spoil.

1. Introduction

The direct shear test (DST) is performed in civil engineering laboratories to investigate the shearing behaviour of soils. Standard 60 to 100 mm sized shear boxes are suitable for testing the majority of soils for civil engineering applications, and 300 mm shear boxes are routinely used for handling more granular materials such as rock fill. For soils tested in boxes up to 300 mm in size, a maximum normal stress of around 1 MPa is the norm for 'off-the-shelf' equipment, and scalping of oversize particles is usually not required. Standard laboratory equipment can provide reliable shear strength data for soils and stress ranges comparable to field conditions, up to a point.

The reliability of the data diminishes when materials tested contain oversize particles, requiring excessive scalping to be performed to meet test standards, or when tests are performed under non-representative stress ranges or non-characteristic saturation conditions. These issues are commonly encountered when performing DSTs on coal mine spoil, where site geotechnical practitioners and laboratory technicians may be unaware that results may be significantly in error when the test procedures do not represent the above constraints. Furthermore, the resultant shear strength parameters are often uncritically accepted by site engineers who are unfamiliar with the practical details of laboratory techniques.

This paper describes key considerations for mine geotechnical practitioners when scoping and validating DSTs performed on coal mine spoils for the purposes of slope stability analysis and design. In particular, it focusses on piles constructed from competent coal mine spoils, either by dragline or end-dumping by haul trucks, where slope heights typically exceed 30 m.

2. Background

2.1. Nature of coal measures spoil piles

Coal mine spoils consist of rocks and soils. Their constituents, fabric and shear strength are governed by the parent rock type, mine processes and post-placement deterioration. Coal measures spoils are generally derived from sedimentary rocks that commonly include sandstones, siltstones, and shales, but may also include volcanics and intrusives.

Mining practices that contribute to the stability of spoil piles include fragmentation, overburden removal, foundation preparation and overburden placement. These processes essentially dictate the foundation condition, spoil pile slope geometry, block size, depositional fabric, density and porosity. Exposure (to air or water) is the most destabilising natural influence on coal mine spoil, especially for clay mineral-bearing, water-sensitive spoils. This is important for stability because groundwater usually enters a spoil pile at the coal seam floor contact; hence spoil pile foundations are generally saturated and weaker than overlying spoil.

Instability mechanisms for coal measures spoil piles are generally classed as either small surficial crest slumps caused by slope undercutting; or deep-seated, multi-wedge type mechanisms that develop on a low-strength layer at the base of the spoil pile. The weak basal layer could be within the spoil, at the spoil/coal seam floor contact, or within the coal seam floor. A distinct backscarp develops to the surface once failure has initiated. Figure 1 shows the multi-wedge type mechanism as described in literature (after Gonano, 1980; Mallet *et al*. 1983, Simmons and McManus, 2004).

Direct shear testing of coal mine spoil (for the estimation of drained shear strength) is applicable to deep-seated instability mechanisms that develop along a planar surface; where confining stresses are large relative to pore pressures, and failure development is not usually contingent on pore pressures.

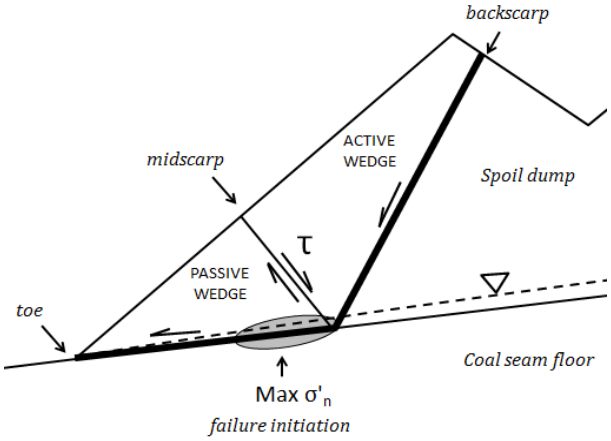

Figure 1. Deep-seated multi-wedge failure mechanism (after Gonano, 1980; Mallet *et al*. 1983, Simmons and McManus, 2004)

2.2. Spoil shear strength framework in the absence of measured data

In the late '80s and early '90s, BHP Engineering and CSIRO conjointly investigated the stability of dragline-scale spoil piles in the Bowen Basin. From this, the BMA Coal strength framework was developed, as described by Simmons and McManus (2004). The framework provides a procedure for classifying coal measures spoil into one of four categories, and for each category provides peak shear strength parameters based on direct shear tests, and back-analysis of spoil pile failures of comparable stress. For each spoil category, parameters for three strength mobilisation modes are provided; these are unsaturated, saturated and remoulded.

The framework is generally adopted in the absence of, or more commonly in preference to, acquiring laboratory data. However, despite proving a reliable tool for shear strength estimation for decades, it is neither perfect, nor impervious to human error or misuse.

The framework is intended to be used for spoil piles 30 to 120 m in height, assuming that the spoil is characterised correctly. However, because the framework is a linear fit to data believed to be non-linear in reality, uncertainty is introduced when the framework is applied to spoil piles outside the intended height range, or to spoil types not covered by the framework. This occurs frequently and sometimes unknowingly by mine geotechnical practitioners.

A common error when using the framework is incorrect spoil characterisation. This often occurs when spoil is assigned to a category without sufficient experience particularly in undertaking the necessary 'visual-tactile' observations. This oversight has the potential for detrimental consequences, because spoil could be assumed to be much stronger or weaker than it actually is.

Another constraint of the framework is that there is no provision for slake-prone spoils. The authors have found that, when saturated, slaking spoils can deteriorate to a completely different category than when in an unsaturated state. The 'remoulded' condition is adopted to describe the strength of saturated, strongly-slaking spoil, although it also used to describe other modes (such as the residual strength in a failed spoil mass, or water-sensitive clays with mineralogy disposed to swelling and dispersion on saturation).

3. Direct shear test and Mohr-Coulomb Criterion

The DST can provide peak, softened or residual shear strength parameters for materials under drained and undrained conditions. Standard shear box dimensions are 60 mm or 100 mm and can handle fine gravels, sands and clays. For coarser materials such as rockfill, 300 mm shear boxes are required.

In a standard 60 mm or 100 mm DST, a representative specimen is placed in the box that is horizontally split into two halves. A vertical load is applied to the specimen, and a horizontal strain is imposed on one of the box halves. The shear force transmitted through the specimen is measured as the reaction force on the other half box. The shear stress, calculated from the shear force divided by the sheared area, is plotted against displacement. Typical stress-displacement curves of normally consolidated (NC) and overconsolidated (OC) soils are shown in Figure 2.

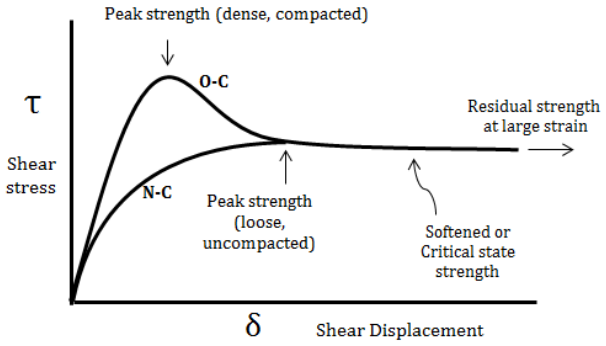

Figure 2. Shear stress- displacement behaviour from DSTs (after Terzaghi *et al.* 1996)

For a given normal stress, the shear stress at failure is recorded. The chosen mobilised failure mode (i.e. peak, softened, or residual) depends on consistency of the material, and the shear strain applicable to the field situation for which the data are to be used. A minimum of three tests is performed, at different normal stresses, to develop

a Mohr-Coulomb failure envelope. For drained tests, effective stress parameters cohesion, *c'* and friction angle, ϕ' are interpreted according to Terzaghi's (1936) theory for saturated soils, given by Eqn. 1; where τ is shear stress, and σ_n' is effective normal stress.

$$\tau = c' + \sigma_n' \tan \phi' \quad (1)$$

The resultant *c'* and ϕ', in addition to the specimen's unit weight, are used by geotechnical practitioners for input into their geotechnical models for slope stability analysis.

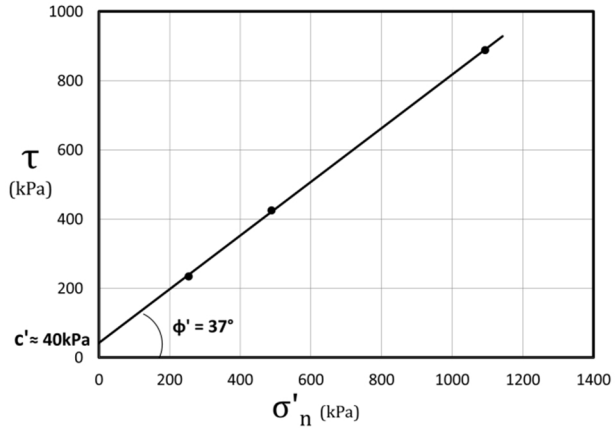

Figure 3. Mohr-Coulomb envelope for 300 mm diameter DSTs on an NC Permian siltstone spoil

3.1. Considerations when Scoping and Validating Direct Shear Tests on Coal Mine Spoil

It is perhaps optimistic to assume geotechnical practitioners recognise the importance of laboratory testing to verify spoil shear strength where a level of uncertainty exists. For example, where the geological or hydrological environment has changed, where spoil piles continually fail at design heights despite models suggesting otherwise, or where spoil types or geometries extend beyond the limitations of the BMA Coal strength framework.

A series of DSTs has been performed to demonstrate some important considerations and to illustrate how laboratory testing may be more routinely adopted by geotechnical practitioners. The spoils tested were derived from Tertiary and Permian coal-measures of the Hunter Valley and Bowen Basin Coalfields, tested in 100 mm, 300 mm and 720 mm-square shear boxes.

Testing for this investigation generally followed the procedures outlined in ASTM D 3080-98. This paper offers suggestions for sample preparation and testing conditions considered specific to coal-measures spoil piles constructed by dragline or end-dumping from haul trucks. Unless specified herein, guidelines for sample preparation, calibration, testing and reporting should be as per the aforementioned test method.

3.2. Geotechnical model

A geotechnical model for a spoil pile should be developed by the geotechnical practitioner prior to engaging a testing authority to perform DSTs. This requires assembling as much as is known about the parent rock geology, mining history, spoil pile construction method and resultant slope geometry, foundation conditions and groundwater behaviour. This geotechnical model should be used to select the sample preparation method, the test saturation condition, the normal stresses for testing, and the strength mobilisation mode.

3.3. Strength mobilisation modes for testing

A prime consideration for scoping and interpreting DSTs is the appropriate strength mobilisation mode. Civil engineers use peak strength to describe the shearing behaviour of compacted soils, soils with no fissuring, and soils with no existing failure surfaces. Softened strength parameters are appropriate to fissured soils and poorly-compacted fills, and residual strength parameters are adopted for existing sheared failure surfaces (Chowdhury *et al*. 2010).

Peak shear strength parameters need only be sought when performing DSTs on mine spoil for a given test saturation condition (explained in Section 3.4). Spoil piles generally exhibit normally consolidated behaviour, as they are loose-dumped, and any compression that occurs is due to their self-weight as compaction by equipment is minimal. Since no further shear strength reduction occurs with continued displacement beyond the peak strength, the peak and softened strengths are equivalent. This behaviour introduces an important practical consideration for testing; in that care should be taken to ensure the specimen has been sheared far enough to allow peak shear strength conditions to fully develop. If the peak is not reached, the resultant shear strength will be conservative. For the spoil samples tested, peak shear strength was observed to develop at relative shear displacements (rsd) ranging from 3 to 10%, depending on lithology and test saturation condition. A value of 10% should be adopted as a minimum rsd to ensure that peak strength is reached.

The softened and residual shear strengths can be assumed equivalent for spoils with a low fines content (i.e. <20%, Fell and Jeffery, 1987). However, with continuing displacement for fines-rich spoils, a further reduction in shear strength may develop due to clay particle reorientation. The residual strength is the minimum shear strength attained at very large displacements, and for high clay mineral-content spoils, it is significantly different to the softened shear strength.

Typically, residual strength is estimated from back-analysis of slope failures due to problems in obtaining the 'true' residual shear strength. Conventional DSTs cannot be performed to the

very large displacements required to reflect the true residual shear strength. Even when a number of shearing reversals (with the normal load removed on reversal and re-applied on re-shearing) are applied in the DST, the residual shear strength can be over-estimated due to particle realignment with each change in shearing direction (Bishop *et al*. 1971). However, within a failed spoil mass, large post-failure shear displacements may develop a failure plane that allows the true residual shear strength to be back-analysed.

It is important to note that the 'softened shear strength' is not interchangeable with 'remoulded shear strength'. The remoulded condition describes a permanent and irreversible alteration of structure that occurs when water-sensitive clay mineral-rich spoils are saturated. Simmons and McManus (2004) found that, for spoils of susceptible mineralogies, the remoulded shear strength can, for practical purposes, be assumed equivalent to the residual shear strength. However, this only holds true for clay mineral-rich spoils. Clay-deficient spoils do not develop the remoulded condition.

Figure 4 illustrates the idealised stress-displacement behaviour observed for the range of normally-consolidated Tertiary and Permian spoils tested for this project in a 720 mm square shear box. 'Unsaturated' tests allowed specimens to air dry from their sampled moisture contents for 24 hours prior to testing. 'Saturated' tests refer to tests on specimens soaked in a water bath for a minimum of 24 hours following compression under the applied normal stress, which assumes a saturated condition was achieved. The remoulded condition was achieved only once in the laboratory for a Tertiary clay sample, by saturating prior to consolidation. Problems with materials handling precluded further successful tests of this nature from being carried out.

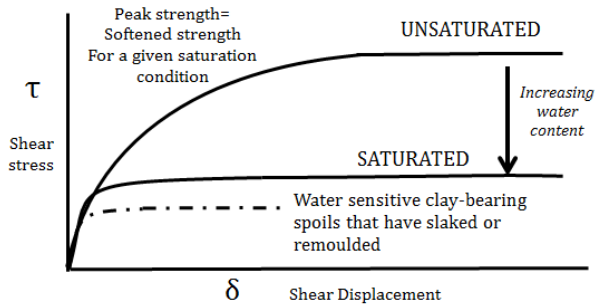

Figure 4. Shear stress-displacement curves observed from DSTs on a range of spoils

3.4. Placement, consolidation and precompression

ASTM D 3080-98 provides instructions for preparing materials to a specific density or void ratio. For coal mine spoils, it is recommended that the specimen be prepared in a loose state, by pouring the spoil into the shear box from a low height. This simulates the condition of spoil placed by dragline or end-dumping by haul truck, as employed when constructing spoil piles. Specimens should then be compressed under a normal stress representative of field conditions.

For very loose spoils under high normal stresses, precompression and refilling of the box prior to shearing may be required to ensure sufficient specimen thickness is achieved for shearing. Following the precompression, the minimum sample thickness (T) should be at least 6 times the maximum particle diameter, (D_{max}), according to ASTM D 3080-98.

In tests with inadequate material above the shear plane, the recorded shear strength may be overestimated due to the rigid top plate interfering with the development of the shear band. Figure 5 shows a series of 300 mm DSTs performed under drained, saturated conditions, on a highly-compressible spoil consisting of Tertiary sediments. Tests sheared under normal stresses of 900 kPa and 1,000 kPa that were not refilled after preloading compressed significantly, leaving an insufficient thickness above the shear plane. Tests were only considered valid if the results were reasonably consistent with other results for similar material, and the observed post-shear surface was not distorted towards the upper or lower boundaries.

The effects of overconsolidation on shear strength were investigated with two additional tests precompressed under 1,500 kPa, and then sheared under normal stresses of 500 and 800 kPa. Although these were performed at different normal stresses to the valid tests, it is evident that precompression resulted in a measured shear strength that is higher than that of the valid normally-consolidated tests.

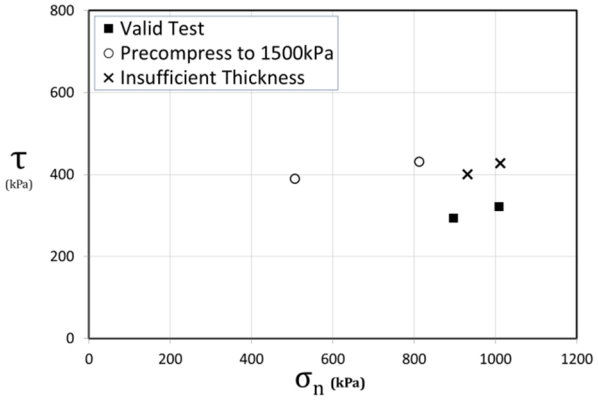

Figure 5. Effects of inadequate preloading on measured shear strength

It is therefore important to ensure that the D_{max}:T ratio complies following the initial compression phase. If it doesn't, the specimen should be topped up. It is equally important to ensure the preload stress does not exceed the normal stress of the test as this will overconsolidate the sample.

3.5. Moisture content and test saturation condition

In regard to dragline-scale spoil piles and a deep-seated multi-wedge failure mechanism (i.e. involving relatively large confining stresses, Figure 1), test results demonstrate that, under the 'dry' condition, variation in gravimetric water content, *w,* has little influence on the failure envelope developed from the measured shear strength. The 'dry' condition refers to spoil that is relatively dry to slightly moist, although *w* could range by as much as 8% under this condition, depending on mineralogy and atmospheric conditions.

Figure 6 illustrates this behaviour for a Permian siltstone spoil tested in the 300 mm and 720 mm shear boxes. 'Dry tests' were conducted at field moisture content, or after air-drying for 24 hours. 'Wet tests' were conducted on samples soaked for a minimum of 24 hours to achieve a condition close to a fully-saturated state.

Dry tests, with *w* between 5 and 11% show little variation in shear strength for the normal stress range considered. In contrast, for wet tests, a marked strength loss with increasing normal stress is apparent beyond 250 kPa; that is, equivalently, the maximum normal stress likely to occur at failure for a 30 m high spoil pile.

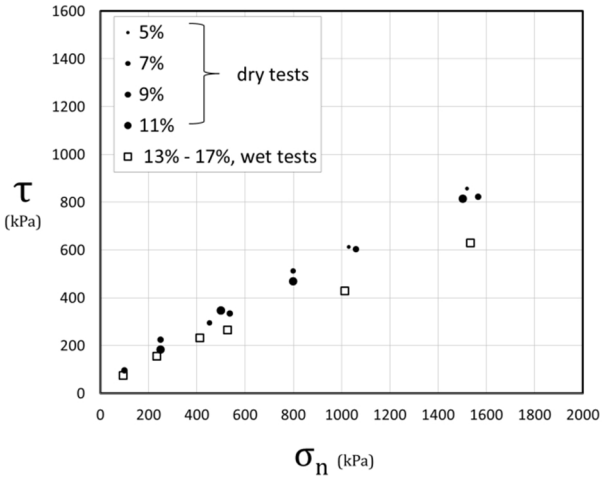

Figure 6. Variation in shear strength according to *w* and test conditions

These findings support the applicability of the 'unsaturated' and 'saturated' strength mobilisation modes of the BMA Coal strength framework, in that unsaturated strengths are higher than saturated strengths. The framework essentially divides the spoil pile into wet and dry zones, with their own unique shear strength parameters. These saturated/unsaturated zones are separated by the phreatic surface, which is assumed to lie 3 to 5 m above the foundation and to drain through the slope toe, with no 'transitional' areas of moisture, or associated strength variation.

It is therefore recommended that coal mine spoil be tested under both the dry and wet states. It is difficult to suggest a blanket guide for nominal soaking time for the 'wet' or 'saturated' tests, because this depends on mineralogy, grading and structure. However, as a general rule, following consolidation, spoils should be soaked until there is no further water uptake by the specimen. This requires refilling the water-bath to a nominal level until the level is maintained. Understandably, clay mineral-rich spoils will require a longer soaking times than cohesionless spoils.

An important consideration when developing geotechnical models for stability analysis from DST data, is that wet (or saturated) shear strengths should be assigned to spoil that has been previously saturated, irrespective of the current phreatic surface location. This is discussed by Simmons and McManus (2004), who recommended that the saturated strength mode be treated as irreversible even when free water has drained from the void spaces. Dry, or unsaturated strength is assigned to the rest of the spoil pile. This is illustrated in Figure 7.

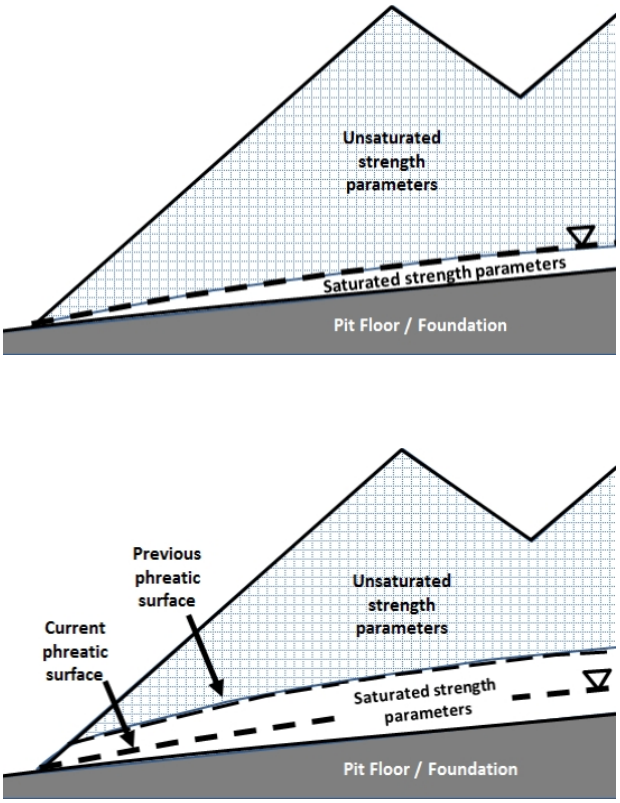

Figure 7. Strengths for geotechnical models when considering saturation

3.6. Scale effects: Apparatus and scalping

Scale effects are acutely pertinent to laboratory testing of coal mine spoil. This is because standard equipment cannot give reliable results for samples containing the large particles typical of coal-measures spoil. Scalping is routinely performed to a maximum particle diameter (D_{max}) to sample

thickness (T) ratio of 6:1 (as recommended by ASTM D3080-98). Figure 8 shows the variation in shear strength when deviating from the nominal ratio of 6:1 for a Permian siltstone spoil. Tests were performed in a 100 mm shear box, and the recommended D_{max} allowed materials passing the 4.75 mm sieve.

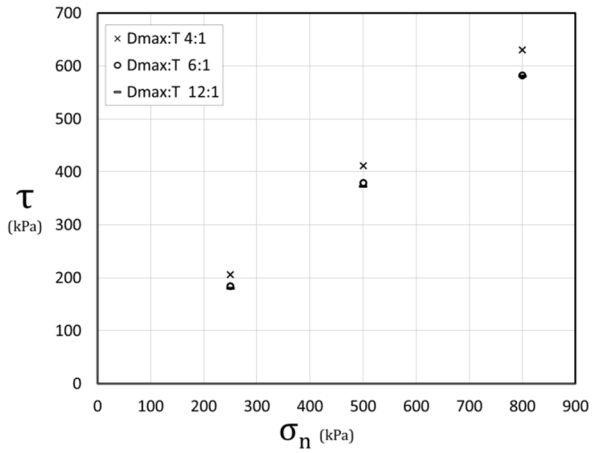

Figure 8. Influence of particle size on shear strength of scalped Permian spoil in a 100 mm shear box

Decreasing the D_{max}/T ratio was found to increase the measured shear strength of the spoil while, as expected, increasing the ratio slightly had little effect. These results highlight the sensitivity of shear strength to oversized material in general for direct shear testing.

It is necessary to note however, that the aforementioned tests required excessive scalping of the spoil to meet the constraints of the 100 mm shear box. Scalping is an issue when a sample is reduced to a fine fraction that is distinctly dissimilar to its original composition, and it is recommended that a shear box with minimum lateral dimension 300 mm be used for coal mine spoil.

Figure 9 compares the shear strengths obtained from the scalped 100 mm DST specimens shown in Figure 8, with those of less-scalped DSTs performed on the same type of spoil in a 300 mm shear box. A D_{max}/T ratio of 6:1 allowed D_{max} passing the 4.75 mm and 26.5 mm sieves for the 100 mm and 300 mm boxes, respectively. It can be seen that the measured shear strengths are higher for the 300 mm DSTs. However, it is acknowledged that differences in machine stiffness may also be playing a part.

This indicates that, for the normal stress range shown (<1MPa), DSTs on spoil scalped to a finer fraction will deliver lower shear strengths than a coarse, less-scalped specimen. This agrees with findings by Nakao and Fityus (2008), who reported a significant underestimation of friction angle for a typical ripped rock material when scalped to a finer fraction and tested in a 60 mm shear box. Due consideration should be given to the shear box size and associated degree of scalping when preparing and reviewing the results of DSTs on coal mine spoil.

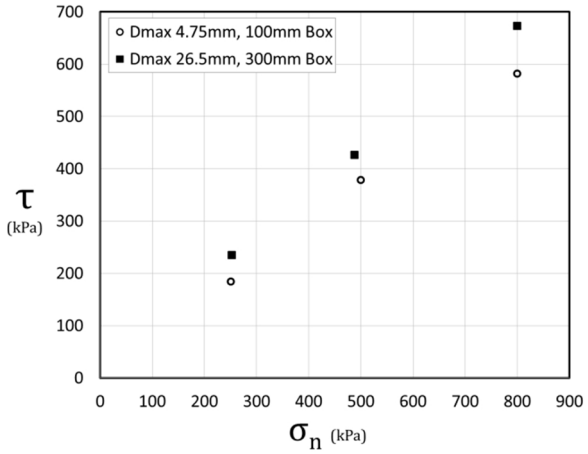

Figure 9. Compares DSTs performed on a Permian spoil in 100 mm and 300 mm boxes, using a D_{max}/T ratio of 6:1

3.7. Scale effects: Stress and extrapolation

Extrapolation of test data to a higher stress range is a common error associated with direct shear testing of mine spoil. This occurs because standard laboratory testing equipment is usually load-limited to around 1 MPa of normal stress; approximately the normal stress at failure for a typical coal measures spoil pile a little over 100 m high (noting that the major principal stress would be around 1.8 MPa, based on a unit weight of 18 kN/m^3).

At present, however, spoil piles commonly exceed 200 m in height, and test data from standard testing equipment are often extrapolated to this stress range. This practice can potentially result in an overestimation of the shear strength due to envelope curvature. Figure 10 is a conceptual model demonstrating how the shear strength of a spoil pile, defined by c_b' and ϕ_b' can be overestimated by the extrapolation of laboratory data (c_a' and ϕ_a').

A large-scale high-stress shear box has been designed and constructed at the University of Newcastle (Bradfield *et al*. 2013) for testing representative samples of mine spoil (720 mm square) at very high normal stresses (~4 MPa).However, where for practical reasons purpose-built apparatus are not available for testing, or standard shear boxes cannot be modified to perform high stress tests, strength reduction factors could potentially be applied to strength envelopes developed from 300mm direct shear boxes if supported by reliable slope performance history.

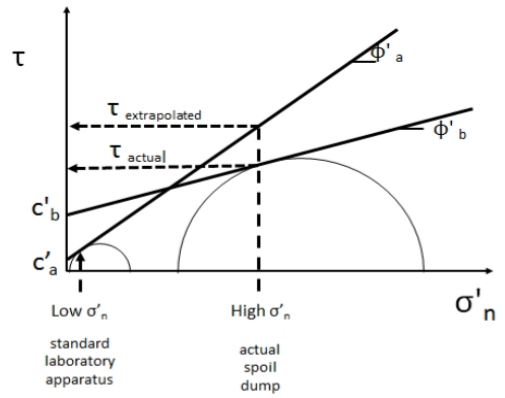

Figure 10. Conceptual model demonstrating an overestimation of shear strength when extrapolating laboratory data

3.8. Selection of normal stress for testing

Another common error is testing at non-representative stress levels, even when the apparatus is of sufficient capacity in terms of normal stress. This can occur if geotechnical practitioners are unsure about how to determine suitable normal stress values for testing to simulate field conditions.

A simple and conservative guide for developing appropriate normal stress values for testing is set out below and illustrated in Figures 11 and 12. *Note that this guide has been developed for dragline-scale (>30 m) spoil piles, where foundations are typically shallow-dipping, and slope batters range between 35^o and 45^o. For non-conforming spoil piles, either in terms of geometry, height, or with steeply-dipping foundations, an alternative method based on analysis of stress distribution should be considered. This approach was developed by the primary author to verify the expected stress conditions for very high spoil dumps in order to design the aforementioned large-scale high-stress shear box. It is based on field observations of typical spoil pile geometries and instability mechanisms, back-analysis of spoil pile failures, and stability analyses for design purposes.*

<u>*Step 1:*</u> Once the slope geometry and geotechnical model are developed, the major principal stress, σ_1 is estimated to a first approximation, by multiplying slope height, *X*, by spoil unit weight, γ. The BMA Coal strength framework can be used to estimate γ if it is not otherwise known. *Note that while the spoil in the basal saturated few metres will have a higher γ than that above the phreatic surface; it can be ignored for this approximation.*

<u>*Step 2:*</u> The maximum normal stress at failure, σ_f can be estimated by multiplying 0.5 by σ_1 (Figure 11). *Note that for deep-seated multi-wedge spoil pile failure mechanisms, the highest normal stress within the failure mass occurs on the base of the passive wedge. By geometry this is approximately half the slope height of spoil cover, if a relatively flat foundation is assumed.*

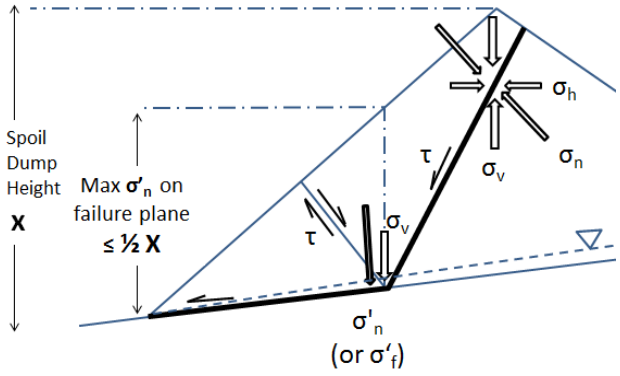

Figure 11: Multi-wedge instability mechanism and approximation of maximum normal stress

<u>*Step 3:*</u> σ_f is then used as one of the three (or more) tests required to develop the Mohr-Coulomb (MC) envelope. Calculation of appropriate normal stresses for the remaining tests will require good engineering judgement. There are a number of ways to approach this, and two suggestions are provided:

(a) The first is to use σ_f as the maximum normal stress, and test at lower stresses to simulate the stress distribution along the base of the passive wedge (Figure 12a). *Note however that envelope curvature is likely to be most pronounced at lower normal stresses.*

(b) The second is to use σ_f as the mid-point and perform tests at, for example ±20% of this to account for variances between field and laboratory conditions (Figure 12b).

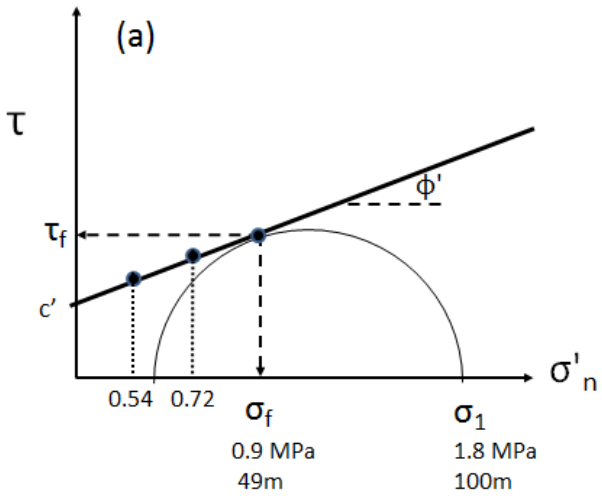

Figure 12a. M-C envelope for a 100 m high spoil pile instability; demonstrating approach (a) for selection of normal stress

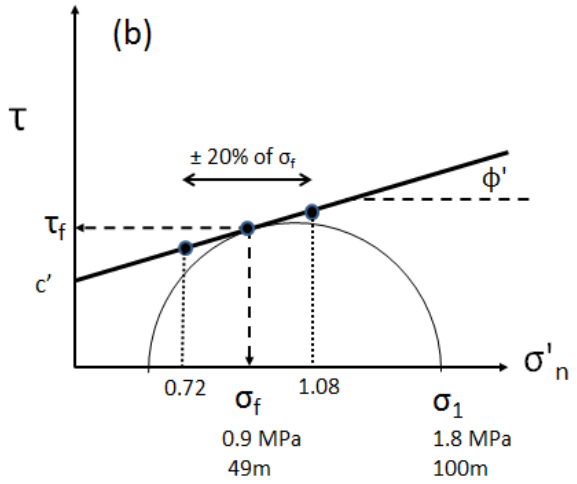

Figure 12b. M-C envelope for a 100 m high spoil dump instability; demonstrating approach (b) for selection of normal stress

4. Conclusions

Considerations for direct shear testing of coal mine spoil to derive geotechnical parameters for stability analysis and design have been presented. These considerations have been developed for coal-measures spoil piles constructed by dragline or end-dumping from haul trucks, consisting of relatively competent material such that typical slope heights exceed 30 m.

The importance of defining the geotechnical model prior to testing has been discussed, so that field conditions can be replicated as best as possible. Aspects of sample preparation and testing that, if disregarded or performed incorrectly, may adversely affect the measured shear strength include: precompression and consolidation; scale, in terms of apparatus capacity, maximum particle size, and available normal stress; strength mobilisation mode; and saturation condition.

The potential for overestimation of the shear strength of coal mine spoil by extrapolating laboratory test data to higher normal stress ranges has been discussed. Ideally, direct shear boxes used for testing mine spoil should be capable of handling large specimens and delivering high stresses. However, the authors know of only one in Australia that has been custom-built for research purposes, which is located at the University of Newcastle. Short of custom-building or modifying standard shear boxes to perform high stress tests, careful consideration of the geotechnical model and stress regimes may allow for shear strength reduction factors to be applied to laboratory-generated shear strength envelopes, if supported by slope performance history.

A simple guide for approximating suitable normal stress values for DSTs relevant to dragline or haul truck spoil piles has also been provided.

5. Acknowledgements

This paper presents aspects of postgraduate research funded by Australian Coal Association Research Program (ACARP Project C20019), which is gratefully acknowledged. Also acknowledged is the in-kind sponsorship of the research provided by Thiess Australian Mining, Mount Arthur Coal Mine (BHP Billiton), and Rolleston Coal Mine (Glencore Xstrata).

6. References

ASTM D3080-98, (1998). Standard Test Method for Direct Shear Test of Soils Under Consolidated Drained Conditions. *ASTM International, West Conshochocken, PA.*

Bishop A.W., Green G.E., Garga V.K., Andresen A., Brown J.D. (1971). A new ring shear apparatus and its application to the measurement of residual strength, *Geotechnique, 21 (4), 273-328.*

Bradfield L., Simmons J., Fityus S. (2013). Issues related to stability design of very high spoil dumps, *Proceedings, 13th Coal Operators' Conference, Woollongong, pp 376-386.*

Chowdhury R., Flentje P., Bhattacharya G., (2010). Geotechnical Slope Analysis. *CRC Press Taylor & Francis Group, London, pp 60-68.*

Fell R., Jeffery R.P. (1987). Determination of drained shear strength for slope stability analysis. *Soil Slope Instability and Stabilisation, Walker, B.F and Fell, R. (eds), Balkema, pp 53-70.*

Gonano L.P. (1980). An Integrated Report on Slope Failure Mechanisms at Goonyella. Technical *Report Number 114, Division of Applied Mechanics, Institute of Earth Resources, Commonwealth Scientific and Industrial Research Organisation, Victoria.*

Mallet C.W., Dunbavan M., Seedsman R.W., Ross D.J. (1983). Stability of Spoil Piles and Highwalls in Deep Surface Mines. *End of Grant Report Number 150, National Energy Research Development and Demonstration Program, Australian Government, Canberra.*

Nakao T., Fityus S. (2008) Direct Shear Testing of a marginal material using a Large Shear Box. *ASTM Geotechnical Testing Journal. Vol 31 No5. pp 393-403.*

Simmons J., McManus D. (2004). Shear strength framework for design of dumped spoil slopes for open pit coal mines. *Proceedings, Advances in Geotechnical Engineering The Skempton Conference*, *pp. 981-991.*

Terzaghi K. (1936). The shear resistance of saturated soils. *Proceedings, 1st International Conference Soil Mechanics Foundation Engineering, vol. 1, pp. 54-56.*

Terzaghi K., Peck R.B., Mesri G.M. (1996). *Soil Mechanics in Engineering Practice, 3rd Edition.* J. Wiley: New York, 549 pages.

Proceedings of the 10th ANZ Young Geotechnical Professional's Conference – 10YGPC
Noosa, Queensland, Australia
10 – 12 September 2014

HAMBLY'S PARADOX AND THE PRACTISING GEOTECHNICAL ENGINEER

David BUXTON
Geotechnical Engineer, Tonkin & Taylor Ltd, Auckland, New Zealand

ABSTRACT – This paper presents four case studies of simple lateral soil loading problems to assess how intuitive the results might be to a young geotechnical professional starting their career. In particular the paper examines if the level of robustness implied by a load factor, partial factor or factor of safety may be misunderstood. It is demonstrated that for the results to be intuitively understood the designer needs to understand the methods and assumptions behind the analysis and the limitations this brings to the results.

The examples are inspired by Hambly's Paradox which comprises a simple example comparing three- and four-legged chairs and eloquently demonstrates the concepts of ductility, robustness and redundancy. The examples demonstrate of how studies of simplified examples can be used to build understanding of an analysis, assess sensitivity of the results and develop the intuition of a young geotechnical professional.

1. Introduction

Lateral soil loads are a fundamental element of geotechnical engineering with the basis for their assessment having been understood for over two centuries. Assessment of active and passive earth pressures using both the Coulomb theory (Coulomb, 1776) and the Rankine theory (Rankine, 1857) remain a basic and key part of the current education and practice of the young geotechnical engineer.

Given the long established earth pressure theory one might expect a graduate geotechnical engineer to be intuitively able to apply active earth pressures. However, John Burland in the "Structural and geotechnical modelling" chapter of the ICE Manual of Geotechnical Engineering (Burland et. al., 2012) presents a simple structural example, Hambly's Paradox (Hambly, 1985). Whilst Hambly's Paradox (or the three- and four-legged stools) is a very simple example, the results are only intuitive if the subtlety of the problem is understood and applied correctly.

Burland's presentation of Hambly's Paradox (summarised below) prompted the author to investigate four case studies of lateral soil loading problems to assess how intuitive the results might be to a young geotechnical professional starting their career. In particular the paper examines if the level of robustness implied by a load factor, partial factor or factor of safety may be misunderstood.

1.1. Hambly's Paradox

Hambly's Paradox (Hambly, 1985) considers how much load is carried by each leg of three-legged and four-legged stools depicted under a central 60kg load, as shown in Figure 1. The three-legged stool is straightforward with 20kg load in each leg. With the four-legged stool 15kg is wrong, one leg does not quite touch the ground and to maintain equilibrium the total load will be carried by two legs with 30kg each.

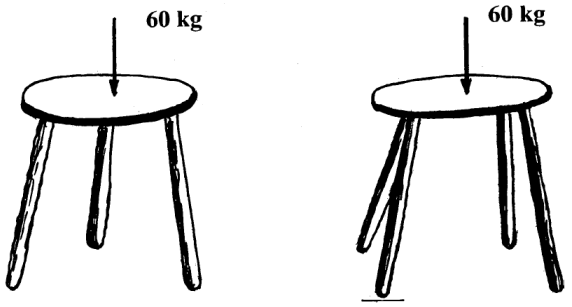

Figure 1. Three- and four-legged stools – Hambly's paradox

The paradox – that the addition of a leg can increase rather than decrease the load carried, can be used to illustrate a number of concepts. In particular the paradox emphasises the importance of ductility, robustness and redundancy. The reader should refer to the "Structural and geotechnical modelling" chapter of the ICE Manual of Geotechnical Engineering for a discussion of these concepts. The aspect of the paradox that prompted this paper was that the answer is not intuitive unless the subtlety of the problem is understood and applied correctly.

1.2. Limitations

In this paper the author does not seek to fully evaluate the field of lateral soil loading but to examine a series of specific situations.

It is noted that the results resented are specific to the geometry and parameters adopted in the case study. The author has not attempted to generalise the results in a way that they can be applied to a wider range of situations. The examples do not include wall friction.

2. Case Study A – Determining Active Earth Pressures using Limit Equilibrium Analysis

Case Study A considers if assessing and applying active earth pressures using limit equilibrium analysis is intuitive. Using limit equilibrium analysis programmes to evaluate earth pressures can be convenient to incorporate the effect of irregular back slopes, surcharges and soil layering or purely as an easy check of another analysis type. The example is extended to consider if a Factor of Safety (FoS) in the limit equilibrium analysis is equivalent to a load factor applied to the active force.

The example comprises a series of analyses in which a vertical face of a single dry soil unit has a horizontal point load equal to the theoretical active earth pressure, with or without a load factor, applied at one-third of the face height. The analyses use the Morgenstern-Price limit equilibrium method in Slope/W with a series of trial surfaces determined by the entry and exit option. The location of the critical slip surface was automatically optimised.

The following range of parameters was considered:

Face Height = 5m*
ϕ' = 30° or 35°
ɣ = 18 kN/m^3
c' = 0 kPa
Load Factor = 1.0 & 1.5 (for ϕ' = 30°)
= 1.0, 1.3, 1.5, 2.0 and 3.0 (for ϕ' = 35°)

[*The principal evaluated here does not appear to be sensitive to face height]

The analysis is illustrated in Figure 2.

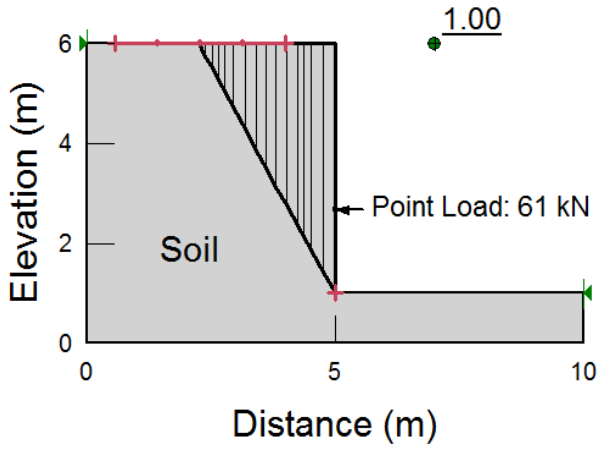

Figure 2. Example of a Case Study A Analysis

2.1. Case Study A - Results

The results of Case Study A are summarised in Table 1.

Table 1. Case Study A Results

ϕ'	Load Factor	Factor of Safety
30°	1.0	1.01
	1.5	1.65
35°	1.0	1.00
	1.3	1.30
	1.5	1.51
	2.0	2.26
	3.0	6.78

2.2. Case Study A - Discussion

Case Study A confirms that active earth pressures (as a force) can be determined using limit equilibrium methods by assessing the force that results in a FoS of 1.0. At a FoS of 1.0 the analysis is in a true equilibrium state equivalent to the active limit state. In this case the answer should be intuitive however several situations can be envisaged where a designer could misunderstand the analysis:

1. The designer may default to a target FoS greater than 1.0 that is typical for demonstrating adequate stability, resulting in an excessively conservative earth pressure.
2. The analysis is determining the active pressure, the designer still needs to separately consider if there will be sufficient displacement to mobilise the active case.

The second part of the example considers if a load factor and FoS are equivalent for this situation and the results are contradictory and therefore not intuitive to someone without understanding of the analysis method. For example in the 35° friction angle case the load factor and FoS are equivalent up to a value of 1.5. At a load factor of 2.0 and 3.0 respectively the FoS increases to 2.26 and 6.78 respectively. For the 30° friction angle case only a load factor of 1.5 is considered however this results in FoS of 1.65.

These results can be understood with a simple conceptual understanding of how the applied force is being incorporated into the limit equilibrium equations, as shown in Equation 1 below (note the point load force will be negative due to its direction):

$$FoS = \frac{F_{Resisting}}{F_{Driving} + F_{Point\ Load}} \qquad (1)$$

As the point load approaches the value of the driving force the bottom line of Equation 1 approaches zero and the resulting FoS will tend to infinity. The bottom line will be zero when the point load is equal to the at-rest condition. For a 30° friction angle the at-rest earth pressure is 1.5 times the active earth pressure, hence the FoS of the result with a load factor of 1.5 is infinity for the theoretical active wedge. The analysis still returns a

result by finding a slip surface encompassing a larger mass with accordingly larger driving and resisting forces in which the modelled force does not result in a zero or negative bottom line in Equation 1. This results in a FoS greater than the load factor.

The ratio of the active to at-rest earth pressure coefficients ranges from 1.34 to 1.64 for soil friction angles of 20° to 40° respectively with no backslope.

3. Case Study B – Retaining Walls with an Inclined Face

Case Study B considers a retaining wall with the face inclined at an angle less than vertical, as shown in Figure 3. It is intuitive that the active force will be less than the case of a vertical wall. It is less intuitive if the level of robustness imparted by a load factor and a partial factor, applied separately to the same results, is equivalent despite the factor being numerically equivalent.

Case Study B comprises limit equilibrium analyses of a 5m high retaining wall with a variety of face inclinations. The following analyses have been undertaken for each face inclination:

Analysis 1. The active force has been determined (ie. the force that results in a FoS = 1.0). From this an active earth pressure coefficient was calculated.

Analysis 2. The FoS of the slope has been assessed with a load factor of 1.5 applied to the active force.

Analysis 3. A factored active force has been determined by both applying a partial factor of 1.5 to the tangent of the soil friction angle in the analysis and applying a load factor of 1.5 directly to the active force results.

The analyses were undertaken using a single dry soil unit and a single horizontal point load applied at one third of the face height. The analyses use the Morgenstern-Price method with a series of trial surfaces determined by the entry and exit option. The location of the critical slip surface was optimised. An example of the analyses is shown in Figure 3.

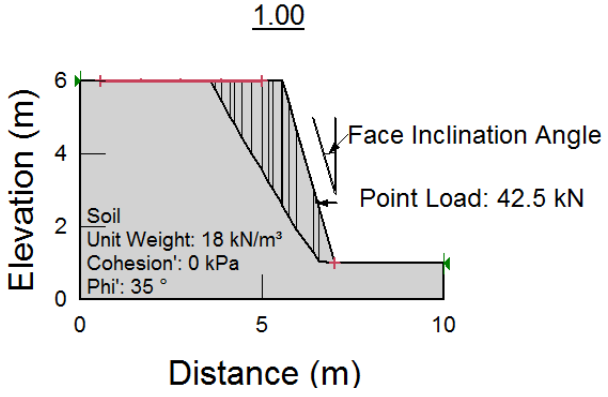

Figure 3. Example of Case Study B Analysis

3.1. Case Study B - Results

The results of Case Study B are summarised in Figures 4 to 6.

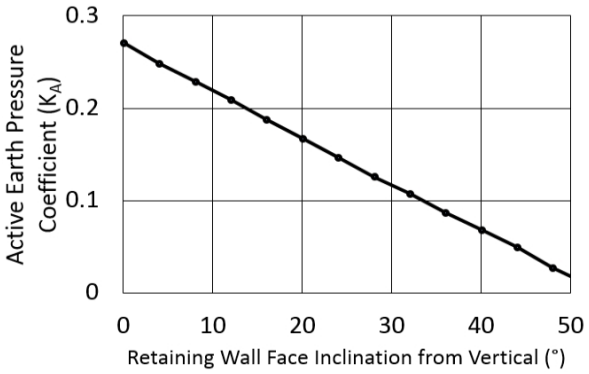

Figure 4. Plot of K_A vs face inclination (Analysis 1 results)

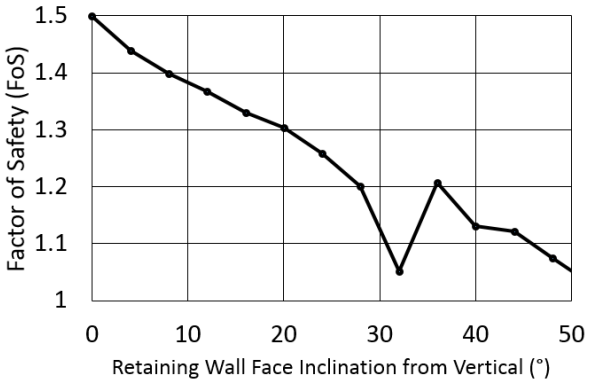

Figure 5. Plot of FoS vs face inclination for a load factor of 1.5 (Analysis 2 results)

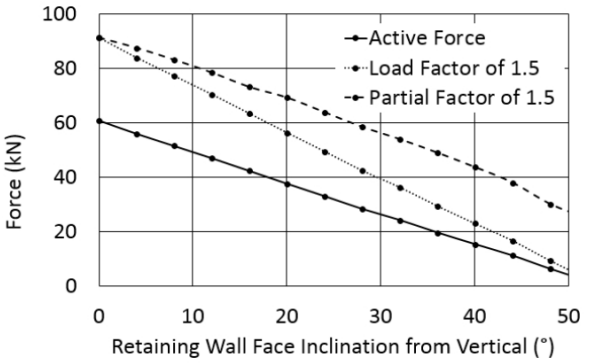

Figure 6. Plot of force vs face inclination for factored and unfactored cases

3.2. Case Study B - Discussion

The results of Analysis 1 show K_A reducing with increasing face inclination, as is intuitive. The trend is linear and although not shown, K_A is nil when the slope angle (90° - face inclination) equals the friction angle.

The results of Analysis 2 (refer Figure 5 above) shows a decreasing FoS with increasing retaining wall face inclination angle, despite a constant load

factor of 1.5 being applied. In this example the level of robustness provided by the load factor varies and may be less than the designer had intuitively expected. To understand this re-consider a modified form Equation 1 from Case Study A that includes the load factor (LF), as given in Equation 2 below, and remembering the point load is negative:

$$FoS = \frac{F_{\text{Re sisting}}}{F_{Driving} + LF \times F_{Po\,\text{int}\,Load}} \qquad (2)$$

As the retaining wall face inclination increases the portion of the total resistance provided by the soil strength (top line of Equation 2) increases and that provided by the active force (on the bottom line but negative) decreases. As only the active force is factored and this is providing a reducing portion of the resisting forces the FoS decreases with face inclination.

Typically most retaining walls have a face inclination of less than about 14° (1H:4V), corresponding to a FoS of 1.35 for a load factor of 1.5 (for a soil friction angle of 35°). In practice a FoS of 1.35 is still likely to be sufficient for most retaining walls.

Analysis 3 considers the comparative level of robustness provided by a load factor applied directly to the active force and a partial factor applied to the soil strength respectively. The results show that the partial factor approach is not sensitive to the relative portion of the resisting force provided by soil strength and the applied force and may therefore be the preferred approach for this situation.

4. Case Study C – The Effect of Drained Cohesion

Case Study C shows the effect that drained cohesion has on retaining wall design actions. The effect of drained cohesion on earth pressures can be very significant, however ignoring it altogether can be excessively conservative. This can result in a situation where the robustness of the design is dependent on the judgement and approach (i.e. intuition) of the designer rather than load/partial factors applied (after all, two times not much is still not much).

An example could be designing a retaining wall on a site where existing un-retained vertical cut faces of greater height exist. In this situation it may be possible to justify parameters that resulted in no soil pressures on the wall, but the resulting design may lack robustness unless it is only intended as a facing element.

Case Study C comprises three figures based on theoretical earth pressure distributions. Of particular note is Equation 3 below, which gives the depth to which the theoretical active earth pressures are negative or alternatively the height to which a vertical cut slope will be self-supporting.

$$z_0 = \frac{2c'}{\gamma\sqrt{K_a}} \qquad (3)$$

Where z_0 is the depth of negative active pressures (m), c' is the drained cohesion (kPa), γ is the soil unit weight (kN/m^3) and K_a is the active earth pressure coefficient.

In this case study active earth pressures have been calculated for a dry soil with no wall friction and a soil unit weight (γ) of 18 kN/m^3. Where theoretical active earth pressures are negative they have been taken as zero.

4.1. Case Study C - Results

Figure 7 plots the "self-supporting height" for a range of soil friction angles and drained cohesion. The self-supporting height is the depth to which a cut slope could stand unsupported and over which the earth pressures are theoretically negative but normally taken as zero in design analysis.

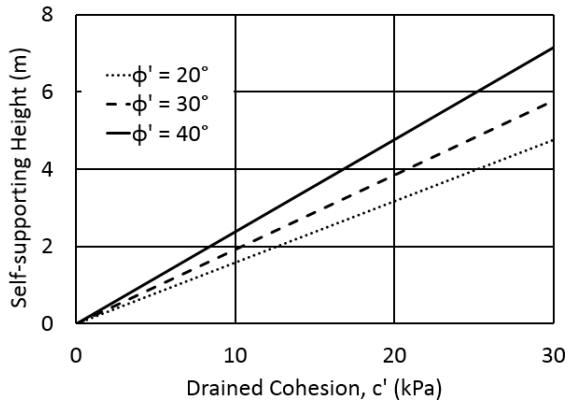

Figure 7. Plot of self-supporting height vs drained cohesion

Figure 8 plots the active earth pressure force vs drained cohesion. The results are normalised by the force with c' = 0kPa.

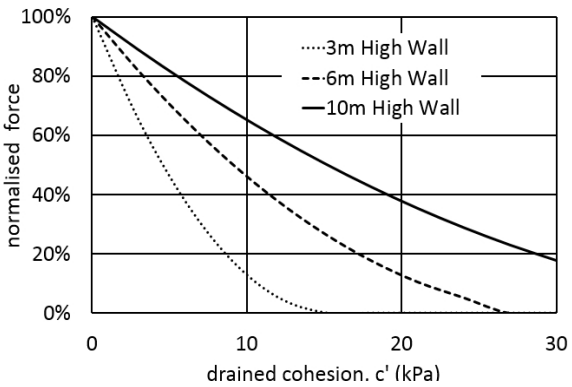

Figure 8. Normalised active force vs drained cohesion (ϕ'=30°)

Figure 9 plots the moment that results from the active earth pressure force at the passive ground

level. The results are normalised by the moment with c' = 0kPa. Note that the maximum moment for a cantilevered retaining wall will actually be larger than the moment at the passive ground level, occurring below the passive ground level. The moment at the passive ground level is however convenient to calculate.

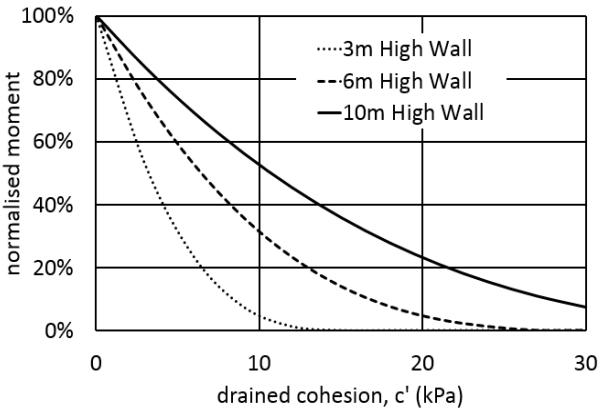

Figure 9. Normalised moment of active force at passive ground level vs drained cohesion (ϕ'=30°)

4.2. Case Study C - Discussion

Figures 7 to 9 show that drained cohesion can significantly reduce retaining wall design actions. Even a seemingly modest 5kPa can result in zero active earth pressure over the upper approximately 1m of a retaining wall, reducing the design active force by approximately 50% for a 3m high retaining wall. For the same 3m high retaining wall the normalised moment of the active force at the passive ground level is only 32%. As the magnitude of this effect can be larger than the typical magnitude of load/partial factors they alone cannot be relied upon to impart robustness into a design with drained cohesion. It is therefore key that the designer understands and treats the situation logically, through intuition from past experience or through an assessment of the model sensitivity.

A commonly adopted recommendation to ensure the design has sufficient robustness is originally found in CP2 (1951) which recommends the use of a minimum equivalent fluid pressure, with the 'equivalent fluid' having a density of 5 kN/m^3.

5. Case Study D – Determining a Lateral Load to Stabilise a Landslip

Case Study D examines a limit equilibrium analysis undertaken to assess the lateral load required to stabilise a landslip. In this example a landslip is located in a paddock adjacent to a rural dwelling. The notional design brief is to stabilise only the upper portion of the landslip, removing risk to the dwelling and reinstating the land at the crest of the slope. The limited design brief is intuitively expected to reduce the size of the retaining structure required.

The case study comprises a series of limit equilibrium analyses as follows:

Analysis 1. A back analysis of the slope is undertaken to determine material strength parameters and to achieve a FoS = 1.0 with design groundwater levels.

Analysis 2. A pile reinforcement is modelled to assess the required force to achieve a FoS > 1.3. The pile location on the slope is varied and is located near the slope crest, mid-slope and near the toe of the slope in analysis 2a, 2b and 2c respectively.

Analysis 3. Analysis 2 is repeated, however the material located downslope of the pile and above the landslip surface is removed from the model.

The analyses use the Morgenstern-Price method with fully specified slip surfaces that are optimised. The groundwater is modelled by a piezometric line and is constant in all analyses. A shear zone is modelled at 4m depth. Sample outputs of analyses are shown in Figures 10 and 11.

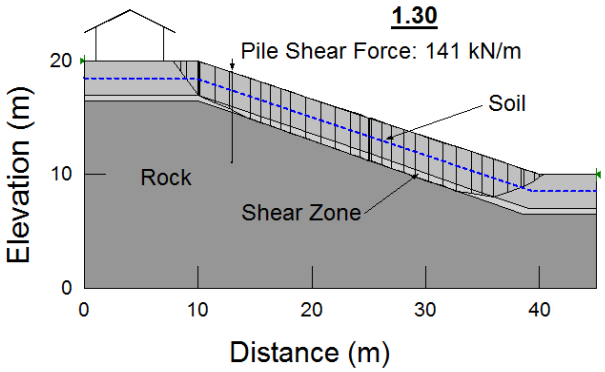

Figure 10. Analysis 2a output.

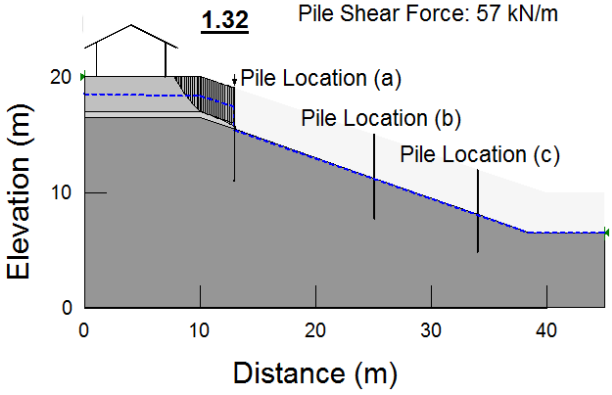

Figure 11. Analysis 3a output, with all pile locations shown.

5.2. Case Study D - Results

The results of Case Study D are summarised in Table 2 below:

Table 2. Case Study D Results

Analysis	Target FoS	Pile Location	Pile Force
1	1.0	n/a	n/a
2a	> 1.3	upper	141 kN/m
2b	> 1.3	middle	133 kN/m
2c	> 1.3	lower	130 kN/m
3a	> 1.3	upper	57 kN/m
3b	> 1.3	middle	217 kN/m
3c	> 1.3	lower	337 kN/m

5.3. Case Study D - Discussion

The back analysis (Analysis 1) confirms that the model and parameters are appropriate. In Analysis 2, one might intuitively assume that the location of the pile reinforcement in the model would have a significant effect on the required pile force. After all it is intuitive that a pile at the top of the slope, retaining only a small portion of the slope, should only require a comparatively small pile force. The results however show a relatively consistent force at each location.

Limit equilibrium analysis only gives a single output for each trial surface, the FoS. The FoS is an average value of all parts of the slope including all slices in the model both above and below the pile. The location of the pile is only changing the required force by a small amount due to the changing effect of the moment arm of the applied force and changes in the inter-slice forces within the model (some of which are negative). To achieve the aim of the design brief, which was to reduce the pile force by stabilising only the upper portion of the slope, a different analysis approach is needed.

In Analysis 3 the soil downslope of the pile is not modelled. In doing this the FoS determined relates only to the soil mass above the pile. In modelling the case study in this way the force required from a pile at the top of the slope (location (a)) reduces by a factor of 2.5 from 141kN/m to 57kN/m and the design brief is met. An alternative approach would be to view the inter-slice forces in Analysis 2a, from which the same reduced load can be determined.

Can this be adopted as a blanket approach? No, consider the mid and lower slope pile locations. The results show that not modelling the soil in these lower pile locations has the opposite effect – the required force increases significantly. This is intuitive as not modelling the downslope soil removes the net stabilising force of the lower portion of the slope that includes the toe.

6. Conclusions

Four simple case studies relating to lateral soil loads have been presented. Each case study has an element like the four-legged chair presented in Hambly's Paradox in that the robustness implied by the results may not be intuitive unless the methods and assumptions behind the analysis with the result are understood.

In the examples it is seen that:

1. A FoS and load factor may or may not imply the same level of robustness.
2. A load factor applied to an active earth pressure and a factored active pressure obtained by a partial factor on soil strength may result in differing levels of robustness.
3. The effect of drained cohesion is sufficiently large that load/partial factors cannot always be relied on alone to provide robustness into a design.
4. Not adequately understanding an analysis can result in a significantly over conservative design (by 2.5 times in the example shown).

For practising young geotechnical engineers starting their career the case studies demonstrate the need to ensure models and assumptions are understood to provide an appropriate, but not excessive, level of robustness in design. The examples also demonstrate how studies of simple models can be used to build understanding of an analysis and develop the intuition of a young geotechnical professional.

7. References

Burland, J. B. et al. (2012*). ICE Manual of Geotechnical Engineering*. Institution of Civil Engineers.

Civil Engineering Code of Practice No. 2 (1951). *Earth retaining structures*. Institution of Structural Engineers.

Coulomb, C.A. (1776). Essai sur une application des maximis et minimis a quelque problemes de statique relative a l architecture. *Memoirs Divers Savants*, Academie Science, vol. 7. Paris.

Hambly, E. C. (1985). Oil rigs dance to Newton's tune. *Proceedings of the Royal Institution*, 57, 79-104.

Rankine, W. (1857). On the stability of loose earth. *Philosophical Transactions of the Royal Society of London*, Vol. 147.

Proceedings of the 10th ANZ Young Geotechnical Professional's Conference – 10YGPC
Noosa, Queensland, Australia
10 – 12 September 2014

CALIBRATION OF THE STANDARD PENETRATION TEST FOR LIQUEFACTION ASSESSMENTS

Holly LE HEUX
Tonkin & Taylor Ltd, Wellington, New Zealand

ABSTRACT – The standard penetration test (SPT) is frequently used in ground investigations as a basis of assessing the relative density and liquefaction potential of granular soils. SPTs are popular due to the fact that they have been used for a long time and a number of accepted empirical correlations for application in design are available. These correlations are based on older SPT hammers which typically had efficiencies around 60%. More modern SPT hammers have much higher efficiencies. These efficiencies need to be measured and allowed for prior to using empirical design correlations. SPT tests are also known to have poor repeatability with variations in energy transfer from different rigs, hammers, operators and other factors. This paper discusses current SPT calibration practices in New Zealand and improvements that could be made. The relevance to a specific site investigation in Wellington is also discussed.

1. Introduction

1.1. Background

The 2010 Canterbury Earthquake and the subsequent aftershocks were a brutal reminder of the importance of creating earthquake resilience in New Zealand. The safety of people is paramount and requires a built environment that is specifically designed to protect lives from this high earthquake hazard. Liquefaction, lateral spreading and ground subsidence during the Canterbury earthquakes caused extensive damage to land and property. Because of this, earthquake effects have been brought to the forefront of people's minds when building, buying or developing property.

A significant sum of money is being invested in developing an appropriate level of resilience. The cost to land and building owners is greatly affected by the outcomes of site liquefaction assessments. Quality ground investigations are crucial to developing options that both provide an acceptable level of earthquake resilience while not being overly conservative resulting in unnecessary costly works.

1.2. Soil penetrometer testing methods

Soil penetrometer testing is commonly used in New Zealand as the basis for assessing the relative density and liquefaction potential of soils. Insitu tests include cone penetration test (CPT) and standard penetration test (SPT) which are commonly available in New Zealand.

CPT has been the preferred method of penetrometer testing for the Christchurch recovery. CPT data is recognized as generally more consistent and repeatable than SPT data. Their relative speed and continuous log make them a more preferable option. However, at some sites the CPT is unable to penetrate through dense sands and gravels.

The SPT is able to penetrate through dense soils and is commonly used in places such as Wellington where this is required. SPT is also popular due to the fact that it has been used for a long time, it is well known and understood and it is inexpensive. Accepted empirical correlations for application in design are available. It also provides samples to visually classify the soil type and/or undertake laboratory testing. A limitation of SPT is that it has relatively poor repeatability with variations in energy transfer from different drill rigs, hammers, operators and other factors.

1.3. SPT correction factors

The output of the SPT test is the value SPT N. This is the measurement of how many SPT hammer blows it takes to push an SPT sampler 300mm through the soil. The effort required for penetration of the soil is used to evaluate the soil's density.

To use SPT data for liquefaction assessments, correction factors are applied to the measured value of SPT N to standardize it. Various correction factors are applied for standardization including energy ratio, borehole diameter, SPT rod length, sampler type and overburden pressure. The energy correction factor takes the efficiency of energy delivered by the SPT hammer and standardizes it to a hammer with a 60% efficiency (SPT N_{60}). This efficiency is used as it was typical of the first SPT hammers. Different types of hammers are currently used. Idriss and Boulanger (2008) reported that the actual delivered energy of current hammers can vary by 30-90%. When the energy efficiency of a trip hammer is not known, it is common practice to assume 60%.

The SPT N_{60} is also normalized to 1 atmosphere effective overburden pressure to become SPT $N_1(60)$. This allows for SPT values measured at different effective stresses to be compared.

In this paper the recommendation of various international standards for SPT practices for the energy correction factor are looked at and compared to current practices in New Zealand. The variation of energy transfer ratios in a sample of

calibrations of New Zealand hammers is assessed and the effects of this on a Wellington liquefaction assessment are discussed.

2. Review of requirements for the energy correction factor in SPT standards

Different countries refer to different standards for undertaking the SPT test. Recommendations from the standards used in United States and the international standard provided by the International Organization for Standardization (ISO) are looked at as these standards have been updated in the last few years and are a good representation of quality SPT practice.

2.1. American standards

The following three relevant American standards are available:

- ASTM D6066-11 (2011) which covers the use of penetration testing for evaluating liquefaction potential.
- ASTM D4633-10 (2010) which provides standard test methods for energy measurement for penetration testing.
- ASTM D1586-11 (2011) which provides a standard test method for SPT.

2.1.1. ASTM D6066-11

Recommendations from this standard include:

- For safety hammers, the energy transfer correction ratio can be assumed on smaller investigations.
- Automatic, trip and donut hammers need to have measured energy transfer for the make and model used to perform measurements. Test method D4633 to be used to measure energy transfer.
- Field monitoring to be undertaken of hammer impact velocity and periodic drill rod energy measurements for critical jobs, such as large ground improvements and liquefaction studies associated with expensive structures.
- For routine foundation investigations, visual confirmation of drop heights developed from known operational characteristics is sufficient.
- Automatic hammers are the preferable type of hammer.

2.1.2. ASTM D4633-10

Recommendations from this standard include:

- Yearly calibration of SPT hammers. It is also desirable to calibrate prior to starting major critical projects.
- The force velocity method is the only fundamentally correct method of measuring energy content.

2.1.3. ASTM D1586-11

This standard reports that:

- Variations in SPT N-values of 100% or more have been observed when using different standard penetration test apparatus and drillers for adjacent boreholes in the same soil formation.
- Field experience indicates that when using the same apparatus and driller, SPT N-values in the same soil can be reproduced with a coefficient of variation of about 10%.

2.2. International standards

ISO 22476-3 (2011) is the international standard for field testing with SPT. This standard recommends:

- The calibration of energy transfer should be made annually and after any changes, repairs and modifications to the driving equipment.
- The energy ratio of the equipment has to be known if the SPT N-values are going to be used for the quantitative evaluation of foundations or for the comparisons of results.
- Force-velocity method is the recommended method used to measure energy.

3. New Zealand practice for the SPT energy correction factor

3.1. NZS 4402 (1988)

NZS 4402 (1988) is the New Zealand Standard that covers the use of SPT to determine the penetration resistance of a soil. No conversion from SPT N value to SPT N_{60} is given in this standard. Energy measurements are not mentioned in this standard but it is stated that the results obtained from hammers with self-tripping mechanisms are not comparable with the results from other driving methods such as the rope and cat-head. Details of correction factors to the SPT N value are required to be stated.

3.2. NZGS guidelines

The New Zealand Geotechnical Society (NZGS) has prepared draft guidelines for assessing liquefaction hazards (NZGS, 2010). This guideline states that the SPT limitations include the potential to overlook susceptible soil strata, relatively poor repeatability and operator dependence. It advises that results should be carefully interpreted and corrected according to the recommendations of Youd et. al. (2001).

Youd, et. al. (2001) recommend that measurement of the hammer energy is undertaken frequently at each site where the SPT is used. Where measurements cannot be made, careful observation and notation of the equipment and procedures are required to estimate an energy

correction factor for use in liquefaction calculations. ASTM 1586-99 standard (now superseded) is recommended for SPT testing procedures.
Youd, et. al. (2001) note that even when procedures are carefully monitored to conform to established standards that some variation in energy transfer occur because of minor variations in testing procedures. Measured energies at a single site indicate that variations in energy ratio between blows or between tests in a single borehole typically vary by as much as 10%.

3.3. MBIE Christchurch rebuild guidelines

Guidelines prepared by New Zealand's Ministry of Business, Innovation & Employment (MBIE) for the Christchurch rebuild, require properly energy rated equipment to be used for ground investigations on TC3 land (land categorized as requiring site specific engineering design).

3.4. Earthquake Commission (EQC) geotechnical investigation project

An extensive post-earthquake geotechnical investigation was undertaken in Christchurch. According to Fairclough and Ashfield (2013) the investigation area covered approximately 28,000 residential properties. SPT tests were undertaken where ground conditions caused shallow refusal of CPT. SPT hammer efficiency was identified to be an important input for using SPT test results in liquefaction assessments. Several SPT hammers were tested in accordance with the recommendations of ASTM D4633-10.

Fairclough and Ashfield (2013) concluded that SPT hammer efficiency should be measured on each rig deployed to ensure reliable and robust analysis is completed.

3.5. Current frequency of SPT hammer energy calibration in New Zealand

Information on SPT hammer efficiency measurements from a sample of drilling companies operating in New Zealand was collected for this paper. The frequency of calibration was inferred from:

- Information verbally supplied by the companies.
- A comparison between the date of calibration certificates provided for SPT hammers and the date they were requested by an engineer for a sample of projects.

A wide range of calibration frequencies was found, with no typical frequency. Out of the drilling companies that measure the energy efficiency of their hammers, the most frequent calibration was every 3 months and the least frequent was 7 years. Not all drilling companies in New Zealand had calibrated their SPT hammers.

4. Variation between energy measurements of New Zealand SPT hammers

SPT hammer calibration measurements of a sample of New Zealand rigs was collected. The sample consisted of 7 automatic hammer calibrations and 16 trip hammers. 13 results were carried out following ASTM D4633-10 standard. 10 results were undertaken under 'refusal conditions' and therefore do not follow ASTM D4633-10 standard. However, they still use the force-velocity method. For the purposes of this paper the different calibration methods has not been considered. Therefore this sample provides only an indication of the energy variation. Results are shown in Table 1.

A significant range of energy transfer ratios is found (48% to 91%). Automatic hammers in this sample were found to have a smaller range than trip hammers.

Fairclough and Ashfield, (2013) reported that during the EQC geotechnical investigation project, SPT hammer calibrations were undertaken in accordance with ASTM D4633-10. For a sample of 8 automatic hammers an average of 85.4% was found with a range of 52.5% to 101.3%. For a sample of 6 trip hammers an average of 65.9% was found with a range of 56.1% to 85.6%.

Some of these SPT calibration test values from the samples in the Fairclough and Ashfield (2013) paper are included in the sample investigated in this paper. The values not included were not available for this paper.

5. Case study – The importance of SPT hammer energy on a specific liquefaction assessment in Wellington

5.1. Background

This case study is of a typical low-lying site in the Wellington area. The importance of the variation in energy transfers of SPT hammers to this case study is considered.
The Wellington region is situated within highly folded and faulted sandstone, siltstone and mudstone.

Table 1. SPT hammer energy measurements for a sample of New Zealand hammers

Hammer Type	Average energy transfer ratio	Coefficient of variation for energy transfer of hammers	Minimum energy transfer ratio	Maximum energy transfer ratio
All hammer types	72%	16.6%	48%	91%
Automatic hammers	85%	6.4%	74%	91%
Trip hammers	67%	14.2%	48%	86%

In the subject area, thick deposits of marginal marine sediments comprising mainly sands with lesser silts and gravels overlie the greywacke bedrock.

The site is located in a low lying area with uplifted greywacke hills on either side. Groundwater is encountered approximately 3m below ground surface. A number of active and inactive faults are close to the site.

During ground investigations for this site SPT tests were carried out. A CPT test was also attempted but was unable to be completed due to the dense ground conditions near the surface. The first 17m of marginal marine deposit was found to to contain layers of fine to coarse sand with gravel. This sand had varying density, with SPT N values ranging from 12 to 50+. Refer Table 2 for soil profile at this site.

5.2. Liquefaction trigger

Idriss & Boulanger (2008) presents the mechanism of liquefaction trigger and the factors that affect whether liquefaction occurs or not. Seismic liquefaction occurs when excess pore pressures are generated in loose, saturated, cohesionless soil and low-plasticity silt during earthquake shaking, causing the soil to undergo a temporary partial to complete loss of shear strength. Such a loss of shear strength can result in ground failures, while the post-cyclic loading reconsolidation of the soil leads to ground settlements. Whether a soil liquefies is dependent on several factors including the intensity and duration of ground shaking, soil density, particle size, and groundwater location. Soils which are susceptible to liquefaction require a certain level of earthquake shaking (trigger) to cause them to liquefy. Denser soils require more intense and/or longer duration of shaking (higher trigger) than less dense soil.

Methods have been developed to correlate SPT N values to earthquake shaking intensity required to trigger liquefaction, for example Idriss & Boulanger (2006). These methods can be used to assess the return period of an earthquake that could be expected to trigger liquefaction at a site. Refer Figure 1 for an example of an evaluation of liquefaction triggers at the case study site.

Table 2. Soil profile for case study

Layer No.	Description	Depth to top of layer (m)	Layer thickness (m)	SPT N (blow/300mm)
1	FILL	0.0	0.0 – 0.5	-
2a	MARGINAL MARINE DEPOSITS Fine to coarse sand with gravel (medium dense)	0.3 – 0.5	2.5 – 3.5	12 – 32
2b	MARGINAL MARINE DEPOSITS Fine to coarse sand with gravel (dense/very dense)	3.0 – 4.0	10.0 – 14.0	30 – >50
2c	MARGINAL MARINE DEPOSITS Fine sand with gravel (dense to medium dense)	13.0 – 17.0	0.4 – 3.0	17 – >50
3	MARGINAL MARINE DEPOSITS Sandy silt (stiff/very stiff)	15.3 – 18.0	14.0	9 – 30
4	MARGINAL MARINE DEPOSITS Organic peat layer (Firm to stiff)	31.0	2.0	-
5	MARGINAL MARINE DEPOSITS Inter-bedded layers of fine to medium sand & silt with some sand (dense)	33.0	7.5	45 – 46
6	RESIDUAL SOIL Silt with some gravel (Hard)	40.5	4.5	33
7	BED ROCK Greywacke	45.0	–	–

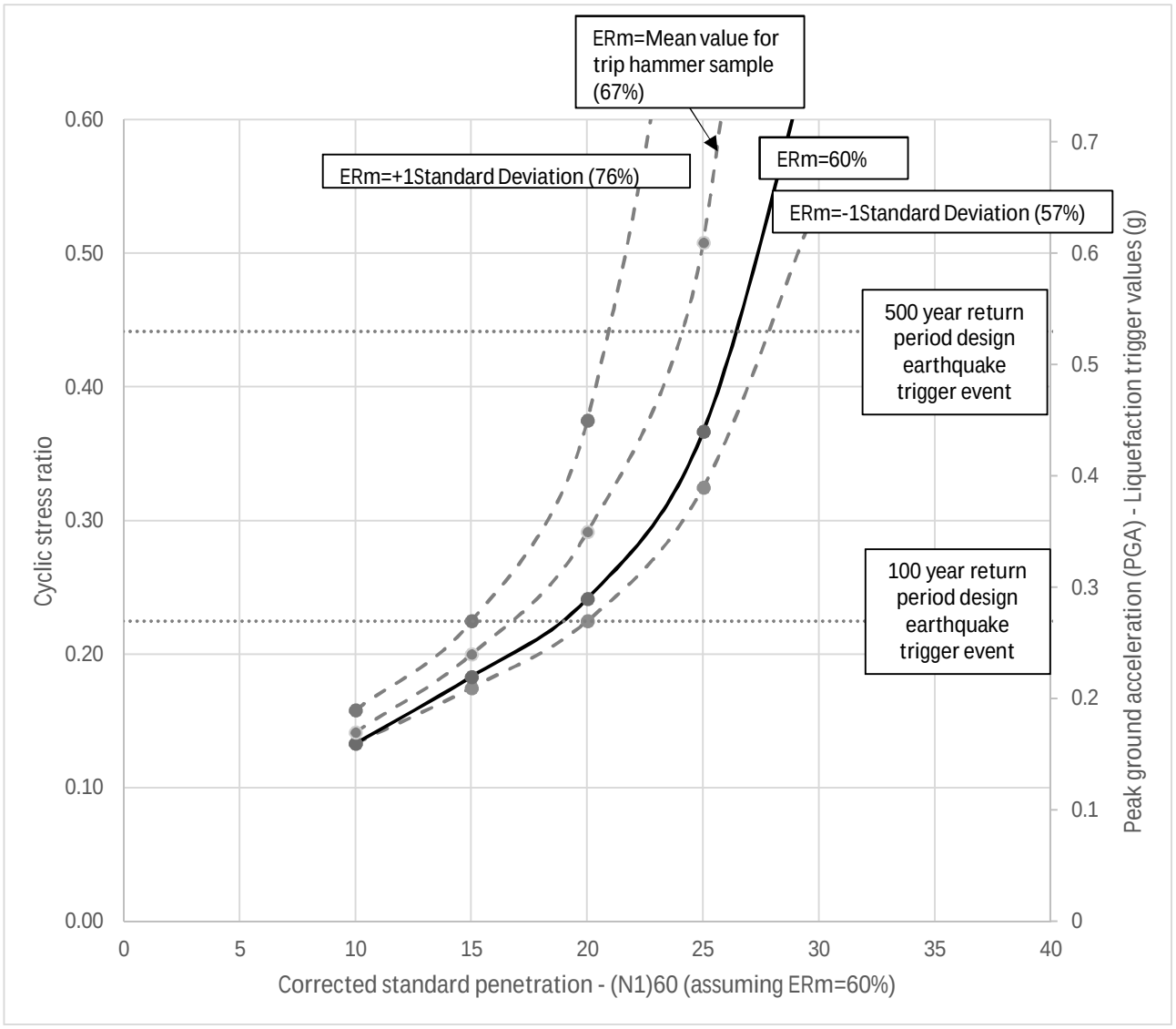

Figure 1. Liquefaction trigger values for a part of the Wellington marginal marine deposit at case study site. [Based on Idriss & Boulanger (2006), Fines Content ≤ 5%; Earthquake Magnitude = 7.5; δ'_{vc} = 1atm]

5.3. Importance of SPT hammer energy variation for case study

Layer 2a from the soil profile (fine to coarse sand with gravel) is potentially liquefiable. This layer has an SPT N range of 12-32, with typical values of 17-25.

Figure 1 shows that using the Idriss and Boulanger (2006) method with the typical assumed energy transfer ratio of 60% has different implications for the range of SPT values found in Layer 2a.

For an SPT N value of 12 and an assumed energy transfer ratio of 60%, the peak ground acceleration (pga) to trigger liquefaction is assessed to be 0.18g. There is only a minor difference in the assessed pga to trigger liquefaction if the SPT hammer has a different energy transfer ratio than the assumed 60%.

For an SPT N value of 17 and an assumed energy transfer ratio of 60%, the pga to trigger liquefaction is assessed to be 0.24g. There is a moderate impact on the assessed pga to trigger liquefaction if the SPT hammer has a different energy transfer ratio than the assumed 60%. If the SPT hammer energy transfer ratio was 67% the pga to trigger liquefaction is assessed to be 0.27g. Assuming an energy efficiency of 60% for this situation could lead to unnecessary conservatism in the liquefaction assessment. For a 100 year design earthquake event, this is the difference between triggering liquefaction and not.

For an SPT N value of 25 and an assumed energy transfer ratio of 60%, the pga to trigger liquefaction is assessed to be 0.44g. There is a large impact on the assessed pga to trigger liquefaction if the SPT hammer has a different energy transfer ratio than the assumed 60%. If the SPT hammer energy transfer ratio was 67% the pga to trigger liquefaction is assessed to be 0.62g. For a 500 year design earthquake event, this is the difference between triggering liquefaction and not.

The current practice of assuming an energy efficiency of 60% for a trip hammer is shown to be generally conservative as 60% is close to one standard deviation below the mean energy for trip hammers. However efficiency values as low as 48% were recorded and for values as low as this, assuming 60% would lead to an unconservative assessment. Liquefaction triggering could be determined as unlikely to occur when the opposite should be predicted.

A hammer energy transfer ratio is shown to make a difference to this case study for SPT values from 17 to 25. This is due to the larger spread in predicted pga values to trigger liquefaction evident in Figure 1 for higher SPT values.

The hammer efficiency for this case study was measured and found to be 63% and so assuming an energy efficiency of 60% had little impact on the design conclusions.

6. Conclusions

The following conclusions have been drawn:

- The energy efficiency of SPT hammers varies widely.
- A wide range of SPT hammer calibration frequencies exists in New Zealand.
- The New Zealand Standard for SPT states that different hammer types are not comparable.
- International standards recommend at least annual calibration of SPT hammers and project specific calibration for critical projects.
- Energy correction can have a significant impact on liquefaction assessment especially for SPT values between 17 and 25.
- When no energy correction is available the current practice of assuming 60% is generally conservative. However as efficiency values as low as 48% were recorded, uncalibrated hammers should not be used to prevent unconservative liquefaction assessments. For assessments that lead to expensive remedial works, confidence of the hammer efficiency could lead to considerable cost savings.

7. Acknowledgements

Richard Cole (Tonkin & Taylor) was the supervisor for this conference paper.

Geotech Drilling Ltd, Griffiths Drilling Ltd., McMillan Drilling Ltd., Websters Drilling and Exploration Ltd were helpful in providing information used in this paper.

8. References

ASTM Standard D6066-11 (2011). Standard practice for determining the normalized penetration resistance of sands for evaluation of liquefaction potential. *American Society for Testing and Materials International*

ASTM Standard D4633-10 (2010). Standard test method for energy measurement for dynamic penetrometers. *American Society for Testing and Materials International*

ASTM Standard D1586-99 (1999). Historical Standard (Superseded) - Standard test method for standard penetration test (SPT) & split-barrel sampling of soils. *American Society for Testing and Materials International*

ASTM Standard D1586-11 (2011). Standard test method for standard penetration test (SPT) & split-barrel sampling of soils. *American Society for Testing and Materials International*

Department of Building & Housing (2012). Guidance for repairing & rebuilding foundations for homes in TC3 areas of Canterbury. *December 2012, Version C. Part C. TC3 Technical Guidance. Appendix/Page C4.11. New Zealand.*

Idriss, I.M., Boulanger, R.W. (2006). Semi-empirical procedures for evaluating liquefaction potential during earthquakes, *Soil Dynamics and Earthquake Engineering vol. 26 pp. 115–130*

Idriss, I.M., Boulanger, R.W. (2008). Soil liquefaction during earthquakes, *Monograph series, No. MNO–12*, *Earthquake Engineering Research Institute.*

Fairclough A., Ashfield D.J. (2013). The EQC Geotechnical Project – Key Issues and lessons learnt during CPT and SPT investigations. *Proc. 19th NZGS Geotechnical Symposium. Ed. CY Chin, Queenstown.*

ISO 22476-3 (2005 with 2011 amendments). Geotechnical investigation & testing-Field testing. Part 3: Standard penetration test. *International Organization for Standardization*

NZGS (2010). Geotechnical earthquake engineering practice. Module 1 – Guideline for method for identification, assessment and mitigation of liquefaction hazards. *New Zealand Geotechnical Society, Rev 0*

Youd et al. (2001). Liquefaction resistance of soils: "Liquefaction resistance of soils: Summary report from 1996 NCEER and 1998 NCEER/NFS Workshops on Evaluation of Liquefaction Resistance of Soils. *Journal of Geotechnical and Geoenvironmental Engineering. vol. 127 No. 10. pp. 817–833*

Proceedings of the 10th ANZ Young Geotechnical Professional's Conference – 10YGPC
Noosa, Queensland, Australia
10 – 12 September 2014

A WELL GeoCONNECTED DESIGN: A HARD ROAD TO A SOLID FOUNDATION

Mark HILL
Beca Ltd, Auckland, New Zealand

ABSTRACT – The NZ Transport Agency's Waterview Connection project is one of the largest and most important infrastructure projects to be undertaken in New Zealand. The project will see 5km of 6 lane motorway constructed through Auckland's Western suburbs, linking two existing motorways to complete a ring route around the city. The project centrepiece is a 14m diameter Earth Pressure Balance Tunnel Boring Machine, used to minimise the impact on surrounding communities. A considerable amount of complex and challenging surface works must also be completed at both ends to connect the tunnels into the motorway network. Geotechnical engineers for the Well-Connected Alliance have contributed to the design of the tunnel, bridges, trenches, embankments, diversions (stream, road and utilities), ancillary buildings and spoil disposal. One of the major geotechnical design challenges was to integrate detailed design packages with other designs that were still at concept stage. Often geotechnical designs were constrained by the needs of other design packages. Having to interface with another Alliance delivering the adjoining SH16 Causeway upgrade added to the challenge and shaped many of the geotechnical design issues on the project, including the design of a 90m long by 4m high retaining wall.

1. Introduction

The Waterview Connection project will see 5km of six lane motorway constructed through Auckland's Western suburbs. This will link State Highway 20 (SH20) to State Highway 16 (SH16) and complete a ring route around the city.

Half of the motorway link will be constructed underground using a 14m diameter Earth Pressure Balance Tunnel Boring Machine (EPB TBM). This will minimise the impact on the communities surrounding the project.

The first part of Auckland's South-western motorway network was constructed in the 1980's. The project has extensive planning history with consultation for the project occurring in the early 2000's.

The project will be delivered through an alliance model. The Well-Connected Alliance (WCA) comprises of the New Zealand Transport Agency, Fletcher Construction, McConnell Dowell, Obayashi Corporation, Parsons Brinckerhoff, Beca and Tonkin and Taylor.

This paper will provide a project overview, a brief summary on some of the major geotechnical works and a discussion on the challenges of designing a Mechanically Stabilised Earth (MSE) retaining wall.

2. Project Overview

Currently all traffic travelling through Auckland is reliant on State Highway 1 (SH1) to provide a motorway connection between north and south Auckland. During peak hours, congestion on SH1 cause significant delays to commuters, freight and tourists.

The western ring route will provide an alternative motorway for through traffic and alleviate congestion on SH1.

Figure 1. Location of the Waterview Connection.

2.1. Construction Zones

The project is geographically divided into three construction zones the southern zone, the tunnel and the northern zone.

2.1.1. Southern Zone

The southern zone extends from the end of SH20 at the Maioro Street interchange through to the tunnel portal openings. The construction work comprises of:

- a connection to SH20;
- an expanded Maioro Street interchange;

- a motorway and pedestrian overbridge;
- The southern approach trench (SAT) to launch the TBM; and
- Realignment of Oakley creek and other major underground infrastructure.

2.1.2. Tunnel Zone

The tunnel zone extends from the Alan Wood Reserve in Owairaka to Waterview adjacent the existing SH16 motorway. The construction work consists of

- Two twin bored tunnels 2.4km long and 13.1m in diameter;
- 16 cross passages connecting the tunnels; and
- Associated mechanical and electrical works

2.1.3. Northern Zone

The northern construction zone links the tunnels to the existing SH16 motorway. The construction work consists of

- Northern approach trench; and
- Four new ramps at the great north road interchange to connect the tunnels to SH16.

3. Overview of Geotechnical Works

The WCA geotechnical engineers have contributed to the design and construction of permanent works such as the tunnels, bridges, retaining walls, embankments and ancillary buildings.

3.1. Southern Approach Trench

The southern approach trench (SAT) is located in the Alan Wood Reserve Owairaka, which is part of the southern zone of works. The SAT is designed to provide the necessary space for reassembly of the TBM that had been shipped in pieces from the factory in Nansha, China. The SAT is approximately 400m long and 29m deep during temporary excavations at the portal sump.

The trench face forms the southern portal where the TBM will begin its first bored tunnel and complete the second bored tunnel.

The SAT is constructed on a circa 100,000 year old basalt lava field sourced from the Mount Albert volcano approximately 1km to the northeast (Wansbone et al, 2013). This strong basalt rock (UCS 25-120 MPa) overlays much weaker East Coast Bays Formation (ECBF) (UCS 1-5MPa) located at depth.

As the TBM is designed to tunnel exclusively through ECBF rock and Tauranga Group soils it was critical to accurately map the basal contact of the basalt lava flow in three dimensions. From a program of ground investigations, a 3D model was developed in 12D and imported into geometric software MX (Wansbone et al, 2013).

The SAT has two separate retention systems for the basalt and the ECBF. Due to the different rock mass types within the basalt, various support types were used to retain the basalt. For poorer quality rock a combination of rock bolts steel mesh and shotcrete was employed. For blocky columnar jointed basalt, fibre reinforced shotcrete was used in combination with rock bolts.

To retain the Tauranga Group and ECBF below the basalt, bored piles with up to three rows of multi strand anchors were used. These were installed through the reinforced capping beams and walers.

Piles were spaced at a maximum of three diameters with drainage and shotcrete lagging installed between piles. By designing the retaining walls as drained, reduced groundwater pressures significantly reduced the structural demands on the retaining wall. (Wansbone et al, 2013).

Figure 2. Aerial view of SAT looking north on 7 August 2013

3.2. Bored Tunnels

The centrepiece of the project is the twin 2.4km bored tunnels. These tunnels are designed to accommodate three lanes of motorway traffic in both the northern and southern directions. The southern extent of these tunnels is the SAT in Alan Wood Reserve and the NAT in the north adjacent the Waterview Reserve. At their deepest the tunnels are approximately 45m below ground and have a bored diameter of 14.5m with an internal diameter of 13.1m.

The tunnels are linked together by sixteen cross passages. These cross passages provide storage for maintenance purposes, house tunnel electrical and mechanical systems and provide emergency exit pathways from the tunnels.

To minimize disruption to the surrounding residential neighbourhoods, bored tunnels using an earth pressure balance (EPB) TBM was selected as the preferred method of tunnelling. An EPB TBM is able to reduce ground surface settlements around the tunnel excavation area by maintaining the pressure on the excavated face. This is achieved through a pressurized compartment directly behind the cutterhead. Spoil from the excavation face is stored in this compartment and used to maintain pressure on the face of the excavation.

Figure 3. Temporary steel segements installed at cross passage opening.

The tunnel will be lined with 2m wide precast concrete segments that will be assembled within the tailskin of the TBM. The rings comprise of nine segments and a key. For the most part the tunnels pass through sandstone (ECBF) of varying strength and weathering, except at the northern portal where the tunnel will be partially within Tauranga Group soil (Well-Connected Alliance 2013c).

Depending on ground conditions and alignment depth, three different types of reinforcement were used within the segmental lining. The cross passages however are not lined with segments and will be mechanically excavated, in a series of advances. Temporary steel segments are installed at the cross passage opening and are then removed later to begin excavation. Shotcrete is applied to the excavated rock lining for support. In areas of poorer quality rock bolts will be installed to provide extra support.

3.3. Great North Road Interchange

A critical part of the project, aside from the tunnels, is the Great North Road interchange (GNRI). The interchange will connect SH 20 onto SH 16. The GNRI comprises of 4 ramps with associated earthworks embankments and retaining walls.

The typical geological profile at the GNRI area consists of Puketoka Formation (alluvium) overlaying weathered and unweathered ECBF. Approximately 28,000 to 30,000 years ago the nearby Mount Albert and Mount Roskill volcanoes erupted. The resulting lava from the eruptions ponded in the valleys of the Oakley Creek catchment. The basalt flows have formed a lobe of basalt in the interchange area that continues into the Waitemata Harbour (Well-Connected Alliance, 2012a).

The construction of these ramps comprises of pre-stressed super T beams integrally supported on cross heads with single piers and piles. The piles are 2.1m diameter bored piles. Where there is sufficient basalt, pad footings will be used instead. (Well-Connected Alliance, 2012b)

There are six retaining walls in the GNRI area. Retaining walls 501, 502 and 503 are mechanically stabilized earth (MSE) walls using stone strong blocks for facing. Retaining walls 601, 602 and 703 use a combination of soil nails, bored piles and ground anchors.

The MSE walls have been designed to transition traffic from the ramps onto SH16. Stone strong blocks were selected as the preferred facing method, as the constructors were able to install them efficiently. Tensar RE geo grid was used as the reinforcement behind the walls.

Figure 4. Aerial view of the Great North Road Interchange and northern retaining walls looking north.

4. RW 503 Design Challenges

Retaining wall 503 (RW503) is located on the western end of Ramp two (Ramp 2). Ramp 2 takes northbound traffic from the tunnel westbound on SH16. The ramp is unique as the traffic from ramp two will merge into the inside lane of SH16 which is referred to as "the flip option".

The retaining wall itself is 90m long and approximately 4m high. It overlaps the Ramp 2 abutment wingwalls and therefore the walls are not connected and are essentially two separate walls. It retains crushed basalt excavated from the SAT excavation.

The retaining wall is constructed with stone strong blocks which are 2.2m long, 1.1m deep and 900mm high and have an exposed aggregate facing. Two rows of Tensar Re geogrid are cast into the back of the block in 0.46m lifts. The grid placed behind the blocks is connected to the cast in grid via a bodkin joint. Due to the large size of the blocks and the gradually diminishing retained height, a special taper top block was developed that could vary in height between 1020mm and 100mm. The taper top block is placed on top of the topmost stone strong block and used to follow the gradient of the ramp down.

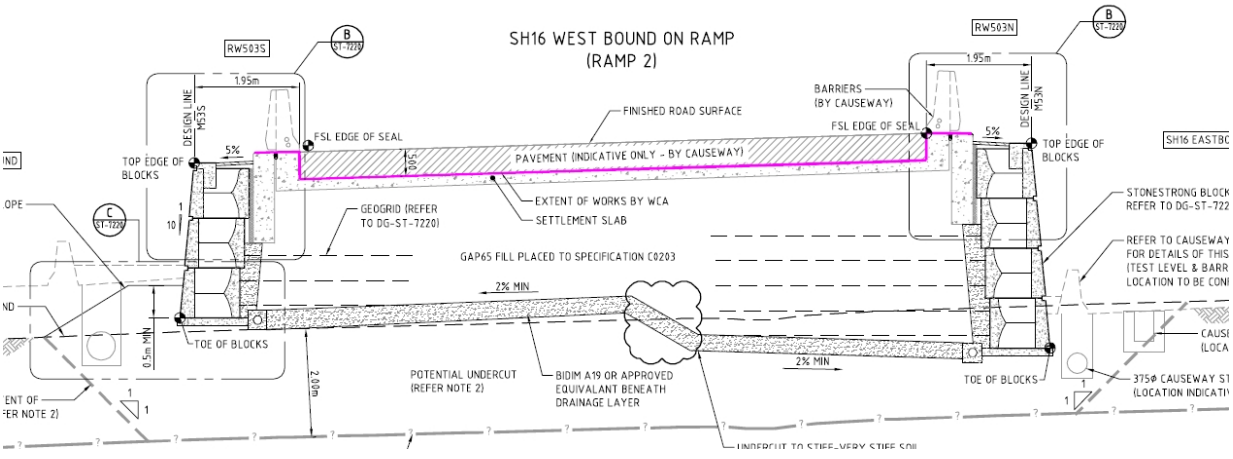

Figure 5. Showing a cross section through Retaining Wall 503.

One of the major challenges on the project was being able to integrate design packages from different disciplines. Often design packages were at different stages of the design process. This makes the design process challenging when a detailed design package requires input from a design package still at conceptual stage. To overcome this, the WCA designers had to be proactive in engaging with other design processes.

Figure 6 Stone Strong block placement for RW502.

4.1. Flip Option

During Total outturn cost (TOC) Ramp 2 was proposed to enter SH16 on the left-hand side of the motorway like a conventional onramp. After TOC was completed it was then proposed that it was more appropriate for Ramp 2 to enter SH16 on the right-hand side of the carriageway. The main reason for this change was to prevent lane weave on SH16. The change in alignment required a retaining wall (RW503) to be built as the ramp landing was now located between the two SH16 carriageways. A challenge in the design of RW503 was the alignment and geometry of the retaining wall wasn't completely confirmed at the start of detailed design. This required close interaction with geometric designers to confirm the retaining wall string lines that were being used for the design of RW503 were accurate.

4.2. Retaining Wall 503 Settlement Issues

One of the challenges for the design of RW503 was confirming that the settlement in the carriageway meets the Project's Minimum Requirement of less than 15mm differential settlement between the settlement slab of the piled Ramp 2 abutment and the approach embankment. This proved quite challenging as the geological profile underneath the retaining wall was 5m of basalt overlying approximately 10m of Tauranga Group soils. Typically adopted analytical methods calculated significantly larger settlements than allowed for in the Minimum Requirements.

Due to RW503 being located in the carriageway of the existing SH16 getting investigation data was very challenging. Geotechnical drilling could only take place at night due to the high traffic volumes on the motorway. The drilling was also time-consuming because of the 5m of basalt above the Tauranga group. It required the drillers to change their drilling equipment once they had drilled through the Basalt and reached the Tauranga Group. This was to ensure representative samples of the Tauranga Group soil could be collected for laboratory testing. The specific borehole was completed at the proposed Ramp 2 abutment and push tubes were undertaken. Laboratory 1-dimensional consolidation tests could then be completed to inform the design process.

A Plaxis model was developed to estimate how the load of the approach embankment would be rafted through the basalt layer and onto the Tauranga group. This involved using Plaxis to provide an average vertical stress onto the top of the Tauranga Group soil. The model confirmed that the cumulative effect over the 25 year maintenance life would exceed these Minimum Requirements.

When the alliance requests a change to the minimum requirements, a departure must be raised. In the case of RW503 a departure was raised in respect to a requirement of less than 15mm differential settlement between the approach embankment and the abutment.

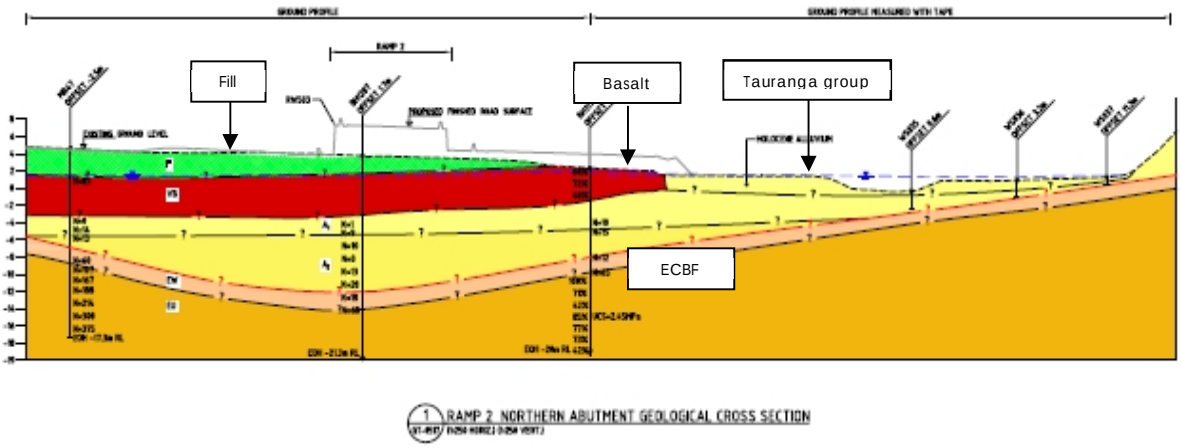

Figure 7 showing geological cross section for RW503

The solution that was presented in the departure centred on the ramp pavement known as Open Graded Porous Asphalt (OGPA). OGPA is resurfaced every 7 years at a maximum and during this scheduled maintenance, minor settlement can be corrected with the OGPA. The alliance could prove that there would be no more than 15mm differential settlement over the 7 year lifecycle of the OGPA and on that basis the departure was approved.

4.3. Interfacing with the Causeway Alliance

Another significant challenge was the integration of the design of retaining wall 503 with the Causeway Alliance (CA). The CA is responsible for raising and widening the causeway which is part of SH16. Retaining wall 503 was unique as it not only had a horizontal interface with the CA but it also had a vertical interface.The WCA was responsible for constructing the retaining wall while the CA was responsible for raising SH16 around the retaining wall and constructing the pavement, barriers and lighting of the ramp.

The Waterview Connection project required close interaction between different design disciplines. The retaining walls at the GNRI area are a good example requiring significant input from geotechnical, civil, structures, urban design, construction and maintenance.

This created challenges, as the project often involved working in confined spaces where design clashes between disciplines were common issues. It was crucial to have communication between the design disciplines and review work packages at the completion of each design stage. It also highlighted the importance of having sound review processes so that potential clashes did not go unnoticed. A good example of this was the stormwater drainage around retaining wall 503 by the CA.

The CA needed to install stormwater pipes at the toe of retaining wall 503. This was picked up early in our detailed design through providing the concept plans to the CA for comment. The pipes were to be located within close proximity. Due to the risk of the retaining wall toe collapsing into the open trench, bracing of the open trenches would be required. This would have been a significant cost to the CA and ultimately the NZ transport agency. By working closely with the CA it was possible to accommodate the stormwater pipes through changing the construction staging around the retaining wall. The stormwater pipes would be installed first followed by the retaining wall itself.

5. Conclusions

The NZ Transport Agency's Waterview Connection project is one of the largest and most important infrastructure projects to be undertaken in New Zealand.

The WCA geotechnical engineers have contributed heavily to the design and construction of structures such as the SAT, tunnels and the GNRI.

A significant challenge for design engineers on any large project is being able to integrate design packages from different design disciplines at different stages of the design process. To achieve this, it becomes crucial to be proactive in engaging other design disciplines and having sound design review processes in place before the design program begins.

6. Acknowledgements

The Author would like to acknowledge the New Zealand Transport agency and the WCA for permission to showcase this project.

The support of my colleagues, in particular Sian France (Associate – Hydrogeology, Beca) and Grant Newby (Technical Director – Geotechnical Engineering, Beca) has been much appreciated and key in the composition of this paper.

7. References

M Wansbone, S Cartwright, S France and B Hill, 2013. 'Wonderland' – Preparing To Send Alice Down The Rabbit Hole, The Southern Approach Trench To The Waterview Connection Tunnels. *NZ Geomechanics News*, Issue 86, pp. 71-82.

Well-Connected Alliance (2012a), *Geotechnical Interpretive Report – Northern Area*

Well-Connected Alliance (2012b), *GNRI Ramp 3 Foundations Stage 2 Report*

Well-Connected Alliance (2013c), *Main Line Tunnels Segmental Lining Design*

Proceedings of the 10th ANZ Young Geotechnical Professional's Conference – 10YGPC
Noosa, Queensland, Australia
10 – 12 September 2014

ESTIMATING THE POSITION OF INFILLED PALAEOCHANNELS BY THREE DIMENSIONAL MODELLING, BURSWOOD PENINSULA, WA

Shane GREENE
Golder Associates Pty Ltd, West Perth, Australia

ABSTRACT – Understanding the characteristics and distribution of infilled palaeochannels beneath the Burswood Peninsula and in the Perth area is fundamental to proposed infrastructure developments along the Swan River. The presence of palaeochannels infilled with soft sediments heavily influences the settlement of infrastructure and selection of suitable foundation options. Point data and geological interpretation have been used to create a three dimensional geological model of the Burswood peninsula. This model has been used to estimate the position of infilled palaeochannels in order to help assess geotechnical risks on the Burswood Peninsula. The relationship between these palaeochannels and their infill sediments plays an important role in understanding Perth's geological history and evaluating geotechnical material characteristics in an area-wide context

1. Introduction

The Swan River is one of the most prominent geomorphological features of the Perth area. It has played an important role in shaping both the physical landscape around Perth and the location of the city.

Variation in the position of the Swan River throughout recent geological history, with particular emphasis on the last 150,000 years, is of particular relevance to development and expansion of buildings and infrastructure on the Burswood Peninsula and in the City of Perth.

The Quaternary geological period has been characterised by fluctuations in sea levels that have resulted in changes in the horizontal and vertical position of the Swan River. These variations in river level have resulted in the formation of ancient river channels, termed "palaeochannels" that have been infilled with a series of sand, gravel, silt and clay sediments. Understanding of the strength, persistence, and extent of these different materials is vital in geotechnical planning and design of developments along the Swan River.

1.1. The Burswood Peninsula

Burswood is one of the southeastern suburbs of Perth, Western Australia, and is located approximately 3km east of the Perth CBD. The majority of the suburb is located on land within a large meander oxbow bend of the Swan River. The area has been previously referred to as "Burswood Island" but since reclamation of the area began in the early to mid-1900's the area has generally referred to as the "Burswood Peninsula".

At the time of European settlement the area was largely comprised of mudflats and a series of sand bars within the greater Swan River. Since the early 1900's reclamation has largely occurred through placement of uncontrolled filled, dredged material from the adjacent Swan River and through use as a disposal site for both industrial and residential waste.

1.2. Regional Geology

The Burswood Peninsula is situated on the Swan Coastal Plain and within the Perth Basin. The Perth Basin contains sediments ranging in age from Permian (280 Ma) to Cretaceous (65 Ma) that represent deposition in a former rift valley.

The geological history most relevant to this study began during the early Tertiary period (35 to 65 Ma) when sediments of the Kings Park Formation were deposited in a shallow marine to estuarine environment within a major river valley.

The Kings Park Formation, including the Mullaloo Sandstone Member, comprises sandstone, siltstone or shale. Beneath the Burswood Peninsula the Kings Park Formation is predominantly comprised of the Mullaloo Sandstone Member within the depth of boreholes completed to date. The Mullaloo Sandstone member is generally very dense, fine to coarse grained, pale grey and white sand with some fine to coarse grained gravel and clay nodules. The shale sequences of the Kings Park Formation proper have been noted in a limited number of boreholes on the northern extent of the Burswood Peninsula.

Changes in relative sea level exposed the Kings Park Formation as a land surface during the late Tertiary Period. Beneath the Burswood Peninsula, retention of subsequent deposition on top of the Kings Park Formation did not occur until alluvium and sand dunes were deposited during the Quaternary period.

The Quaternary period has been characterised by periodic sea level fluctuations largely attributed to glacial and interglacial periods. Sea level fluctuations are thought to have ranged from 150 m below, to 9 m above current sea level in the Perth area (Gordan, 2003). The alluvium deposited during the Quaternary is the geological unit of principal interest in this paper.

This alluvium has been deposited by the ancient Swan River and includes both the Swan River Formation and the Perth Formation. Beneath the Burswood Peninsula, the Swan River Formation predominantly comprises soft and compressible silt and clay while the Perth Formation comprises dense to very dense sands, silts and clays.

1.3. Geotechnical Considerations

Estimation of the position of the palaeochannels is important in developments along the Swan River as their presence may affect the geotechnical considerations for any particular site.

The presence of a palaeochannel infilled with relatively soft and compressible sediment can affect the choice of foundations. Settlement of soft sediments due to both natural compression, and that added by placement of engineered fill or buildings, can make shallow foundations too risky or costly to meet restrictions on long term vertical and horizontal movements.

The position and cross section of palaeochannels are also important. If piled foundations are selected in vicinity of the paleochannels, the depth to suitable foundation materials can change significantly over a relatively short distance. This uncertainty carries a project risk that if not properly understood, can have adverse effects on design considerations as well as the project budget and time schedule.

1.4. Global Sea Level Change and Palaeochannels

Oxygen isotopes from deep sea sediment cores have been used to estimate climatic temperature fluctuations throughout approximately the past 700,000 years.

During colder glacial periods global sea levels are lower because a significant portion of the earth's water is bound up in continental ice sheets and alpine glaciers.

In contrast, during the warmer interglacial periods, sea levels are higher because ice sheets and glaciers melt and release water. Consequently, there is a direct relationship between global temperature and sea level. Worldwide changes in sea level are known as eustatic changes.

Based on the relationship between oxygen istopes, temperature and sea level change, Shackelton and Opdyke (1973) have developed a worldwide eustatic curve for the last 700,000 years. Gordon (2003 & 2012) present a relative sea level for the last 270,000 years for the Swan Coastal Plain that has incorporated sea level height data from local outcrops and bridge investigation sites.

Their interpretation of the relative sea level variation has been reproduced in Figure 1. Glacial and interglacial events have been given numbers and letters based on their Marine Isotope Stage (MIS). Three of the main Marine Isotope Stages with respect to palaoechannels in the Perth area are marked as MIS2, MIS4 and MIS6 on Figure 1 and correspond to times when channel elevations were likely lowest during glacial periods. Figure 1 also shows the author's interpretation of the geological units infilling the palaeochannels based on information presented in Gozzard (2007) and Gordon (2012).

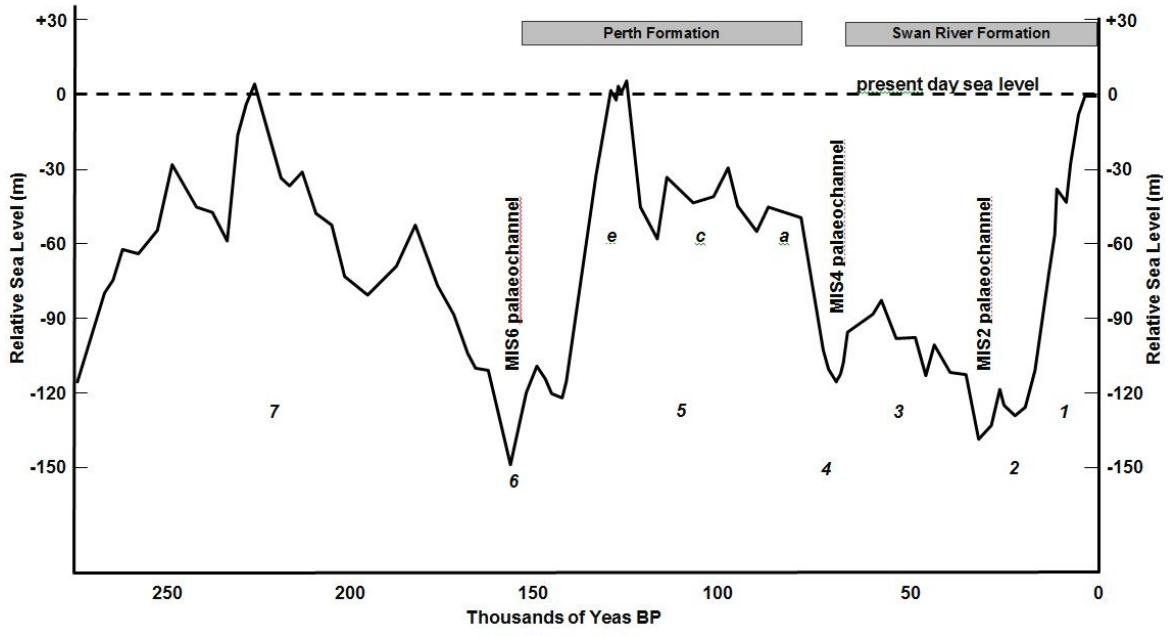

Figure 1. Eustatic sea level curve for the past 270,000 years with oxygen isotope stages indicated (modified from Gordon, 2003; Gozzard, 2007 and Gordon, 2012).

During glacial periods, when sea level is lower, existing river channels experience down-cutting and erosion. During interglacial periods and higher sea level, the hydraulic gradient of rivers decreases and these river channels experience depositional process and are generally infilled with sediments. The erosion and depositional processes may also result in horizontal movement of the river's alignment position.

During each deposition or erosion cycle, river channels may follow different courses, or may not erode as deeply into underlying sediments. The variation in the course of the Swan River from offshore Fremantle to Barkers Bridge in Guildford has previously been identified by Gordon (2003 & 2012), Tutton (2003) and various other private reports.

2. Three Dimensional Modelling of Burswood Peninsula Geology

As previously outlined, one of the main geotechnical considerations for construction over the infilled palaeochannels is associated with identification of the relatively soft and compressible infill sediments of the Swan River Formation within the MIS2 palaeochannel. Consequently, detailed delineation of the extent of these soft sediments has been one of the main objectives of recent and historical geotechnical investigations in the Burswood Peninsula area.

On the other hand, the relatively dense and less compressible sediments infilling the MIS4 and MIS6 palaeochannels have not been considered as critical to delineate from one another (or from the underlying Kings Park Formation). Furthermore, a large proportion of the MIS4 palaeochannel infill sediments may have already been eroded during formation of the MIS2 palaeochannel and re-filled with the MIS2 aged sediments.

In order to confirm the presence and estimate the position of palaeochannels beneath the Burswood Peninsula, current and historical geotechnical investigation data has been reviewed and interpreted. Historical photographs and maps have also been used to understand reclamation history.

2.1. Available Data

Over 1000 geotechnical investigation locations have been reviewed and interpreted to create a three dimensional geological model of the Burswood Peninsula and to estimate the alignment of the major palaeochannels. The geotechnical investigations comprised machine drilled boreholes, cone penetration tests (CPTs), test pits and hand auger holes.

Approximately 850 investigation locations within the current geological model penetrate through the full depth of the MIS2 infill sediments and only 78 penetrating through the MIS4 and/or MIS6 infill sediments into the underlying bedrock. The variation in the number of tests fully penetrating these units is a result of the focus of geotechnical investigations on identifying the MIS2 palaeochannel infill as well as on the inability of CPTs to fully penetrate the denser sediments of the MIS6 infill.

This means that the confidence in the location of the MIS2 palaeochannel is significantly higher than that of the MIS4 or MIS6 palaeochannels. Delineation of these deeper palaeochannels is further complicated by similarities in material type between MIS4 and MIS6 infill sediments as well as similarities with the sediments of the Mullalloo Sandstone.

2.2. Methodology

The geological data for each of these test positions has been interpreted and materials grouped within units in order to produce a 3D geological model of the area. Geological data has been mapped using Environmental Visualisation Software (EVS); a 3D modelling package that is primarily used for analysing and modelling borehole geology data. The end result can be a series of surfaces for each geologic unit base that can be exported in several formats.

The geologic modelling method used is a hierarchical method that allows for extrapolating the geology based on existing unit thicknesses and is ideal for "pinching out" layers. The point data input into the model is comprised of interpreted borehole data for the base elevation of each unit and available surface elevations. The interpolation method used is 'Kriging' which makes use of geostatistic principals with regard to data variability to estimate the surface elevations. All data was equally weighted during the Kriging process.

In addition to the geological investigation locations, a significant amount of geological interpretation was completed in ArcGIS. This involved creation of false points and contours in order to provide a better visual estimate of palaeochannel positions.

3. Palaeochannels and Geologic Interpretation for the Burswood Peninsula

Previous work by Gordon (2003 & 2012) on historical geological data at bridge sites identifies that the three palaeochannels mentioned (MIS2, MIS4, and MIS6) occur in the vicinity of the Burswood Peninsula.

This work was used to help target geological interpretation including evaluation of the thalweg, or line of lowest channel elevation, for each palaeochannel.

The position of the MIS2, MIS4 and MIS6 palaeochannels beneath the Burswood Peninsula and surroundings has been estimated. These positions are presented graphically in Figure 2. A

conceptual cross section across the Burswood Peninsula showing the relative position of the three palaeochannels is shown in Figure 3.

3.1. MIS6 Palaeochannel (MIS6)

MIS6 is the oldest of the identifiable palaeochannels and is associated with a glacial period when sea level reached a low point of approximately 150 m below current level approximately 150,000 years ago. The MIS6 channel has eroded the underlying sedimentary rocks of the Kings Park Formation (KPF); including the Mullaoo Sandstone Member.

Beneath the Burswood Peninsula the main part of the MIS6 channel is between 100 m and 150 m wide with a thalweg elevation of about -35 m AHD.

Sediments infilling MIS6 are included in the Perth Formation (Gordon, 2012). Geotechnical investigations show that in the vicinity of Burswood, these materials generally comprise grey to yellow, medium dense to very dense sand dominated deposits with an overall fining upwards trend. Deposits range between approximately 3 m and 30 m in thickness. Lenses of gravels, silts and clay are also present and may be up to approximately 10 m in thickness. Clay lenses may comprise stiff to very stiff red, blue and grey mottled clay.

The thalweg for MIS6 is often characterised by gravel that may represent lag deposits laid down at the base of this palaeochannel. The presence of organics, that may represent a palaeosol, has been noted at the contact with the Kings Park Formation. In addition, the base of this palaeochannel has also been interpreted based on Standard Penetration Test (SPT) results. A rapid increase in the SPT N values greater than 50 was often used to help delineate the base of this palaeochannel from the underlying Mullalloo Sandstone.

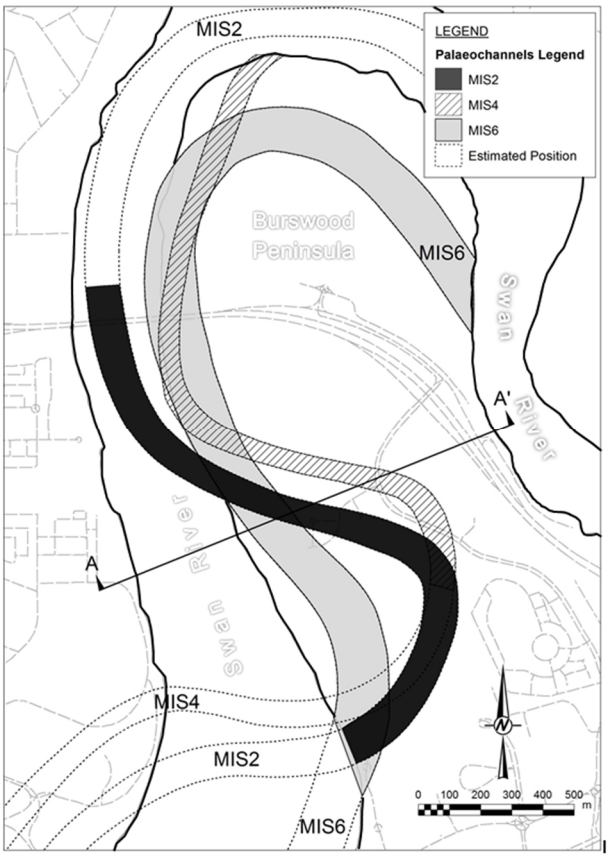

Figure 2. Approximate position of the MIS2, MIS4, and MIS6 palaeochannels beneath the Burswood Peninsula and surroundings.

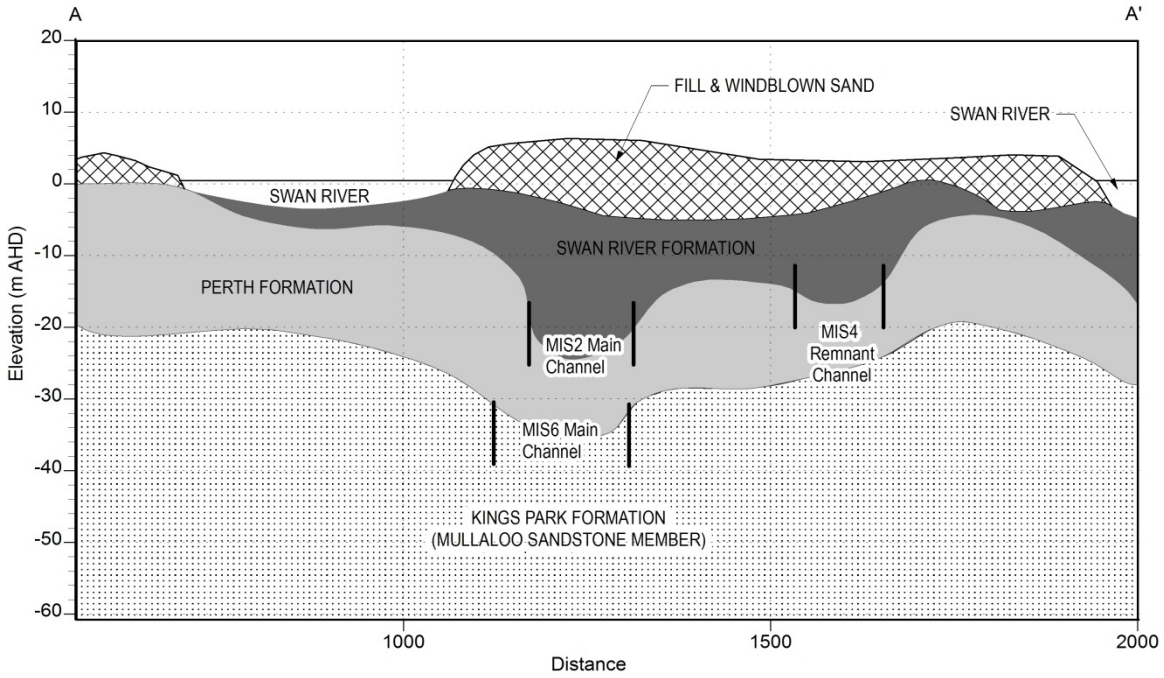

Figure 3. Conceptual cross section through the Burswood Peninsula showing the relationship of infilled palaeochannels.

3.2. MIS4 Palaeochannel (MIS4)

MIS4 is associated with the beginning of the most recent glacial period and would have reached a maximum depth approximately 70,000 years ago when sea level was approximately 115 m below current level. Once this maximum depth was reached, a period of deposition occurred prior to continuation of the sea level drop associated with the last glacial period and formation of MIS2.

Of the three palaeochannels, the position of MIS4 carries the most uncertainty as most of the infill sediments appear to have been eroded by MIS2 or are difficult to differentiate from deposits of MIS6. The position of MIS4 is based on its elevation with a thalweg of approximately -20 m AHD and its agreement with the position estimated by Gordon (2003).

Geotechnical investigations have shown that at the Burswood Peninsula, infill sediments of the MIS4 channel are scarce but are likely dominated by silty sands.

Beneath the Burswood Peninsula and Swan River, the main part of this channel is estimated to be between 50 to 100 m wide.

3.3. MIS2 Palaeochannel (MIS2)

MIS2 is the youngest and the most well defined of the identifiable palaeochannels within the Burswood Peninsula and surroundings. It is believed that MIS2 reached its maximum incised depth during the later stages of the last glacial period approximately 20,000 to 30,000 years ago when sea level was approximately 130 m below current level.

Around the Burswood Peninsula MIS2 has cut into the sediments deposited by both MIS4 and MIS6, and in a limited number of boreholes, it has eroded into the Kings Park Formation as well.

Sediments infilling MIS2 are termed Holocene Alluvium by Gozzard (2007) and have been included in the Swan River Formation by Gordon (2012). These sediments have also been previously referred to as "Swan River Alluvium" (Hudson-Smith and Grinceri, 2007) and "Blue" and "Black" muds of the Swan River. This paper has adopted Gordan's (2012) approach and included these sediments in the Swan River Formation.

Beneath the Burswood Peninsula and surroundings, geotechnical investigations show that the Holocene Alluvium generally comprises very soft to firm, dark grey to black and blue high plasticity silty clay or clayey silt. Organics, shells and shell fragments may be present either in trace amounts or as significant interbeds within the silty clay and clayey silt matrix. These muds are still being deposited by the Swan River at present.

The main part of MIS2 is between 100 and 150 m wide with a thalweg elevation of about -25 m AHD. Within the test locations, MIS2 has an identifiable thickness of between approximately 0.5 m and 25 m.

3.3.1. Further Subdivision of the MIS2 Infill

It has been identified that the MIS infill contains two sequences of estuarine muds (Marsh,1967; Quilty, 1974). The older, more consolidated sequence is locally referred to as "Blue Mud" and was deposited between about 6700 years and 4500 years ago (Kendrick, 1977). The younger sequence, known locally as the "Black Mud", is still being deposited by the modern Swan River.

Analysis of CPT traces, compression indices and particle size distribution curves suggest that a division between these two vertical sequences is present at an elevation of about -8 m AHD beneath the Burswood Peninsula.

Analysis of CPT traces also suggests a horizontal change in the alluvium. Toward the central part of the channel, the alluvium appears to be more homogenous in nature with minor sand interbeds and a corresponding greater percentage of fine grained material. Towards the outer channel and banks, the alluvium contains significantly higher percentages of interbedded sand units.

These horizontal differences may be related to different flooding events when a higher sediment load is carried downstream. During floods, the Swan River is also higher and extends beyond its normal flow path. Although flow velocity in the main channel may be high enough to carry the coarser sediment load further downstream, flow velocities on the overflow banks would likely be lower resulting in deposition of coarser sediment. The higher percentage of sand and interbeds of sand near the sides of the main channel may also be attributed to deposition of windblown sand between flood events.

4. Limitations and Further Work

4.1. Limitations

The geotechnical assessment completed to estimate the position of palaeochannels beneath the Burswood Peninsula has involved interpretation of test results in order to create geological units. This interpretation has attempted to simplify a relatively complex geological system in order to provide a better overall understanding of site geology and provide input into specific geotechnical assessments.

All interpretation of geological information must contain a certain degree of subjective assessment and this interpretation along with the surface estimation completed with the EVS software will invariably introduce error into the model. It is important to understand the assumptions used to create the model in order to evaluate potential errors and understand the limitations of geological models.

4.2. Further Work

The geological and geotechnical information available could be further differentiated, particularly components of the Perth Formation. Further differentiation of the Perth Formation could;

- better define the extent of MIS4 and MIS6;
- better define the depositional extent of MIS6 sediments in the wider Perth area
- highlight differences with the Guildford Formation, which these sediments have previously been in
- provide insight into the depositional history of the greater Perth Area.

5. References

Commander, P. (2003). Outline of the geology of the Perth Region, *Australian Geomechanics*, Vol. 38 (3), p. 7 – 16.

Gordon, F.R. (2012). *Geology of quaternary coastal limestone of Western Australia*. PhD Thesis, Department of Applied Geology, Curtain University, Western Australia, September 2012.

Gordon, F.R. (2003). Sea Level Change and Palaeochannels in the Perth Area, *Australian Geomechanics*, Vol. 38 (4), December, 85 – 90.

Gozzard, B. (2007). The Guildford Formation Re-Evaluated. *Australian Geomechanics*, Vol. 42 (3), p. 59 – 80.

Hudson-Smith, E., Grinceri, M. (2007). Ground conditions and building protection for the new metrorail city project, Perth. *Australian Geomechanics*, Vol. 42 (3), p. 33 – 58

Kendrick, G.W., Wyrwoll, K-H. and Szabo, B.J., 1991, Pliocene-Pleistocene coastal events and history along the western margin of Australia. *Quaternary Science Reviews*, Vol. 10, p. 419 – 439.

Marsh, J.G. (1967). Planning of Projects – Earthworks. An application of sand drains to road embankments construction in Western Australia. *Permanent International Association of Road Congresses. XIII Congress*, Tokyo, 1967.

Quilty, P.G. (1974). Cainozoic stratigraphy of the Perth area. *Journal of the Royal Society of Western Australia*, Vol. 57, p. 16 – 29.

Shackleton, N.J. Opdyke, N.D. (1973). Oxygen isotope and paleomagnetic stratigraphy of equatorial Pacific core V 28. Vol. 238. Oxygen isotope temperatures and ice volumes. *Quaternary Research*, Vol. 3, p. 39 – 55.

Tutton, M.A. (2003). Engineering geology of Fremantle harbour. *Australian Geomechanics*, Vol. 38 (4), p. 91 – 102.

Proceedings of the 10th ANZ Young Geotechnical Professional's Conference – 10YGPC
Noosa, Queensland, Australia
10 – 12 September 2014

DESTROYING THE STRUCTURE OF HALLOYSITE CLAY THROUGH OVEN DRYING

Christopher LENTHALL
Golder Associates, Melbourne, Australia

ABSTRACT – Halloysitic soils may develop in areas where volcanic ash is exposed to intense tropical weathering in high rainfall climates. It can exhibit unusual characteristics when tested using conventional geotechnical laboratory techniques due to the sensitivity of the clay minerals and soil structure to high temperatures and low humidity. The effect of low temperature oven drying on Atterberg Limit classification testing is analysed through comparison of a range of drying and rehydration tests. Test results indicate that low temperature oven drying at 40^{o}C alone does not prevent the transition of halloysite to metahalloysite and may lead to the incorrect classification of halloysite soil. However, analysis of the results of drying tests in conjunction with Atterberg Limit classification test results may better represent the behaviour of halloysite clay in accordance with USCS protocols and the Casagrande plasticity chart.

1. The genesis of halloysitic clay

Halloysite is formed when alternating kaolinite clay minerals and water molecules form delicate hollow cylindrical nanotubes. Typically derived from the weathering of volcanic ash soils and rock in tropical environments, halloysite can exist in two distinct wet states; as hydrated halloysite or dehydrated metahalloysite. Like other soils of the Andosol group, such as allophane, halloysite develops where intense weathering processes leach minerals such as silica and magnesium oxide from the soil profile, resulting in remnant soils rich in iron and aluminium oxides. Although more abundant in tropical climates, halloysite may develop in temperate environments under contain conditions, such as those found in New Zealand (Wesley 2009). In some areas with very high rainfall and no significant dry season, strong interparticle bonding resulting from the dehydration of aluminium and iron sequioxides to form aggregations (Fookes, 1997) is prevented, allowing halloysite rich residual soils to remain in a natural hydrated form.

The structure of natural hydrated halloysite clay retains water in three distinct ways; as adsorbed water on the outside of the halloysite tubes, as interlayer water within the tubes as depicted in Figure 1 and as water molecules within the kaolinite crystalline lattice structure.

Some adsorbed water may be drawn out of the soil mass at room temperature, as for many soils, whereas the interlayer water may be partially expelled at temperatures over 50^{o} C or relative humidity less the 50% (Fookes, 1997). The mobilisation of the interlayer water (also referred to as "water of hydration") marks the transition from hydrated halloysite to metahalloysite. The dehydration of halloysite to metahalloysite is an irreversible process and may result in the splitting or unrolling of the tubes (Mitchell, 1976). Ross and Kerr (1934) provide evidence that suggests the water retained in the kaolinite lattice of halloysite is

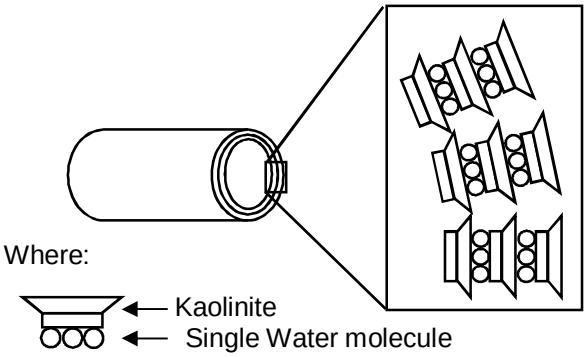

Figure 1. Interlayer water within a halloysite nanotube

expelled at a temperature of approximately 400^{o}C to 550^{o}C. The specific conditions required for the formation and preservation of hydrated halloysitic residual soil are key to understanding the behaviour of the clay if conditions are changed. How changing conditions affect soils is a fundamental question of geomechanics, but it's the dramatic and irreversible nature of the changes that can occur in halloysite that can be misinterpreted if viewed under the microscope of conventional soil mechanics.

This paper describes one instance in which both conventional and specialist laboratory testing was used to identify residual hydrated halloysite at an earthworks site. The identification of halloysite through this assessment enabled the project to revaluate the suitability of the local soil for use as engineered fill. The original prescribed earthworks specification was replaced with a method specification for the placement of the local soils, resulting in significant project savings.

2. The site

At a construction site in Papua New Guinea, an earthworks programme was designed to level a

mildly undulating greenfields site to establish a base on which an array of low rise structures with interconnected pavements would later be constructed.

The site has a recorded mean annual rainfall of 3400 mm and a mean relative humidity of between 67% and 94%. The region has relatively constant and predictable weather patterns with records showing the area experiences light to moderate rainfall on 25% of days throughout the year (www.weatherspark.com, 2014). However, it is the author's experience that very light rainfall occurs on a near daily basis. The region does not experience a dry season.

The region is scattered with volcanic cones, both active and dormant and is a geologically young land mass experiencing rapid uplift. The prevailing near surface geological units are understood to be Quaternary Age and include basalt, tuff and 'uplifted marine sediments' (Geological Survey of PNG, 1989).

3. The soil investigation

Two independent intrusive geotechnical investigations were undertaken across the project site. The first investigation, which included the drilling of 16 solid auger boreholes, aimed to broadly classify the soil at the site and to confirm information from publically available sources. The second was instigated by the primary contractor to confirm the findings of the first investigation and provide geotechnical recommendations for the development. The author was involved in the second investigation and supervised the excavation of 71 test pits.

The timeline of the project was such that the results of the first investigation were made available to the author following completion of the secondary site investigation.

The scope of the second investigation was established to classify the soil for use as engineered fill in accordance with a typical earthworks specification, provided by a third party consultant.

A suite of geotechnical laboratory tests was planned, involving nine different test types, including Atterberg Limit Classification testing, to test the soil compliance against the specification.

Between the completion of the secondary field investigation and commencement of the laboratory testing programme, the author received the final report from the first geotechnical investigation, indicating the local soil was not suitable for use as engineered fill because the soil exhibited the behaviour of a high liquid limit silt, which is identified as generally unsuitable material for engineered fill in Section 4.3 of Australian Standard AS3798-1997.

3.1 Initial laboratory investigation

The majority of Atterberg Limit classification tests undertaken on samples recovered during the first investigation recorded liquid limits in excess of 70-90% and plastic limits of around 20-40%. The soils, initially identified as high plasticity clay in the field by a geotechnical engineer, were re-classified in accordance with USCS protocols as silt, based on the laboratory test results. The geotechnical field engineer coordinating the first investigation noted the discrepancy between the field and laboratory classifications and questioned the preparation procedures of the laboratory undertaking the testing. However, based on the high liquid limit test results, the field engineer recommended that the site be classified as Class H1 to E in accordance with Australian Standard AS2870-2011. Further to this, the first geotechnical report recommended that 'alternate material be used as engineered fill'.

3.2 Secondary laboratory investigation

During the secondary test pit investigation, a visual and tactile assessment of the soil profile by the author indicated it has cohesive properties, typical of high plasticity clay. The discrepancy between the author's field observations and the results of the laboratory test results from the first investigation provided a clear indication that the soil would not behave as typical clay.

At the request of the client, further Atterberg Limit classification testing was undertaken on a broad range of samples collected during the test pit investigation. The results of the classification tests are presented in Figure 2. The classification tests presented in Figure 2 were undertaken in accordance with AS1289 and indicate the tested soil has the mechanical properties of an organic clay or high liquid limit silt. The samples were oven dried at 40°C and sieved prior to classification using the one point Casagrande cup method.

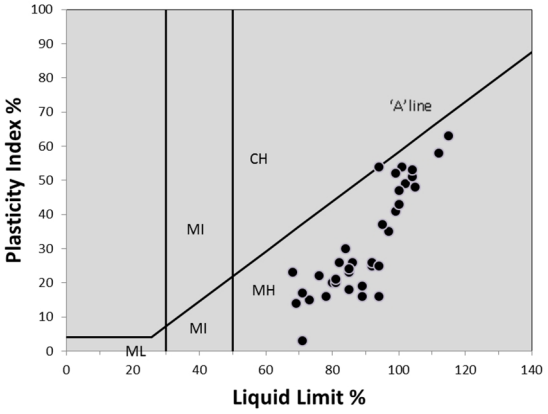

Figure 2. Atterberg Limit test results - oven dried during preparation at 40°C (36 Samples)

During preparation and testing, laboratory personnel indicated that the soil was difficult to work with and noted that it exhibited non plastic properties during testing. The Atterberg Limit test results, plotted on Figure 2, support the notion that the soil samples behave as silt during testing even though they display plastic properties prior to testing.

A side by side visual assessment of retained field samples and the sample subset used during classification testing showed a clear change in the soil structure. Hard spherical aggregations up to 2 mm in diameter were evident within the oven dried (40^{o}C) samples. A literature review revealed that the observations were consistent with the findings of Mitchell and Sitar (1982) who noted that "when allowed to dry, hydrated halloysite clay may form aggregates in the silt and sand size ranges resulting in a complete loss of plasticity." A further literature review of both the results of the Atterberg Limit tests and geological setting supported the notion that the soil may contain sensitive soils such as halloysite or allophane.

4. Confirmation of halloysite

The results of the laboratory testing indicated the potential presence of structurally sensitive soil. Further laboratory testing was requested to assess the mineralogy and structure of the soil with the aim of potentially developing a method to use the local soil as engineered fill. Fookes' (1997) assertion that the water within the clay mineral structure of halloysite is "inert and has no influence on the mechanical behaviour" of the soil mass raised the question of whether the initial recommendation to source alternate fill material was still valid, based on a potentially flawed interpretation of the test results.

Select samples were sent to Adelaide University for mineralogical testing to confirm the potential presence of halloysite and or allophane. The testing programme included scanning electron microscopy (SEM), x-ray diffraction and oxalate chemical analysis.

SEM images were captured with a maximum magnification of 300,000. Figure 3 shows the results of one SEM image

The results of the SEM analysis indicated that the soil samples sent for testing predominantly consisted of hydrated halloysite clay. The measured tube lengths and diameters were similar (slightly less) to the findings of Bordeepong et al, (2011). The SEM results were supported by the results of X-ray diffraction testing and oxalate analysis.

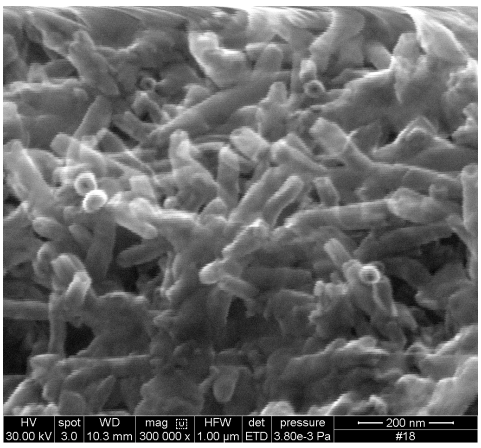

Figure 3. Hollow tubes approx. 35 - 50 nanometres in diameter and 150 - 190 nanometres in length.

5. Influence of oven drying halloysite

To further investigate the influence of oven drying halloysite clay, three suites of tests were performed on select samples. The first suite was undertaken to compare the difference between Atterberg Limit classification test results for samples tested at natural moisture content and samples oven dried at 40^{o}C during preparation. The second suite was undertaken to compare the difference in Atterberg Limit classification test results for samples oven dried at 40^{o}C during preparation and samples allowed to air dry. The third test was undertaken to investigate the capacity of a 40^{o}C oven (compared to a 105^{o}C oven) to remove the water of hydration from the halloysite clay. The sub-samples used during test 1 and test 3 were taken from the same bulk samples, the samples used for test 2 were taken from alternate, but visually similar bulk samples.

5.1 Natural moisture vs 40^{o}C oven drying (1st Test)

Seven soil samples were split for Atterberg Limit classification testing, both at natural moisture content (as sampled in the field – non-dried) and following standard dry-sieve preparation procedures using a 40^{o}C oven (non-humidity controlled) . A visual assessment indicated that negligible oversize material (>425 µm) was present in the non-dried samples. The results of the classification tests are presented in Figure 4.

The results indicate a distinct difference in liquid limit and corresponding plasticity index between the two data sets, with the non-oven-dried samples recording a higher liquid limit on each occasion. On average, the plastic limit was observed to remain the same for each data set. A summary of the results is provided in Table 1.

Table 1. Difference in Atterberg Limit test results for oven dried (40°C) and samples prepared at natural moisture content

Sample ID	Difference in Liquid Limit	Difference in Plastic Limit
1	31	-4
2	46	0
3	17	2
4	18	-9
5	28	4
6	25	-3
7	38	4
AVERAGE	**29**	**-1**

The difference in liquid limit and plasticity index is consistent with the findings of Morin and Todor (1975) for a site in Papua New Guinea, demonstrating the effect of similar testing.

The variability in results shown in Figure 4 demonstrates that sample preparation procedures did affect the Atterberg Limits for the samples tested and that the observed variability is consistent with the findings of similar testing on samples of inferred andosol soils. Interestingly, the test results for the natural moisture content samples also plotted below the A-line, indicating the soils still behaved as silt, despite having observable cohesive properties.

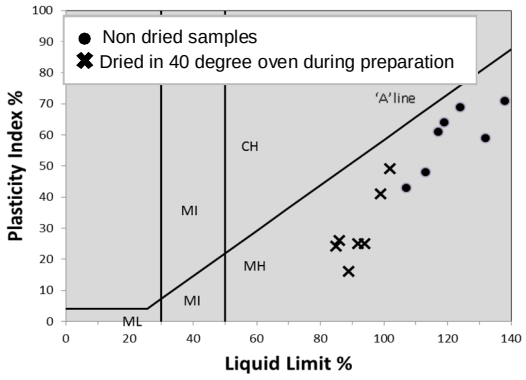

Figure 4. Atterberg Limits obtained form samples prepared via low temperature oven (40°C) and at natural moisture content (7 Samples)

5.2 Air dried sample preparation (2nd test)

For this suite, six samples were air dried in a room open to outdoor air flow, prior to testing. The average ambient air temperature during this time in Melbourne was 18°C with an average relative humidity of 56% (www.bom.gov.au, 2014). The results of the tests are shown in Figure 5 and indicate that samples not subjected to high temperature or low humidity conditions plotted closer to the A-line than those oven dried at 40°C.

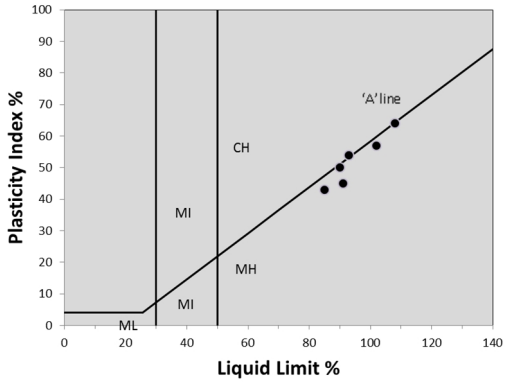

Figure 5. Air dried Atterberg Limit results (6 Samples)

5.3 Drying Test (3rd test)

Seven samples were split and placed in either a 40°C oven or 105°C oven for a period of 103 hours.

The ovens used for the drying test were simultaneously used to undertake non-project related laboratory testing for other projects. Although the influence of temperature variation due to the sporadic addition and removal of samples from the ovens during the drying test has not been considered in this assessment, it is however expected that during the test, oven temperatures will have temporarily dropped below the target temperature and the relative humidity in the ovens will have spiked when new samples were added to the oven, before returning to equilibrium conditions.

Although not a strictly controlled environment, this is typical of a commercial geotechnical laboratory and reflects typical industry standard testing conditions. It is expected that the humidity in the ovens would return to near zero after an extended period, depending on the moisture content of the samples in the oven.

Over the 103 hour drying period the moisture content of all the samples was measured nine times and was seen to stabilise in the final 24 hours to within 0.4% (by mass) for the samples in the 40°C oven and 0.1% (by mass) for the samples in the 105°C oven. The total measured moisture loss in the samples dried in the 105°C oven was used to infer the initial moisture content of the split bulk sample (i.e. the samples in the 105°C oven are assumed to have reached a moisture content of zero after 103 hours for the purposes of this comparison).

The stabilised moisture contents of the samples dried in the 40°C oven were generally greater than those in the 105°C oven. The moisture content differential after 103 hours of drying is shown in Table 2.

Table 2. Variation in moisture content of samples from 40°C and 105°C ovens after 103 hours drying

Sample ID	Natural MC	Variation in final MC of 40°C Sample from 105°C sample
1	69.3 %	+3.2 %
2	54.0 %	+1.3 %
3	72.6 %	+4.0 %
4	61.0 %	+2.6 %
5	59.4 %	+3.0 %
6	51.6 %	0.0 %
7	55.7 %	+4.9 %
AVERAGE	**60.5 %**	**+2.7 %**

A plot showing the average of the calculated moisture content for the seven samples over time is shown in Figure 6. The shape of the curve shown in Figure 6 generally reflects the pattern seen in each individual sample, except for Sample 6, in which the calculated moisture content for the sample in the low and high temperature ovens was seen to converge between 60 and 103 hours.

Following the 103 hours of oven drying, all samples were stored on a shelf and allowed to rehydrate in room temperature conditions for a further 180 hours, during which time the mass of the samples was measured seven times. The mass of all samples was measured to increase by between 2.4 and 5.7 %. The increase in mass is inferred to be the result of water adsorbing to the clay from the humidity in the atmosphere.

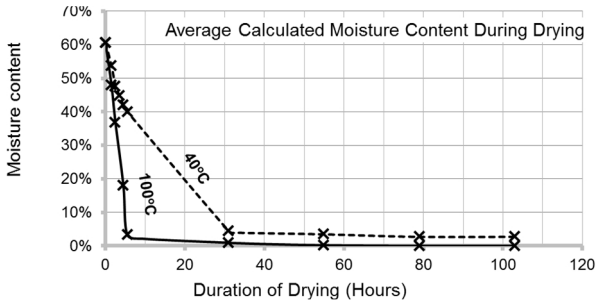

Figure 6. Average Calculated MC during Drying

After 190 hours the mass of adsorbed water from the atmosphere was seen to stabilise, as shown on Figure 7. The measured mass of the samples was seen to fluctuate between 190 hours and 280 hours (with a reduction in average moisture content during this time of 0.1%). This fluctuation is inferred to reflect the changes in atmospheric condition (temperature and humidity) in the room over the rehydration period. The average relative humidity for Melbourne over the drying period was 56%.

To quantify the effect of oven drying the samples, a third subset of the original seven samples was allowed to air dry from the as-sampled field moisture content. After 220 hours, the samples allowed to air dry had reached a constant mass. The results for air drying are summarised in Table 3 and are plotted on Figure 7.

Table 3. Moisture content of samples after 240 hours of air drying at room temperature

Sample ID	Natural MC	Moisture content after 240 hours of air drying
1	69.3 %	44.0 %
2	54.0 %	25.6 %
3	72.6 %	47.9 %
4	61.0 %	38.4 %
5	59.4 %	34.1 %
6	51.6 %	27.1 %
7	55.7 %	30.1 %
Average	**60.5 %**	**35.3 %**

If it is assumed that the percentage of adsorbed water (as a percentage of the soil mass) was similar for all samples in equilibrium conditions (stored in the same location), then the difference in final moisture content of the samples dried in the 40°C and 105°C ovens (then allowed to rehydrate) and the air dried samples is inferred to represent the water of hydration in the samples tested.

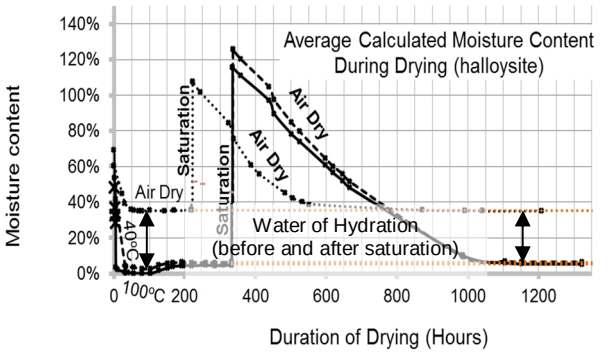

Figure 7. Equilibrium MC of samples in ambient air conditions (7 sample averages)

Fookes (1997) asserts that "the loss of water of hydration in a pure halloysite is equal to 14% of the dry soil weight." The samples analysed in this study were assessed to be predominantly halloysite. However, other clay minerals were inferred to be present within the samples during x-ray diffraction and oxalate analysis.

The measured difference in the equilibrium moisture content of the air dried samples and the samples dried in the 105°C oven was 29.9 % ± 0.1%. This suggests the water of hydration in the samples analysed is approximately 29.9%. By extension, this suggests that the low temperature oven was able to expel 27.2% of the 29.9% water of hydration in the samples. The inference that the difference in moisture content after 220 hours reflects the water of hydration was further tested by saturating all sample sets then allowing them to air dry for a further 1000 hours (approximate). The moisture contents of the samples after 1200 hours

were measured to be the same as they were prior to saturation (See Figure 7). This confirms the permanent nature of the loss of water of hydration.

For comparison, three samples of residual basaltic clay (inferred to be predominantly montmorillonite) were dried for 270 hours then allowed to rehydrate. The moisture contents of the samples were seen to converge during rehydration, following drying (see Figure 8), suggesting the moisture loss is temporary in montmorillonite.

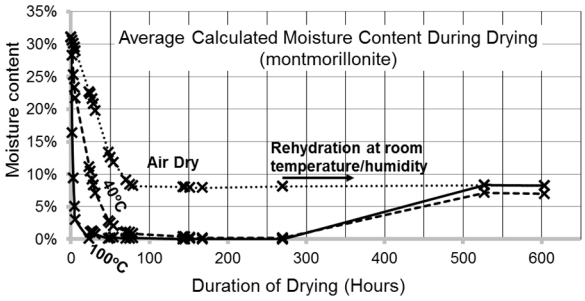

Figure 8. Equilibrium MC of montmorillonite samples in ambient air conditions (3 samples)

6. Discussion

From the results of the drying test it can be inferred that, in industry standard conditions, a low temperature (40°C) non-humidity-controlled oven can expel the water of hydration from halloysite clay samples. If the high temperature oven is assumed to remove 100% of the water of hydration from the samples and the water of hydration is assumed to represent 29.9% of the soil mass, the low temperature oven may be inferred to expel up to 91% of the water of hydration, if the relative humidity is allowed to approach zero. This suggests that an industry standard laboratory oven at 40°C (in which the humidity in the oven is not controlled), will mostly convert hydrated halloysite to metahalloysite. This is consistent with the findings of Brindley and Goodyear (1948), that suggest a relative humidity of 15% (even at low temperatures) may expel the majority of interlayer water from halloysite.

If the interlayer water within the halloysite tubes is "inert and has no influence of the mechanical behaviour" (Fookes, 1997), then a true account of the physical behaviour for a soil mass (reflected in Atterberg Limits) should exclude this water.

The long term air dry test indicated that the samples lost, on average, approximately 25.2% moisture from as-sampled condition when left open to the ambient air conditions in Melbourne.

If the soils tested contained approximately 29.9 % water of hydration and this quantity is subtracted from both the Liquid and Plastic Limits for the samples analysed in Test 2 (plotted on Figure 5) then the 25.2 % water estimated to have been lost during air drying is added to the Atterberg Limits, then the results generally plot above the A-line, as shown in Figure 9.

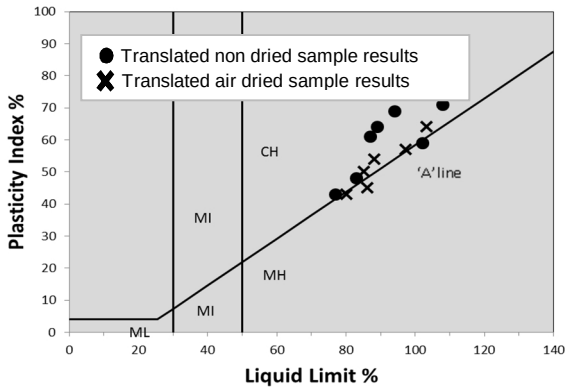

Figure 9. Revised Atterberg Limit plot

In Figure 9 the Atterberg Limits (less the calculated water of hydration, plus the water lost during air drying) are shown as crosses. Similarly, if the Atterberg Limits of the non-dried samples (plotted as dots on Figure 5) are reduced by 29.9% for comparison with the air dried samples, they plot in a similar location on Figure 9. The results shown in Figure 9 match the author's expectation of the physical behaviour of the soil.

The translation in position on the Atterberg Limit chart cannot be applied to the results presented on Figure 2 or the low temperature oven dried results presented on Figure 4. These results reflect the properties of the soils after the clay structure has been changed from halloysite to metahalloysite.

7. Conclusions

Test results indicate that low temperature (40°C) oven drying of hydrated halloysite clay does not prevent the destruction of the soil structure for Atterberg Limit classification testing. However, characteristic Atterberg Limit test results can be used to identify halloysite.

For the soil tested at this project site, results indicate that up to 91% of the water of hydration may have been expelled from the halloysite clay during oven drying at 40°C. This suggests that even when halloysite clay is identified at a site, conventional wisdom, requiring the use of low temperature ovens, may also lead to Atterberg Limit classification results that do not reflect the in situ mechanical behaviour of the soil. However, by measuring the water of hydration lost during testing, it may be possible to derive Atterberg Limit test results that reflect the in situ mechanical behaviour of the soil.

8. References

Australian Government Bureau of Meteorology, accessed 2 May 2014, <http:www.bom.gov.au>

Bordeepong et al, (2011). Characterization of halloysite from Thung Yai District, in Southern Thailand. Songklanakarin *J. of Sci. and Tech*.

Brindley, G.W and Goodyear, J (1948). *X-ray studies of halloysite and metahalloysite*. University of Leeds, Parts 2 and 3

Cedar Lake Ventures, Inc, 2014, accessed 5 May 2014, <http:www.weatherspark.com>

Fookes, P.G (1997). Tropical residual soils. *The Geological Society.*, London

Geological Survey PNG, 1:1000000 map, (1989)

Mitchell, J.K (1976). *Fundamentals of Soil Behavior*. John Wiley and sons Inc., New York

Mitchell, J.K., Sitar N. (1982). Engineering Properties of Tropical Residual Soils. *Proc. of the ASCE Geotechnical Eng. Specialty Conference*

Morin, W.J., Todor, P.C. (1975). Laterite and Lateritic Soils and other Problem Soils of the Tropics. *U.S Agency for International Development, Lyon Associates Inc., Baltimore.*

Ross, C.S and Kerr, P.F (1934). *Halloysite and allophane*. U.S Department of the Interior

Wesley, L. (2009). Behaviour and geotechnical properties of residual soils and allophane clays. *Obras y proyectos* 6, p. 5 – 10

This page intentionally left blank

Proceedings of the 10th ANZ Young Geotechnical Professional's Conference – 10YGPC
Noosa, Queensland, Australia
10 – 12 September 2014

DESIGN ASPECTS OF RAIL INFRASTRUCTURE OVER SOFT GROUND

Cillian McCOLGAN (BA, BAI, MSc, DIC)[1], Ben DENING (BSc, IEng, MICE)[2] and Bryn THOMAS (BSc, MSc, PhD, CEng, MIMM, CGeol, EurGeol, FGS)[2]
[1] *Pells Sullivan Meynink (PSM), North Ryde, NSW, Australia (formerly of GHD)*
[2] *GHD, Artarmon, NSW, Australia*

ABSTRACT – A new rail maintenance and refueling facility is to be constructed on a low lying tidal river floodplain with deep deposits of very soft clay in NSW. The proposed facility requires the construction of a fill development platform over 3 km in length and up to 150 m across at its widest point.

A combination of local experience and settlement analysis of existing embankments was used to develop and interrogate design parameters. Settlements of more than 2 m have been predicted at the site. A discussion of the adopted design approach in terms of best estimate, lower and upper bound is also presented.

This paper discusses some of the more challenging geotechnical aspects of the design including; (i) accounting for the effect of re-ballasting to maintain flood levels and rail design criteria (ii) areas where predicted settlements and the interfaces between track and buildings were managed using ground improvement or piled solutions (iii) the design of an embankment under-drainage system capable of accommodating the predicted settlements, and (iv) the design of lighting columns to accommodate excessive settlements.

1. Introduction

Deep soft soils present significant geotechnical design challenges to site development. Such soils will be subject to significant ongoing settlement under loading and design solutions must accommodate or reduce the effect of this. This paper focuses on some geotechnical design aspects for a rail maintenance and refueling facility to be constructed over a site with deep soft soils. Rail embankment formations were required to provide sufficient support to the rail structure whilst presenting manageable maintenance requirements to the infrastructure over the life of the asset. The asset was designed to accommodate predicted settlements of up to 2.8 m over a 50 year facility design life, allowing for track re-ballasting and maintenance.

In addition to providing a suitable platform for track construction, significant challenges were presented with regard to the geotechnical design of buildings and other structures such as signaling and lighting columns. Solutions such as piling and mass ground improvement can provide foundation support though on large sites can result in significant cost. Ground improvement using concrete injected columns (CICs) was adopted where structures required a rigid solution. Where settlement could be tolerated or managed at reduced cost, settlement was allowed to occur.

Specifically this paper discusses:

- The site geology and the formulated geotechnical model
- Settlement prediction and management
- Design of transition zones between buildings and track
- Design of lighting columns to accommodate settlements
- Design of an under drainage system to accommodate settlements

Figure 1 provides a schematic illustration of some key design aspects of the facility.

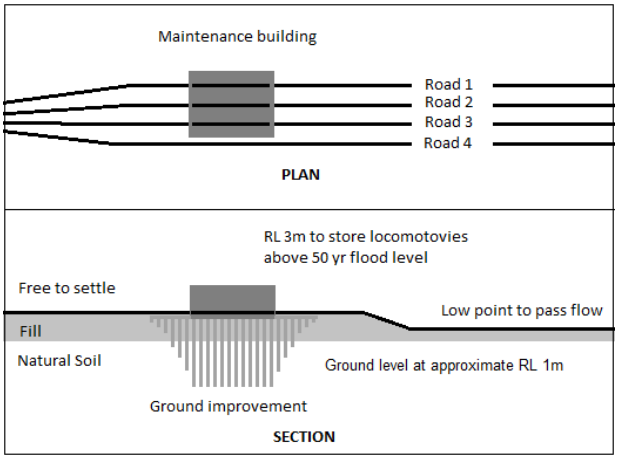

Figure 1 Schematic illustration of different facility requirements at different locations

2. Site Geology and Geotechnical model

The project site is located within a floodplain environment underlain by extensive deep compressible estuarine deposits generally consisting of very soft medium to high plasticity clays with a firm to stiff clay surficial crust of varying thickness. The very soft clays are underlain by older alluvium of stiff clay and occasional bands of

medium dense sand. Bedrock consisting of interlayered sandstone, siltstone and shale was generally not encountered across the site within the majority of available ground investigation exploratory holes, but exists at over 20 m depth based on a single test location. A variable sand – gravel fill layer with old railway ballast and colliery washery waste material was also present on the site reflecting previous site uses. The thickness of the fill layer was highly variable ranging from absent to more than 3 m.

Time and access constraints limited geotechnical investigations to selected locations and where possible focused on buildings. The detailed design was therefore based upon a limited field investigation consisting of boreholes, cone penetration tests (CPT) and test pits. The project data set was complimented by a number of sources of existing information from previous works at the site and on directly adjacent sites. Project specific ground investigations were used to verify the data derived from the existing investigations.

Figure 2 shows an extract from the geotechnical model indicating some of the more prominent features of the site:

- Areas with existing fill material
- The generally horizontally layered sediments
- The presence and absence of sand lenses and a sand under drain
- The thickness of the residual soils, and
- The sedimentary bedrock

The sand lenses were generally found to be randomly distributed across the site. This made it difficult to assess the drainage conditions for consolidation analysis. It is possible that with a denser coverage of ground investigation these lenses could be properly delineated, though their interconnectivity would also need to be assessed and properly accounted for in the analysis.

The over consolidation ratio (OCR) profile of the very soft soil was derived using the relationship of the measured undrained shear strength correlated from the CPT testing with the expected undrained shear strength determined from Mesri (1973). Based on Mesri (1973) a coefficient of 0.22 was selected for the ratio of expected and measured undrained shear strength.

In general typical desiccated soft clay OCR profiles were observed across the site as would be expected in an estuarine environment. Lower OCR's were found where the site was overlain by fill material reflecting the more recent change in stress and the reduced relative impact of desiccation in the crustal layers.

3. Settlement prediction

3.1. Design approach

Settlement prediction is often carried out to assess a range of values on the following basis:

- Best guess – an assessment of what the likely amount of settlement will be
- Lower bound –the likely minimum predicted settlement
- Upper bound –the likely maximum predicted settlement

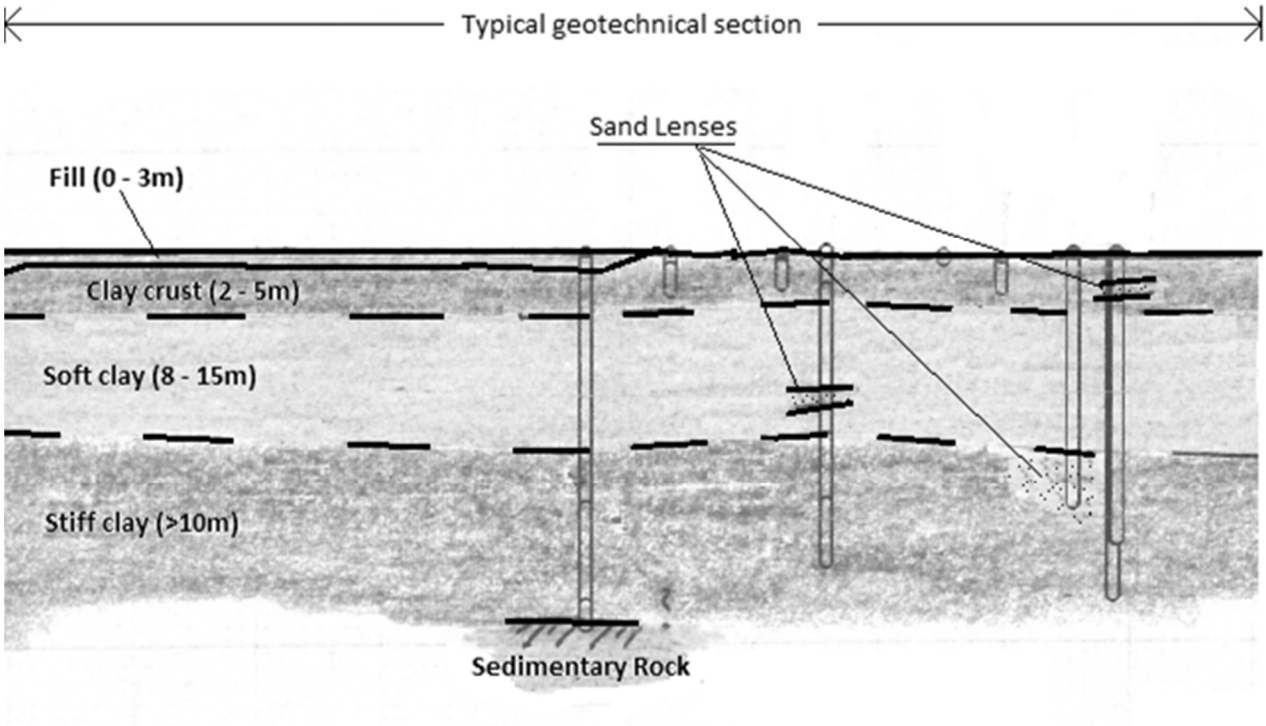

Figure 2. Typical geotechnical section with material thicknesses

An upper bound approach to settlement prediction was adopted for this project. This reflects the following aspects of the site:

- The site will be frequently re-ballasted to maintain operational rail tolerances
- Re-ballasting volumes needed to be costed
- Differential settlements needed to consider the worst possible scenario to understand long term operational risk
- Parts of the site were required to remain above design flood levels for flood immunity

3.2. Parameter selection

Parameter selection for settlement prediction was based on a review of historic and recent projects both within the locality and the same geological environment. Oedometer and soil classification tests for the site were compared to those from these projects and a good agreement was observed. With several site derived parameter sets available from other projects and limited site specific data, the historically derived parameters were adopted as the consolidation parameters. The adopted parameters are listed in Table 1.

Table 1. Consolidation parameters

Parameter	Value
Compression ratio $c_c/(1+e_0)$ (%)	31
Recompression ratio c_r/c_c (%)	15
Creep coefficient c_α (%)	0.143
Creep ratio $c_{\alpha r}/c_\alpha$	10
Vertical coefficient of consolidation c_v (m^2/yr)	8
Coefficient of consolidation ratio c_h/c_v	1.5

3.2 Settlement analysis of tailings dam

A 15 m thisk former coal washery tailings dam was located adjacent to the site and was also founded on the very soft compressible soils. Boreholes through the tailings dam indicated both its thickness and total amount of settlement that had occurred. This information was used in conjunction with the tailings dam operational history to assess the selected parameters. Figure 3 shows the results of the settlement analysis. The investigations indicated that the tailings had settled approximately 3.0 – 5.0 m and the settlement analysis yielded a predicted settlement of approximately 4.0 m.

While a number of assumptions were required to undertake the analysis, (chiefly the rate at which the level of the tailings dam was raised), the

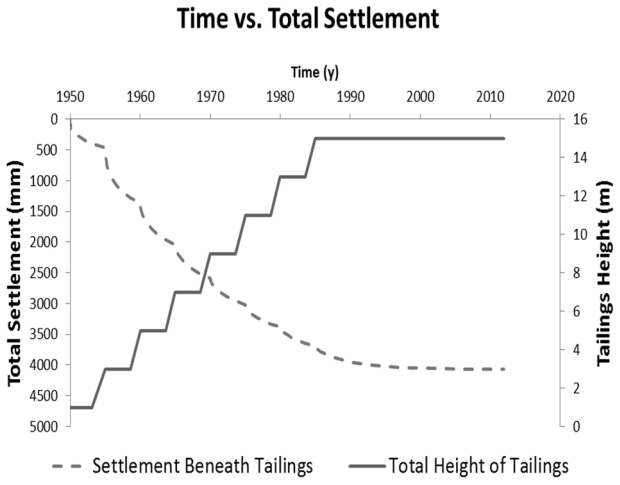

Figure 3. Tailings back analysis

settlement analysis provided a useful sanity check against the derived consolidation parameters. The consolidation parameters were adopted for the project

3.3 Design settlement

Construction of the facility was required to commence less than 12 months after completion of detailed design. The use of preloading was quickly ruled out as an option for management of settlement with the allocated timeframes. Therefore the adopted design approach was to estimate the settlement that would occur at the site taking into account embankment filling and the periodic re-tamping of rail ballast to maintain design levels. The facility was designed such that the predicted settlements would be managed throughout the design life with periodic maintenance and adopting a design that could tolerate the large predicted settlements.

An iterative approach was used to account for periodic refilling and this was modeled using Settle-3D (i.e. 1D consolidation of a 2D stress distribution). The following steps were used in the settlement modeling:

- Load equivalent to the proposed fill height placed at ground level and allowed to settle for 6 months (to simulate construction period)
- Load placed equivalent to the fill required to raise the platform after construction to design level
- Addition load placed following each additional 100 mm of settlement to bring the platform back to design level

For the "worst case' section of the proposed fill platform, total predicted settlement after 50 years of re-ballasting was estimated at between 2.3 and 2.8 m. This is far greater than the 1.3 m to 1.5 m of settlement that would have been predicted if no refilling was accounted for as illustrated in Figure 4.

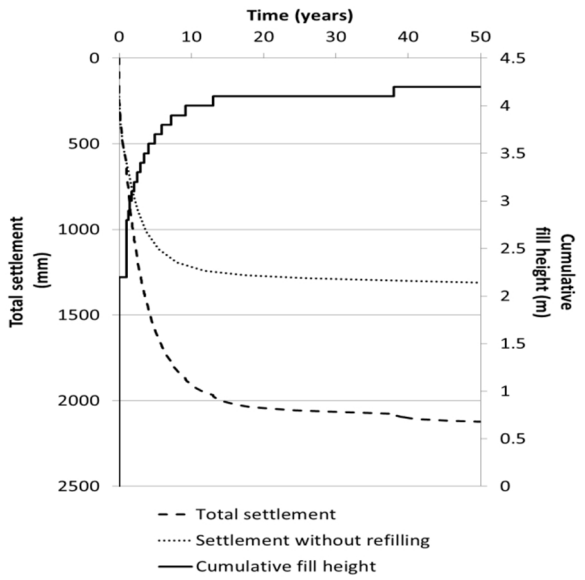

Figure 4. Cumulative fill placed and settlements over 50 year design life

Despite the uncertainties associated with the settlement prediction and the actual timeframe for refilling to occur, it was necessary to make an estimate to better inform the client for planning purposes. It was found that after 50 years of settlement the total settlement was not dramatically affected by the timing of the additional fill placement, rather it was affected by the total amount placed. After 50 years all consolidation is likely to have occurred, with only creep remaining.

4. Managing interfaces with rigid structures

4.1. Transition zones

The earthworks development platform was to be constructed to a level above design flood levels to allow safe locomotive storage and maintenance adjacent to and within buildings. While settlement of the fill platform could be tolerated and remediated by refilling, settlements of the buildings cannot be accommodated. The clients design criteria for the buildings were that settlement should not exceed 50 mm over the 50 year design life. To satisfy this criteria the buildings were construction on fill platforms founded on CICs as shown in Figure 1.

As the railway tracks were to run in and out of the maintenance buildings (Selig and Waters 2000) consideration was required as how to manage the interface between the continuously settling tracks and the (relatively) rigid buildings.

As settlements at the site are very large (up to about 2.8 m), transitioning from <50 mm to up to 2.8 m settlement over a short distance was quickly identified as being a problem for the facility and was likely to lead to unmanageable maintenance requirements in the long term. The rate at which track differential settlement criteria would be violated and track tamping and realignment applied was considered to be unacceptable.

In order to reduce the maintenance frequency at the entrances to these buildings, 'settlement reducing' transition zones consisting of reducing depths of CIC improved ground were designed. 50 m long transition zones were selected based on consideration of capital expenditure versus maintenance in consultation with the client. Longer transition zones would have been expected to further reduce maintenance but would have also increased the capitol cost of the facility and increased the duration of construction

Figure 5 shows the effect of the transition zones. The building is located at chainage 0, where negligible settlement was predicted. The figure shows an increasing amount of track settlement with increasing distance from the building until the unimproved ground is encountered at a distance of >50 m from the building.

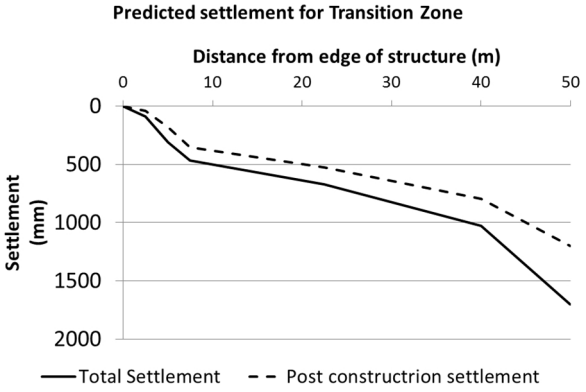

Figure 5. Predicted settlement along a typical transition zone (without refilling)

Table 2 shows the adopted transition zone ground improvement depth profile for one of the buildings. Note that most of the transitioning is focused adjacent to the structure where the maximum differential settlements would be expected to occur.

Table 2 Transition zone CIC improved depths

Distance from edge of structure (m)	Depth of CIC (m)
0 – 5	16*
5 – 10	12.5
10 – 15	7.5
15 – 40	5
40 – 50	2.5

* This corresponds to full depth ground improvement and a 1 m socket in stiffer material from 15 m depth

4.2. Lighting columns

As predicted site settlements were so significant a number of minor structures on the site required incorporation of settlement mitigation measures

within the design to accommodate these predicted displacements to ensure that they would remain serviceable throughout the design life.

Overhead lighting was required to enable 24 hour operation of the facility. This is provided by lighting columns which require provision of access to the lighting column electronics for periodic maintenance. The adopted foundation solution for the lighting columns was floating continuous flight auger (CFA piles). Where the facility was predicted to settle up to 2.0 m or more, these lighting column access points could eventually be underground buried in ballast. Access to the electronics would require construction of a trench (which would itself need to be supported). Alternately re-commissioning a new lighting system could be budgeted for in the future.

To overcome this problem the lighting columns were designed to be installed with a 2.0 m 'upstand' above ground level. This allows for maintenance access to the lighting columns for the majority of the duration of the facilities operation. A higher upstand was considered but 2.0 m was agreed upon after consideration of capital expenditure versus maintenance costs. The lighting columns were also designed with adjustable mountings to accommodate some rotation of the footings due to differential settlement. Figure 6 shows details of the lighting column on a piled foundation with a 2.0m high concrete block upstand and indicated initial and predicted ultimate ground levels.

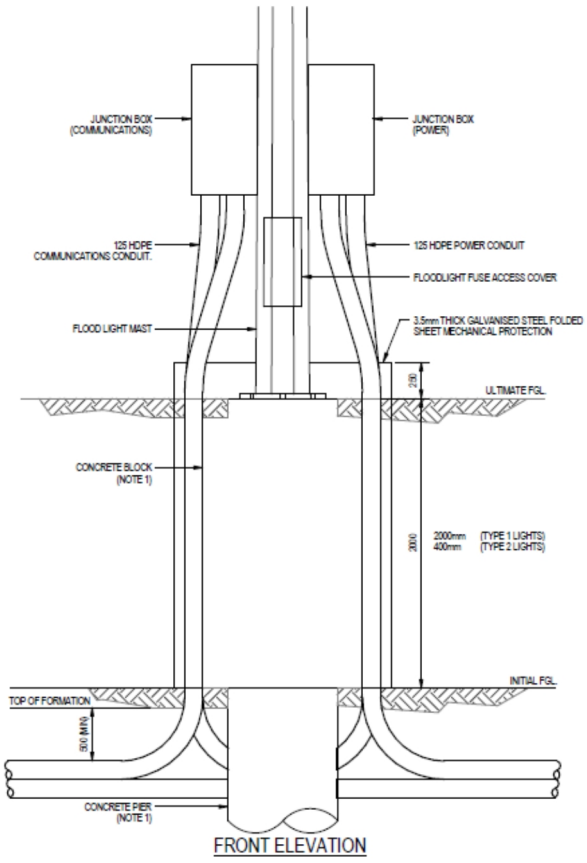

Figure 6. Lighting column upstand and foundations

4.3 Drainage system

The design of the subsurface drainage system was carried out with consideration of the predicted settlements of the development platform, and its likely influence on long term performance of the drainage system. A pit and pipe system was adopted at one end of the site, where the original site level had been raised by approximately 1.0 m to 1.5 m by placement of fill associated with previous site developments. The rationale for this was, as a consequence of the consolidation estuarine clay due to fill placement settlement would be reduced. A drainage layer at the base of the rail pavement was also provided in order to accelerate consolidation settlement and reduce long term impacts on the performance of the site drainage regime.

At the other end of the site, a drainage blanket solution was adopted, due to the lack of existing fill materials and higher predicted settlements.

Where pipes were specified perpendicular to the proposed rail tracks, multiple joints were required to allow for potential deflections resulting from differential settlement due to train and embankment loading.

The fill development platform is underlain by a series of underdrains to redirect surface runoff beneath the tracks to side drainage channels and then drainage basins for later disposal. As predicted settlements at the site were in excess of 2.0 m the drainage system had to be designed to accommodate the following:

- Differential settlement between areas with varying heights of fill
- Rotation resulting from differential settlement
- Elongation resulting from differential settlement

The drainage pits were designed with flexible and extensible connections to accommodate the predicted ground movements as shown in Figure 7.

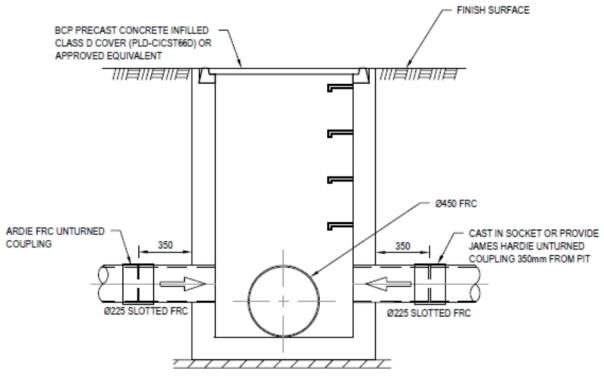

Figure 7. Drainage pit
(note detailing of connections to accommodate rotation and some extension at the joints)

As for the lighting columns, the drainage pits would be subject to changing finished site ground levels over the facilities design life. The pits were designed with this in mind and to allow extension upwards prior to re-ballasting to avoid future burial.

5. Conclusions

The project presented a number of challenges during design which will impact on the construction and operation of the facility. These challenges are related to the settlement that is a result of constructing the facility on soft estuarine soils. The key design aspects considered are:

- Deep very soft soils subject to long term settlements which will have design and operational implications over the 50 year design life of the project
- Geotechnical design parameters were carefully interrogated. Back analysis of settlements experienced by a nearby colliery waste tailings dam proved to be a useful validation exercise in the derivation of consolidation parameters for design
- Transition zones for railway track approaches from the settling development embankment into rigid facility buildings required special consideration. They were designed to be constructed using tapering length CIC's which were used as controlled settlement reducing zones
- Maintenance implications had to be considered in settlement prediction. This design element has long-term cost implications for the client over the 50 year design life of the project
- The design of lighting columns needed to consider long term ground settlements and required a bespoke column foundation design
- A drainage system design was required to accommodate future settlements of the development platform: a flexible pipe to pit drainage solution was adopted where existing fill had consolidated the underlying clay; a drainage blanket solution was used where no existing fill was present
- The overall success of the project has required a flexible detailed design approach based upon fundamental soil mechanics principles and backed up by sound engineering judgment.

6. References

Arulrajah, A., Abdullah, A, & Bouazza, A. (2009). *Ground improvement techniques for railway embankments*. Proc. ICE, Ground Improvement 162, Issue G11, pp.3-14, February.

British Standards (2010). *BS 8006-1: 2010. Code of Practice for strengthened / reinforced soils and other fills.* British Standards Institution, London.

Charles, J.A. (1993). *Building on fill: geotechnical aspects. BRE Report 230*, BRE, Watford, UK.

Hewitt et al (2009) *Bridge Approach Treatment Works on the Coopernook to Herons Creek Section of the Pacific Highway Upgrade*, Australian Geomechanics Symposium October 2009, Sydney

Robertson, P.K. & Cabal (Robertson) K. L. (2010). *Guide to cone penetration testing for geotechnical engineering*. Gregg Drilling & Testing Inc., California. 4th Ed., July.

Selig, E.T. & Waters, J.M. (2000). *Track Geotechnology and sub-structure management*. Thomas Telford, ISBN 0 7277 2013 9.

Standards Australia (2009). *Piling design and installation. (AS2159-2009),* Standards Australia, Sydney.

Mesri, G. "New Design Procedure for Stability of Soft Clays." Discussion, *Journal of the Geotechnical Engineering Division,* ASCE, 101, GT4 (1975): pp. 409 412.

Proceedings of the 10th ANZ Young Geotechnical Professional's Conference – 10YGPC
Noosa, Queensland, Australia
10 – 12 September 2014

UNFIT 24: A COMMONLY USED ROCK STRENGTH MULTIPLIER COMPARED TO SANDSTONE MULTIPLIERS IN SE-QLD and NE-NSW

Mike EVERT[1], John WORDEN[2] and Patrick KIDD[3]
[1] *Civil Engineer, Queensland Transport and Main Roads, Gold Coast, Australia*
[2] *Associate Professor, University of Southern Queensland, Toowoomba, Australia*
[3] *CPGeo CPEng RPEQ NPER, Snowy Mountains Engineering Corporation, Gold Coast, Australia.*

ABSTRACT - This paper examines the engineering issues relating to the utilisation of a commonly used rock strength multiplier with Sandstone in Southeast Queensland (SE-QLD) and Northeast New South Wales (NE-NSW).

For this paper, rock strength results in SE-QLD and NE-NSW are compared to results of other published studies made in SE-QLD.

1. Introduction

A common practice is to estimate uniaxial compressive strength (UCS) by multiplying the point-load strength index of 50mm core (I_{s50}) by a factor of 24 when planning civil infrastructure (i.e. UCS ≈ 24 I_{s50}). The use of the multiplying factor of 24 was established by the collective work of E. M. Broch and J. A. Franklin (1972) and accepted by the *International Journal of Rock Mechanics and Mining Science* later that year. UCS and I_{s50} are both measured in units of megapascals (MPa). I_{s50} values are also used in *AS1726-1993 Geotechnical site investigations* to indicate the scale of strength of rock material.

The original intention of this common multiplier was for use in testing high strength rocks, however, there has been wide spread use in the geotechnical engineering community of using 24 as a general multiplier, leading to deficiencies in estimating rock strength at various locations, as significant departure from this multiple value has been identified to occur in various rock types and various grades of weathering.

The problem arises as the commonly used multiplier of 24 can often overestimate, and sometimes underestimate, the actual rock strength in a specific area. Site specific parameters, rock types and degrees of weathering are important modifiers of UCS values and cannot be represented with one generalised integer multiplier. Rock fabric has an important impact on point load tests, as well as UCS tests. An inaccurate UCS may yield a Factor of Safety (FoS) that can be grossly inaccurate and result in an under-designed civil engineering structure that can fail, ultimately putting public safety at risk.

In contrast to using a universal multiplier, using I_{s50} with a site specific multiplier holds a significant advantage in allowing the testing of a large number of samples in the field at a modest cost, providing a better impression of the variability in intact rock strength than afforded by a comparatively small number of UCS tests, which incur a greater expense.

2. Background

The pivotal paper by Broch and Franklin (1972), was one of the first to recognise a relationship between the results of UCS and point-load testing. The authors proposed that a standard testing procedure be employed for point-load tests, and that the point-load test should be used as standard for strength classification of rock material replacing the UCS test usually employed for this purpose. Furthermore, they nominated a ratio for UCS : I_{s50} of 23.7, although this was derived from testing completed upon a limited number of rock types.

Broch and Franklin (1972) based their proposal on fifteen rock samples; 15 UCS tests and 15 point-load tests on 38mm core corrected to 50mm which, when plotted, provides with a straight line correlation whose slope (23.7) passes very near to the origin. The Broch and Franklin (1972) regression is reproduced in Figure 1.

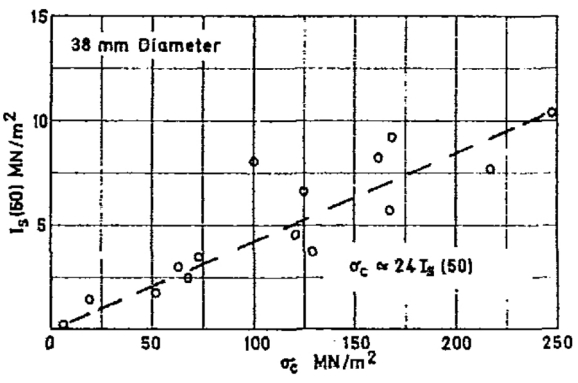

Figure 16. UCS & I_{s50} correlation (from Broch & Franklin, 1972)

The value of 23.7 was stated by the authors as conditional since it was based on limited results for a limited number of mostly high strength rock types, and the authors had only limited experience in using the test or interpreting the results in terms of field performance. It is noted that the Broch & Franklin core samples were smaller than core samples typically used in practice today such as NQ3 (50mm), HQ3 (65mm) or PQ3 (85mm).

Since Brock and Franklin published their paper in 1972, many authors have also conducted reviews of this topic worldwide and have conclusively established that rock strength multipliers are relevant to specific rock types and affected by degrees of weathering (e.g. Read, Thornton & Regan, 1980; Tomlinson, 1995; Thuro & Plinninger, 2001; Look & Griffiths, 2001; Look & Griffiths, 2004; Ferner, Kahraman, Bilgil & Gunaydin, 2005; Basu & Aydin, 2006; Look, 2007; Cobanoglu & Celik, 2008; Gu, Tamblyn, Lamb & Ramsay, 2008).

To elaborate further, Ferner et al. (2005) listed twenty-six studies published between 1964 and 2004 (refer in Table 1) in which the correlation between UCS to the I_{s50} on a range of locations, rock types and degrees of weathering. The multipliers and equations were shown to vary widely. The wide dispersion of multipliers and variable regression intercepts between 9 and 60 (when I_{s50} = 1 MPa) for weak and strong rocks demonstrate the need to regularly re-assess the applicability of the original multiplier of 24 on a site- or material-specific basis.

It is noted that some studies included in Ferner et. al. (2005) (i.e. Table 1) target weaker rocks (Singh, 1981; Smith, 1997; Palchik & Hatzor, 2004; Tsiambaos & Sabatakakis, 2004), with Marinos & Hoek (2001) also stating that UCS estimates from I_{s50} are highly ambiguous when UCS < 25 MPa.

Thuro and Plinninger (2001) encapsulate this theme, inferring there is no single factor applicable to all rock types.

Data from Tomlinson (1995), and also Look & Griffiths (2004), published in the *Handbook of Geotechnical Investigation and Design Tables* (Look, 2007), outline rock strength multipliers for Brisbane and the Gold Coast that include data from within the coastal sediments (i.e. sandstone). Ratio data for sandstone from the City of Gold Coast (CGC) and Brisbane (BNE) region (Look op. cit.) varied from 10 to 12.

Table 6. Equations correlating UCS to Is50 on a variability of locations, rock types and weathering. (Ferner et al., 2005)

Reference	Equation
D'Andrea et al. (1964)	$UCS \approx 15.3\ I_{s50} + 16.3$
Deer and Miller (1966)	$UCS \approx 20.7\ I_{s50} + 29.3$
Broch and Franklin (1972)	$UCS \approx 24\ I_{s50}$
Bieniawski (1975)	$UCS \approx 23\ I_{s50}$
Hassani et al. (1980)	$UCS \approx 29\ I_{s50}$
Read et al. (1980) Sedimentary	$UCS \approx 16\ I_{s50}$
Read et al. (1980) Basalts	$UCS \approx 20\ I_{s50}$
Singh (1981)	$UCS \approx 18.7\ I_{s50} – 13.2$
Forster (1983)	$UCS \approx 14.5\ I_{s50}$
Gunsallus and Kulhawy (1984)	$UCS \approx 16.5\ I_{s50} + 51.0$
ISRM (1985)	$UCS \approx 20…25\ I_{s50}$
Vallejo et al. (1989)	$UCS \approx 8.6…16\ I_{s50}$
Cargill and Shakoor (1990)	$UCS \approx 23\ I_{s50} + 13$
Tsidzi (1991)	$UCS \approx 17…82\ I_{s50}$
Ghosh and Srivastava (1991)	$UCS \approx 16\ I_{s50}$
Grasso et al. (1992) Power relation	$UCS \approx 25.67\ I_{s50}^{0.57}$
Grasso et al. (1992) Linear relation	$UCS \approx 9.30\ I_{s50} + 20.04$
Chou and Wong (1996)	$UCS \approx 12.5\ I_{s50}$
Smith (1997)	$UCS \approx 14.3\ I_{s50}$
Kahraman (2001) 22 different rock types	$UCS \approx 8.41\ I_{s50} + 9.51$
Kahraman (2001) Coal measure rocks	$UCS \approx 23.62\ I_{s50} – 2.69$
Quane and Russel (2003) Strong rocks	$UCS \approx 24.2\ I_{s50}$
Quane and Russel (2003) Weak rocks	$UCS \approx 3.86\ (I_{s50})^2 + 5.65\ I_{s50}$
Tsiambaos and Sabatakakis (2004) Power relation	$UCS \approx 7.3\ I_{s50}^{1.71}$
Tsiambaos and Sabatakakis (2004) Linear relation	$UCS \approx 23\ I_{s50}$
Palchik and Hatzor (2004)	$UCS \approx k_1 e^{-k} 2^n\ I_{s50}$

3. Experimental Approach & Methodology

The 1:500,000 Moreton Geological Map (Cranfield et al., 1980) indicates that SE-QLD and NE-NSW are underlain by Neranleigh-Fernvale beds, coastal sediments, Chillingham volcanics and Tweed volcanic basalts. The rock types that are commonly encountered within the Neranleigh-Fernvale beds comprise phyllite, argillite, meta-greywacke, arenite, quartz-arenite, quartzite and shale. The Neranleigh-Fernvale beds have been subject to variable regional metamorphisms resulting in weak to strongly foliated, interbedded rock types of varying weathering and strength. The coastal sediments have produced cemented sandstone and the Chillingham volcanics are mostly rhyolitic pyroclastics of late Triassic age.

The rock type evaluated in this study is sandstone. The rationalised sandstone data is

compared to other work previously completed in SE-QLD (Look, 2007). Core samples were extracted in accordance with *AS 4133.5-2002*, whilst UCS and point-load tests were conducted in accordance with *AS 4133.4.2.1-2007 and AS 4133.4.1-2007.*

The compilation and publishing of this rock testing data was directed towards determining the relevance of rock strength multipliers as a general assumption and recommendations for revised rock strength multiplier for a:

- Different rock type.
- Similar rock type in different areas (i.e. variability or range within a rock type).
- Different degree of weathering for the evaluated rock type.

Interestingly there was one common element (rock type) between local studies and that is sandstones from a range of sites within the region:

- FR sandstone (Wyaralong Dam, SE-QLD),
- DW sandstone (Banora Point, NE-NSW)
- DW sandstone (Gold Coast, SE-QLD) and
- DW sandstone (Brisbane, SE-QLD).

4. Results and Discussion

4.1. R^2 analysis

SMEC kindly provided access to some unpublished data to the senior author when he undertook a final year engineering project at University of Southern Queensland. The provided data was obtained to assess the rock strength underneath major infrastructure projects; the Wyaralong Dam in SE-QLD and the Banora Point Road Upgrade in NE-NSW to establish the strength of rock for foundation design.

The collection of this data provided an opportunity to conduct regression analysis on the Fresh (FR) and distinctly weathered (DW) sandstone to produce both a fitted linear equation and an estimate of the strength of the derived relationship, in the form of a co-efficient of correlation (R^2). The derived relationships for each of the sites are summarised in Table 2

.

Table 2. Details of fitted PLI : UCS linear relationships

Rock Type, Weathering & Location	No. of Samples	Linear Regression Equation	R^2
Sandstone, Fresh, Wyaralong Dam	9	y ≈ 5.6x + 14.3	0.6
Sandstone, Distinctly Weathered, Banora Point	8	y ≈ 4.9x + 0.4	0.6

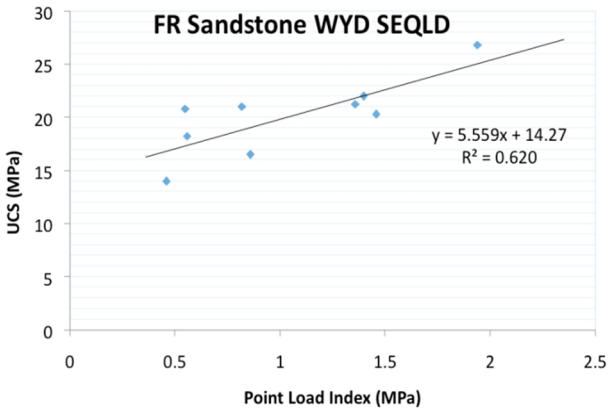

Figure 17. PLI:UCS fitted linear relationship - Sandstone, fresh, Wyaralong Dam (SE-QLD)

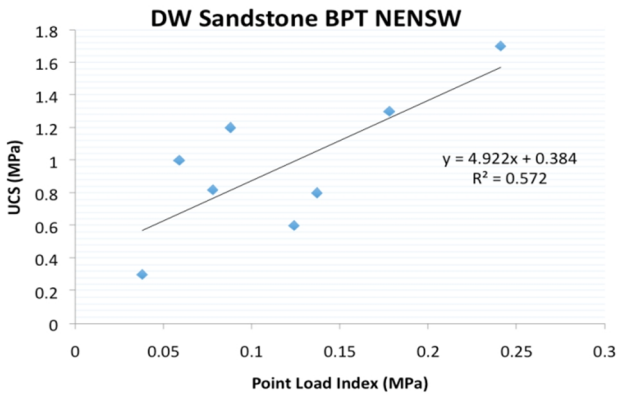

Figure 18. PLI:UCS fitted linear relationship - Sandstone, distinctly weathered, Banora Point (NE-NSW)

Figures 2 and 3 present the derived linear relationships relating PLI and UCS rock strength test results for sandstone materials obtained from Wyaralong Dam (WYD) in SE-QLD and Banora Point (BPT) in NE-NSW respectively.

From this rationalised analysis the higher strength (FR) sandstone has a much higher *y* (UCS) value than the weaker (DW) sandstone as shown in Table 2. This observation supports the previously identified recommendation that the multiplier adopted for transformation of point-load results to UCS values for a specific rock type should also be further derived for the weathering state of the rock.

The use of the origin *(0,0)* as an additional data point / forced intercept was the method adopted by Broch and Franklin (1972) for all rock types, and no variance based on weathering state was made in their data analysis. It is also understandable that test results associated with DW (low strength) rock materials would result in points falling close to the origin.

4.2. Comparative rock type

Data relating to one rock type, sandstone, was extracted from the SMEC data and compared with existing data published by Look, (2007) to provide a comparison of the rock strength variation over the general location (SE-QLD / NE-NSW) and degree of weathering. The difference between the rock strengths of the DW (BPT) to the FR data (WYD) is approximately a factor of 3.8. The difference between the DW data (BPT) to the DW (CGC) and DW (BNE) datasets reported by others (Look, 2007), was a factor of between 1.9 and 2.3.

However, the use of the term distinctly weathered (DW) may have been applied by professional staff differently as the weathering description and lithology is subjective in many cases. This highlights a general problem when applying descriptive geological terms in engineering studies. It is also possible that DW rock is too broad a category.

4.3. Effects of weathering

A response to the lack of consistent and uniformly applied standards for DW was to recognise two additional descriptive weathering classes intermediate between DW and slightly weathered (SW) – i.e. highly weathered (HW) and moderately weathered (MW). There is evidence that HW & MW have been used by Moye and Sharp (1961) at the Snowy Mountains Hydro-Electric Authority. Hence, DW rock in *AS1726-1993* is replaced by some consultancy firms in the geotechnical industry with this wider array of HW and MW rock, and the use of this extra discrimination may clarify the rock strength estimate of DW rock.

In this study, the commonly used multiplier of 24 would overestimate the equivalent UCS values; the strength of the FR sandstone (WYD) by a factor of 1.2; the DW sandstone (BPT) by a factor of 4.5; the DW sandstone (BNE) by a factor of 2; and the DW sandstone (CGC) by a factor of 2.4.

If the HW and MW system was adopted this may give a progressive result which may establish more appropriate regression relationships. While the authors acknowledge that different degrees of cementation can affect the UCS of arenites (sandstones), and furthermore that each arenite may contain differing quantities of clay minerals, a common practice of using HW & MW in the geothechnical community may influence the ability to directly compare datasets.

5. Recommendations

What Broch & Franklin (1972); Thuro & Plinninger (2001) and equations mentioned in Ferner et al. (2005) have tried to achieve is to provide an empirical relationship between the results of UCS and point-load tests for all rocks as a homogenous multiplier. This includes a single multiplier that does not vary based on degree of material weathering.

Since the beginnings of the point-load test in the late 1960's, much work has been done via trial and error on this topic. It is the heterogeneous and anisotropic nature of the differing rock types including an exponential relationship between different grades of weathering (Basu & Aydin, 2006) that are at variance with a universal multiplier.

There is little evidence in this research to support the commonly used rock strength multiplier of 24 that is in the recent guidelines used by government agencies and other consulting firms in the geotechnical industry, therefore, it is unfit for this purpose. This research is supportive of previous researchers of rock strength in SE-QLD and around the world that concludes that rock strength equations are dependent on different rock types, their inherent internal variability, the extent of weathering and site location. The issue is further complicated by the lack of defined and standardised terms for recognising the degree of weathering in common practice.

The relationship produced via linear regression for the FR data set (WYD, SE-QLD) produced UCS values approximately 4 times higher than if the same point-load value was used for the relationship defined by use of the DW data (BPT, NE-NSW). This finding supports that observation that multipliers relating to FR rock and DW rock should be calculated by independent analyses, and any multipliers should be defined with the weathering state to which they relate. Analysis of a combination of FR and DW data leads to an underestimation of the FR rock strength and overestimation of the DW rock strength.

The multiplier related to the DW data set (BPT, NE-NSW) was approximately 0.5 of that published in the *Handbook of Geotechnical Investigation and Design Tables* for comparable rocks and location (CGC & BNE, SE-QLD). This result again supports the recommendation that the data should be analysed on a site-specific basis, even if similar rock materials and weathering states exist.

Further analysis of UCS versus I_{s50} data of different rock types from different areas in SE-QLD and NE-NSW, coupled with enhanced rock type discrimination, confirms the rock strength multiplier variability detailed in this paper. Although the rock strength data has been sourced from a limited data set, its purpose is to give an indication of rock strength at specific sites.

6. Conclusions

From the completed review of the published literature and the analysis undertaken in the current study, it is concluded that all I_{s50} correlations for estimating UCS should be applied with considerable caution.

For initial UCS strength estimation, or where the risk associated with overestimating UCS is manageably low, then the correlations published here could be considered appropriate for sandstone at sites in SE-QLD and NE-NSW. However, when the risk is high then laboratory tests are necessary to establish UCS.

The I_{s50} is indicative of the UCS and by no means replaces the accuracy of the UCS test.

7. References

Australia, S. (1993). *Geotechnical site investigations* (Vol. AS 1726 - 1993, pp. 22-23). Sydney: Standards Australia Limited.

Australia, S. (2007a). *Method of testing for engineering purposes Method 4.1 Rock strength tests - Determination of point load strength index* (Vol. AS 4133.4.1). Sydney: Standards Australia Limited.

Australia, S. (2007b). M*ethods of testing rocks for engineering purposes Method 4.2.1: Rock strength tests - Determination of uniaxial compressive strength of 50MPa and greater* (Vol. Method 4.2.1). Sydney: Standards Australia Limited.

Basu, A., & Aydin, A. (2006). Predicting Uniaxial Compressive Strength by Point Load Test: Significance of Cone Penetration. *Rock Mechanics and Rock Engineering*, Vol. 39 (5), pp. 483-490.

Bieniawski, Z. T. (1975). Point load test in geotechnical practice. Eng. Geol., 9(1), 1-11.

Broch, E., & Franklin, J. A. (1972). Point-load strength test. *International Journal of Rock Mechanics and Mining Sciences*, Vol. 9 (6), pp.669-697.

Cargill, J. S., Shakoor, A. (1990): Evaluation of empirical methods for measuring the uniaxial compressive strength of rock. *International Journal of Rock Mechanics and Mining Sciences,* Vol. 27 (6), pp. 495-503.

Chou, K. T., Wong, R. H. C. (1996): Uniaxial compressive strength and point load strength. *International Journal of Rock Mechanics and Mining Sciences,* Vol. 33, pp. 183-188.

Cobanoglu, I., & Celik, S. B. (2008). Estimation of uniaxial compressive strength from point load strength, Schmidt hardness and P-wave velocity. *Bulletin of Engineering Geology and the Environment*, Vol. 67, pp. 491-498.

Cranfield, L. C., Whitaker, W. G. & Green, P. M., (1980). Geoscience.gov.au. (1980). *Moreton Geological Map*. Available from Australian Government, from Department of Resources, Energy and Tourism http://www.geoscience.gov.au/geoportal-geologicalmaps/download?map=250dpi/moreton.jpg

D'Andrea, D. V., Fisher, R. L., & Fogelson, D. E. (1964). Prediction of compressive strength from other rock properties. *Colorado School of Mines Quarterly*, Vol. 59 (4b), pp. 623-640.

Deere, D. U., Miller, R. P. (1996): Engineering classification and index properties for intact rock. *Air Force Weapons Lab. Tech. Report, AFWL-TR 65-116*, Kirtland Base, New Mexico.

Ferner, M., Kahraman, S., Bilgil, A., & Gunaydin, O. (2005). A Comparative Evaluation of Indirect Methods to Estimate the Compressive Strength of Rocks. [Technical Note]. *Rock Mechanics and Rock Engineering*, Vol. 38 (4), pp. 329-343. doi: 10.1007/s00603-005-0061-8.

Forster, I. R. (1983): The influence of core sample geometry on the axial point-load test. *International Journal of Rock Mechanics and Mining Sciences Abstracts,* Vol. 20 (6), pp. 291-295.

Ghosh, D. K., Srivastava, M. (1991): Point-load strength: an index for classification of rock material. *Bulletin of International Association for Engineering Geology*, Vol. 44, pp. 27-33.

Grasso, P., Xu, S., Mahtab, A. (1992): Problems and promises of index testing of rocks. *Proc. 33rd US Symp. Rock Mech.*, Sante Fe, NM, Balkema, Rotterdam, 3-5 June 1992.

Gu, D. X., Tamblyn, W., Lamb, I., & Ramsey, N. (2008). Effect of Weathering on Strength and Modulus of Basalt and Siltstone. *Paper presented at the 42nd US Rock Mechanics Symposium and 2nd U.S.-Canada Rock Mechanics Symposium*, San Francisco.

Gunsallus, K. L., Kulhaway, F. H. (1984): A comparative evaluation of rock strength measures. *International Journal of Rock Mechanics and Mining Sciences,* Vol. 21, pp. 233-248.

Hassani, F. P., Scoble, M. J. J., Whittaker, B. N. (1980): Application of point-load index test to strength determination of rock and proposals for size-correction chart. In: Summers, D. A. (ed.) *Proc. 21st US Symp. Rock Mech.*, Rapid City, 1985, pp. 549-555.

ISRM (1985): Suggested method for determining point load strength. *International Journal of Rock Mechanics and Mining Sciences Abstracts,* Vol. 22 (2), pp. 53-60.

Kaharaman, S. (2001): Evaluation of simple methods for assessing the uniaxial compressive strength of rock. *International Journal of Rock Mechanics and Mining Sciences,* Vol. 38, pp. 981-944.

Look, B. G (2007). *Handbook of Geotechnical Investigation and Design Tables*. The Netherlands: Taylor and Francis Publishers.

Look, B. G., & Griffith, S. G. (2001). An Engineering Assessment of the Strength and Deformation Properties of Brisbane Rocks. *Australian Geomechanics*, pp. 17-30.

Look, B. G., & Griffiths, S. G. (2004). Rock strength properties in south east Queensland. *9th Australian New Zealand conference in Geomechanics*, Auckland New Zealand.

Marinos, P., & Hoek, E. (2001). Estimating the geotechnical properties of heterogeneous rockmasses such as flysch. *Bulletin of Engineering Geology and the Environment*, Vol. 60, pp. 85–92.

Moye, D. G., & Sharp, K. R. (1961). *Report on the geology of Murray 1 project and associated works*. Snowy Mountains Hydro-Electric Authority (SMEC), Cooma, Australia.

Palchik, V., Hatzor, Y. H. (2004): The influence of porosity on tensile and compressive strength of porous chalk. *Rock Mechanics and Rock Engineering*, Vol. 37 (4), 331-341.

Quane, S. L., Russel, J. K. (2003): Rock strength as a metric of welding intensity in pyroclastic deposits. *European Journal of Mineralogy,* Vol. 15, pp. 855-864.

Read, J. R. L., Thornton, P. N., & Regan, W. M. (1980). A rational approach to the point load test. *Third Australia-New Zealand conference on Geomechanics*, Wellington.

Reichmuth, D. R. (1968). Point load testing of brittle materials to determine tensile strength and relative brittleness. Paper presented at the *Proc. 9th US Symposium on Rock Mechanics*, Golden.

Singh, D. P. (1981): Determination of some engineering properties of weak rocks. *Proc. Int. Symp. Weak Rock*, Tokyo, 1981, pp. 21-24.

Smith, H. J. (1997): The point load test for weak rock in dredging applications. *International Journal of Rock Mechanics and Mining Sciences,* Vol. 34 (3/4), pp. 702.

Thuro, K. (1996). *Drillability in hard rock tunneling by drilling and blasting.* Technische Universitat Muchen, Muchen.

Thuro, K., & Plinninger, R. J. (2001). Scale effects in rock strength properties. Part 2: Point load test and point load strength index. *EUROCK 2001 Rock Mechanics - a Challenge for Society*, Espoo, Finland.

Tomlinson, M. J. (1995). *Foundation Design and Construction* (6th ed.): Longman.

Tsiambaos, G., Sabatakakis, N. (2004): Considerations on strength of intact sedimentary rocks. *Engineering Geology*, Vol. 72, pp. 261-273.

Tsidzi, K. E. N. (1991): Point load-uniaxial compressive strength correlation. *Proceedings of the 7th ISRM Congress*, Aachen, Germany, vol. 1, 1991, 637-639.

Vallejo, L. E., Welsh, R. A., Robinson, M. K. (1989): Correlation between unconfined compressive and point load strength for Appalachian rocks. *Proceedings of the* 30th *US Symposium on Rock Mechanics*, Morgantown, 1989, pp. 461-468.

Proceedings of the 10th ANZ Young Geotechnical Professional's Conference – 10YGPC
Noosa, Queensland, Australia
10 – 12 September 2014

HIGH IMPACT ENERGY COMPACTION OF COAL MINE SPOIL

Seth HAMILTON (MEng (Hons I))
GHD Pty Ltd, Sydney, Australia

ABSTRACT – The reuse of mine spoil in civil applications presents significant geotechnical design and construction challenges. The Bulga Optimisation Project (BOP) is a Glencore initiative to consolidate and relocate existing underground and open cut coal mining facilities to enable the expansion of the Bulga mine open cut operations. The project incorporates the realignment of approximately 9 km of roadway including sections that will traverse remediated and existing mine spoil dumps (approximately 2 km of single lane carriageway).

Achieving sufficient compaction of the underlying coal mine spoil prior to road construction without removal, replacement or re-grading of subgrade materials while using conventional compaction techniques is challenging. Achieving this outcome this would allow for significant time and cost savings.

Compaction trials were conducted to investigate the use of High Impact Energy Compaction (HIEC) (also known as impact roller compaction or rolling dynamic compaction) as an alternative to conventional compaction techniques for the densification of the coal mine spoil materials at Bulga.

This paper presents the findings of HIEC trials including an assessment of settlement and densification resulting from varying degrees of dynamic compactive effort. Indicative compaction characteristics are presented to assist in geotechnical design including the expected depth of compaction, degree of densification achievable using HIEC and suggested compaction mechanisms.

The reported benefits of HIEC over conventional methods are reviewed following observations made during the trial. Recommendations for future work, particularly the use of non-intrusive testing methods in future trials and practical considerations when using HIEC, are also presented.

1. Introduction

The Bulga Optimization Project (BOP) is a Glencore initiative to consolidate and relocate existing underground and open cut mining facilities at the Bulga Mine Complex. The BOP project will enable the expansion and improve the efficiency of mine open cut operations. The project incorporates the rerouting of approximately 2 km of single lane public carriageway across remediated and existing mine spoil dumps.

Providing reliable geotechnical parameters such as subgrade strength or estimation of expected short- and long-term settlements for the pavement design of this single lane public carriageway presented a number of challenges. It was therefore determined that ground improvement was required to modify the engineering characteristics of the in situ material to allow the provision of pavement design parameters with greater confidence and with less conservatism.

This paper presents the findings of compaction trials undertaken to investigate the effectiveness of High Impact Energy Compaction (HIEC) techniques (also known as impact roller compaction or rolling dynamic compaction) in ground improvement of coal mine spoil. The reported benefits of HIEC over conventional methods of compaction including those reported by Scott and Jaksa (2012) and others, such as a greater depth of compaction make the technique well suited to use in developments upon mine spoil if these purported benefits are found to be reliable.

2. Geotechnical design challenges with mine spoil

Mine spoil presents significant geotechnical design and construction challenges. Mine spoil materials are characteristically non-homogeneous with material properties dependent on the source geology, the stratigraphic sequence from which the material was won, the method of excavation (blast or otherwise) and any sorting/grading prior to placement. As a result mine spoil can comprise materials with a range of particle sizes and variations in particle durability, strength and weathering/weathering potential. Oversize material greater than 500 mm minimum diameter is not uncommon in mine spoil.

Mine spoil is typically hauled to site by truck and spot dumped in thick layers (1.2 loose thickness typically) and is often uncompacted. The presence of oversize material, little (if any) grading control and the method of placement of the material mean that in areas underlain by mine spoil it is particularly difficult for practitioners to provide geotechnical parameters and/or recommendations with confidence. Due to this heterogeneity of material and treatment geotechnical investigations of mine spoil to assist in the development of geotechnical parameters can be particularly difficult (Scott and Jaksa, 2012). The presence of high strength, oversize particles, voiding etc. mean that conventional in situ testing methods, such as the Standard Penetration test (SPT) can be unreliable and provide little feedback to the geotechnical practitioner.

Given the heterogeneity of the mine spoil, and the challenges associated with defining appropriate design parameters, the designer might be inclined to recommend the removal, replacement or re-grading of mine spoil with appropriate compaction control prior to development. This is likely to impose a significant even prohibitive time and cost imposition upon the developer. Ground improvement therefore in mine spoil without the need for removal, replacement, re-grading and re-compaction offers significant benefits.

3. High Impact Energy Compaction (HIEC)

Also known as 'impact roller compaction' or 'rolling dynamic compaction', HIEC is a type of roller compaction where instead of using the more common circular drum, heavy (6 to 18 tonne) non-circular modules with 3 to 5 sides are used (refer Figure 1). These are towed by typically greater than 200 kW towing units, commonly 4WD tractors (Broons, 2014). As the HIEC module is towed it rotates around its non-circular circumference and it imparts compactive energy to underlying material.

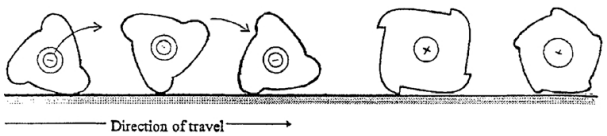

Figure 1. Common HIEC non-circular modules (Scott, Jaksa, & Lik Kuo, 2012)

HIEC technology first entered the Australian market in the mid-1980's with the principal Australian based manufacturer of the modules being based in South Australia. There are also a number of other manufactures worldwide supplying the Australian market, most from the USA.

Within Australia HIEC has been used in numerous applications including, as detailed by Broons (2014):

- Compaction of uncontrolled fill, landfill, reclaimed land
- Compaction of water storages and channel banks
- Mining haul roads and mine spoil compaction
- Rural road improvement

4. Benefits of HIEC over conventional compaction methods

There are a number of benefits purported by suppliers of the technology and various authors of HIEC over conventional compaction methods, some of which are presented below.

4.1. Increased depth of compaction

Scott and Jaksa (2012) reported that HIEC has the ability to compact thicker loose layers, between 0.5 m to 1.5 m during conventional filling earthworks, compared to conventional rollers, which typically compact 300 mm lifts.

Greater depths of compaction can also be achieved in the compaction of existing uncontrolled fill, estimated at 1 m to 4 m depth, depending on the nature of the material.

4.2. Higher travelling speeds

HIEC is typically conducted at higher travelling speeds relative to other methods common methods of roller compaction (refer Table 1). In part this is because the compactive energy imparted by HIEC is proportional to the travelling speed, thus in order to achieve the compactive effort desired impact rollers must achieve a sufficient travelling speed. However, this higher travelling speed also leads to improved efficiencies because larger areas of compaction can be achieved in a given period of time.

Table 1. Typical roller travelling speeds (Scott, Jaksa and Lik Kuo, 2012)

Roller type	Typical roller speed
Steel wheeled rollers	Not exceeding 5 km/h
Vibratory rollers	8 to 10 km/h
Pneumatic-tyred rollers	6 to 10 km/h
Impact roller	10 to 12 km/h

4.3. Reduction in moisture conditioning

Given the higher compactive energy that can be applied by HIEC, compaction can to be undertaken on materials at a greater range of soil moisture contents than by conventional compaction techniques (Scott, Jaksa, and Lik Kuo, 2012). As a result less/or no moisture conditioning is required to achieve satisfactory compaction, which can be particularly advantageous in the dry climatic conditions found in inland Australia.

5. Compaction trials

5.1. Background

The HIEC compaction trials were undertaken by GHD and Robson Civil Projects at Mount Thorley open cut coal mine, located 15 km south west of Singleton in the Hunter Valley region of New South Wales.

This site was selected as it was in close proximity to the Bulga Mine open cut operations (site of the BOP project) and located in a similar geological environment, namely the Singleton Coal Measures which are characterized by sedimentary sequences of sandstone, shale, mudstone,

conglomerate and coal seams (Rasmus, Rose and Rose, 1969). The mine spoil sourced from the Mount Thorley Warkworth (MTW) mine has broadly similar characteristics to that of Bulga Mine including similar particle sizes, grading, and particle durability.

The earthworks plant needed for the trial, including graders, haul trucks and impact roller where already on site as part of existing an earthworks project to construct a tailings storage facility and leave was given by the mine owner Rio Tinto for this plant to be made available for the duration of the trial. The trial was undertaken over two consecutive days, the 22 and 23 April 2013.

The weather during the trial was fine, with maximum daily temperatures ranging from 24.9 °C to 25.7 °C and minimum daily temperatures ranging from 5.5 °C to 8.4 °C. During the preceding seven-days 13.6 mm of precipitation was recorded in the local gauges. No rain fell during the trial.

The compaction trial had three principal objectives, to:

- Evaluate the compaction capabilities of HIEC in coal mine spoil materials
- Assess the suitability of using a HIEC for pavement subgrade improvement in the Bulga mine spoil dump materials where traversed by the proposed Broke Road realignment
- Provide information for design of earthworks at Bulga mine, including input into a method earthworks specification.

5.2. Trial location and materials

The trial was conducted over an approximately 50 m by 25 m lot. Moisture conditions of the placed material varied, but no ponding or surficial water was observed over the trial area. Prior to the trial a broad topographical survey of the site was conducted to provide a base/reference survey.

Discussions with the contractor and other site observations, such as existing tyre marks, suggested the lot had been subjected to trafficking by earthworks plant prior to the trial; no other formal compaction had taken place on the surficial layer of material under investigation.

The trial area was underlain by mine spoil material (rockfill) sourced from pit excavations at MTW mine. This material was sourced from two stratigraphic sequences, as follows:

- Upper 5 m of pit excavations, comprising "free dug" material, a mixture of soil and weathered rock particles including weathered sandstone, shale, mudstone and/or conglomerate particles, with isolated oversize particles greater than 500 mm minimum diameter.
- 5 m to 10 m depth of pit excavations, comprising generally "free-dug" or rippable material, comprising a mixture of soil and weathered rock particles including weathered sandstone, shale, mudstone and/or conglomerate particles, with isolated oversize particles greater than 500 mm minimum diameter, typically less weathered and higher strength than that obtained from upper sequences.

The fill was delivered to the site by haul truck and spot dumped over the previously compacted fill layer. The contractor then spread the fill material in continuous horizontal layers of nominal 1.2 m loose thickness. Rolling compaction was undertaken in a direction parallel to the longitudinal axis of the trial area.

Discussions with the contractor indicated that the depth of existing fill was approximately 13.5 m deep over the trial area prior to the trial. The fill had been watered for dust control and better workability at the discretion of the earthworks contractor.

Figure 2. Typical excavated mine spoil, including oversize material. A ten-pound sledge hammer can be seen at centre as a scale reference

5.3. Trial methodology

The trial utilised a 17.75 tonne operating mass, four-sided impact roller, manufactured by Impact Roller Technology (IRT), USA. The manufacturer's maximum recommended operating speed for the roller was given as 13 km/h. The roller was pulled by a rubber-tyred mine specification agricultural tractor (refer Figure 3).

The trial comprised in-situ density testing and sampling after zero, 5, 10, 15 and 20 overlapping passes with the IRT impact roller. The first pass was conducted at an average speed of approximately 8 km/h. All subsequent passes were conducted at the target average speed of approximately 10 to 12 km/h. Roller speeds were monitored by the plant operator using onboard instruments.

Due to the corrugations formed by the impact roller, surface re-grading was required after passes 1 and 3 to allow the roller to reach the target average speeds. Passes 5 through 10 were conducted without grading. It was found that the

Figure 3. Four-sided impact roller pulled by mine specification agricultural tractor

corrugations left by the impact roller caused great discomfort to the operator and made it difficult to achieve the target speed. For the remainder of the trial grading was conducted after each pass.

For reasons of dust suppression the trial area was watered by water cart once between passes 5 to 10 and after pass 12. Given the magnitude of the compactive energy imparted by the impact roller it is assumed that any additional compaction attributable to passes by the water cart would be negligible. The direction of travel for passes 1 through 10 was reversed for passes 11 through 20.

5.4. In situ testing

The compaction trial was designed so that the effectiveness of HIEC might be assessed principally by review of densification and induced settlements, if any, resulting from the applied compactive effort.

The original testing schedule comprised Dynamic Cone Penetrometer (DCP) testing, supplemented by determination of the field density and field moisture content using a nuclear surface moisture-density gauge.

Six DCP probes were conducted initially, prior to any HIEC, to depths ranging from 1.1 m to 1.2 m below surface level. During testing the DCP equipment was damaged twice, presumably in part because of the deleterious nature of the mine spoil. With further replacement parts for the DCP not available onsite it was decided that the trial should proceed with nuclear densometer testing only, with the DCP testing being abandoned.

A revised testing schedule was adopted with a total of twelve nuclear densometer tests per set of passes, as follows:

- Prior to compaction and after each subsequent set of five passes with the impact roller, nuclear densometer testing was undertaken at the surface at three locations
- Prior to compaction and after each subsequent set of five passes with the impact roller, nuclear densometer testing was undertaken over the full depth of the lift at three locations

The nuclear densometer used had a maximum test depth of 300 mm below the gauge. Thus to assess the density over the full depth of the fill lift (1.2 m loose thickness), nuclear densometer testing was conducted at the surface and at two subsequent depths, nominally 400 mm depth and nominally 800 mm depth, by excavating a trench and testing on the exposed floor of the trench.

At all test locations the nuclear densometer probe was extended to the maximum 300 mm below the nominated test depth, viz. a 300 mm layer thickness was tested. To achieve the nominated test depth frequently required attempting more than one pilot hole at each test location, as many pilot holes refused at depths shallower than 300 mm because of underlying oversize material.

Figure 4. Side wall of test pit showing typical mine spoil material. A ten pound sledge hammer has been placed in the foreground for scale

The excavation to the nominal depths was conducted by a 36.5 tonne hydraulic excavator (CAT Model 336D), utilising a blade bucket. All efforts were made to limit the disturbance of the underlying fill. After each set of five passes sample locations were relocated so that testing was not conducted where the excavation / full depth testing had previously taken place. Bulk fill samples were collected from selected test locations and depths for compaction, CBR and other laboratory testing.

6. Compaction trial results

The variability of the mine spoil including a significant fraction of material coarser than 37.5 mm minimum dimension meant the assessment of material properties such as in situ density during the trial proved challenging. That said a number of trends may be observed from the data collected.

6.1. Field moisture content

Field moisture content values obtained from laboratory testing suggest that the in situ moisture

content of fines at the time of the trial (6.8% to 10.1%) was below the typical Plastic Limit (16% to 18%) of samples collected at the site but near the modified optimum moisture content (8.6 to 9.9%) of the same material.

6.2. Sieve analysis

The sieve analysis conducted on samples obtained during the HIEC trial identified the material as 'dirty', i.e. material with greater than 12% fines content ('fines' defined as particles with diameter less than 75 µm, as per Standards Australia, 2000), sufficient to bind coarse grains and reduce permeability.

The percentage fines after 20 passes with a dynamic impact roller ranged from 21% to 36%, with an average fines percentage of 28%. The material would typically be characterized as sand, with a sand fraction ranging from 41% to 56% and with an average sand fraction of 47%. The material also contained significant gravel and cobble fractions, ranging from 16% to 35%, and an average gravel/cobble fraction of 26%. It should be noted that the sampling process is likely to underestimate the percentage coarse/oversize materials, with much of the larger cobble and boulder size material not being sampled.

Table 2. Particle size variance following compaction

No. of passes with impact roller	Average % fines	Average % sand	Average % gravel & cobbles
10	27.7	41.3	31.3
15	28.3	43.3	28.3
20	27.3	46.8	25.5
% change (10 to 20 passes)	*+0.3*	*+5.5*	*-5.8*

The sieve analysis also illustrates the effect of HIEC on particle size distribution, through particle break-up. Table 2 presents a summary of change in particle size between 10 and 20 passes of the dynamic impact roller. The results suggest that the majority of the particle break up occurs amongst the coarsest material (gravel and cobbles), with the largest proportion of material grading to sand (approximately 5.5%). There is also a minor increase in the fines percentage as a result of HIEC (approximately 0.3% - 1.0%). Grading envelopes for selected samples after 10 and 20 passes with the dynamic impact roller, as presented in Figure 5, also demonstrate this particle break-up and average particle size reduction.

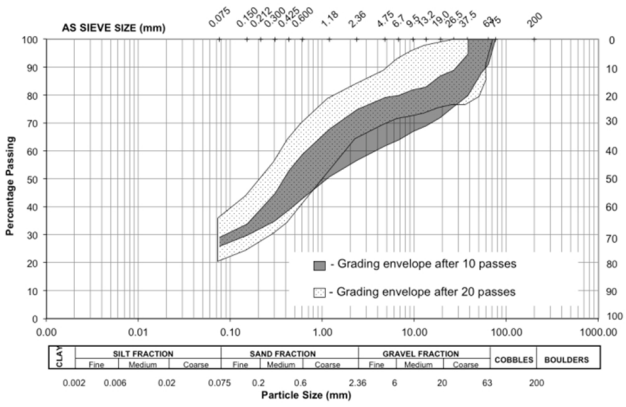

Figure 5. Grading envelopes for selected samples after 10 & 20 passes with impact roller

6.3. In situ density

Figure 6 shows aggregated density ratios from all nuclear densometer testing plotted against the number of passes with the dynamic impact roller. The data has been presented as a mean of the full data set and as a mean of the full data set excluding outliers greater than one standard deviation from the mean; values for the latter are presented on the chart.

The HIEC trial data has also been segregated to show the relative compaction at the surface and nominal depths of 0.4 m and 0.8 m. Error bars have been included to show the spread of data, with error bars set at +/- one standard deviation from the arithmetic mean for each respective data series.

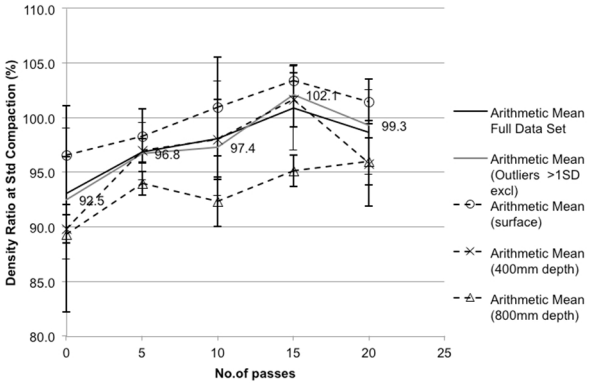

Figure 6. Mean density ratio at standard compaction

The results show a general trend to increasing density ratio with increase in compactive effort as might be expected with the field density nearing 98% of standard maximum dry density (i.e. a density ratio of 98%) after approximately 10 passes. The data also suggests that beyond 15 passes the attained increase in density begins to attenuate, with limited increase in density ratio for increased compactive effort, certainly at depths shallower than 0.8 m. It should be noted that this trend was not investigated beyond 20 passes and

so the appropriate caution should be applied to this assertion with the limited data at hand.

There also appears to be a statistically significant difference in densification over the full depth of the lift. The surficial material achieves a higher density ratio after 20 passes than material from 0.3 to 1.1 m depth. However the increase in density ratio is most pronounced at depth, with an increase in density ratio at 0.8 to 1.1 m depth from zero to 20 passes of 6.7 % compared with 4.9% at the surface to 0.3 m. This appears consistent with the observations at other locations (Scott and Jaksa, 2012), which suggest that the greatest compactive effect of HIEC is up to at least 1 m depth in mine spoil type material.

6.4. Settlement

The trial confirmed that an impact roller is not a finishing roller due to the corrugations left following HIEC and the shearing and kneading effect as the module travels over the surface. There is always a need for final trimming, watering and rolling of HIEC compacted areas with conventional plant to achieve a suitable running surface.

Accordingly attempts to assess compaction by calculating induced settlements were unsuccessful. Aggregated surface survey results relative to base survey conducted prior to the trial were reviewed. The data showed significant scatter. Any changes in settlement relative to compactive effort were within an assumed margin of error of 1.5 times standard deviation; accordingly it is difficult to draw any identifiable trends or conclusions from the data. The high variability of the data is likely to be attributable to a number of factors including the grading required during the trial between passes and disturbance of surface material such as the corrugations left as the HIEC module travels over the surface.

7. Recommendations for future work

Due to the significant quantities of oversized particles in mine spoil the use of intrusive geotechnical investigation methods proved challenging during the trial. Alternate methods have been suggested by various authors – including Scott and Suto (2007) and Avalle and Mackenzie (2005) – including geophysical techniques such as MASW (Multi-channel Analysis of Surface Waves) and CSWS (Continuous Surface Wave System).

However these have limited application because of the potential for signals to be overwhelmed by local noise sources, if the trial is conducted near to active earthworks plant.

Plate load testing is another technique previously utilized by the authors of this report to assess the degree of compaction of quarried material, by determination of the Modulus of Subgrade Reaction or a measure of the shear strength of pavement components.

Utilisation of such techniques above together with further trials or validation testing will provide a valuable comparison to the intrusive geotechnical investigation methods used during this trial.

As previously indicated the trial was conducted upon coal mine spoil, derived from the sedimentary Singleton Coal Measures. It is anticipated that in case of 'hard rock' mining spoil, such as that derived from hematite or iron ore mines the findings may be different, and worthy of further investigation.

8. Conclusion

Mine spoil should not necessarily act as a prohibitive restraint on road and other infrastructure developments. Given appropriate geotechnical consideration and aided by the use of non-conventional compaction techniques such as HIEC development upon areas of mine spoil is feasible.

The HIEC trial conducted at Mount Thorley in April 2013 and subsequent laboratory testing indicates that HIEC has the ability to compact coal mine spoil of characteristics defined herein to 98% standard compaction after approximately 10 passes with a 17.75 tonne dynamic impact roller.

HIEC was observed to achieve compaction in layers up to 1 m thickness depending upon material composition; the number of passes applied and specified target density ratios. This is in comparison to conventional rollers which can satisfactorily compact fill in layers up to 400 mm loose lift thickness.

The trial identified the challenges with compaction testing of mine spoil materials, using conventional intrusive techniques. It is also noted that the mine spoil materials investigated during the trial, are at the limit of the applicability of the test procedures for in situ determination of dry density ratio specified in the relevant parts of AS 1289 (Standards Australia, 2000).

HIEC achieves higher roller speeds than comparative compaction rollers, leading to time and cost efficiencies.

The outcomes of the HIEC compaction trials provided valuable inputs in to the geotechnical and pavement design of approximately 2 km of single lane public carriageway across remediated and existing mine spoil dumps at Bulga Mine.

9. Acknowledgements

The Author would like to thank Bryn THOMAS (BSc, MSc, PhD, CEng, MIMM, CGeol, EurGeol, FGS) for his assistance in reviewing the work and mentorship of the Author.

Thanks are also extended to Glencore – Bulga and Rio Tinto for their assistance with facilitating this work.

10. References

Avalle, D. L., & Mackenzie, R. W. (2005). Ground improvement of landfill site using the "square" impact roller. *Australian Geomechanics*, Vol. 40 (No. 4).

Broons Pty. Ltd. (2014). Impact Rollers. Retrieved August 15, 2014, from: http://www.broons.com/index.php

Rasmus, P. L., Rose, D. M., & Rose, G. (1969). Singleton 1:250 000K Geological Sheet SI/56-01 (1st edition ed.).Geological Survey of NSW.

Scott, B. T., & Jaksa, M. B. (2012). Mining Applications and Case Studies of Rolling Dynamic Compaction. *ANZ 2012*, (pp. 961 - 966). Melbourne, Australia.

Scott, B. T., Jaksa, M. B., & Lik Kuo, Y. (2012). Use of Proctor Compaction Testing for deep fill construction using impact rollers. *ICGI 2012,* (pp. 1107 - 1112). University of Wollongong, Australia.

Scott, B. T., & Suto, K. (2007). Case study of ground improvement at an industrial estate containing uncontrolled fill. *Proceedings 10th Australia - New Zealand Conference on Geomechanics*, *Vol. 2, 150-155.* Brisbane.

Standards Australia International Ltd. (2000). *AS 1289.0-2000: Methods of testing soils for engineering purposes - Part 0: General requirements and list of methods.* Sydney, NSW.

This page intentionally left blank

Proceedings of the 10th ANZ Young Geotechnical Professional's Conference – 10YGPC
Noosa, Queensland, Australia
10 – 12 September 2014

PRACTICAL CONSIDERATIONS FOR THE TRIAXIAL TESTING OF MINE WASTES

Kai KOOSMEN[1], Leonie BRADFIELD[1], John SIMMONS[2], Stephen FITYUS[1]
[1] *The University of Newcastle, Newcastle, Australia*
[2] *Sherwood Geotechnical and Research Services, Peregian Beach, Australia*

ABSTRACT – Triaxial testing of mine wastes is commonly undertaken to provide shear strength estimates for stability assessments of mine waste storage facilities. When planning triaxial tests however, the omission of carefully planned testing instructions may produce shear strength parameters which are inaccurate, or not suited to the assessments being undertaken.
This paper details various issues that should be considered when planning triaxial testing of mine wastes. Test results have demonstrated that; test type and initial confining stress are important to define failure envelopes over appropriate stress ranges (which may be particularly important for mine wastes exhibiting curved failure envelopes); laboratory saturation of unsaturated mine wastes may return conservative shear strengths; oversize particles may compromise the reliability of calculated shear strengths, and multistage tests may provide reasonably reliable drained shear strengths, but may overestimate undrained shear strengths.

1. Introduction

Triaxial testing of mine wastes is commonly undertaken to provide shear strengths for stability assessments of mine waste storage facilities such as waste dumps, co-disposal facilities, or tailings dams. Often however, practitioners are not well versed in the science of triaxial testing and as such, may fail to provide laboratories with detailed testing instructions. In the absence of detailed instructions, laboratories may be forced to employ arbitrary test conditions that may produce sub-optimal results.

Mining practitioners typically opt for consolidated drained (CD) or consolidated undrained (CU) test types, where CD tests permit drainage of excess pore pressure (Δu) during shearing, whilst CU tests do not. As a result, when tested using the same initial confining stress (s'_0), CD and CU tests produce different effective stress paths (ESPs), which ultimately define the failure envelope over different stress ranges. When planning triaxial tests, failure to recognise the importance of test type and s'_0 conditions may result in the extrapolation of failure envelopes beyond the stress ranges employed during testing. For mine wastes that exhibit curved failure envelopes, this may introduce significant errors into slope stability assessments.

Another element often overlooked is the effect of saturation. Commonly mine wastes are saturated as part of standard triaxial testing procedures; however the same wastes may be unsaturated in the field. According to the extended Mohr-Coulomb criterion, first proposed by Fredlund et al. (1978) for unsaturated soils, it is widely accepted that unsaturated soils are stronger than saturated soils. As such, laboratory saturation of material that is unsaturated in the field may considerably underestimate the field shear strength. The effects of back saturation during triaxial testing are typically overlooked, though they may be significant.

Due to their often coarse granular nature, triaxial testing of mine wastes may require that oversize particles be removed or scalped from samples to facilitate use of laboratory scale equipment. However, the removal of oversize particles alters laboratory specimens from the material in the field. Thus it is desirable to minimise scalping through use of the largest particle size (D_{max}) possible. However, if D_{max} is too large, oversize particles may compromise the reliability of the results. To reduce the erroneous effects of oversize particles, AS 1289.6.4.2 recommends that the diameter ratio (specimen diameter / D_{max}) be greater than 6 during triaxial testing. Often however, diameter ratios below 6 are used with little knowledge of the effect this can have on results.

Multistage testing is another technique that may be used for triaxial testing. In comparison to multiple single stage tests, multistage testing reduces the potential for material variability and offers economies in terms of reduced costs, smaller required sample volumes and shorter test times. Despite these benefits, many practitioners are wary of adopting multistage tests, as it is generally perceived that specimen deformation incurred during early stages may compromise results from later stages. If confidence in the results from multistage tests could be improved, their use may allow practitioners to increase the efficiency of triaxial testing programs.

The purpose of this paper is to summarise various findings from the triaxial testing of granular coal mine wastes, to provide practitioners with a tool to assist in making guided decisions when scoping triaxial testing programs. Although testing only considers coal mine wastes, it is expected that findings may be applicable to mining wastes from other commodities also.

Table 1. Details of triaxial tests undertaken as part of this investigation

Test	1 – 3	4 – 6	7	8 – 10	11 – 13	14 – 16	17 – 18
Material type	Spoil	Spoil	Spoil	MPR	MPR	MPR	MPR
Test Type	CD	CU	UCD	CU	CU	CU	CU
Test stages	Single	Single	Single	Single	Single	Single	Multi
Specimen diameter (mm)	100	100	100	50	50	50	50
D_{max} (mm)	19	19	19	6.7	9.5	13.2	9.5
Diameter ratio	5.3	5.3	5.3	7.5	5.3	3.8	5.3
Shearing rate (mm/min)	0.025	0.06	0.0025	0.01	0.01	0.01	0.01
s'_0 (kPa)	50, 100, 250	50, 100, 250	50	125, 250, 400	125, 250, 400	125, 250, 400	125, 250, 400

2. Methodology

2.1. Materials

Materials tested as part of this investigation included a coal mine spoil sample, and a mixed plant reject (MPR) sample.

Spoil samples were classified as a poorly-graded gravel, had a D_{max} of 19 mm, were non-plastic and had an initial gravimetric moisture content (GMC) of approximately 6%.

MPR samples were manufactured by mixing 80% coarse coal rejects and 20% dewatered coal tailings to produce a "typical" MPR mixture. Prior to mixing, coarse coal rejects were prepared with a D_{max} of 6.7-13.2 mm. The tailings material was classified as a high plasticity clay, with a liquid limit of 71%, and plasticity index of 42%. The resulting MPR mixture was classified as silty clayey gravel, with an initial GMC of 31%. Particle size distributions for each material are shown in Figure 1.

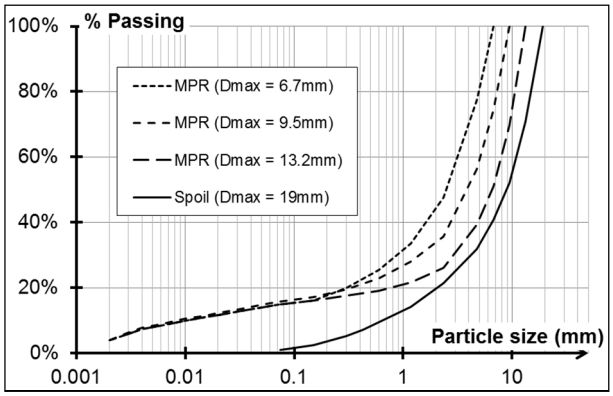

Figure 1. Particle size distribution of mine wastes

2.2. Triaxial Testing

Eighteen triaxial tests were conducted comprising 14 saturated CU tests (with pore pressure measurement), 3 saturated CD tests, and 1 unsaturated CD (UCD) test. All tests were loosely prepared at their initial GMCs, and normally consolidated to reflect field conditions in a mine waste dump. Specific details for each triaxial test are provided in Table 1.

Saturated tests included back saturation, B-value check, consolidation and shearing stages. The unsaturated test was conducted using a conventional triaxial cell with the omission of the saturation and B-value check stages. The two multistage tests were conducted by subjecting the same specimen to three consecutive consolidation then shear phases at increasing cell pressures.

Triaxial tests results are presented herein by plotting the effective stress paths (ESPs) using the MIT convention, which plots the mean effective stress (s') against the shear stress (t). More information regarding stress paths can be found in Head (2006).

3. Results

3.1. Comparison of CD and CU tests

CD and CU triaxial tests vary in that CD tests allow drainage of water from the test specimen during shearing, whilst CU tests do not. Because of the drained conditions, when sheared at a slow enough rate, CD tests do not develop excess pore pressure (Δu). Conversely, CU tests do develop Δu as drainage is prevented during shearing.

Figure 2 shows ESPs from CD tests 1-3 (referred to herein as CD ESPs), and ESPs from CU tests 4-6 (referred to herein as CU ESPs). CD and CU tests were conducted using the same s'_0 values of 50, 100 and 250 kPa. From the figure it is apparent that the CD and CU ESPs tested under the same initial conditions have very different shapes, which is due to the development of Δu during undrained shearing, but not during drained shearing.

During drained shearing in the CD tests, the effective stress was equal to the total stress due to the absence of Δu. This resulted in the CD ESPs being equal to the total stress paths (TSPs); which are observed to have 1:1 slope up to the failure envelope.

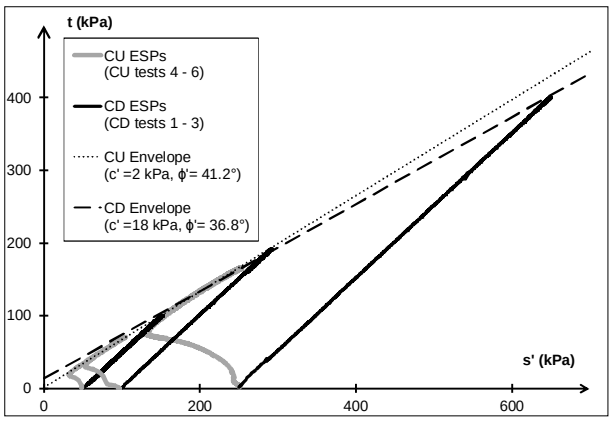

Figure 2. ESPs from CU and CD tests conducted under the same initial conditions.

During undrained shearing in the CU tests however, the development of Δu caused a drop in the mean effective stress (s') and a divergence (to the left) of the CU ESPs from the TSPs (and CD ESPs). The observed offset between the CU and CD ESPs for a given s'_0 is therefore equal to the Δu generated during undrained shearing. Once the maximum Δu (point of phase transformation) was reached, the CU ESPs began converging back towards the CD ESPs and TSPs. Such behaviour is said to be contractive-dilative and is typical of loose, normally consolidated soils during undrained shearing.

As a consequence of their undrained contractive behaviour (diverging to the left), the CU ESPs define the failure envelope over an s' range of 30-260 kPa. This is considerably lower than the s' range of 150-650 kPa, over which the CD ESPs define the failure envelope.

Given most normally consolidated mine wastes exhibit contractive behaviour during CU testing, it follows that CD tests may be more suitable for defining the failure envelope at high stresses. Contractive CU tests may otherwise require very high s'_0 values; much higher than the s' being targeted at failure. Very high s'_0 values may then lead to experimental difficulties such as exceeding conventional apparatus pressure limits and/or the puncture of latex membranes, particularly for angular or granular mine wastes.

When defining the failure envelope at very low stresses however, use of CU ESPs may be preferable as they intersect the failure envelope at a lower s' than a CD ESP (with the same s'_0). Theoretically, although any s' value could be targeted using CD tests, when specifying very low s'_0 values, there is a risk that specimens may inadvertently be overconsolidated during sample preparation. In the authors' experience, this is typically avoided for s'_0 values >100 kPa.

CU tests also allow calculation of undrained shear strengths, whilst CD tests do not. Typically the peak undrained shear strength is taken as the conditions at phase transformation, that is, where a CU ESP switches from contractive to dilative and Δu_{max} is reached (Chern, 1985; Tsukamota et al., 2009; Yoshimine et al., 1999). The undrained shear strength cannot be calculated from CD tests as the inherent nature of the test method does not generate Δu or undrained conditions. Thus, if undrained failure is also of concern, CU tests with pore pressure measurement should be used in preference to CD tests, as they allow estimation of drained and undrained shear strength parameters.

Further to their inability to provide undrained shear strength parameters, CD tests may also be unsuitable for use with low-permeability fine-grained soils, such as high-plasticity tailings or clay-rich overburden intervals. This is because CD tests typically require shear rates much slower than CU tests in order to maintain drained conditions and prevent generation of Δu during shearing. In low-permeability materials, required shear rates for CD tests may be so low that a single test may run for months (even with side-drains), and times required to determine failure envelopes from multiple CD tests may therefore extend well beyond practical timeframes. In such materials CU tests could be used to facilitate faster testing times, and also provide data on undrained shear strengths which presumably may be of concern for low permeability soils.

3.2. Curvature of the failure envelope

Two linear Mohr-Coulomb envelopes are shown in Figure 2, where the CD envelope was derived from the CD ESPs, and the CU envelope was derived from the CU ESPs. Each of these linear envelopes is seen to provide a reasonably good fit to their respective data sets. However, both envelopes have significantly different Mohr-Coulomb parameters, with the effective friction angle (ϕ') varying by 4.4° and the effective cohesion (c') varying by 16 kPa. As a result of these variations, if the CU envelope is extrapolated up to an s' of 650 kPa, the shear strength is overestimated by 7.5% compared to that estimated using the CD envelope. Similarly extrapolating the CD envelope into the low stress range (s' <150 kPa) overestimates the CU envelope.

At first, these significant variations between the two envelopes may seem surprising given that the CD and CU tests were conducted on the same material. However, these differences can be attributed to the selection of linear Mohr-Coulomb parameters from a curved failure envelope at different stress ranges. Curvature of the failure envelope becomes apparent in Figure 3 in which a single non-linear failure envelope is fitted to the combined CD and CU ESPs. Here the CU ESPs intersect the curved failure envelope at lower stresses (s' <250 kPa) when compared to the CD ESPs (s' of 150-650 kPa).

Therefore the CU envelope from Figure 2 is in fact a linear approximation of the curved failure envelope in Figure 3 at low stresses (s' <250 kPa), whilst the CD envelope in Figure 2 is a linear

approximation of the same curved envelope at a higher stresses (*s'* of 150-650 kPa). Because the curved envelope in Figure 3 flattens out with increasing stress, the CU envelope sampled from the low stress range has a higher ϕ' and lower *c'* than the CD envelope sampled from the higher stress range where the curved failure envelope is flatter.

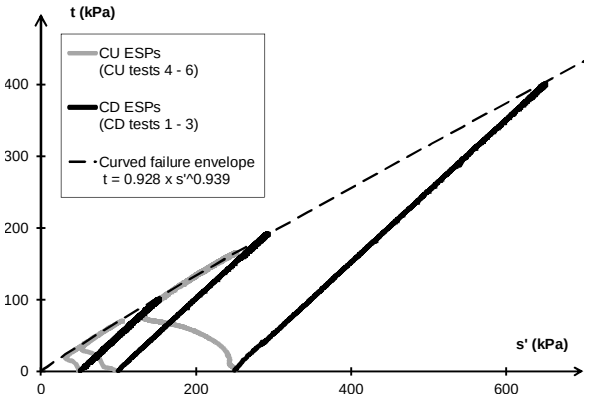

Figure 3. Curved failure envelope fitted to ESPs from CD tests 1 – 3 and CU tests 4 – 6

To highlight possible implications of extrapolating linear failure envelopes into "undefined" stress ranges, two limit equilibrium models were constructed and adopted shear strength parameters from the CU and CD envelopes shown in Figure 2. Both models which are shown in 4 consisted of a 30m high tiphead, assumed a unit weight of 17 kN/m^3, had no equipment loading, and used the Spencer method to calculate the factor of safety (FOS).

The results in Figure 4 show that the FOS was calculated to be 1.32 when using *c'* and ϕ' from the CU envelope, and increased significantly to 1.55 when using *c'* and ϕ' from the CD envelope. Assuming the FOS calculated using the CU envelope to be correct (based on shallow depth of failure surfaces) application of the CD envelope parameters overestimates the FOS by ~17%. This is because the CD envelope has an artificial cohesion much higher than the true cohesion, thus predicting artificially high strengths in the low stress range.

This same concept is discussed by Simmons and McManus (2004) in relation to their commonly adopted coal mine spoil shear strength framework, which has proven to be effective for coal mine waste dumps ranging from 30-120 m in height. The authors noted that shear strength envelopes for coal mine spoils may exhibit distinct non-linearity, and as such application of shear strength framework to dump heights below 30 m or above 120 m may significantly overestimate the available shear strength. This notion is strongly supported by the data in Figure 2 and 3 and subsequent analysis presented in Figure 4.

For mine wastes which commonly exhibit curved failure envelopes, it is therefore important that triaxial shear strength testing be conducted so that the failure envelope is defined over a stress range consistent with stresses expected in the field. This first requires determination of the target stress range by assessing the stresses associated with the possible slope failure mechanisms. Following this, triaxial test type/s can then be coupled with various s'_0 values to produce ESPs that define the failure envelope over the target stress range. For most normally-consolidated mine wastes, it is reasonable to assume that (contractant) CU ESPs will reach failure at stresses below s'_0, whilst CD ESPs will reach failure at stresses above s'_0. Coupling of CD and CU tests may also help to define the failure envelope over a wider stress range and identify potential curvature.

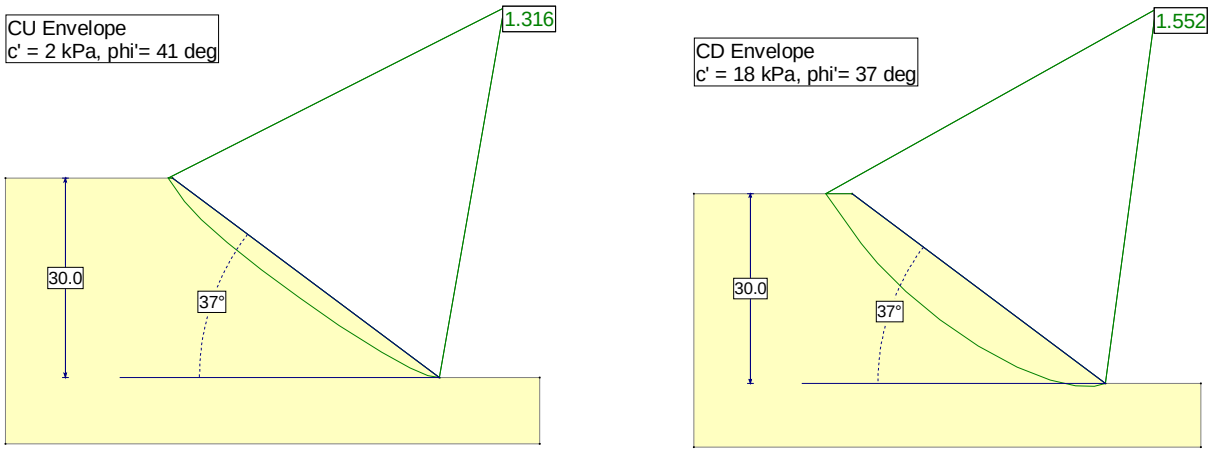

Figure 4. Left) *c'* and ϕ' adopted from CU envelope, and right) *c'* and ϕ' adopted from CD envelope

3.3. Moisture content and saturation

Figure 5 shows the shear stress plotted against the axial strain for tests 1 and 7, both of which were conducted on spoil material, with an s'_0 of 50 kPa. Prior to consolidation and shearing, test 1 was back-saturated as per standard triaxial procedures (outlined in AS 1289.6.4.2), resulting in a GMC of 17%. Test 7 however was not back-saturated, and instead remained unsaturated during testing, and at its run-of-mine GMC of 6%.

Comparing the results in Figure 5 it is apparent that the effects of saturation were to reduce the peak shear strength of the spoil from 123 to 100 kPa. This reduction in shear strength is due to a decrease in matric suction resulting from the saturation process. In an unsaturated soil, the water phase develops a negative tensile stress (known as matric suction) which increases the contact force between soil particles, and ultimately increases the shear strength. When the degree of saturation in a soil increases however, the matric suction and associated shear strength decrease. Once fully-saturated conditions are achieved, matric suctions trend to zero and no longer contribute to the shear strength.

Unfortunately, estimating the change in shear strength due to a change in matric suction is a complex multi-dimensional problem, largely dependent on soil type, structure and moisture content. As a qualitative rule however, it should be recognised that the effects from matric suctions are typically more pronounced in fine-grained soils, and increasing the moisture content will typically decrease soil shear strength.

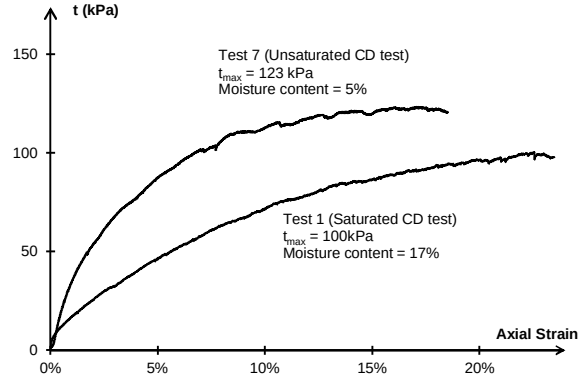

Figure 5. Comparison of stress-strain curves for saturated and unsaturated tests.

Quantifying the effects of saturation in terms of Mohr-Coulomb parameters, based on direct shear testing of a coal-mine spoil material derived from a weathered claystone, Seedsman et al. (1988) reported that ϕ' reduced on average by 9° upon saturation, whilst the BMA shear strength framework in Simmons and McManus (2004) suggested that ϕ' for saturated spoil within a spoil pile is 5 – 7° lower than ϕ' for unsaturated spoils.

Further complicating the effects of saturation and changes in moisture content on shear strength, is the propensity for some clay-mineral-rich mine wastes to slake and degrade on wetting. This may liberate individual clay particles from larger aggregates, reduce aggregate particle interlock, and alter the internal fabric of a material. Seedsman and Emerson (1985) note that the degree to which this occurs depends on the mineralogy, intact rock strength, pore water chemistry and handling practices.

Given the influence that moisture content can have on shear strength, it is therefore important that the effects of laboratory saturation be considered when scoping the testing program Laboratory saturation of mine wastes which are unsaturated under field conditions may otherwise underestimate the field shear strength. To provide accurate assessments of field shear strength, as applicable, unsaturated triaxial testing should be considered. The potential for changes in moisture content after deposition in the field should also be considered when specifying moisture contents for testing. If materials may saturate and slake after deposition, consideration should be given to induce slaking of the test specimens to reflect this.

3.4. Particle size and specimen diameters

Figure 6 shows results from triaxial tests 8-16, in which samples had diameter ratios of 7.5 (compliant), 5.3 (marginal) and 3.8 (low). Specimens with a "compliant" diameter ratio of 7.5 were the only ones that complied with AS 1289.6.4.2 (requiring a diameter ratio >6), and were therefore used as the control case to validate results from specimens with "marginal" and "low" diameter ratios.

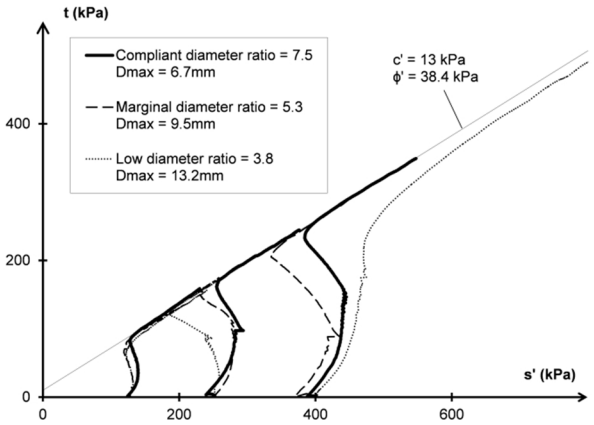

Figure 6. Comparison of ESPs for samples with different diameter ratios

Figure 6 shows that the ESPs for the marginally compliant specimens are reasonably consistent with the ESPs for the compliant specimens, terminating on approximately the same failure envelope. For the tests conducted at s'_0 of 250 and

400 kPa, the marginally compliant ESPs are slightly more contractive than the compliant ESPs. As a result; the marginally compliant ESPs intersect the failure envelope at slightly lower *s'* values, and would produce slightly lower undrained shear strengths, if this was taken at phase transformation.

In contrast, the ESPs for the specimens with the low diameter ratio do not compare very well with those for the compliant specimens. In Figure 6 the low diameter ratio ESPs are seen to be considerably more contractive when s'_0 = 250 kPa, yet considerably less contractive when s'_0 = 400 kPa. Furthermore, the low diameter ratio ESP for the s'_0 = 400 kPa stage does not appear to converge to the same failure envelope as the marginally compliant and compliant specimens, instead converging on a slightly lower failure envelope.

Based on the results shown in Figure 6, it would appear that test specimens with marginal diameter ratios as low as 5.3 produced reliable results, with little compromise in reliability due to the presence of oversize particles. Thus to limit scalping requirements for the triaxial testing of mine wastes, a diameter ratio of 5.3 could be coupled with the largest possible specimen diameter. Typically the largest specimen diameter offered by most commercial laboratories is 100mm, which would permit a D_{max} of 19mm if adopting a diameter ratio of 5.3. Also based on the results in Figure 6, it would appear that adopting a diameter ratio of 3.8 may produce unreliable results due to the presence of oversize particles. Although it is possible that some ratios between 5.3 and 3.8 may still produce reliable results, these remain untested and should not be used without further validation.

Regardless of the diameter ratio used, triaxial testing of granular mine wastes will still typically require scalping of a large fraction of oversize particles. Findings in the literature are not unanimous as to whether this increases or decreases shear strength (see for example Varadarajan et al., 2003) and the effects appear to be dependent on material characteristics. The literature does suggest however that the effects of scalping may be significant, where data presented by Bradfield et al. (2014) indicates that calculated shear strengths of a coal mine spoil material are sensitive to D_{max}. This reinforces that the largest available apparatus with the largest D_{max} should be used for shear strength testing of mine wastes. Consideration should also be given to whether removed oversize is simply omitted, or crushed and recombined, particularly in materials such as MPR where material behaviour is largely dependent on the coarse:fines ratio.

3.5. Multistage testing

Figure 7 shows the CU ESPs from multistage (MS) tests 17 and 18, compared with the CU ESPs from single stage (SS) tests 11 – 13. MS and SS tests were conducted using the same material (MPR) and same s'_0 values (125-400 kPa), with the only difference being the number of stages performed on each specimen, and the axial strains (ε_a) used for each stage. SS tests were sheared to 30% ε_a, whilst the two MS tests 17 and 18 were respectively sheared to 5% and 10% ε_a per stage. Each MS specimen was consolidated and sheared three times.

Figure 7 shows that the ESPs for both MS tests converge very near to the failure envelope from the SS tests, despite slightly underestimating the SS envelope when *s'* > 600 kPa. When compared in Table 2, the Mohr-Coulomb parameters from the MS tests are very similar to those calculated from the SS tests.

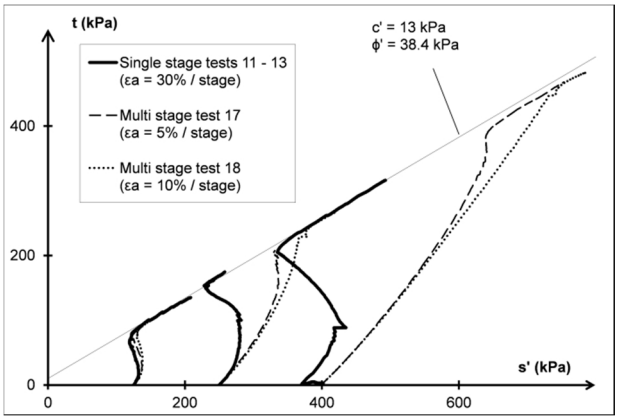

Figure 7. Results from single and multi-stage tests

Table 2. Mohr-Coulomb parameters for single stage and multi stage tests.

Mohr-Coulomb Parameter	SS Tests 11 – 13	MS Test 17 (ε_a = 5%)	MS Test 18 (ε_a = 10%)
c' (kPa)	13	5	10
ϕ' (°)	38.4	38.0	37.8

However, on reviewing Figure 7 it is evident that the MS ESPs in the latter stages are much less contractive than the SS ESPs, indicating Δu is much lower during undrained MS shearing. Furthermore, the MS ESPs from test 18 (10% ε_a per stage) are less contractive than the MS ESPs from test 17 (5% ε_a per stage). This suggests that the effect of shearing during early stages is to reduce contractive tendency and generation of Δu in latter stages, and these effects increase for higher cumulative $\varepsilon_a s$. These findings agree with comments by Head (2006), who suggested that although the effective shear strength parameters from MS tests are practically indistinguishable from those obtained by SS tests, other factors such as compressibility, dilatancy, pore pressure changes and void ratio changes do not compare well with SS tests. As a result of their reduced contractive behaviour, the MS ESPs undergo phase

transformation and reach the failure envelope at much higher stresses than the SS tests.

In practice, the above results indicate that MS triaxial tests could be used to derive effective strength parameters with little compromise in accuracy when compared to results from SS tests. Although the results in Figure 7 only include results from CU tests, Saeedy and Mollah (1988) report similar findings for CD tests. During undrained shearing in MS tests however, Δu was observed to be much lower in comparison to SS tests, and was attributed to the deformation and shearing in earlier stages. As such, the MS ESPs were much less contractive than SS ESPs, and grossly overestimated the undrained shear strength (if taken at phase transformation).

4. Conclusions

Results from triaxial testing of mine wastes have been presented to highlight various considerations that may often be overlooked when planning and conducting triaxial testing of mine wastes.

For normally-consolidated mine wastes, undrained triaxial testing typically results in contractive behaviour. Because of this; CU ESPs will typically define a failure envelope at lower stresses than CD ESPs (if CU and CD tests are conducted using the same s'_0). Because mine waste failure envelopes often exhibit curvature it is important that triaxial testing defines the failure envelope over a stress range similar to that expected in the field. An example was provided demonstrating how failure to do so may otherwise produce erroneous stability assessments in the event that linear envelopes are extrapolated into undefined stress ranges. Integral to the definition of the failure envelope over an appropriate stress range is the coupling of triaxial test types with appropriate s'_0 conditions.

The importance of conducting triaxial tests at expected field moisture contents was also discussed, as laboratory saturation of mine wastes that are unsaturated in the field may return conservative estimates of shear strength.

Although AS 1289.6.4.2 recommends that a diameter ratio of 6 or greater be maintained for triaxial testing, results have indicated that diameter ratios of 5.3 may be used with little compromise of results. Thus, coupling a diameter ratio of 5.3 with largest possible specimen size could be used to minimise scalping requirements.

It was also found that multistage tests may provide reasonably accurate effective (drained) shear strength parameters, but may grossly overestimate the undrained shear strength due to the effects that pre-deformation in early stages has on the generation of Δu in latter stages.

5. Acknowledgements

The authors gratefully acknowledge the financial assistance from the Australian Coal Association Research Program (ACARP).

6. References

Fredlund D. G., Morgenstern N. R., Widger, R. A. (1978). The shear strength of unsaturated soils. *Can. Geotech. Journal, vol. 15, pp. 313-321.*

Saeedy H. S., Mollah M. A. (1988). Application of multistage triaxial test to Kuwaiti soils. Advanced triaxial testing of soil and rock. ASTM STP 997

Head K. H. (2006). Manual of soil laboratory testing, Volume 3: Effective stress tests. Whittles Publishing – Dunbeath, Scotland, 412 pages.

Yoshimine M., Robertson P. K, Wride C. E (1999). Undrained shear strength of clean sands to trigger flow liquefaction. *Can. Geotech. Journal, vol. 36, pp. 891-906.*

Chern J. (1985). Undrained response of saturated sand with emphasis on liquefaction and cyclic mobility. PhD thesis – Uni. of British Columbia.

Tsukamota Y., Ishihara K., Kamata T. (2009). Undrained shear strength of soils under flow deformation. *Geotechnique,* vol. 59, pp. 483-486.

Simmons J. V., McManus D. A. (2004). Shear strength framework for design of dumped spoil slopes for open pit coal mines. *Proceedings, Advances in Geotechnical Engineering The Skempton Conference*, pp. 981-991.

Seedsman R. W., Richards B. G., Williams D. J. (1988). The Possibility of Undrained Failure in Bowen Basin Spoil Piles. *Proceedings, Fifth ANZ Conf. on Geomechanics, pp.* 404-409.

Seedsman R. W., Emerson W. W. (1985). The role of clay-rich rocks in spoil pile failures at Goonyella Mine, Queensland, Australia. *Int. J. Rock Mech. & Mining Sciences,* vol. 22, pp. 113-118.

Varadarajan, A., Sharma, K. G., Venkatachalam, K. & Gupta, A. K. (2003). Testing and Modeling Two Rockfill Materials. *Journal of Geotech. and Geoenviro. Eng.,* 129, 206-218.

Bradfield, L., Koosmen, K., Simmons, J. V., Fityus, S. G. (2014) Practical considerations for direct shear testing of mine spoils. *Proceedings, Tenth Young Geotech. Professionals Conf. (in press)*

This page intentionally left blank

Proceedings of the 10th ANZ Young Geotechnical Professional's Conference – 10YGPC
Noosa, Queensland, Australia
10 – 12 September 2014

LIQUEFACTION COUNTERMEASURES AT THE WELLINGTON WATERFRONT

Emilia BELCZYK
Tonkin & Taylor Ltd, Wellington, New Zealand

ABSTRACT – Wellington waterfront was reclaimed in a number of stages beginning in the 1850s. Most of the reclamations were constructed by end tipping of gravels obtained from excavation works or from local quarries. Other reclaimed areas were formed using hydraulic fill. The reclamation fills, which can be up to 15m thick, overlie a thin layer of soft harbour bed deposits which in turns overlies dense alluvium. Based on the material type and its density, liquefaction of the reclamation fills could be expected during strong earthquake shaking (magnitude M6 or greater). This paper presents an overview of the risk of liquefaction on the waterfront, plus a case study of a proposed five story development. Various foundation systems have been proposed to reduce liquefaction and its consequences at this site. The relative merits of these foundation systems considered are discussed. A cellular deep soil mixing with raft foundation and tension piles was selected. A description of this ground improvement method and its benefits and design requirements are presented.

1. Introduction

The Wellington waterfront covers the reclaimed land between Wellington's central business district (CBD) and the foreshore. In the past, the land was formerly occupied by railway and port facilities. However, nowadays due to its proximity to the CBD it presents unique opportunities for developers.

Construction of a new five story building with a basement has been proposed for one of the Wellington waterfront sites currently occupied by a carpark. The building design includes base isolation to provide high seismic performance by preventing the building's superstructure from absorbing earthquake energy. To support the base isolation system and ensure this high seismic performance, ground improvement has been proposed to reduce liquefaction and lateral spreading.

This paper discusses the geotechnical issues associated with the new development. The first part of the paper sets the geology and seismicity of Wellington Harbour. The second part presents Foundation system options considered for the specific development, as well as their advantages and limitations. From these foundation systems, a cellular deep soil mixing (DSM) with raft foundation and tension piles was selected as the preferred option. A description of this ground improvement method as well as its benefits and some specific design requirements are presented.

2. Geology and seismicity

2.1. Geology

The geology of Wellington is complex. Prior to the reclamation of the Wellington Harbour shoreline, the site was subject to deposition by alluvial and colluvial processes (Begg and Johnston, 2000). The deposited materials, transported from the surrounding hills, in-filled the steeply graded valleys of the inner Wellington Harbour during periods of elevated sea level. The changes in sea level built up the alluvium in layers of sand and silt.

On top of the alluvium, in very recent geological time, a layer of harbour bed deposits has built up. This generally consists of loose sand. The sand is often overlain by a layer of soft black silt, which is a result of human occupation of the area such as port activities.

Greywacke bedrock underlies the alluvium at depths ranging from 10m to 200m below the existing ground level (Semmens et al. 2011). Bedrock in the Wellington Region comprises folded and faulted indurated sandstone (greywacke), siltstone and mudstone (argillite). A typical soil profile at the Wellington waterfront is presented in Figure 1.

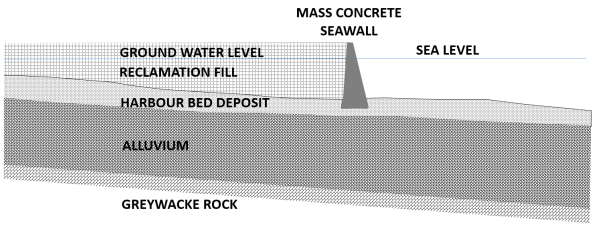

Figure 1. Typical soil profile

2.2. Reclamation history

A number of reclamations have been constructed since Europeans settled in Wellington in 1839. The initial reclamations were carried out in stages between 1852 and 1973, extending the shoreline 250m to 700m seaward (see Figure 2).

Most of the reclamations were constructed by end-tipping of gravel originating from quarries and nearby road and building excavations. There are

also areas of hydraulic fill constructed by pumping dredged sea bed sand and silt behind mass concrete seawalls.

The nature of the reclamation materials varies from soft silts and loose sands (dredged sea bed material) to loose silty gravel comprising weathered greywacke rock (end-tipped material). The depth of reclamation can be up to 15m and the mean sea level is approximately 2m below ground surface level. The reclamation fills overlie a thin layer of soft / loose harbour bed deposits which in turns overlies dense alluvium (refer Section 2.1).

The specific site considered in this paper consists of up to 7m of end-tipped granular reclamation fill overlying 1m of harbour bed deposits. The depth to rock is between 80m and 100m. The site is approximately 10m from the reclamation edge, which is supported by a mass concrete seawall.

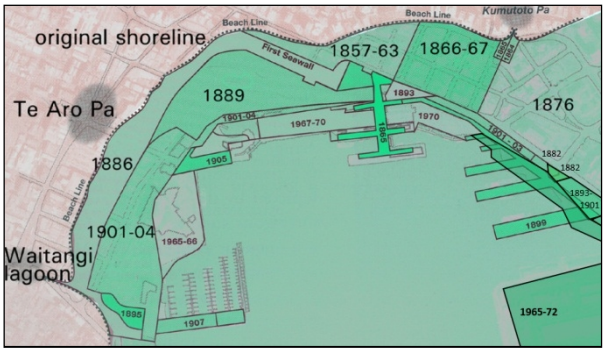

Figure 2. History of Wellington reclamation (source: Positively Wellington Waterfront website)

2.3. Wellington faults

The frequency of large earthquakes affecting the Wellington region is very high. There are a number of active faults identified as a seismic hazard to the Wellington region – the closest being the Wellington Fault (see Figure 3).

The Wellington Fault has a maximum credible earthquake event of moment magnitude 7.6 and the probability of its rupture in the next 100 years is considered to be 11% (Rhoades et al., 2011).

Other faults around the Wellington region, like the Wairarapa and Ohariu Faults, are also active and capable of generating major earthquakes.

3. Risk of liquefaction and consequences

3.1. Liquefaction

Seismic liquefaction occurs when excess pore pressures are generated in loose, saturated, generally cohesionless soil during earthquake shaking. This causes the soil to undergo a partial to complete loss of shear strength. Case histories indicate (e.g. Kobe, Japan in 1995) that liquefaction of gravels has been observed (Hara et al, 2004).

Figure 3. Wellington region faults lines (source: GNS Science website)

Such a loss of shear strength can result in settlement, bearing capacity failure and/or horizontal movement of the soil mass. The occurrence of liquefaction is dependent on several factors, including the intensity and duration of ground shaking, soil density, particle size distribution, and depth of the groundwater table.

Liquefaction of the reclamation at the Wellington waterfront could be expected during moderate to large earthquakes (Modified Mercalli Felt Intensity MM7 / Richter magnitude M6 or greater).

3.2. Liquefaction consequences

3.2.1. Lateral spread

Lateral spreading is the movement of ground toward a free edge (i.e. the sea) as a result of shearing of weak liquefied ground under seismic and/or gravity forces. It occurs in a series of slips extending back from the reclamation edge. The magnitude of displacement reduces with distance from the reclamation edge. With increasing magnitude and acceleration of earthquakes, greater lateral displacement and greater extent of lateral spreading from the reclamation edge can be expected.

The site is approximately 10m from the reclamation edge. Lateral spread of the Wellington reclamation fills of the order of 300mm or greater could be expected as a consequence of earthquake shaking with felt intensity of MM7 / magnitude M6 or greater.

3.2.2. Loss of vertical support and subsidence of foundations

Liquefaction may result in a loss or reduction of vertical bearing capacity of foundations. This can cause differential subsidence of structures.

In the event of liquefaction, the following contribute to the structures settlement:

- Shakedown consolidation type settlement of the liquefied layers (free field settlement).

- Strain within weak liquefied layers under the foundations loads.
- Sand boils and loss of soil to the surface.
- Settlement associated with lateral spread.

For this specific site, only a shakedown consolidation type settlement of up to 300mm has been estimated for the average 7m thick layer of reclamation fill. Loaded foundations could be subject to even greater settlement / subsidence.

3.2.3. Increase of lateral earth pressure

Earthquakes create unfavorable effects on underground structures such as basements. During earthquake shaking lateral earth pressure on buried structures increases from the pre-existing at rest earth pressure (K_0) by the following factors:

- increase of excess pore water pressure (pore pressure ratio (ru) increase to 1),
- potential ground movement toward the buried structure.

3.2.4. Buoyancy effects

Buoyancy can be caused by excess pore water pressure increase during liquefaction. Building basements, manholes and other underground vessels buried below the level of liquefaction could be subject this uplift pressure. This pressure could result in damage to underground services and basement floor heaving and cracking allowing ingress of water and sand.

4. Foundation system

4.1. Specific development

Construction of a new five story building with a basement extending over approximately 60% of the building footprint has been proposed for a specific site on the Wellington waterfront. A base isolated reinforced concrete structure is proposed. The foundation system for this structure needs to:

- mitigate lateral spread,
- mitigate basement buoyancy forces in the event of liquefaction,
- support building gravity and seismic compression loads without adverse differential settlement,
- resist high local tension actions from the structure during severe earthquake shaking,
- resist base shear from the structure.

4.2. Options considered

The following foundation systems have been considered:

- *Option 1:* Grid of gravel compaction columns over the building footprint area plus a foundation raft slab with bored belled piles acting in tension and temporary sheet pile wall to control ground water
- *Option 2:* Grid of dynamic compaction over the building footprint area plus a foundation raft slab with bored belled piles acting in tension and temporary sheet pile wall to control ground water.
- *Option 3:* Wet cellular deep soil mixing over the building footprint area plus a foundation raft slab with bored belled piles acting in tension.
- *Option 4:* High pressure jet grouting over the building footprint area plus a foundation raft slab with bored belled piles acting in tension
- *Option 5:* Bored belled piles plus temporary sheet pile wall.

A description of each foundation option is listed in Table 1. Advantages and disadvantages are highlighted for each option.

4.3. Evaluation of options

The relative advantages and disadvantages of each option has been identified. For the specific site, an initial option evaluation was undertaken in conjunction with a structural engineer as summarized Tables 1 and 2. During these evaluations, the DSM method with raft foundation and tension piles was identified as the preferred foundation option (see Option 3 in Tables 1 and 2).

5. Deep Soil Mixing

5.1. Performance

Deep soil mixing has been commonly used worldwide since the 1970s. However, this is a relatively new method in New Zealand.

Deep soil mixing can be used to improve the performance of a specific site by reducing the shear strains imposed and excess pore water pressures generated in the enclosed soil. It provides resistance against lateral deformations and reduces vertical settlement potential. It provides a barrier against high excess pore pressures migrating from surrounding unimproved soils to the enclosed area.

Case histories, although limited, demonstrate that DSM can perform well during earthquake shaking and liquefaction (O'rourke et al, 1997).

5.2. Process, types and geometry

During construction, soils are mixed in-situ with cement or any other stabilizing binders, which chemically react with the soil and/or groundwater. The binders are injected through a hollow mixing shaft equipped with various cutting tools (i.e. auger flights, mixing blades) to increase the efficiency of the mixing process.

Table 1. Foundation system options for the Wellington waterfront development

Option	Description of foundation system	Advantages	Disadvantages
1	Grid of gravel compaction columns to densify the soil mass over the building footprint. Foundation raft slab. Bored belled piles acting in tension. Temporary sheet pile wall to control ground water. Gravel is placed through the tip of a vibrator at a specified improvement depth followed by progressive raising and re-penetration of the vibrator to densify the gravel.	• Reduce liquefaction potential • Increases bearing capacity • Reduces total and differential settlements • Relatively cheap cost of construction • Suitable for installation in limited space • Relatively low carbon footprint	• Inadequate lateral restraint to seaward edge of reclamation • Some settlement potential remains.
2	Grid of dynamic compaction to densify the soil over the building footprint. Foundation raft slab. Bored belled piles acting in tension. Temporary sheet pile wall to control ground water. The compaction is achieved by impact energy that is caused by dropping a heavy weight from a relatively great height.	• Well known method (used at Museum of New Zealand, Wellington) • Increases bearing capacity • Reduces total and differential settlements • Sustainable technique, low carbon footprint • Relatively cheap cost of construction • Relatively low carbon footprint	• High vibration during construction • Inadequate lateral restraint to seaward edge of reclamation • Some settlement potential remains.
3	Wet cellular deep soil mixing to solidify the soil mass over the building footprint. Foundation raft slab. Bored belled piles acting in tension (refer Section 5 for method description).	• Resists cyclic strains mitigating liquefaction between DSM walls • Resists lateral spread • Increases bearing capacity and provides suitable base for shallow foundations • Reduces total and differential settlements • Provides ground water control and temporary lateral restraint for basement excavation • Low noise and vibration during construction • Suitable for installation in limited space and near existing structures	• Difficulty penetrating very dense or very stiff soils • Difficulty mixing in organic soils • Produces a considerable quantity of soil / grout waste material • Underground utilities and obstructions may pose problems • High carbon footprint
4	Cellular high pressure jet grouting to solidify the soil mass over the building footprint. Foundation raft slab. Bored belled piles acting in tension. Improvement is achieved by placement of grout material under pressure using a combined process of cutting soil by high pressure jet and filling the space with grout.	• As per Option 3	• Relatively high cost of construction • Produces considerable large quantity of soil / grout waste material • High carbon footprint
5	Belled bored piles to provide tension, compression and lateral capacity. Temporary sheet pile wall to control ground water.	• Commonly used in Wellington • High uplift and compression resistance • Flexibility of going deeper if weak ground encountered • Relatively low settlement on loading	• Relatively high cost of construction • High carbon footprint • Bell collapse risk

Table 2. Relative merits of options

Feature	Options				
	1	2	3	4	5
Proven design and construction in Wellington					
Ability to resist severe earthquake without significant damage					
Simplicity of construction					
Limit construction noise and vibration					
Carbon footprint (Zöhrer, Wehr and Stelte, 2001)					
Relative construction cost					

Applied ranking:	expected to be best	average	expected to be worst

Two types of DSM are available: wet mixing and dry mixing. Wet mixing involves injecting binders in slurry form to blend with the soil. Dry mixing uses binders in powder form that react with the water already present in the soil.

DSM is installed in many different layouts with the most commonly used shown in Figure 4.

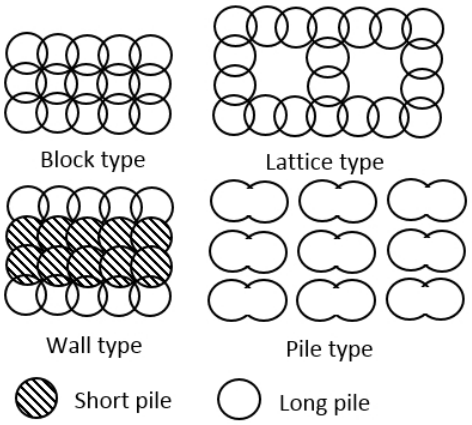

Figure 4. Typical layout of DSM improvement

Deep soil mixing for liquefaction mitigation generally uses a lattice or wall layout. They have a large resistance against horizontal forces. The improved ground restricts shear deformation of the unimproved soil inside reducing potential for liquefaction. Since the DSM improvement can prevent transmission of excess pore water pressure, the area required to be improved outside of the construction is relatively small compared to the densification method.

An approximate 6m by 6m DSM cell layout with 1m wall width penetrating up to 7.5m depth is proposed for the new development in order to match the geometry of the proposed building and depth of fill and harbour bed deposits (see Figure 5).

The typical cell spacing is generally 5m to 6m. The expected performance of this layout has been assessed based on currently available literature including Bradley et al. (2013) and Kitazume and Takahashi (2010). Based on the literature review, it is expected that the proposed DSM cell spacing is sufficient to mitigate liquefaction effects during earthquake shaking.

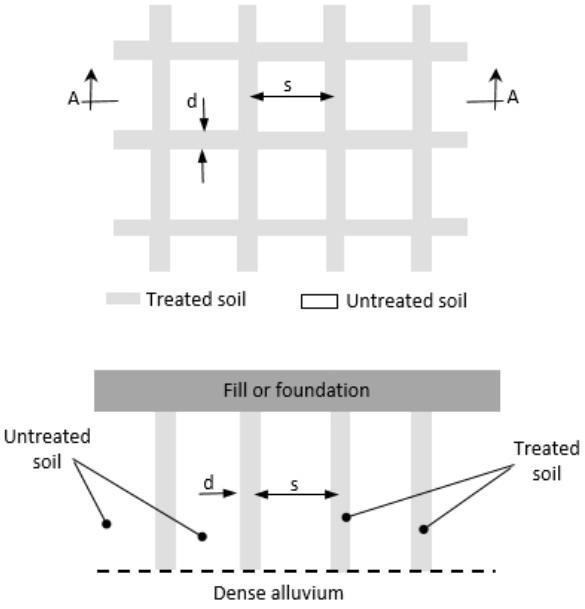

Figure 5. Typical layout and cross-section of DSM

The DSM ground improvement provides a 7.5m thick non-liquefiable "raft", mitigating settlement arising in this upper 7.5m of the ground profile and reducing differential settlement resulting from any potential liquefaction below 7.5m.

5.3. Geotechnical properties

The improved material has a higher strength. For this specific site it is expected to achieve 28 days unconfined compression strength (UCS) between 2MPa and 4MPa. However, based on the experience gained in Japan, it is not possible to predict the strength of the ground improvement based on in-situ characteristics of soil. Consequently, laboratory tests of DSM core samples are required to determine the actual strength (U.S. Department of Transportation, 2013).

Permeability values in treated sandy soils can be as low as 10^{-9}m/sec to 10^{-7}m/sec, which allow the DSM walls to be used as hydraulic cut-off walls during basement excavation. The same wall can serve as a temporary retaining wall for the excavation by installing UC steel columns within

the constructed walls to increase its bending capacity (Kitazume and Terashi, 2013).

5.4. Implementation

A foundation raft slab plus bored belled piles acting in tension are proposed as the foundations system for the waterfront development. This raft slab is supported on the proposed 6m by 6m DSM grid. The depth of improvement is approximately 7.5m with reduced grouting in the first 3.5m, which will be excavated for the basement construction (see Figure 7). This foundation system and ground improvement provides; reliable liquefaction mitigation, sufficient vertical (compression and tension) and lateral capacity to resist large earthquake loading.

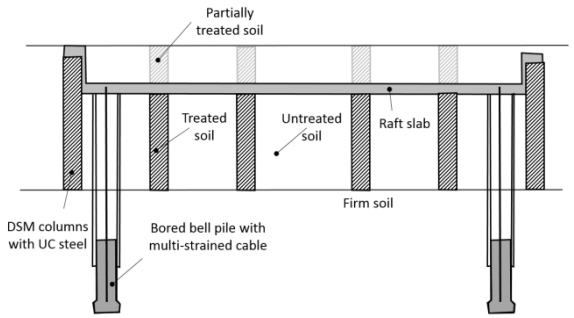

Figure 7. Foundation system

A water cut off barrier and temporary retaining wall required for the basement excavation is provided by perimeter DSM walls with UC steel columns in every 3rd DSM column.

6. Conclusions

A high risk of liquefaction exists in the reclamation fill material at the Wellington waterfront including the selected site for the new development.

The proposed building will feature a base isolated foundation structure to mitigate seismic loads to the superstructure. To support this system raft foundations on improved ground plus tension piles are proposed.

A number of ground improvement options have been considered and cellular wet deep soil mixing was selected as the preferred one to mitigate liquefaction and its consequences at this site. This method presents the following benefits:

- Resists cyclic strains, mitigating liquefaction between walls
- Resists lateral spread
- Increases bearing capacity and provides a base for shallow foundations
- Reduces total and differential settlements
- Provides ground water control and temporary lateral restraint for basement excavation
- Suitable for installation in limited space and near existing structures
- Relatively small area required to be improved outside of the construction
- Low noise and vibration during construction, making it more desirable for constructions within urban areas such as Wellington CBD.

The combination of the base isolation system, raft foundation, DSM ground improvement and tension piles provides a reliable liquefaction mitigation system plus sufficient vertical and lateral capacity to resist large earthquake loading.

Due to the limited experience of DSM method in Wellington, allowances are required for flexibility in the design and construction procedures to address variations in the encountered ground conditions.

7. Acknowledgements

The author wishes to express her great appreciation to Stuart Palmer from Tonkin and Taylor Ltd for his support during the writing of this paper.

8. References

Begg, J. G., and Johnston, M. R. (2000). Geology of the Wellington area. *1: 250 000 Geological Map 10. Lower Hutt, New Zealand. Institute of Geological and Nuclear Sciences Ltd.*

Bradley, B.A. et al. (2013). Effect of Lattice-Shaped Ground Improvement Geometry on Seismic Response of Liquefiable Soil Deposits via 3-D Seismic Effective Stress Analysis. *Soil Dynamics and Earthquake Engineering Vol. 48 pp. 35–47*

Hara T., et al. (2004) Undrained strength of gravelly soils with different particle gradations. *13th World Conference on Earthquake Engineering,* Vancouver, Canada

Kitazume, M. and Takahashi, H., (2010). Centrifuge model tests on effect of Deep Mixing wall spacing on liquefaction mitigation, *Proc. of the 7th International Conference on Urban Earthquake Engineering (7CUEE) & the 5th International Conference on Earthquake Engineering*

Kitazume, M., and Terashi M. (2013) The Deep Mixing Method. Leiden, *The Netherlands: CRC Press / Balkema*

Nguyen, T. et al. (2013). Design of DSM Grids for Liquefaction Remediation. *Journal of Geotechnical and Geoenvironmental Engineering Vol. 139, Issue 11, pp. 1923-1933*

O'rourke, T. D, et al. (1997) Reduction of liquefaction hazards by deep soil mixing. *National Center for Earthquake Engineering Research*

Rhoades, D. A., et al. (2011). Re-evaluation of conditional probability of rupture of the Wellington-Hutt Valley Segment of the Wellington Fault. *Bulletin of the New Zealand*

Society for Earthquake Engineering, Vol. 44, No. 2, pp. 77-86

Semmens, S., et al. (2011). NZS 1170.5: 2004 site sub soil classification of Wellington city. *Proceedings of the ninth Pacific conference on earthquake engineering pp.14-16*

U.S. Department of Transportation. (2013). Federal Highway Administration Design Manual: Deep Mixing for Embankment and Foundation Support. *Report No. FHWA-HRT-13-046*

Zöhrer, A., et al. (2001). Is ground engineering environmental friendly? *Proceeding of the 11th International EFFC-DFI Conference, Session 3: Sustainability in the Foundation Industry*

This page intentionally left blank

Proceedings of the 10th ANZ Young Geotechnical Professional's Conference – 10YGPC
Noosa, Queensland, Australia
10 – 12 September 2014

NUMERICAL ANALYSIS OF A SLOPED EXCAVATION IN ORGANIC CLAY

Akula PAVAN and Tamilmani THRIUVENGADAM[2]
[1] *AECOM Singapore Pte. Ltd., Singapore*
[2] *Bachy Soletanche, Singapore*

ABSTRACT – Singapore is a rapidly growing economy and its urbanization has led to vast developments in infrastructure along the coastal regions of Singapore. The presence of Peaty clay in urban areas poses a threat to the design of new underground structures. The design and construction of these structures should have minimal influence on the existing critical structures (basement of Mass Rapid Transit stations and Piles). This paper concentrates on the design methodology used in the design of a sloped excavation (Waterway) in Peaty clay located in an urban area. Peaty clay is a very soft (SPT 1 to 6) clay with high organic content and is acidic (PH>7) in nature. The excavation is assumed to be 15m deep. The presence of critical structures demands stringent measures to reduce the influence of excavation on the critical structures. The flowchart for an effective design solution is also discussed. Geotechnical Finite Element modeling is adopted to study the effect of excavation of untreated and treated soil on the critical structure. It is divided into parts based on the presence of critical structures. 1) Waterway near critical structure 2) Waterway in green field. Separate schemes are developed for the two parts. Jet Grouted Piles (JGP) and grouted Stone Columns are designed for the waterway. Validity and Impact of ground improvement to surrounding structures have been studied using advanced finite element modeling.

1. Introduction

The geographical size of Singapore and its increase in population has forced extensive infrastructure developments even in areas with challenging geotechnical conditions. The geological strata of these sites can be made favorable by the use of ground improvement techniques. Soft soils such as marine clay, pose a problem in excavation as the shear strength of these soils is very low. Ground improvement techniques using chemical admixtures adopted for peaty clay should take into consideration the acidic nature of the soils. For example, Jet grout piles use cement for increasing the shear strength. The shear strength of the soil is improved by the formation of calcium silicate hydrate. Peaty clay being highly acidic in nature, affects the target shear strength. In order to achieve the target shear strength of excess volume of cement is used for the Jet Grout Piles (JGP). In this technical paper, two schemes of ground improvements such as Jet Grout piles and stone column and their effectiveness in reducing the impact on surrounding structures are studied. In general, peat is a complex material consisting of organic matter which starts under aerobic and anaerobic conditions through incomplete decomposition of plant and animal matter. Research to understand the creep behavior has been carried out (Mesri et al.1997, Elsayed 2003, Fox et al 1992). One of the major concerns of peaty clay is its creep behavior especially in long term problems.

Finite element modeling is used to substantiate the viability of the proposed schemes for various constitutive models such as Mohr-Coulomb, Hardening soil model etc. The constitutive soil models are based on various conservative assumptions and hence will prevent under design of the ground improvement technique adopted. Modeling the ground improvement and predicting the ground settlement is also accomplished using finite element modeling.

2. Geological Conditions

The varying geological strata are presented in Figure 1. The geological condition analyzed in this paper is a 10 m thick organic clay (acidic in nature, PH > 7) with a SPT value of 4 – 7. The organic clay layer overlies a thick layer of peaty sand.

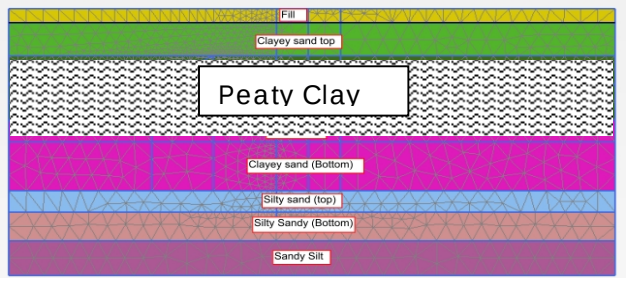

Figure 1. Geological Strata

Peaty Clay belongs to the Kallang Formation of Singapore. Kallang formation is relatively recent formation in Singapore which has alluvial soils of marine, estuarine and littoral origins. Peaty clay is a transition member of the Kallang formation. Civil Design Criteria (LTA CDC, Singapore) for determining the undrained shear strength of peaty

clay is presented in Figure 2. Depending on the depth where estuarine clay is encountered, the shear strength varies accordingly.

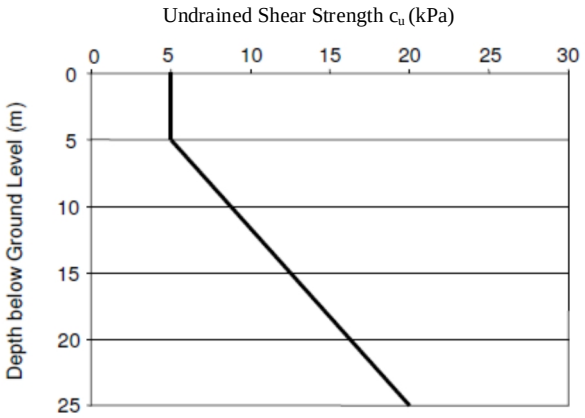

Figure 19. Undrained Shear Strength of Peaty Clays (Source: LTA CDC, Singapore)

3. Sloped Excavation

Excavation width of 30 m and depth of 15m respectively is shown in Figure 3. Most of the excavations are in peaty clay. Hence, the need for ground improvement arises. The type of ground improvement is dependent on factors such as cost, time, nearby critical structures, etc. This paper discusses the effect of two types of ground improvements techniques (Stone Column and Jet Grout Piles). The type of ground improvement technique adopted is based on the presence of critical structures nearby.

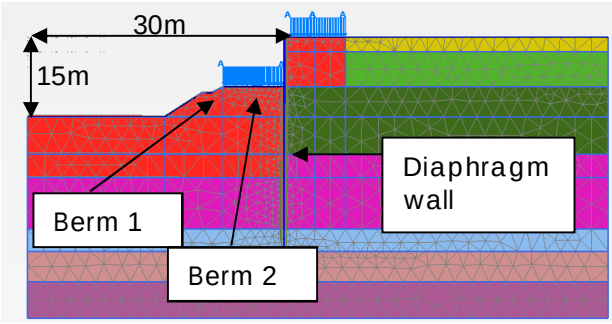

Figure 3. FEM Model

4. Finite Element Model

The numerical tool used in this work is the commercial PLAXIS (finite element program. PLAXIS 2D V12) which is a 2 Dimensional Finite element program. All analysis in this paper use 15 node elements unless otherwise stated. Closed boundary conditions were adopted for the model as shown in Figure 4. Two types of constitutive models are adopted for the present study: Mohr Coulomb (MC), a simple linear elastic perfectly plastic model - and Hardening soil model, the so-called advanced soil model.

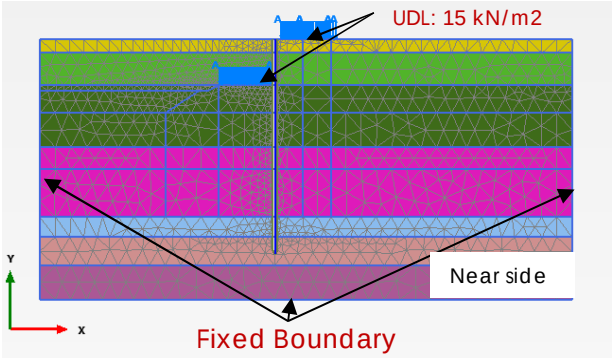

Figure 4. PLAXIS Model-Initial Phase

The objective of ground improvement is to satisfy the stringent displacement allowance for the critical structure set by the stakeholders. The limit of allowable displacement has been set at 10 mm.

4.1. Model geometry

The presence of critical structures nearby necessitates the need for different ground improvement techniques. Ground improvement by JGP was adopted in areas where the critical structures are within the zone of influence of excavation and stone column was adopted where the critical structures are outside the zone of influence.

4.1.1 Near Critical structure (Near Side)

Two berms along with diaphragm wall as shown in Figure 3 facilitate the excavation near critical structure. The Diaphragm wall reduces the soil movement. The distance of the critical structure from the Diaphragm wall is 40 m

4.1.2 Green Field

Diaphragm wall is not used in this section because the soil movement is not the deciding criteria for the excavation. The Water table was assumed to be 2m below the ground level. The diaphragm wall and peaty clay will prevent seepage of water into the excavation side. Steady state conditions were adopted for the model.

Stone columns are proposed, In order to reduce the long-term settlements in the waterway. Stone Columns not only reduce settlement but also minimize the overall cost of ground improvement.

Stone columns are proposed in a triangular pattern with each individual columns being 1m in diameter since triangular pattern covers more area with lower number. A friction angle for Stone Columns of 40° was used to design the stone column.

The problem was modeled in PLAXIS and the assumptions with the modeling are as follows:

- The elastic settlement of the ground and the column are insignificant when compared to the consolidation settlement
- Darcy's law is valid and the flow of water through the soil is purely horizontal. In other words, it is radial towards the column (Indraratna et. al., 2013)

The improvement factor is a term used to describe the extent to which the soil can be improved. The basic equation for calculating the improvement factor of stone column is given below (Equation 1 and Figure 5):

$$n_0 = 1 + \frac{A_c}{A}\left[\frac{1/2 + f(\mu_s, A_c/A)}{K_{ac}.f(\mu_s, A_c/A)} - 1\right] \quad (1)$$

Where: $f(\mu_s, A_c/A) = \frac{(1-\mu_s)(1-A_c/A)}{1-2\mu_s + A_c/A}$

K_{ac} = $\tan^2(45^\circ - \phi/2)$
μ_s = Poisson's ratio of soil
A_c = Area of column
A = Area of the grid

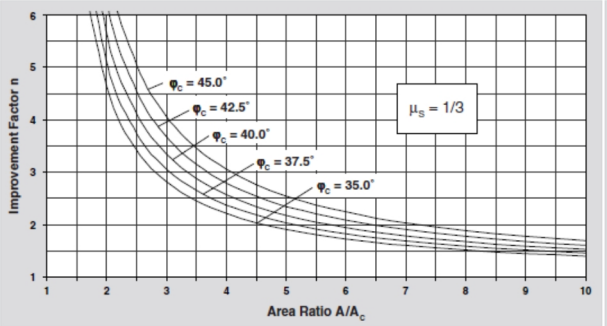

Figure 5. Design Chart for Stone Columns

4.2. Model Parameters

Moderately conservative parameters were chosen for the analysis. Organic Clay was modeled with undrained parameters and Peaty sand was modeled with drained parameters respectively. The undrained analysis (peaty clay) is a critical condition. The parameters used in Peaty clay and Peaty sand are presented in Table 1. A uniform water table of 2 m below ground level was adopted for the analysis. In order to avoid numerical instability, negligible undrained shear strength (c_u) of 0.1 kPa for Peaty sand was used.

Table 1. Soil Parameters

Soil Type	Type	E'(MN/m^2)	c_u (kPa)	ϕ
Peaty Clay	Undrained	5200	25	-
Peaty sand	Drained	4150	0.1	28°

4.3. Ground Improvement techniques

The objective of the ground improvement technique adopted was to increase the shear strength of the soil.

4.3.1. Near Critical Structure (Near Side)

The ground improvement scheme for critical structures nearby is shown in Figure 6. Jet Grout piles (JGP) with an average shear strength of c_u 500 kPa was adopted. The target shear strength was derived from previous achieved strength in peaty clay. JGP is executed for the entire length of Peaty clay. A diaphragm wall 1 m thick was adopted nearby the critical structure, to prevent the lateral movement of soil near the critical structure. A small stretch of JGP is adopted on the other side of the diaphragm wall to provide support for the diaphragm wall during casting.

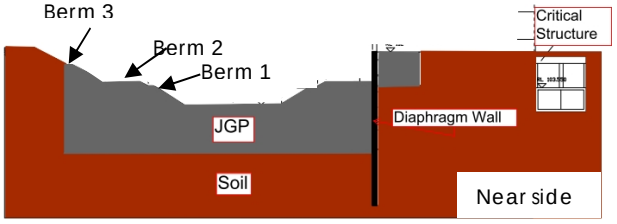

Figure 6. Ground Improvement Scheme

4.3.2. Green field

In the Green field zone, Ground improvement techniques such as Dynamic Compaction and Dynamic replacement are proposed.

Dynamic compaction is to be provided with 6m × 6m grid. 6 passes are to be applied with a 15 ton hammer, dropped from a height of 12 m. A sand blanket of 2 m is applied throughout the area. Finally, an ironing pass should be performed with low energy. The velocities of soil particles with which they are travelling (peak particle velocity) must be checked. With the above mentioned conditions, the induced vibrations are to be less than 23mm/s, which are less than acceptable limits.

4.4. Calculation steps

A brief overview of the calculation steps is presented in Figure 7.

The initial stress was computed based on K_o conditions. Ground Improvement was then activated for the entire length of peaty clay. The excavation was carried out in two stages of 7.5m each. A c-phi reduction was implemented to find the factor of safety for the current model. c-phi reduction will reduce the shear strength of the soil and will determine the slip circle. Thus, the slip circle determines the optimum area of ground improvement needed.

Initial phase	0	N/A	K0 procedure
<Phase 1>-Install Dwall	1	0	Plastic
<Phase 2>- Install JGP	3	1	Plastic
<Phase 3>-Excavate to Level 1	4	3	Plastic
<Phase 4>-Excavate to Level 2	5	4	Plastic
<Phase 5>-Final Excavation Level	6	5	Plastic
<Phase 6>-Factore of Safety	7	6	Safety

Figure 7. Calculation steps

5. Results

5.1. Untreated soil condition with ERSS

The analysis indicated a maximum horizontal displacement of 5 m for the Diaphragm wall as shown in Figure 8.

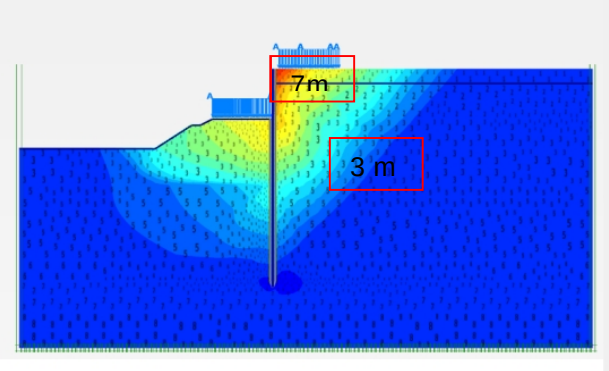

Figure 8. Horizontal Displacement

Generation of excess negative pore water pressure due to the excavation resulted in shear failure as shown in Figure 9. The plastic points indicate the propagation of shear failure.

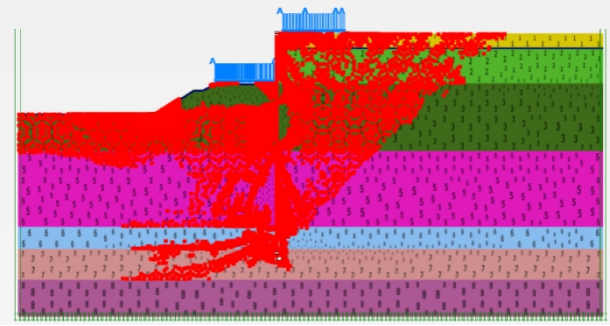

Figure 9. Plastic Points

5.2. Ground improvement

5.2.1. Jet Grout Piles with ERSS

Jet Grout Pile with ERSS (1m thick diaphragm wall) was modeled using two Mohr-Coulomb and hardening soil constitutive models. The maximum horizontal movement at a distance of 40m from the critical structure is 30mm as deduced from the Mohr-coulomb model and 10 mm for the hardening soil model. Hardening soil model takes into account the change of stiffness with strain while the Mohr-Coulomb model is a perfectly elastic plastic model, thus exhibiting reduced maximum horizontal movement.

A comparison of horizontal movement behind the diaphragm wall for the two constitutive models is shown in Figure 10.

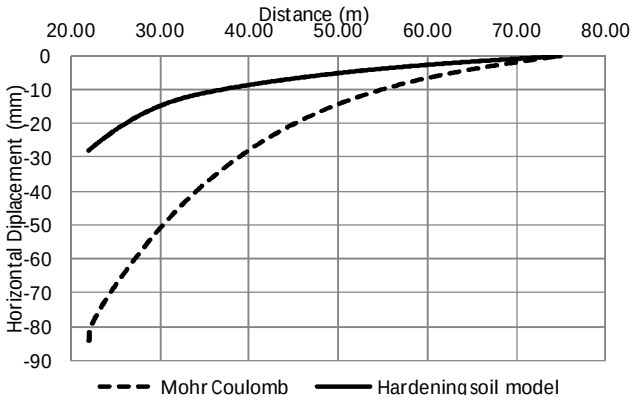

Figure 10. Horizontal Displacement Vs Distance

The Mohr-Coulomb model exhibits a maximum horizontal displacement of 80 mm just behind the wall. This displacement gradually decreases as the distance from the excavation increases. The critical structure is located 40 m away from the diaphragm wall and experiences a maximum deflection of 10 mm (Hardening soil model). The maximum deflection is less than the 10 mm criteria set for critical structures.

5.2.2 Diaphragm wall - Bending moment and shear force

A maximum bending moment of 1457 kNm and shear force of 540 kN/m was calculated using Finite Element Modeling (FEM).

A 1m thick diaphragm wall has a maximum capacity of 2000 kNm and Shear force of 1500 kN. A Factor of safety of 1.4 (for maximum allowable shear force and maximum allowable bending moment)was used as the criteria for the diaphragm wall

5.2.3 Stone Columns

The depth of the stone columns is 8.5 m below the existing ground level. The settlement of the waterway was calculated to be 72 mm before improvement. It has been reduced to 25 mm after the ground improvement with 64% reduction.

6. Conclusions

The combined resistance provided by Jet Grout pile and diaphragm wall reduces the displacement

caused due to excavation, thus negligible impact is induced on the critical structure nearby.

Stone columns also prevents slope stability failure during excavation but does not significantly reduce the lateral displacement. The absence of critical structures in the vicinity justifies the non-requirement of a more expensive ground improvement technique

7. Acknowledgements

We would like to thank AECOM Singapore Pte. Ltd, Bachy Soletanche and Reviewers for their continuous support and encouragement

8. References

Biarez, J. and Hicher, P.Y. (1994), Elementary Mechanics of Soil Behaviour.

Civil Design Criteria for Road and Rail Transit Systems (2010), Land Transport Authority, Singapore

CP4: Code of Practice for Foundations (2003), Spring Singapore, Singapore

Dames and Moore (1983), Detailed geotechnical study – engineering report and detailed interpretative report, Mass Rapid Transit System, Singapore.

Indraratna.B., Basack.S., Rujikiatkamjorn.C (2013). Numerical Solution of Stone Column–Improved Soft Soil Considering Arching, Clogging, and Smear Effects. *Journal of Geotechnical and Geoenvironmental engineering,* ASCE, Vol.139, No.3, pp.377-394

Sina et al. A review of stablisation of soft soils by injection of chemical grouting. Australian Journal of Basic and Applied Sciences, pp 5862-5868

South Carolina Department of Transportation (2010), *Geotechnical Design Manual*, pp 1-90

This page intentionally left blank

Proceedings of the 10th ANZ Young Geotechnical Professional's Conference – 10YGPC
Noosa, Queensland, Australia
10 – 12 September 2014

NOVEL SELF-FILTRATION CRITERIA FOR SUFFUSION ASSESSMENT

Huu Duc TO[1] and Alexander SCHEUERMANN[1]
[1]*School of Civil Engineering, The University of Queensland, Australia*

ABSTRACT - Suffusion is one major reason for the creation of sinkholes and dysfunctions of hydraulic structures. When suffusion occurs, fine soil grains are mobilized and dislodged by seepage flow. There are two types of suffusion assessment methods, developed based on the consideration of self-filtration processes: (1) quick and easy-to-use correlation methods, which correlate some specific and characteristic sizes of the grain size distribution (GSD) to ensure that coarse grains are capable of keeping fine grains in place regardless of the seepage flow; and (2) separation methods, which divide the GSD of soils into two separated fractions, primary fabric and loose grains, before specific filter criteria are used for the GSDs of the both fractions. This study presents two novel approaches in both of the above introduced groups. The first approach acknowledges the fact that suffusive soils are often characterized with a steep slope in the coarse fraction and a flat slope in the fine fraction of the GSD. This assessment approach assesses the suffusion potential of a soil via the farthest distance a GSD can go from its mean line, i.e. how hard it is kinked. The second approach suggests a new way to separate soil primary fabric from loose grains taking into account the fact that there is an overlapping zone between the both fractions. Both criteria show a good coherence with data from experimental studies.

1. Introduction

Suffusion is one of the main reasons for the development of sinkholes and is considered to be causative for almost 50% of dysfunctions in embankment dams (Foster, Fell, & Spannagle, 2000).

Although narrow-graded soils are more likely non-suffusive, local wide–graded materials are preferable to be used in order to circumvent the great expense on buying, transporting and replacing materials. In the last century, many empirical studies have been conducted with the aim to develop reliable criteria for the assessment of suffusion. Recently, a simple, but effective, method for internal stability assessment of wide–graded materials correlated slopes of coarse and fine parts in the soil Grain Size Distribution (GSD) (Wan & Fell, 2008). Though this method, as well as some other similar ones (Burenkova, 1993; Sherard, 1979), can cover a large number of soils, there are still cases where these criteria are not able in identifying suffusive soils. (To & Scheuermann, 2014).

This paper represents two novel assessment methods based on self–filtration criteria, which divides the GSD into filter and loose fractions to apply filtration criteria. Filter fraction builds up a soil *primary fabric* to support loads, and, thereby, its grains would be kept firmly in place by the load transfer. Thereby, these grains form a porous structure which actually acts as a filter. Meanwhile, loose grains can be mobilized and transported through series of pores in that porous structure by seepage flows because they are stabilized by their self–weight and/or weights of just only few other lose grains above them.

The first new method inherited a traditional point of view that stable soils often have a straighter GSD line in comparison with unstable soils. The bend of GSD line is assessed through the farthest distance it goes from its mean line. This method is easy to apply in engineering work.

The second method is developed from a recent numerical simulation discovery that there is transitional interval between those two fractions, where a grain can be a loose grain, while another grain with the same size can be involved in the filter fraction (To, Galindo-Torres, & Scheuermann, 2014). This method employs an assumption that loose grains sized *d* will be kept in pore of grains sized 4*d* or larger (Kenney & Lau, 1985). This method correlates the loose grain size distribution with the pore constriction size distribution formed by filter fraction to find out the transportable fraction. In a short explanation, the constriction is the narrowest place along the path connecting neighbour pores. A grain can be transported from a pore to another if it is smaller than the constriction size (Indraratna, Raut, & Khabbaz, 2007).

Both of new methods were tested with experimental data and showed a good agreement.

2. Some important existing assessment methods

This part of the paper is not only simply a literature review section, but also gives a brief summary of excellent ideas, which was considered by the new assessment methods.

One of the most comprehensive methods which must be summarized in this section is the Russian standard, which assesses many factors, such as

the soil porosity, uniformity, hydraulic gradient and seepage directions (ВНИИГ, 1976). The largest size of suffusive grains, d_{smax}, is calculated by (Goldin, Rasskazov, & Zeidler, 1992):

$$\boldsymbol{d_{smax} = 0.35 k_u \sqrt[6]{C_u}\frac{n}{1-n} d_{17}} \quad (1)$$

Where: C_u – coefficient of uniformity, $C_u = d_{60}/d_{10}$; k_u – coefficient of non-uniformity arrangement, $k_u = 1+0.05C_u$; n – porosity. In this paper, d_x indicates the opening size of sieve, which allows x% of soil mass to pass through, if there is not any other indication.

If the cumulative mass of suffusive grains is smaller than an acceptable loss, i.e. $d_{smax} \leq d_3 \div d_5$, soil is considered as stable. In addition, suffusion might not occur if the hydraulic gradient of seepage flow is smaller than its critical value I_{cr}:

$$\boldsymbol{I_{cr} = \varphi_0 d_{suf}\sqrt{\frac{ng}{vk}}} \quad (2)$$

Where: v – kinematic viscosity of water; k-hydraulic conductivity and φ_0 defined by:

$$\varphi_0 = 0.6\left(\frac{\gamma_{grain}}{\gamma_{water}} - 1\right)[0.82 - 1.8n + 0.0062(C_u - 5)]sin\left(\frac{\pi}{6} - \frac{\theta}{8}\right) \quad (3)$$

Where: θ – angle between seepage flow and gravity force; γ_{grain}, γ_{water} – density of soil grain and water respectively.

Although this method is very sophisticated, it is still based on only few key sizes, and, therefore, can be inapplicable to some specific soils such as multi gap–graded. In addition, it does not assess well the influence of soil grain arrangements (To et al., 2014).

An alternative method based on the correlation of gradation slope between fine and coarse fractions pointed out that soil might be instable if it has a steep slope in the coarse part and a flat slope in the fine part of GSD (Wan & Fell, 2008). Although the accuracy of this method is still under consideration, it led the authors to an idea that the stability of a GSD can be assessed through the distance how far it goes from its mean line.

There is another recent study developed from Constriction Size Based Method, which should be described here because of its reflection on self-filtration essence (Indraratna, Nguyen, & Rujikiatkamjorn, 2011). If a grain is transported from one pore to another, it must be smaller than the constriction size d_c between those pores. The constriction size with a probability P_c and a relative density R_d can be calculated by:

$$d_c(P_c, R_d) = 1.11\left[d_{c3}(P_c) + P_c(1 - R_d)\left(d_{c4}(P_c) - d_{c3}(P_c)\right)\right] \quad (4)$$

Where: d_{c3}, d_{c4} – constriction size at densest state formed by three grains and loosest state formed by four grains respectively.

There are two problems with this method. Firstly, a recent study on porous structure point out that if a pore formed by four grains, it will not form a joined constriction, but two intersecting non-coplanar constrictions. Secondly, the separation of GSD into loose grains and filter fraction is subjective at some level, which might lead to different assessment results by different engineers.

The last method would be described in this section is a popular method based on gradation slope control (Kenney & Lau, 1985; Loebotsjkov, 1969). It suggested that for any size of grain d, the mass of soil fraction smaller than this size f_d must satisfy:

$$f_d \geq 0.6\left(\frac{d}{d_{60}}\right)^{0.6} \quad (5)$$

This condition can be expressed in terms of f_d and f_{4d}:

$$f_{4d} \geq 4^{0.6} f_d \cong 2.3 f_d \quad (6)$$

This method employed a consideration that grains sized d will be kept by other grains sized $d \div 4d$. Therefore, if there is a lack of grains sized $d \div 4d$, grains sized d and smaller grains can be eroded. This assumption is good for sandy soils where grains have nearly spherical shapes. The slope control is often checked from finest grains up to d_{20} or d_{30}. This fact inspired a new way to determine the primary fabric of soils by an inverted method.

3. New assessment method based on key sizes

As mentioned above, assessment methods based on only few key sizes are simple, quick, and good for engineering work. This section is devoted for a new method assessing suffusion potential of a GSD by the farthest distance it makes from its mean line connecting two points (d_3,3) and (d_{100},100) (Figure 20).

The mean line is assumed to start from (d_3,3) because 3% is the acceptable loss of soil mass, while the internal stability of soils is preserved (Goldin et al., 1992). The distance from any point (d,f_d) on GSD to the mean line is estimated by:

$$D = \frac{\left|\frac{97}{lg\left(\frac{d_{100}}{d_3}\right)} \cdot lg\left(\frac{d}{d_3}\right) - f_d + 3\right|}{\sqrt{\left(\frac{97}{lg\left(\frac{d_{100}}{d_3}\right)}\right)^2 + 1}} \quad (7)$$

Because the farthest point can be estimated approximately first by visual estimation before taking a more precise calculation, this identification

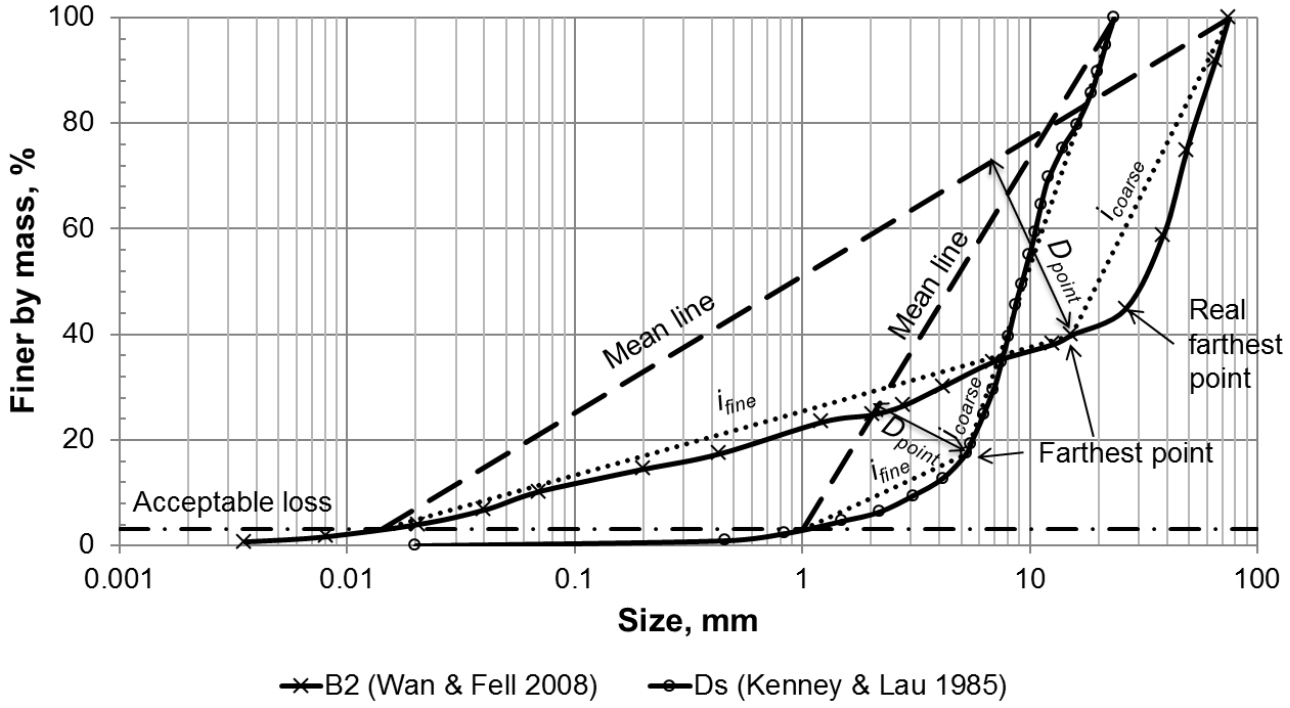

Figure 20. Farthest point identification.
(Note: When the real farthest point is above 40%, it is not selected)

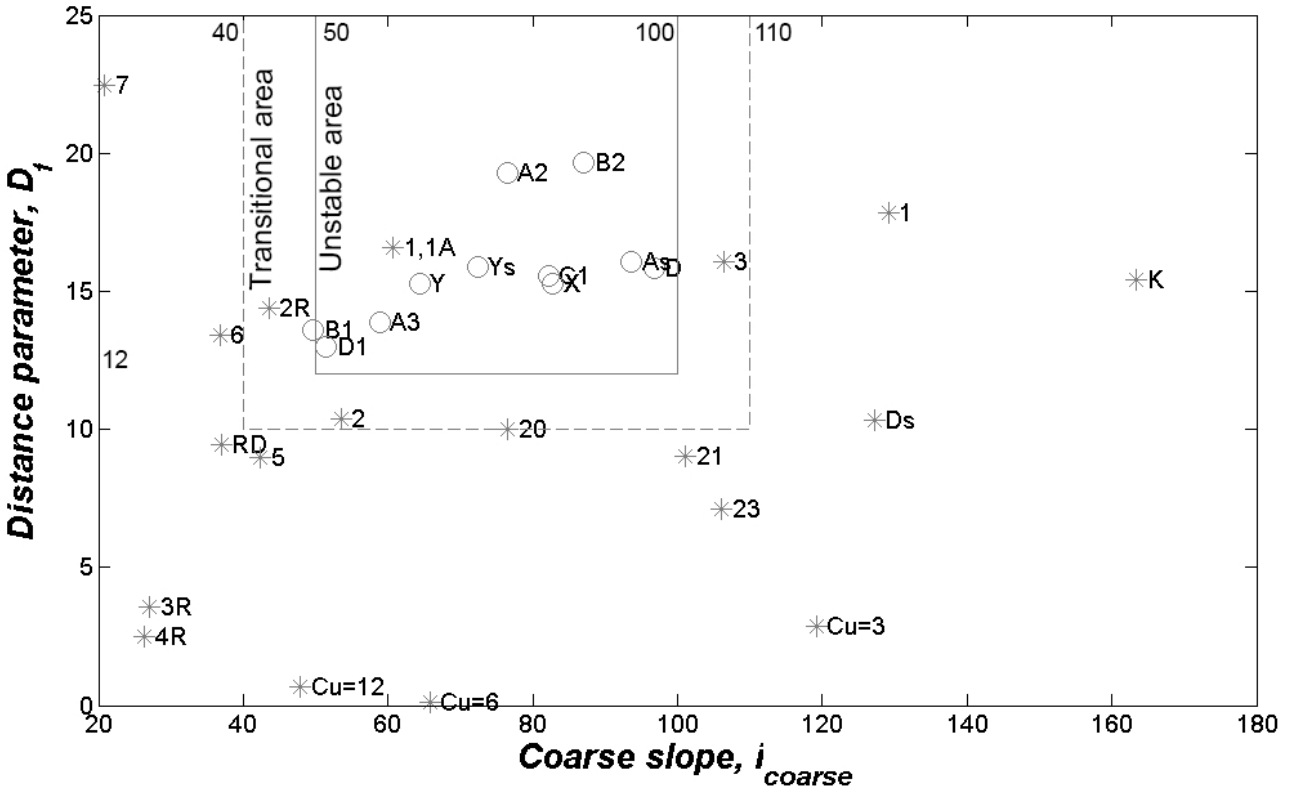

Figure 21. Self–filtration criterion based on key sizes.

✳ - Stable soils, ○ - Unstable soils.

should not take a lot of time. The coordinates of the farthest point is marked as (d_{point}, f_{point}). The distance from that point to the straight line is noted as D_{point} respectively.

Also noteworthy is the fact that when f_{point} is too high, the coarse fraction may not have enough grains to build the primary fabric (To et al., 2014). In that case, the primary fabric will restructure itself under loads and self-weight to reach a firm state, where more grains are involved in the primary fabric. Therefore, the farthest point is selected with a condition that $f_{point} \leq 40\%$ (Figure 20).

In order to assess the suffusion potential, the new method employs the correlation between the slope of the coarse fraction i_{coarse} and distance parameter D_f:

$$\begin{cases} \mathbf{i_{coarse}} = \frac{\mathbf{100-f_{point}}}{\mathbf{lg\left(\frac{d_{100}}{d_{point}}\right)}} \\ \mathbf{D_f} = \mathbf{D_{point}} \cdot \mathbf{i_{fine}} = \mathbf{D_{point}} \cdot \frac{\mathbf{f_{point}-3}}{\mathbf{lg\left(\frac{d_{point}}{d_3}\right)}} \end{cases} \quad (8)$$

Actually, the physical meaning of the farthest point is a break point in GSD, which makes soils easy to be eroded. Therefore, this method is inapplicable to gap–graded soils, which has one or some significant intervals with small gradation slope:

$$i_{interval} = \frac{f_{end\ interval} - f_{begin\ interval}}{lg\left(\frac{d_{end\ interval}}{d_{begin\ interval}}\right)} \leq 2 \quad (9)$$

However, the calculated results for continuously graded soils showed some coherence with experimental data (Figure 21). The stable and unstable soils are separated clearly and a small transitional zone is located for safety.

There are only two types of stable GSD with high D_f. In the first case, soils have only very big i_{coarse}, i.e. having almost vertical slope in coarse fraction. Although the fine, loose fraction can be washed out, these soils remain stable and behave such a uniform or narrow graded soil. Regard to the second type, where soils have very small i_{coarse}, i.e. having mild slope. In this case, the slope coarse fraction is close to the mean line, which leads to a small value of the farthest distance D_{point}. Therefore, these soils must have a steep slope in fine fraction, which make fine grains hard to be eroded.

However, like many other methods based on key sizes, this method might be inapplicable for some specific GSD such as multi-bended gradation 1,1A (Wan & Fell, 2008). This GSD widely spreads through all soil grain classifications to get a big enough value of distance parameter D_f, while still has a medium slope of coarse fraction. Nevertheless, this is a *scot-free error*, where a stable soil is considered as an unstable one, i.e. the material selection is safer. In addition, a laboratory stable soil can be an unstable one in reality because of inappropriate laboratory conditions.

4. New assessment method based on constriction size distribution

As stated in the second section, an essential method for suffusion assessment is the correlation between the loose fraction and the constriction size distribution formed by filter fraction, or better says, soil primary fabric. However, the identification of the filter fraction is currently not necessarily clear. This section will contribute an approximate way to estimate it.

The first idea for the separation is a sharp boundary at the farthest point estimated above. However, the recent numerical simulation proved the existence of a transitional interval between the filter and loose fractions (To et al., 2014). The later idea came from the inversion of Kenney's assumption that soil grains sized d are kept by soil grains sized $d \div 4d$, and if $f_{d\div4d} < 1.3f_d$ (Equation 6), soils might be unstable. While this assumption is applied for fine fraction of GSD, its inversion for coarse fraction states that if there are not enough soil grains sized $4d$ or larger to store soil grain sized d in their pores, the excessive amount of soils sized d will be involved in the primary fabric, i.e. filter fraction.

Inheriting the Kenney assumption above, the new method defined the loose fraction in the interval from d to $4d$, $FL_{d\div4d}$, by filter fraction in the interval from $4d$ to $16d$, $FF_{4d\div16d}$:

$$\boldsymbol{FL_{d\div4d}} = \frac{\boldsymbol{FF_{4d\div16d}}}{\mathbf{1.3}} \quad (10)$$

Obviously, all of soil grains sized $0.25d_{100}$ and larger should be included in the soil primary fabric because there is no large enough pore to store them. The inverted estimation of the soil primary fabric is illustrated on Figure 22

. The primary fabric fraction is calculated sequentially from the largest grain size. The milder the mean line is, the more steps primary fabric can have. In contrast, if GSD has an abrupt slope of GSD, where the coarse fraction is big enough to store all finer grains, the process will be ended only after one or two steps.

After the division of GSD, the constriction size distribution of the filter fraction is computed. Actually, there are several ways for this distribution calculation, each of those have its own advantages and drawbacks. This new assessment employs a modified Schuler method, which has been compared with experimental results (Witt, 1993). Full details of this method can be found in (Scheuermann & Bieberstein, 2007).

The next step is the correlation of the calculated constriction size distribution with loose grain size distribution (Steeb & Scheuermann, 2014). Both distributions are divided into several intervals respectively. Each of intervals will be represented by a mean size d_i and probability of occurrence p_i. The possibility of grains in an interval i to be transported to the next pore, P_{wi}, is calculated by the fraction, 1-f_{csdi}, of constriction larger than d_i.

$$\boldsymbol{P_{wi}} = \boldsymbol{p_i} \cdot (\mathbf{1} - \boldsymbol{f_{csdi}}) \quad (11)$$

The proportion of transportable grains is estimated as the sum of those mounts from all intervals:

$$\boldsymbol{P_w} = \sum \boldsymbol{P_{wi}} = \sum \boldsymbol{p_i} \cdot (\mathbf{1} - \boldsymbol{f_{csdi}}) \quad (12)$$

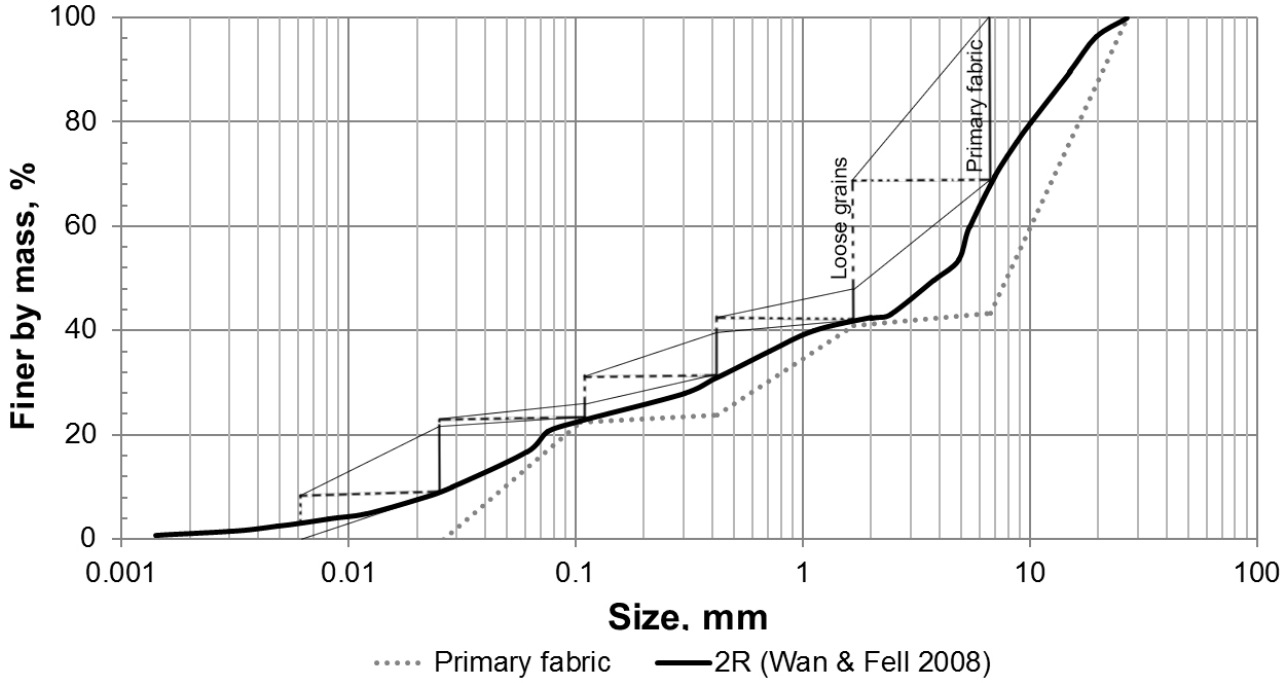

Figure 22. Soil primary fabric estimation by inverted assumption

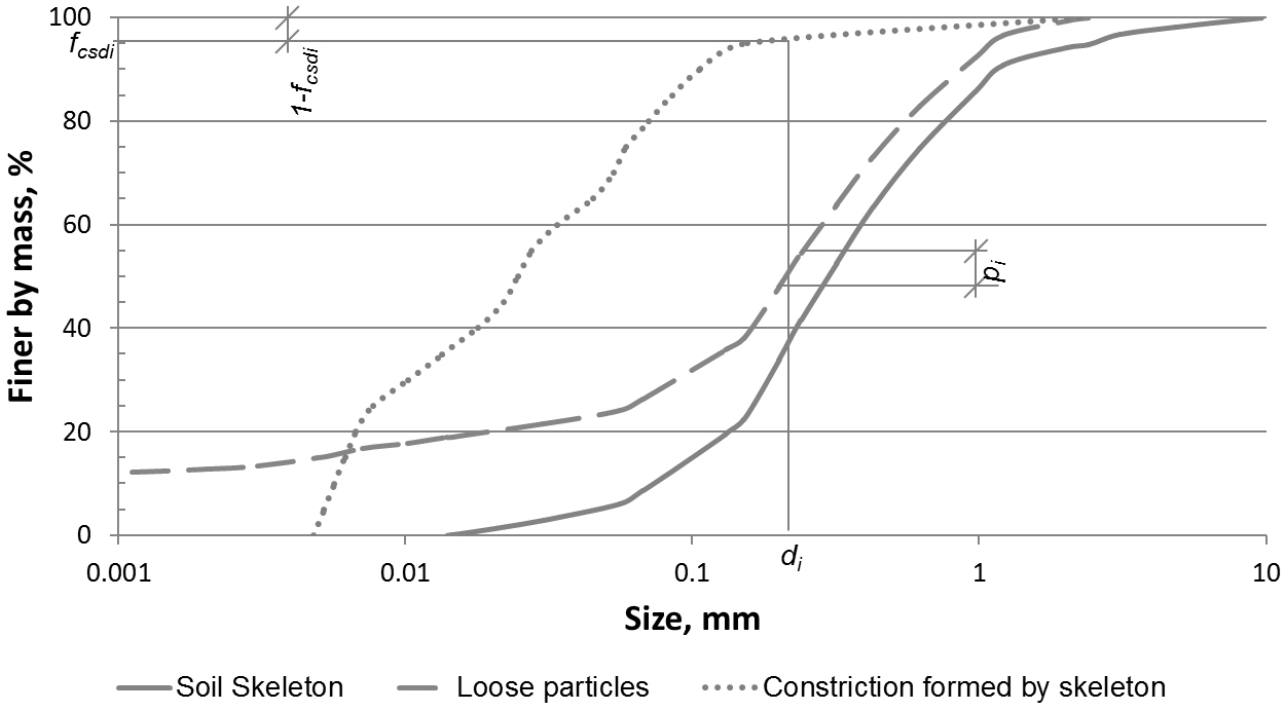

Figure 23. Correlation of loose grains and constrictions formed by filter fraction

This new method assumes that soil is instable when Pw is more than 50%, i.e. soil grains seem to be transported rather than be kept in pores (Table). When Pw is smaller than 40%, soil can be considered as stable because the transportation seems to be ended after several pores. Other soils are located in the transitional zone.

The uncertainty of the transitional zone is explained by the influence of some other decisive factor such as the creation of pipe, which depends on the grain arrangement.

It is evident from the Table 1 that the new method does not provide any serious errors on surveyed soils. However, there are some scot-free errors when several stable gradations are considered as unstable. As mentioned in section 3, scot-free error is an acceptable incompetence of internal stability assessments. In addition, the transitional zone has been narrowed down, which increases the certainty of the assessment despite the scot-free errors.

On the top of these, the biggest advantage of the new method is its comprehensive consideration of the whole GSD, which makes it applicable even to some specific soil type such as multi gap-graded soils.

This new method is facilitated by a comprehensive computer program to enable the application in engineering work.

5. Conclusion

This paper has presented two novel self-filtration criteria for soil internal stability assessment.

The first method inherits the prior point of view that instable gradations often have a steep slope in coarse fraction and flat slope in fine fraction. This new method tries to assess the instable potential by the farthest point on GSD from its mean line. The stability of soils is classified by the graph of the distance parameter and slope of coarse fraction.

The second new method makes an effort on assessing GSD comprehensively by the correlation of the loose grain size distribution and constriction size distribution, which has been denoted in a prior authorial research. The loose grains are separated from GSD by an inversion of Kenney's assumption that grains sized d will be kept by grains sized $d \div 4d$. This correlation will identify the proportion of transportable soil grains. When more than 50% of loose grains are transported, soil can be estimated as unstable.

Although the accuracy of the assumption is very difficult to be tested because of the small size of soil grains, the new method shows a good coherence while it is applied for some typical experimental data.

Table 1. Internal stability assessment by constriction correlation

Reference	Soil names	Lab. results	Assessed result	P_w
Wan & Fell (2008)	15	U	U	67.2
	14A	U	T	48.2
	10	U	T	50.0
	A2	U	U	72.8
	B1	U	U	74.4
	D1	U	U	74.1
	A3	U	U	70.9
	B2	U	U	82.1
	C1	U	T	47.0
	7	S	***U****	77.3
	6	S	S	31.0
	RD	S	S	39.1
	13	S	S	26.4
	5	S	***U****	53.2
	3R	S	S	18.5
	11	S	***U****	78.1
	2R	S	S	10.2
	1,1A	S	***U****	60.3
	9	S	S	31.2
	4R	S	T	40.4
Kenney & Lau (1985)	X	U	T	49.5
	D	U	U	67.3
	Y	U	U	69.8
	As	U	U	64.1
	Ys	U	U	65.8
	A	U	U	77.3
	3	S	***U****	54.7
	1	S	***U****	51.8
	2	S	S	10.9
	Ds	S	S	30.2
	23	S	S	15.8
	21	S	S	20.6
	20	S	T	47.0
	K	S	S	33.2
	$C_u = 3$	S	S	0.0
	$C_u = 6$	S	S	0.1
	$C_u = 12$	S	S	1.6

U – Unstable; T – Transitional; S – Stable; * Scot-free error

6. Acknowledgements

This research is funded by and included in the Discovery Project (DP120102188) "Hydraulic erosion of granular structures: Experiments and computational simulations", granted by Australian Research Council. The first author would like to acknowledge the Graduate School International Travel Award (GSITA) and Professor Nguyen Chien, Vietnam Water Resources University for his useful comments on the farthest point.

7. References

Burenkova, V. (1993). Assessment of suffusion in non-cohesive and graded soils. *Filters in geotechnical and hydraulic engineering. Balkema, Rotterdam*, 357-360.

Foster, M., Fell, R., & Spannagle, M. (2000). The statistics of embankment dam failures and accidents. *Canadian Geotechnical Journal, 37*(5), 1000-1024.

Goldin, A. L. v., Rasskazov, L. N., & Zeidler, R. B. (1992). *Design of earth dams*: AA Balkema.

Indraratna, B., Nguyen, V. T., & Rujikiatkamjorn, C. (2011). Assessing the potential of internal erosion and suffusion of granular soils. *Journal of Geotechnical and Geoenvironmental Engineering, 137*(5), 550-554.

Indraratna, B., Raut, A. K., & Khabbaz, H. (2007). Constriction-based retention criterion for granular filter design. *Journal of Geotechnical and Geoenvironmental Engineering, 133*(3), 266-276.

Kenney, T., & Lau, D. (1985). Internal stability of granular filters. *Canadian Geotechnical Journal, 22*(2), 215-225.

Loebotsjkov, E. (1969). *The calculation of suffusion properties of non-cohesive soils when using the non-suffosion analogue.* Paper presented at the Proceedings of the International Conference on Hydraulic Research, Brno, Czechoslovakia. Technical University of Brno, Svaze B-5, Brno, Czechoslovakia.

Scheuermann, A., & Bieberstein, A. (2007). Determination of the soil water retention curve and the unsaturated hydraulic conductivity from the particle size distribution *Experimental unsaturated soil mechanics* (pp. 421-433): Springer.

Sherard, J. L. (1979). *Sinkholes in dams of coarse, broadly graded soils.* . Paper presented at the 13th Congress on Large Dams, New Delhi, India.

Steeb, H., & Scheuermann, A. (2014). Modeling of internal erosion of cohesionless soils. A continuum-based model enriched by microstructural information. *Acta Geotechnica-submitted*.

To, H. D., Galindo-Torres, S., & Scheuermann, A. (2014). A numerical approach for the determination of the primary fabric of granular soils. *Applied Mechanics and Materials, 553*, 489-494.

To, H. D., & Scheuermann, A. (2014). *Separation of grain size distribution for application of self-filtration criteria in suffusion assessment*. Paper presented at the 7th International Conference on Scour and Erosion, Perth, Australia.

Wan, C. F., & Fell, R. (2008). Assessing the potential of internal instability and suffusion in embankment dams and their foundations. *Journal of Geotechnical and Geoenvironmental Engineering, 134*(3), 401-407.

Witt, K. (1993). *Reliability study of granular filters.* Paper presented at the Proc. 1. Int. Conf.„Geo-Filters ", Brauns, Schuler, Heibaum (Hrsg.): Filters in Geotechnical and Hydraulic Engineering, Balkema.

ВНИИГ. (1976). *Руководство по расчетам фильтрационной прочности плотин из грутовых материалов* (Vol. П55-76/ВНИИГ). Ленинград.

This page intentionally left blank

Proceedings of the 10th ANZ Young Geotechnical Professional's Conference – 10YGPC
Noosa, Queensland, Australia
10 – 12 September 2014

GEOTECHNICAL ISSUES IN FOUNDATION DESIGN IN RECLAIMED GROUND OVER SOFT MARINE DEPOSIT

Vinay TRIVEDI[1], Payam SADEGHI[2] and Bill KOUL[3]
[1.] *Project Geotechnical Engineer, 4DGeotechnics Pty Ltd, Perth WA*
[2.] *Associate Geotechnical Engineer, 4DGeotechnics Pty Ltd, Perth WA*
[3.] *Principal Geotechnical Engineer, 4DGeotechnics Pty Ltd, Perth WA*

ABSTRACT – This paper discusses the effects of iron ore stockpile loading on the stability of the foundations of a stockpile shed, founded on reclaimed ground conditions, comprising engineered fill over high plastic, soft, marine deposits, underlain by low to medium strength mudstone. Consolidation settlements in the order of 1,200 mm were anticipated to occur in marine deposits, over a period of about 25 years. Surcharge loading due to iron-ore stockpile was expected to exacerbate both vertical and lateral ground movements, potentially affecting the stability of shed footings. Preloading of the ground was not considered due to time constraints. The geotechnical design challenges were, therefore, to (a) limit the maximum height of stockpile for global stability of the ground and (b) provide a stable and robust foundation system for the shed. Shallow pad and strip footings, and short bored piers, were found to be unsuitable, using Plaxis 3D computer program, due to potential rotational failure considerations. Pile foundations were, therefore, recommended to support the shed, which incorporated additional lateral and vertical loadings due to the consolidation ground.

1. Introduction

This paper is based on a geotechnical study related to iron ore stockpile shed at Lautoka Port, Fiji. The stockpile footprint was underlain by challenging ground conditions, comprising reclaimed ground conditions (Fill) over deeper soft marine sediments. Geotechnical analyses were carried out using both empirical and FE methods (PLAXIS 3D) to (i) study the response of soft marine mud to superimposed loadings from the existing fill and the future iron ore stockpile and (ii) assess appropriate foundation system(s) for supporting the stockpile shed.

2. Background

The proposed site for the construction of stockpile shed is located towards the east of the Queens Wharf. The site is bounded by a Customs storage yard to the south, to the east and northeast by a water injection canal and by tidal flats to its northwest.

The geological map of Lautoka area (1:50,000, revised edition, 1983) indicates that the site could be underlain by recent unconsolidated muds, sands and shell beds, deposited during the early Pliocene.

Due to environmental requirements, the stockpile was proposed to be covered by a shed, with a mobile crane mounted within it for operation purposes. For smooth operations of the crane, the shed structure was understood to be sensitive to differential settlements.

3. Subsurface Condition

Two separate ground investigations had initially been conducted on site by others, in 1990 and 2001, prior to the commencement of reclamation works (fill placement), which comprised six and eight boreholes, respectively, for the whole reclaimed area.

An additional five boreholes and nine CPTu probes, along with dissipation tests, were carried out to ascertain the current site conditions in 2012. Laboratory tests included soil characterisation tests (Particle Size Distribution, Atterberg Limits and Moisture Content tests), 1-D Oedometer tests, Tri-axial tests on soil samples and Point Load Strength Index and UCS tests on rock samples.

The updated generalised subsurface profile under the stockpile shed area was identified as follows:

- Engineered Fill, about 4 m thick, comprising soapstone – Suva Marl, overlying,
- SAND, about 1.5 m thick, very loose to loose, with variable silt and gravel content, overlying,
- Clayey SILT (marine deposits, 7 m to 14 m thick, very soft to soft, high plasticity, overlying,
- SILTSTONE / MUDSTONE, very low strength, extremely weathered.

Based on the CPTu logs, the average depth to groundwater was estimated to be about 1.5 m below the existing pad surface

3.1. Groundwater

As iron-sand was expected to be placed in stockpile in a wet condition, leaching of moisture was expected from the stockpile. Due to a close proximity with sea and possible fluctuations in the groundwater depth, and leaching of moisture from the stockpile, groundwater was considered close to the ground surface in geotechnical analyses.

4. Geotechnical Assessment

4.1. Earlier Work

Settlement monitoring of reclaimed ground was conducted between November 2006 and August 2011, which indicated the engineered fill area had settled by up to 1.1 m in the first five years, primarily due to consolidation settlement of marine sediments. The survey data also indicated that the settlement rate had reduced with time. Based on the settlement data, about 85% consolidation settlement was anticipated to be completed by early 2012.

4.2. General Stability Check

Due to the presence of underlying soft marine deposits, it was assessed that the surficial Fill could potentially fail in general shear failure mode if the loading on the ground exceeded the ultimate bearing capacity of marine sediments. The previous geotechnical reports noted that a section of bund failed on each of the reclamation stages, carried out in 1991 and 2001, due to a combination of weak seabed materials, the presence of an adjacent gully in the seabed and high pore pressures due to rapid loading during the filling process. It was also noted that the piezometer were not effective in identifying the excess pore water pressures and preventing the bund failures.

Based on the previous geotechnical investigations, the original shear strength (C_u) of sub-soil (prior to the fill placement) was estimated to be in the order of about 10 kPa. Therefore, the ultimate bearing capacity of the original ground was estimated about 60 kPa. However, after five years of fill placement, and assuming 85% completion of consolidation settlement, the revised ultimate bearing capacity of consolidated marine sediments was estimated to be in the order of 220 kPa.

The results of stability analyses, using SLOPE/W software, indicated a global failure if the height of iron sand (unit weight was considered as 28 kN/m^3) stockpile reached about 8.4 m. Therefore, to provide a minimum Factor of Safety (FoS) of 1.5, the fill height was recommended to be limited to 5 m.

4.3. Bearing Capacity

For large shallow footings (B ≥ 2 m), the values of bearing capacity, based on shear failure considerations, were estimated to be high. However, the zone of influence, for the larger footings was expected to extend into the softer marine deposits.

Due to highly compressible marine deposits and stringent differential settlement criteria for shed footings, the bearing capacity of the large shallow footings was governed by the settlement consideration rather than by shear failure consideration. Therefore, the width of shallow footings was recommended to be limited to larger than 1 m.

5. Ground Deformation under Loading

Further to settlement monitoring survey results, it was anticipated that the consolidation process for the soft marine sediments was still ongoing.

The shed structure and stockpile on the ground surface were, therefore, expected to exacerbate the consolidation process and cause further elastic (initial) and consolidation settlements of soft marine deposits. The ground surface was also expected to be undergoing an ongoing settlement process reflecting the settlement process of the underlying marine deposits.

Due to variable thickness of marine deposits, the magnitude of settlements was also expected to be variable, which would potentially result in significant differential settlements across the footprint of the stockpile and the shed structure.

The maximum total settlement (initial and consolidation), for a 5 m high iron-sand stockpile loading, was estimated to be in the order of about 1,200 mm under the centre of the stockpile footprint and occur over a period of about 25 years. As indicated in Figure 1, due to variable thickness of marine deposits, the estimated settlements ranged between 300 mm and 1,200 mm across the stockpile footprint. The initial settlement was estimated to be around one third of the total settlement.

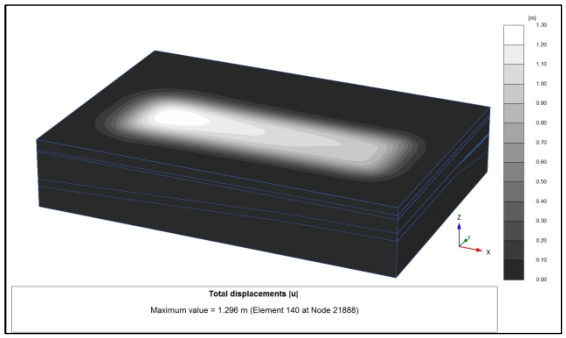

Figure 1. Total Settlements under stockpile loading (light to dark shade indicates high to low settlement range.)

Due to alternate loading and unloading cycles of iron-sand, it was expected that the thickness of stockpile would vary during the loading and unloading cycles. An average stockpile thickness of 2.5 m of constant stockpile loading was assumed in the analyses, after discussions with the client. The maximum consolidation settlement, due to 2.5 m high iron-sand loading, was estimated to be in order of about 550 mm under the centre of the stockpile footprint.

5.1. Time Bound Settlement

The Coefficient of Consolidation (C_v) was considered as 6 m^2/day based on the results of dissipation tests carried out during CPTu probing and the laboratory test results. This value was in agreement with the actual time rate of settlement estimated from the previous settlement surveys.

The maximum settlement under the stockpile was estimated to be about 350 to 500 mm in the first 30 days after the placement of 5 m high stockpile. Ongoing consolidation settlement was anticipated to continue to occur over the design life of 25 years. Based on the actual stockpile loading and time of loading, the ground settlement was estimated to vary between 300 mm and 1,200 mm at the end of 25 years.

The magnitude of consolidation settlement due to a constant 2.5 m high stockpile, over the design life of 25 years, was estimated to be about 550 mm to 650 mm at the centre of the stockpile footprint.

It was expected that 90% consolidation settlement of the ground would occur within a period of about 7 to 9 years (Ref. Figure 2).

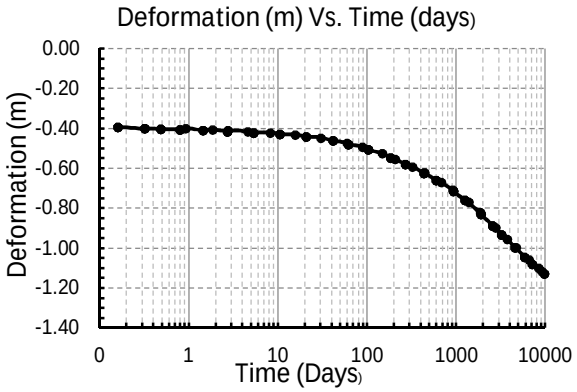

Figure 2. Time vs. Consolidation Settlement

Plaxis 3D computer program was used to observe the ground behaviour under the stockpile loading.

6. Effect of Ground Movements on Foundations

Due to the stockpile loading, additional ground settlements were anticipated to occur both in short and long term. Significant ground movements were anticipated to occur in softer marine deposits underlying the surficial fill. It was also anticipated that the vertical ground movements would be associated with corresponding lateral ground movements in marine deposits. The results of analysis indicated that the maximum values of lateral grounds would be within the marine deposits, although relatively lesser but significant, lateral movements would also be expected to occur within the surficial fill. The horizontal deformation, due to stockpile loading, in the surrounding soil was estimated to be in the order of 50 mm to 70 mm. It was anticipated that the maximum deformation would take place below the fill material, therefore, settlements along the foundation line were estimated using Plaxis 3D software. The estimated settlements are shown in Figure 3.

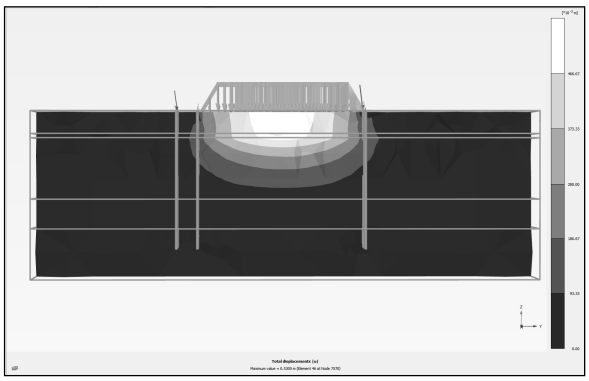

Figure 3. Ground deformation along the foundation line. (Scale 1:5)

6.1. Shallow Foundations

The main purpose to construct the shed structure was to cover the stockpile. Due to limited space, the shed columns were also designed to support a mobile crane for operation purposes. Due to large footing size, the zone of influence was found to extend into deeper, softer, marine deposits. As such, settlement governed the bearing capacity. Settlements calculated due to structural loadings were found to be acceptable.

Due to the presence of soft marine deposits with variable thickness, the vertical ground movements were anticipated to be accompanied by significant lateral ground movements under the effect of stockpile loading. Therefore, in addition to the structural loading, shallow footings would also be subjected to lateral loadings generated due to the settlement of the ground. Due to horizontal movements, the shallow footings were anticipated to undergo differential settlements higher than the acceptable limits. Plaxis 3D software was used for undertaking the analyses, which included the crane loading. A typical settlement profile of a shallow footing under the stockpile loading is shown in Figure 4(a).

The results of analyses indicated that differential settlements under shallow footings would be in the

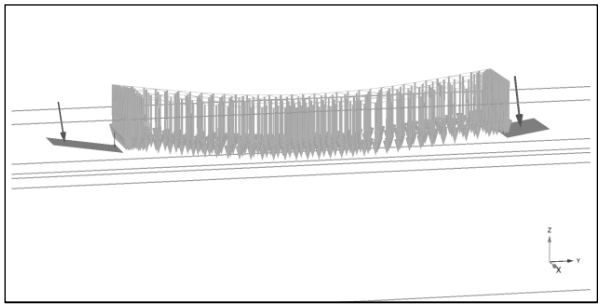

Figure 4 (a). Effect of stockpile loading on Shallow Foundations. (Scale – 1:10)

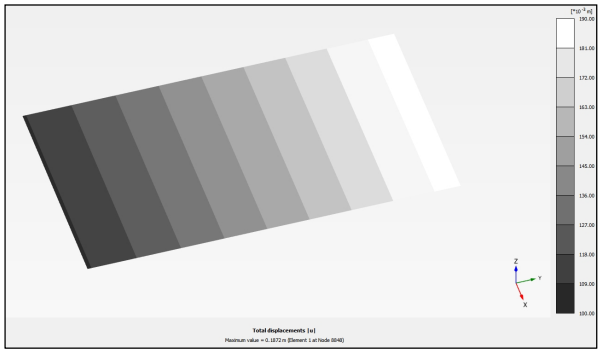

Figure 4(b). Differential settlement in left side footing

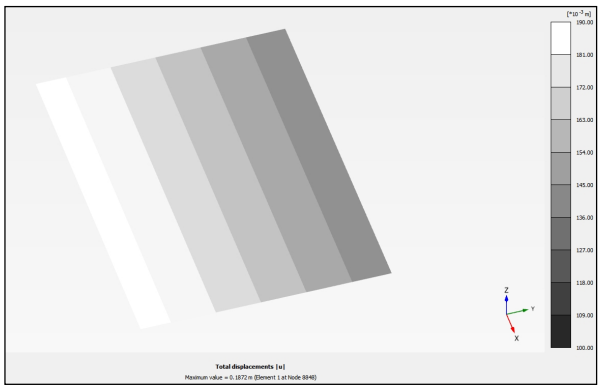

Figure 4(c). Differential settlement in right side footing.

range of 100 mm to 190 mm, with 100 mm under the edge of the footing away from the stockpile and 190 mm under the edge of the footing near the stockpile.

The settlement contours under the footings are shown in Figures 4b and 4c. As the differential settlements exceeded acceptable limits, shallow footings were not recommended for supporting shed structures.

6.2. Shallow bored piers

Due to high ground settlements and lateral deflections anticipated in shallow footings, shallow bored piers were also assessed, as an option, for their suitability to support the shed footings. To minimise differential settlements, the bored piers were considered to be structurally connected with a common rigid reinforced concrete (RC) beam at the top.

The magnitude of the initial settlement was estimated to be one third of the total settlement, therefore, to reduce the effect of settlement on the bored piers, preloading of the ground, with a maximum preload of 100 kPa, was recommended to be carried out over the stockpile footprint, and nominally 3 m beyond it, before the construction of bored piers. The minimum preloading period was recommended as 90 days. The following assumptions were considered during the analysis:

- The steel structural columns will be supported by a nominal 2 m wide by 0.5 m thick continuous RC beam which will, in turn, be supported on a series of equally spaced shallow bored piers.
- The footings under the RC beam will comprise nominal 0.9 m diameter and 4 m deep cast-in-situ RC bored piers.
- The iron-sand stockpile footprint extends to the inner edge of the RC beam.
- The average height of the iron-sand stockpile, for a majority of the time, was considered to be 2.5 m (i.e. an average surcharge pressure of nominally 70 kPa);
- The long-term settlement and ground movement, due to the ground consolidation, was required to be estimated for a time period of 25 years, involving alternate loading and unloading cycles.

Plaxis 3D software was used for analyses. Figure 5 shows a deformed profile of bored pier after the completion of consolidation period of 25 years.

The results indicated that the bored piers were subjected to about 135 to 140 mm of vertical settlement and about 40 to 45 mm of horizontal deformation. Due to high settlement values, shallow bored piers (connected with RC beam) were anticipated to fail due to rotational failure during the life span of the structure.

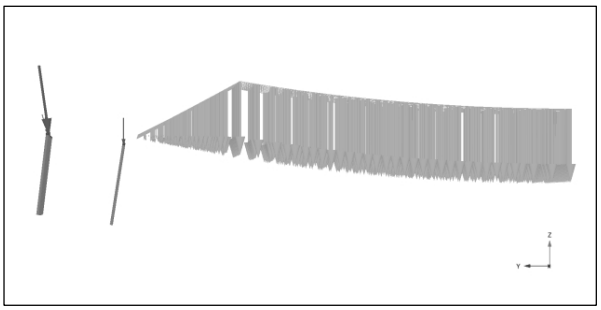

Figure 5 (a). Deformed shape of Shallow Bored Pier Left side of footing (Scale – 1: 50)

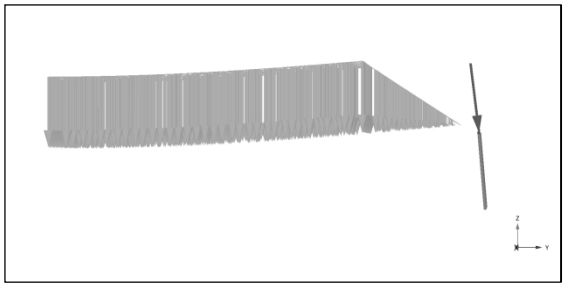

Figure 5 (b) Deformed shape of Shallow Bored Pier (Right side of footing (Scale – 1: 50)

7. Deep foundation

As discussed in the above sections, shallow foundations systems were found to be unsuitable for supporting the shed structure unless significant ground improvement works and/or footing under-pinning works were carried out. Therefore, due to time constraints, pile foundations were considered.

7.1. Pile Types

Driven hollow steel section (HSS) / tubular piles were considered to be more suitable at the site as compared to bored piles. Three pile sizes, with outer diameters of nominally 0.6 m, 0.9 m and 1.2 m, as single piles and as 2-pile groups, were analysed.

7.2 Pile Design

The following design issues were identified:

- The SILTSTONE / MUDSTONE bedrock was found to be of low strength. Therefore to provide adequate resistance against horizontal ground movements, pile embedment depth was estimated to be high for anchorage.
- Due to vertical ground settlements, the piles were expected to be subjected to negative skin friction, in addition to the structural load.
- Due to the large horizontal ground movements, the piles were expected to be subjected to the additional Shear Force (SF) and Bending Moments (BM) within the soft marine deposits, as shown in Figure 6.

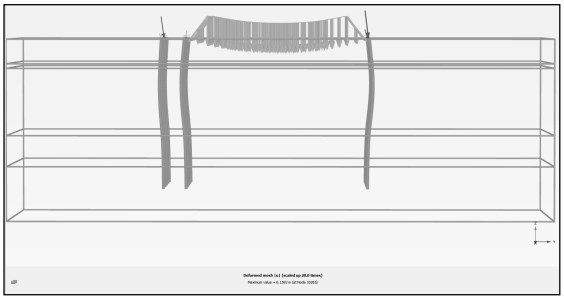

Figure 6. Pile deformation in soft marine deposit (Scale – up to 5 times)

- Due to the additional SF and BM from soil movements in marine deposits at deeper depths, the pile stiffness needed to be assessed for adequacy.
- As expected, larger piles (1.2 m diameter) showed lower pile movements as compared to smaller (0.6 m diameter) piles. It was also noted that 0.6 m diameter piles showed higher overall deformations, however, due to 'rotate back effect', these piles showed lower deformations at the ground surface as compared to 1.2 m diameter piles (Figure 7).

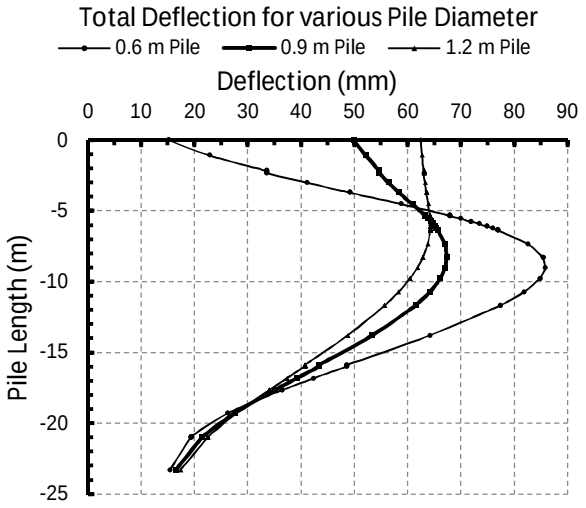

Figure 7. 'Rotate back effect' for 0.6 m, 0.9 m and 1.2 m diameter piles.

- An optimised pile diameter of 0.9 m was suggested due to geotechnical considerations, however, subject to structural design requirements.
- To reduce the friction between the pile and surrounding soft marine deposit, bitumen coating was recommended in the upper portion of the pile surface.

8. Conclusion

Driven HSS piles, with 0.9 m outer pile diameter and a minimum length of 33 m long pile, with a minimum rock plug of 6 m, were found to meet structural and geotechnical design requirements of a robust foundation system to support the proposed stockpile shed.

The vertical settlements of the proposed pile foundation system were estimated to be in the range of 10 to 15 mm, which was within the tolerance limits of the proposed shed structure and a mobile carne within it.

The maximum horizontal pile deflections were estimated to be in the range of 65 to 70 mm, which would require a flexible structural design and periodic maintenance during the life of the project.

9. References

Das B.M. (2008). *Advanced Soil Mechanics*. Third Edition. Taylor & Francis, New York

Bowles J.E. (1996). *Foundation Analysis and Design*. Fifth Edition, McGrow-Hill.

Standards Australia, *AS2159-2009, Piling-Design and installation*, SAI Global Limited.

Proceedings of the 10th ANZ Young Geotechnical Professional's Conference – 10YGPC
Noosa, Queensland, Australia
10 – 12 September 2014

STATE OF PRACTICE OF CPT TESTING IN 2014

Ross KRISTINOF
Jacobs Engineering, Melbourne, Australia

ABSTRACT – This paper provides an overview of some themes and learnings from the 3th International Symposium on CPT testing, held in Las Vegas in May, 2014. The symposium presented papers in the subject areas of equipment and procedures, interpretation, and applications. Key learnings taken away from the conference, and discussed in this paper, include: 1. Seismic CPT testing is underused, and provides the opportunity both to reliably assess small strain stiffness, and provide improved interpretation of other geotechnical parameters, by comparing correlations of V_s with correlations of q_c and f_s. 2. The measurement and interpretation of f_s is still far from reliable and work is being done to improve it. The sources and impacts of this inaccuracy are discussed. 3. The evaluation of CPT-based methods of assessing liquefaction benefit from recently available case studies. These case studies highlight the need to refine these approaches and improve predictions for the future. 4. New advancements in CPT based methods for pile design include more reliable techniques to predict load-settlement behavior of piles based on sCPT results, and improved CPT based *p-y* methods.

1. Introduction

The 3rd International Symposium on Cone Penetration Testing (*CPT'14*) took place in May 2014 in Las Vegas in the United States. 272 delegates took part representing 36 countries. Delegates represented academia, contractors and consultants, and papers presented covered the categories of equipment and procedures, interpretation and application. The purpose of this paper is to provide a summary of the key themes discussed at CPT'14 and to highlight a few areas of specific interest to the author. The topics discussed in this paper are by no means intended to be an exhaustive list of what the industry currently finds important, and many topics, particularly those which involve case studies of current applications, are not discussed here. Furthermore, papers and authors from CPT'14 will be referenced by *name* without date; other references will be cited in the conventional manner. All the papers included in CPT'14 have been made available, free of charge, at the symposium website: www.CPT14.com and delegates to 10YGPC are encouraged to explore this useful technical resource.

2. Seismic CPT

A consistent theme across many of the presentations at CPT'14 was the desire to make better use of seismic cone penetration testing. Despite being around since the late 1980s, as reported separately by both *Mayne* and *Massarsch*, the 'sCPT' is not yet universally in use as a means of in situ-testing and site characterization. This author contends that the reasons for this are twofold:

1. Availability of seismic modules in the market place is currently still limited (here in Australia, fewer than half of the CPT operators known to the author have a seismic cone penetrometer);

2. Practitioners are not yet convinced of the benefits of the additional seismic readings in everyday geotechnical practice, and moreover are wary of the cost implications to 'routine' site investigation. It is this second reason which should be of most interest to the industry, as overcoming this reason necessarily also solves the first.

As discussed by *Mayne*, geophones installed in the penetrometer can measure arrival times from surface waves, and from these infer the down-hole shear wave velocity (V_s), at vertical spacings of around 0.5m. Thus, the sCPT allows collection of four independent parameters: cone resistance (q_c), shaft resistance (f_s), pore water pressure (u) and shear wave velocity (V_s). V_s can be used directly to assess small strain stiffness, G_s as shown in equation (1), which approximates G_0 and thus is useful for finite element analyses and design methods which utilise the full stiffness-strain degradation curve.

$$G_s = \rho V_s^2 \quad (1)$$

Less common however, as far as day-to-day practice is concerned, is the application of V_s in assessing other geotechnical strength parameters. Just as q_c, f_s, and u can be used to infer undrained shear strength, friction angles, density, state parameters and a host of other geotechnical parameters (Robertson, 2010), so too can V_s. Rarely in a small, low budget investigation are sufficient laboratory tests undertaken to provide, with high confidence, a site specific correlation for factors such as N_{kt}. Such factors are needed to transform the measured CPT data into useful geotechnical parameters, such as undrained shear strength (s_u). Thus we rely on experience and judgment, which, for young geo-professionals,

usually means the experience and judgment of our more senior colleagues!

Experience and judgment can be improved upon with independent measurement and confirmation using V_s. For example, in assessing s_u in the absence of a site-specific correlation with laboratory or vane shear tests, one might normally assume an N_{kt} of between 15 to 20. This is despite the current industry consensus of the possible range (based on published data at various test sites) being nearly twice as wide. Cabal and *Robertson*, for example, quote a laboratory verified value of N_{kt}=8 for the Young Bay Mud in San Francisco. Without laboratory testing, or specific local experience based on the same, how does one settle on a value of 15, or a value of 20? V_s can be used to independently calculate s_u, via correlation, and this additional independent data set can be used to validate site assumptions in the absence of expensive laboratory testing. Figure 1, reproduced from *Mayne*, shows such a correlation, valid for intact normally consolidated clays, based on Equation 2.

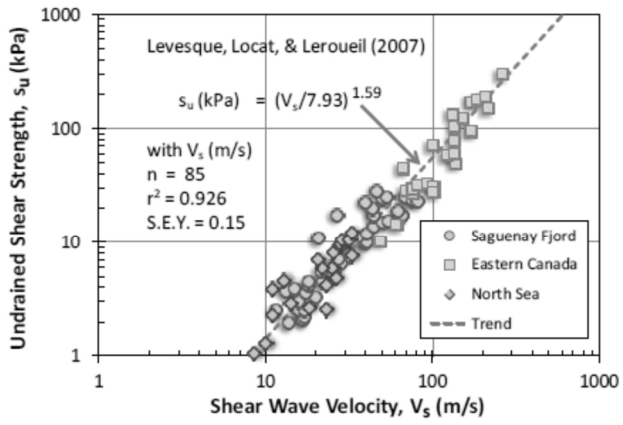

Figure 1. Correlation between shear wave velocity and undrained shear strength for intact clays (from *Mayne*).

$$s_u = \left(\frac{V_s}{7.93} \right)^{1.59} \qquad (2)$$

It is evident that the ability to collect an independent data set (V_s) alongside conventional q_c data provides a useful check on inferred s_u profiles at a site, and can provide a ready means by which to check one's inferred N_{kt} parameter. This is of course just one example of the applicability of V_s measured by the sCPT, and this author strongly encourages the industry to make better use of this technology as part of routine investigation practice.

3. Reliability and measurement of f_s

Several authors at CPT'14 focused their research on either attempting to improve, or highlight the issues surrounding, measurement of CPT sleeve friction, f_s. Previous work by Lunne et al (1986) and others has shown that f_s is the least reliable of the parameters measured by the CPT, and could vary considerably between operators in otherwise controlled conditions. There are several reasons for this, including sleeve size, temperature effects, adhesion of clay to the sleeve surface, and the design of components of the apparatus, such as seals. *Peuchen and Terwindt* provide a comprehensive overview of the contributing factors to CPT accuracy more generally, as well as those specific to sleeve friction. What is clear from their work is that significant inaccuracy is possible in f_s measurements, even when the CPT design and operation is fully compliant with the tolerances in the ISO and ASTM standards.

Holtrigter et al and *Cabal and Robertson* discuss the effect of sleeve diameter on the measurement of f_s. Figure 2 below, reproduced from *Cabal and Robertson*, compares CPT tests taken side by side at a site north of San Francisco. One test is undertaken with a friction sleeve equal in diameter to the cone, whilst the other has an oversized sleeve. Of particular interest is the fact that the oversized sleeve is still within the size tolerance allowed in international testing standards. Whilst q_c and u (not shown) have good repeatability, it is clear that the friction sleeve readings are affected by sleeve diameter.

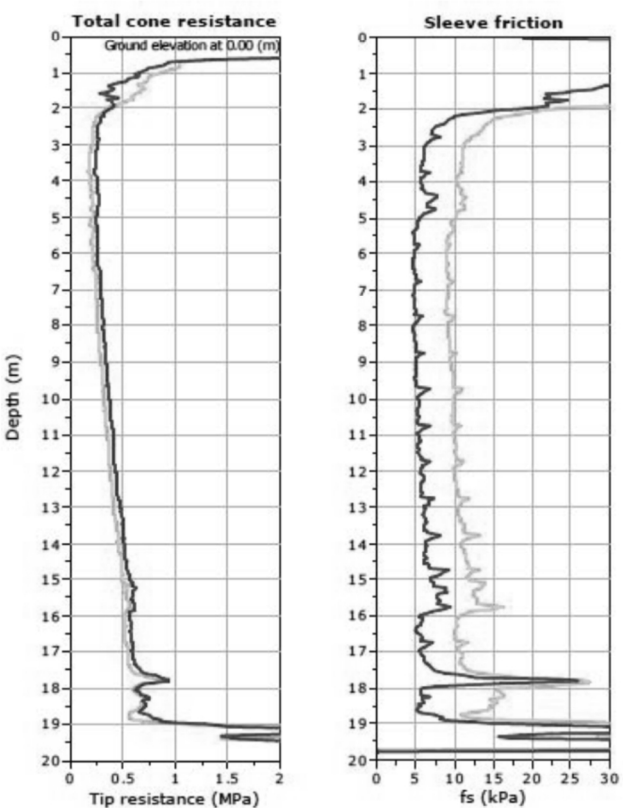

Figure 2. Comparison of f_s measurements for a same sized and oversized friction sleeve (from *Cabal and Robertson).* NB oversize sleeve shown as pale-grey trace.

The discrepancy is reduced on subsequent tests with the cone with the oversized friction sleeve, which is postulated to be due to wear on the sleeve reducing the degree of oversize. This of course, is concerning for another reason. Not only may measurements of f_s vary between CPT rigs, they may vary with the *same* rig, after completion of only a handful of tests.

Cabal and Robertson show how inaccuracies in the measurement f_s can affect interpretation of the soil profile. Figure 3 shows a soil behavior type (SBT) chart interpreting ground conditions with both the same sized and oversized cones. The data clearly shows that at the test site, the use of the oversized cone incorrectly classify the soil as Zone 2 (organic), instead of Zone 3 (normally consolidated clay).

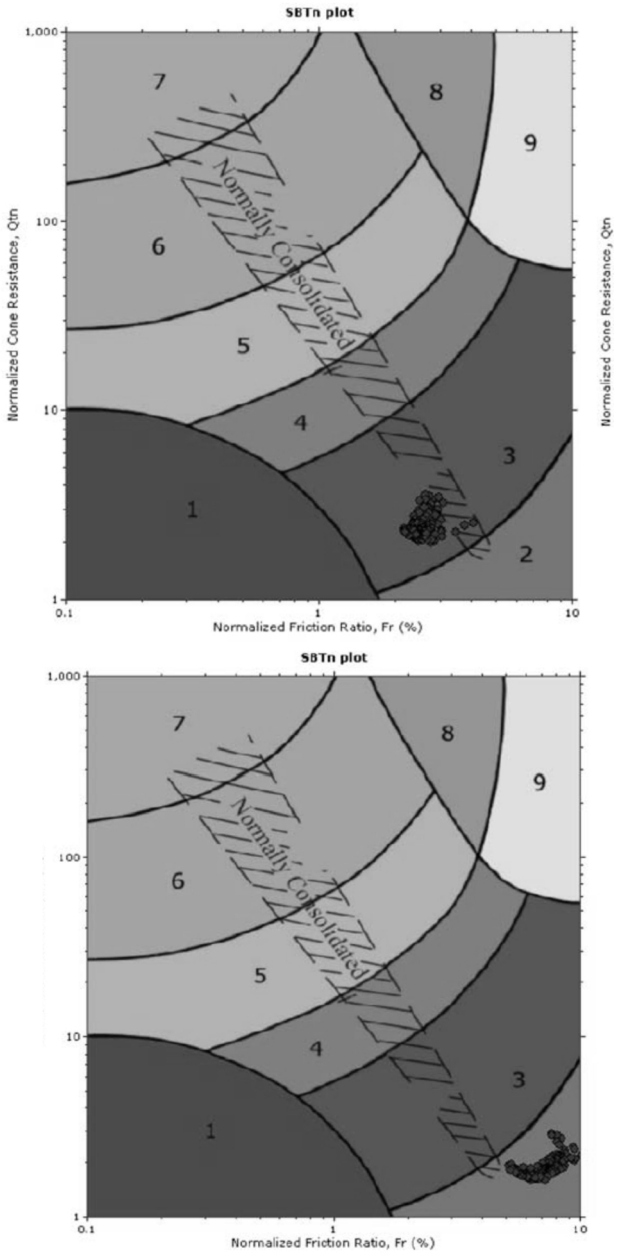

Figure 3. Soil Behavior type chart for a) same-sized sleeve, and b) over-sized sleeve. (after *Cabal and Robertson)*

Santos et al show that friction associated with o-rings and dirt seals also affect accuracy of f_s measurements, and report variances of more than 7kPa in tests undertaken at Onsøy, in very soft sediments with undrained shear strengths less than 15kPa. Such an error band is clearly unsatisfactory when dealing with such soft soils. The work of *Santos et al* showed that improvements in the design of o-rings and seals can measurably improve the accuracy of these measurements.

The work presented at CPT'14 in quantifying errors in f_s and improving its reliability is a step in the right direction for the industry, however it is clear there is still further to go if this parameter is to become acceptably reliable. As well as highlighting the impact of apparatus design, the potential for errors in f_s measurements to affect interpretation of ground conditions also serves as a reminder for all young geo-professionals to critically analyse their data sets. Soil behavior type (SBT) for example is becoming a pseudo-standard for CPT test interpretation around the world, and is built into virtually all CPT interpretation software. It is thus becoming a 'black box' for interpretation, and whilst incredibly useful, must always be understood for what it is: a correlation, based on an extensive but ultimately finite data set which *predicts*, but does not unequivocally determine, soil behavior.

4. Applications of the CPT to geotechnical practice

It is clear from a review of papers from CPT'14 that there is an incredibly wide spread of uses for the CPT, with its utility as a site investigation tool undeniable. *Lehane* provides an overview of the papers at CPT'14 with specific emphasis on application of the test method, and this author has elected to highlight two uses of particular interest.

4.1 Liquefaction

It comes as no surprise that a great deal of the recent studies into liquefaction phenomena are taking place in Christchurch, New Zealand, following the devastation of the 2011/12 earthquakes. A great deal of high-quality data on the occurrence of liquefaction and resulting settlements are available, with extensive CPT, drilling, geophysical and LiDAR surveys undertaken across the Christchurch region. *Bray et al* report that over 15,000 CPTs and over 3,000 boreholes have been undertaken in the Christchurch area in the last 3 years.

The consensus amongst the CPT industry, at least insofar as the work in Christchurch is concerned is that no one method of CPT interpretation adequately predicts the factor of safety against liquefaction (FS_L). In all the cases this author has looked at, practitioners have undertaken an evaluation using most (if not all) of the following four methods:

- Robertson & Wride (1998)
- Moss et al (2006);
- Idriss & Boulanger (2008)
- Robertson (2009).

Zhang et al (2002) provides a method of prediction of liquefaction-induced surface settlements, assuming level ground and green-field conditions, and has been widely adopted in partnership with the above listed FS_L methods to predict the liquefaction risk at a particular site. The former provides a prediction of volume change and settlement which provides a quantification of 'consequence', whilst the later provides quantification of the probability of occurrence. Thus, combining both the FS_L methods with settlement approaches such as Zhang et al allow the risk equation to be assessed.

The extensive datasets available from Christchurch afford the opportunity to assess the adequacy of the above methods. Rarely if ever in the past has there been so much high-quality data available from which to compare both the *predicted* and *actual* ground performance due to a liquefaction event. *Bray et al* present several case histories which describe the performance of buildings founded on both shallow and deep foundations, following liquefaction events. They conclude that the current suite of FS_L methods are conservative, based on the observation of several smaller earthquake events failing to trigger liquefaction, despite predictions to the contrary. This is not of serious concern; as a designer one would certainly want to err on the side of caution in this regard.

Current methods for predicting surface settlements seem to perform reasonably well for larger events, but are less reliable for smaller events. *Bray et al* concede that these methods do not capture settlement induced by shear deformation mechanisms, such as ratcheting, bearing failure or volume loss of soil as ejecta.

The work reported by *Bastani* is also of particular note. *Bastani* compared predicted versus actual earthquake-induced settlements at 6 sites with at least 4 CPTs and a borehole with SPT data available at each site. Unique about this study was the availability of pre and post-earthquake LiDAR data which allowed reasonably accurate measurements of the actual amount of settlement due to the earthquake events. *Bastani* found that the methods listed above, combined with Zhang et al (2002) resulted in highly variable predictions of settlement, ranging from under prediction by 50% to over prediction by 250%.

Clearly, the above studies highlight the need for more case histories to be made available in literature against which to compare various methods of predicting earthquake induced ground movements. This author encourages the publishing and sharing of case histories, such as those discussed in the above referenced papers, such that methods of evaluating liquefaction risk can be refined.

4.2 Pile design

The CPT has always been seen as a useful tool for pile capacity estimates, particularly with reference to driven piles. Current research work is focusing on both refining capacity assessments of axial piles, in particular the estimation of load-deflection curves using sCPT data, and expanding the applicability of the CPT for use in predicting lateral pile behavior and assessing setup.

Niazi et al have built on work done by Vardanega and Bolton (2013), which derives modulus degradation curves based on the plasticity index of the soil, and Randolph and Wroth (1979) who developed a closed-form elastic solution for the axial load – displacement (Q-w) response of a pile. *Niazi et al*s' work shows that sCPT data can be used to estimate G_s, and when combined with the methods of the other mentioned authors can be used to develop a reliable estimate of the Q-w response of a pile. The method can be readily applied in a spreadsheet, following the methodology shown in the flowchart in Figure 4, and using the design charts and equations provided in their paper.

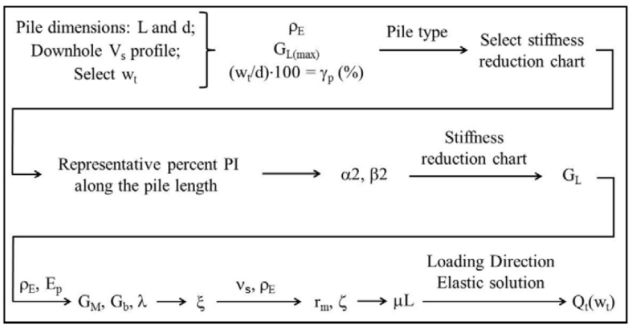

Figure 4. Evaluation of Q-w response of a pile (from *Niazi et al)*

A program of works is currently being undertaken at the University of Western Australia (UWA), investigating the prediction of *p-y* curves and lateral soil behavior from CPT data. Papers by *Suryasentana and Lehane*, *Guo and Lehane, and Truong and Lehane* explore the validity of *p-y* relationships estimated from CPT data. The work compares both analytical and empirically derived *p-y* relationships. Equation 3 presents one such relationship for sands, and Equations 4 and 5 present relationships for clay. These relationships have been validated for Kaolin clay, with OCR=1 and OCR=2 and an assumed rigidity index (I_r) of 150. The work presented, whilst requiring further validation against real test sites, is promising. It is also worth noting that work done by *Truong and Lehane* suggests that once the *p-y* response has been defined, sophisticated 3D finite element analysis, despite the amount of effort involved,

produces no better predictions than analysis undertaken with much more straight forward lateral pile software, such as Oasys. This observation highlights the importance of selecting the right tool for the task, and not assuming that finite element modelling, despite being theoretically more robust, is always the best way to tackle a problem.

$$\frac{p}{\gamma z D} = 2.4\left(\frac{q_c}{\gamma z}\right)^{0.67}\left(\frac{z}{D}\right)^{0.75}\left(1 - exp\left(-6.2\left(\frac{z}{D}\right)^{-1.2}\left(\frac{y}{D}\right)^{0.89}\right)\right) \quad (3)$$

$$N_{pq} = \frac{P_u}{q_{net}} = \left(\frac{3}{4.7 + 1.6\,ln I_r}\right) + [1.5 - 0.14\ln I_r]\tanh\left[0.65\frac{z}{D}\right] \quad (4)$$

$$\frac{P}{P_u} = tanh\left[(0.26I_r + 3.98)\left(\frac{y}{D}\right)^{0.85}\left(\frac{z}{D}\right)^{-0.5}\right] \quad for \quad 0 < \frac{z}{D} < 3$$

$$\frac{P}{P_u} = tanh\left[(0.15I_r + 2.3)\left(\frac{y}{D}\right)^{0.85}\right] \quad for \quad \frac{z}{D} \geq 3 \quad (5)$$

5. Concluding remarks

The work presented at CPT'14, and discussed herein highlights the utility and applicability of the CPT. Few geo-professionals would argue that the CPT has a role to play in the vast majority of geotechnical site investigations. Key learnings which have arisen for the author at the symposium, and which are worthy of consideration by other young geo-professionals, include:

1) The seismic CPT needs to play a more prominent role in site investigation practice. The additional costs and time are negligible when compared to the additional value gained by measuring V_s, whether it is used as a stand-alone parameter in the derivation of geotechnical parameters such as G_s, or as a useful check against correlations for parameters such as s_u, based on q_c or f_s;
2) Interpretation and reliability of f_s is still questionable, and appears to be limited by apparatus design;
3) Point (2) reminds us that closed-form solutions to geotechnical problems are rare, if they exist at all. Soil behavior type is an example of an approach which is becoming a 'black-box' used by practitioners. Yet this interpretation tool relies on an accurate and repeatable measurement of f_s, which, as shown, is not always achievable;
4) Case histories for complex problems such as liquefaction are essential for the refinement of our understanding of these phenomena, and geo-professionals should share these valuable datasets to improve the industry's body of knowledge;
5) Progress is being made by researchers to improve the prediction of pile behavior using the CPT and sCPT, which will increase the tool's utility even further. Again, case histories are necessary to allow validation of theoretical approaches;
6) Finally, the author reminds all young geo-professionals of the value of choosing the right analysis tool for the job. Whilst this paper has focused on the merits of the CPT and its variants, the use of the tool must always be considered in the context of the purpose of the investigation, and the anticipated geology. Reference has been made to one example where a complex, 3D finite element analysis was seen to provide little benefit compared with a more straight-forward pile analysis procedure, despite the additional time and effort involved. Occam's Razor, in this instance, holds true.

6. Acknowledgements

The author would like to extend his appreciation first of all to Insitu Geotechnical Services for sponsoring the Young Geo-professional's Prize. The prize has provided the opportunity to attend CPT'14 and learn from some of the pioneers in the CPT industry, and to be able to share those valuable learnings with the delegates of 10YGPC.

Without doubt, further thanks must also go to the authors and organizes of CPT'14 who have made their research public and in particular freely accessible online for anyone interested. Not only have the papers of the most recent symposium been shared, but all published works from previous CPT symposia, dating back to 1974, have been made freely available on the internet.

6. References

Bastani S.A. (2014) Comparison of observed and claculated earthquake-induced settlements at 6 sites in Christchurch, NZ. *Proceedings, 3rd International Symposium on Cone Penetration Testing, pp. 797-807.*

Bray J.D., Zupan J.D., Cubrinovski M., Taylor M. (2014) CPT-based liquefaction assessments in Christchurch, New Zealand. *Proceedings, 3rd International Symposium on Cone Penetration Testing, pp. 75-95.*

Cabal K., Robertson P.K. (2014) Accuracy and repeatability of CPT sleeve friction measurements. *Proceedings, 3rd International Symposium on Cone Penetration Testing, pp. 271-278.*

Guo F., Lehane B.M. (2014) Experimentally derived CPT-based *p-y* curves for soft clay. *Proceedings, 3rd International Symposium on Cone Penetration Testing, pp. 1021-1028*

Holtrigter M., Thorp A., Hoskin P.W.O. (2014) The effect of sleeve diameter on f_s measurements. *Proceedings, 3rd International Symposium on Cone Penetration Testing, pp. 189-198.*

Idriss I.M., Boulanger R.W. (2008) Soil liquefaction during earthquakes*, Earthquake engineering research institute MNO-12.*

Lehane B.M. (2014) Session report 3 CPT applications. *Proceedings, 3rd International Symposium on Cone Penetration Testing, pp. 165-178.*

Lunne T., Eidsmoen T., Gillespie D., Howland J.D. (1986) Laboratory and field evaluation on cone penetrometers. *Proceedings of ASCE Specialty Conference In Situ'86: Use of in situ tests in geotechnical engineering,* Blacksburg, ASCE, 714-729.

Massarsch K.R. (2014) Cone penetration testing – A historic perspective, *Proceedings, 3rd International Symposium on Cone Penetration Testing, pp97-134.*

Mayne P.W (2014) Interpretation of geotechnical parameters from seismic piezocone tests. *Proceedings, 3rd International Symposium on Cone Penetration Testing, pp. 47-73.*

Moss, R.E.S., Seed R.B., Kayen R.B., Stewart J.P., Der Kiureghian A., Cetin K.O. (2006) CPT-based probabilistic and deterministic assessment of in situ seismic soil liquefaction potential. *Journal of geotechnical and geoenvironmental engineering*, *vol 132, no. 8.*

Niazi F.S., Mayne P.W., Woeller D.J. (2014) Pile axial load-displacement response from geophysical component of seismic CPT. *Proceedings, 3rd International Symposium on Cone Penetration Testing, pp. 1103-1111.*

Peuchen J., Terwindt J. (2014) Introduction to CPT accuracy *Proceedings, 3rd International Symposium on Cone Penetration Testing, pp. 1-45.*

Randolph M.F., Wroth C.P. (1979) A simple approach to pile design and the evaluation of pile tests. *Behaviour of deep foundations, STP 670, ASTM, West Conshohocken, PA, pp. 1575-1589.*

Robertson P.K., Wride C.E. (1998) Cyclic liquefaction and its evaluation based on the CPT. *Canadian Geotechnical Journal*, Vol 35.

Robertson P.K. (2009) Interpretation of cone penetration tests – a unified approach. *Canadian geotechnical journal, vol 46, no. 11, pp. 1337-1355.*

Robertson PK., Cabal K. (2010) *Guide to Cone Penetration Testing 4th edition.* Gregg Drilling & Testing, Inc, California.

Santos R.S., Barwise A., Alexander M. (2014) Improved CPT sleeve friction sensitivity in soft soils. *Proceedings, 3rd International Symposium on Cone Penetration Testing, pp. 239-248.*

Suryasentana S., Lehane B.M. (2014) Verification of numerically derived CPT based p-y curves for piles in sand. *Proceedings, 3rd International Symposium on Cone Penetration Testing, pp. 1013-1020.*

Truong P., Lehane B.M. (2014) Numerically derived CPT based *p-y* curves for a soft clay modeled as an elastic perfectly plastic material. *Proceedings, 3rd International Symposium on Cone Penetration Testing, pp 975-982.*

Vardanega P.J., Bolton M.D. (2013) Stiffness of clays and silts : normalizing shear modulus and shear strain. *Journal of geotechnical and geoenvironmental engineering, 139(9), pp. 1575-1589.*

Zhang G., Robertson P.K., Brachman R. (2002) Estimating liquefaction induced ground settlements from the CPT*, Canadian geotechnical journal, vol 39, pp. 1168-1180.*

Author Index

Major Sponsors of 10YGPC:

reducing geotechnical uncertainty

IGS

Insitu Geotech Services Pty Ltd

CPTS

cone penetration testing services

Additional Sponsorship and Support provided by:

Global Synthetics

GEODRILL
Geotechnical & Environmental
Drilling Specialists

Foundation Specialists Group

Tonkin & Taylor

aurecon

Douglas Partners
Geotechnics · Environment · Groundwater